

Dinâmica de elementos traço em bacias de drenagem e suas exportações para o Oceano Atlântico

LUÍSA MARIA DE SOUZA VIANA

UNIVERSIDADE ESTADUAL DO NORTE FLUMINENSE DARCY RIBEIRO

CAMPOS DOS GOYTACAZES – RJ

SETEMBRO – 2022

Dinâmica de elementos traço em bacias de drenagem e suas exportações para o Oceano Atlântico

LUÍSA MARIA DE SOUZA VIANA

Tese apresentada ao Centro de Biociências e Biotecnologia da Universidade Estadual do Norte Fluminense Darcy Ribeiro, como parte das exigências para a obtenção do título de doutor em Ecologia e Recursos Naturais.

Orientador: Prof. Dr. Carlos Eduardo Veiga de Carvalho

Coorientador: Prof.^a Dr.^a Taíse Bonfim de Jesus

CAMPOS DOS GOYTACAZES – RJ

SETEMBRO – 2022

FICHA CATALOGRÁFICA

UENF - Bibliotecas

Elaborada com os dados fornecidos pela autora.

V614

Viana, Luísa Maria de Souza.

Dinâmica de elementos traço em bacias de drenagem e suas exportações para o Oceano Atlântico / Luísa Maria de Souza Viana. - Campos dos Goytacazes, RJ, 2022.

192 f. : il.

Inclui bibliografia.

Tese (Doutorado em Ecologia e Recursos Naturais) - Universidade Estadual do Norte Fluminense Darcy Ribeiro, Centro de Biociências e Biotecnologia, 2022.

Orientador: Carlos Eduardo Veiga de Carvalho.

1. bacias de drenagem; . 2. fluxo de elementos.. 3. estuário de Serinhaém; . 4. elementos traço; . 5. Oceano Atlântico; . I. Universidade Estadual do Norte Fluminense Darcy Ribeiro. II. Título.

CDD - 577

Dinâmica de elementos traço em bacias de drenagem e suas exportações para o Oceano Atlântico

LUÍSA MARIA DE SOUZA VIANA

Tese apresentada ao Centro de Biociências e Biotecnologia da Universidade Estadual do Norte Fluminense Darcy Ribeiro, como parte das exigências para a obtenção do título de doutor em Ecologia e Recursos Naturais.

Aprovada em: 30/09/2022

Comissão Examinadora:



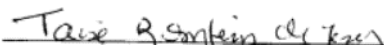
Dr. Aginaldo Marques Nepomuceno Júnior (IBM/UFF)



Dr. João Paulo Machado Torres (IBFCCF/UFRJ)



Dr. Marcos Sarmet Moreira de Barros Salomão (LCA/UENF)



Dra. Taíse Bomfim de Jesus (UEFS) (Coorientadora)



Dr. Carlos Eduardo Veiga de Carvalho (UENF) (Orientador)



Governo do Estado do Rio de Janeiro
Universidade Estadual do Norte Fluminense Darcy Ribeiro
Pró-Reitoria de Pesquisa e Pós-Graduação

DECLARAÇÃO

Eu, Marina Satika Suzuki, coordenadora do Programa de Pós-Graduação em Ecologia e Recursos Naturais (PPG-ERN) da Universidade Estadual do Norte Fluminense Darcy Ribeiro (UENF), seguindo a Resolução CPPG nº2 de 2021, declaro validadas as assinaturas constantes da Folha de Assinaturas da Dissertação intitulada “**Dinâmica de elementos traço em bacias de drenagem e suas exportações para o Oceano Atlântico**” de autoria de Luisa Maria de Souza Viana, defendida no dia 30 de setembro de 2022.

Campos dos Goytacazes, 24 de outubro de 2022

Marina Satika Suzuki
Coordenadora PPG-ERN / UENF
ID. Funcional 641333-1



Documento assinado eletronicamente por **Marina Satika Suzuki, Coordenadora**, em 24/10/2022, às 14:51, conforme horário oficial de Brasília, com fundamento nos art. 21º e 22º do [Decreto nº 46.730, de 9 de agosto de 2019](#).



A autenticidade deste documento pode ser conferida no site http://sei.fazenda.rj.gov.br/sei/controlador_externo.php?acao=documento_conferir&id_orgao_acesso_externo=6, informando o código verificador **41565957** e o código CRC **14D6A74D**.

Dedico essa tese ao meu avô, Ernani Leodônio, que me ensinou a sempre tentar ser uma pessoa melhor e, independentemente, de como a tratem deve-se sempre retornar o bem e o que for para ser seu ninguém tem o poder de tirar.

AGRADECIMENTOS

Agradeço primeiramente a Deus, que me permitiu chegar ao fim dessa etapa.

Aos meus pais por terem me concedido a chance de realizar os meus sonhos, por todo o apoio que me deram durante toda essa caminhada e por serem exemplos de boas pessoas.

Ao orientador, Prof.: Dr. Carlos Eduardo Veiga de Carvalho por todo o apoio durante a caminhada do doutorado e todo o suporte emocional e financeiro para que a pesquisa fosse realizada, além da parceria e amizade construída ao longo desses anos. Obrigada pela confiança depositada no meu trabalho.

Ao meu grupo de pesquisa, principalmente Eloá Tostes, Wendel Constantino e Felipe Rossi, por toda ajuda e ombro amigo durante esse processo.

A coorientadora, Prof.: Dr^a. Taíse Bonfim de Jesus por todo suporte e ajuda concedido durante a nossa estadia na Bahia e pela parceria.

Ao professor, Dr. Marcos Sarmet Moreira de Barros Salomão por sempre se fazer presente durante o doutorado, por todos os ensinamentos, parceria e amizade construídos ao longo desses anos e pela sua dedicação durante toda a minha formação.

Aos meus amigos Gabriel Cardoso, Julya Braga, Matheus Moura, Viviane Campos, Beatriz Muniz, Pedro Miranda, Marianne Caiado, Wesley Pires, Arícia Leone, Roberta Paschoa, Gildeíde Costa, Priscila Bittencourt, Keltony Aquino, Échily Sartori e Pedro Gatts por todo o apoio durante esses quatro anos, todo o suporte emocional, por terem ouvido todas as reclamações durante esse processo e pelos momentos de distração importantíssimos para a conclusão dessa etapa.

SUMÁRIO

LISTA DE ABREVIACÕES.....	xi
LISTA DE FIGURAS.....	xiii
LISTA DE TABELAS	xv
LISTA DE ANEXOS	xvi
ABSTRACT	xix
ESTRUTURA DA TESE	xx
Introdução Geral.....	1
CAPÍTULO 1	9
Seasonal variation, environmental parameters and their importance for the control of As and Pb concentrations: A case study	9
Abstract	10
1. Introduction.....	10
2. Data processing and analysis.....	13
2.1 Study Area.....	13
2.2 Database used	14
2.2.1 Analysis methods used.....	14
2.2.2 Average rainfall.....	15
2.2.3 Flow estimation.....	15
2.2.4 Preparation of geochemical maps	16
2.3 Statistical analyses	16
3. Results and Discussion	16
3.1 – Seasonal variation of As an Pb along the Doce River Basin	16
3.2 - Controlling parameters of As and Pb concentrations in the Doce River Basin	18
3.3 – As and Pb Fluxes along the Doce River Basin and export to the Atlantic Ocean ..	21
4. Further considerations and suggestions for future studies	26
5. Acknowledgements	27
6. Conflict of interest.....	27
7. Data Availability	27
8. References	27
CAPÍTULO 2	56

Comparison of stochastic and machine learning models in streamflow forecasting of a small basin in northeast Brazil	56
Abstract	57
1. Introduction	57
1.1 Autoregressive Moving Average Models	59
1.2 Artificial Neural Network	61
1.3 Statistical comparison.....	61
1.4 Case Study.....	62
2. Methodology	63
2.1 Stationarity	64
2.2 Development of ARMA and ARIMA models	65
2.3 Development of ANN models	65
3. Results and Discussion.....	65
3.1 Performance evaluation of ARMA, ARIMA and SARIMA models.....	65
3.2 Performance evaluation of MLP models.....	67
3.3 Performance evaluation of Linear Regression models	68
4. Statistical comparison between the performance of the approached models	69
5. Conclusion.....	70
CAPÍTULO 3	91
Seasonal variation, contribution and dynamics of trace elements in the drainage basin and estuary of the Serinhaém river, BA.....	91
Abstract	92
Graphical Abstract.....	93
1. Introduction.....	94
2. Materials e Methods	95
3. Results and Discussion	98
3.1. Environmental parameters	98
3.2. Trace elements.....	101
3.2.1 - Essentials trace elements	101
1. Iron (Fe).....	101
1. Vanadium (V).....	103
2. Chromium (Cr)	103
3. Zinc (Zn)	104

4. Cooper (Cu).....	105
5. Manganese (Mn).....	106
3.2.2 Non-Essentials trace elements.....	107
6. Lead (Pb).....	108
7. Aluminum (Al).....	108
8. Cadmium (Cd).....	109
9. Barium (Ba).....	111
3.3. Relationship between physical-chemical parameters and trace elements.....	113
3.4. Export of trace elements to the Atlantic Ocean.....	115
3.4.1. Export via dissolved flux.....	115
3.4.2 – Export via particulate fraction (SPM).....	119
4. Conclusions.....	124
Acknowledgements.....	125
Conflict of interest.....	125
Referências.....	126
Discussão geral.....	164
Considerações Finais.....	166
Referências.....	167

LISTA DE ABREVIações

ACF – Autocorrelation

AIC – Akaike's Information Criterion

AICc – Akaike Information Criterion with Correction

ANA – National Water Agency

ANN – Artificial Neural Network

AR – Autoregression

ARIMA – Autoregressive Integrated Moving Average

ARMA – Autoregressive Moving Average Model

As – Arsenic

BIC – Bayesian Information Criteria

CONAMA - National Environment Council

DO – Dissolved oxygen

DOC – Dissolved Organic Carbon

EPA – Environmental Protection Area

Fe – Iron

HPP – Hydroelectric Power Plant

LR – Linear Regression

MA – Moving average

MAE – Mean Absolute Error

MAPE – Mean Absolute Percentage Error

MASE – Mean Absolute Scaled Error

MBC – Mass Balance Calculation

MLP – Multilayer Perceptron

MLR – Multiple Linear Regression

Mn – Manganese

MSE – Mean Square Error

NRMSE – Normalized Root Mean Square Error

PACF – Partial Autocorrelation

Pb – Lead

PC – Principal Component

PCA – Principal Component Analysis

R² - Coefficient of Determination,

RMSE – Root of Mean Square Error

SARIMA – Seasonal Autoregressive Integrated Moving Average

SPM – Particulate Material in Suspension

TN – Total Nitrogen

LISTA DE FIGURAS

Capítulo 1

- Figure 1** - Division of the watershed of the Doce River in sub-regions. The ES01 region was assigned by the author due to the lack of an official nomenclature.....39
- Figure 2** - Seasonal differences in the flows of As. Asterisks indicate statistical difference. Values of p: 2012 p = 0.0009765, 2015 p = 2.401e-10, 2016 p < 2.2e-16, 2018 p = 0.012399. The y-axis is logarithmic to facilitate understanding. The values were transformed to meet the assumptions of ANOVA. N: number of samples.40
- Figure 3** - Seasonal differences in Pb flows. The year 2017 only presented data on the rainy season. Asterisks indicate statistical difference. Values of p: 2012 p = 0.000542, 2015 p = 2.401e-10, 2016 p < 2.261e-16, 2018 p = 0.0578667, 2019 p = 0.0145725. The y-axis is logarithmic to facilitate understanding. The values were transformed to meet the assumptions of ANOVA. N: number of samples.41
- Figure 4** - PCA between As concentrations and environmental parameters found in the reviewed studies. Mg - Magnesium, Fe - Iron, K - Potassium, Cl- - Chlorides, STD - Total Dissolved Solids, T - Temperature, Mn - Manganese, Alc - Alkalinity, EC - Electrical Conductivity, Ca⁺² - Calcium, Na⁺ - Sodium, SO₄^{- 2} - Sulfates, As - Arsenic, Alt - Altitude, OD - Dissolved Oxygen and pH - Hydrogenionic Potential.....43
- Figure 5** - PCA between Pb concentrations and environmental parameters found in the reviewed studies. Mg - Magnesium, Fe - Iron, K - Potassium, Cl- - Chlorides, STD - Total Dissolved Solids, T - Temperature, Mn - Manganese, , Alc - Alkalinity, EC - Electrical Conductivity, Ca⁺² - Calcium, Na⁺ - Sodium, SO₄^{- 2} - Sulfates, As - Arsenic, Alt - Altitude, OD - Dissolved Oxygen and pH - Hydrogenionic Potential.....44
- Figure 6** - As flow in the dissolved fraction of the water column (mg s⁻¹) calculated for the years 2009 to 2019. The maps were plotted by Kriging interpolation, except for the year 2014.45
- Figure 7** - Pb flow in the dissolved fraction of the water column (mg s⁻¹) calculated for the years 2009 to. The maps were plotted by Kriging interpolation, except for the years 2011, 2012, 2013, 2014 and 2018.....46

Capítulo 2

Figure 1 – Map of the study area in which the case study was carried out.....	80
Figure 2 – A) Time series of the flow of the Serinhaém estuary, BA from 1966 to 2019; B) ACF and C) PACF graphics.....	81
Figure 3 – Scatter plot of model regressions in both time intervals (T1 and T2).....	87
Figure 4 – Flow series predicted by the models used.....	88

Capítulo 3

Figure 1 – Map of the Pratigi EPA, collection points and main tributaries. The cities are represented by the black dots and the red stars refer to the collection points.	146
Figure 2 – Physico-chemical parameters of the water column in both collections.	147
Figure 3 – Concentrations of trace elements (Al, Ba, Cd, Cr, Cu, Fe, Mn, Pb, V, Zn) in the dissolved fraction of the water column in the two collection campaigns.	148
Figure 4 - Concentrations of trace elements (Al, Ba, Cr, Fe, Mn, Ti, V, Zn) in the particulate fraction of the water column in the two collection campaigns.	149
Figura 5 – Flow of trace elements (Al, Ba, Cd, Cr, Cu and Z) in the dissolved fraction of the water column in both collection campaigns.	150
Figura 6 – Flow of trace elements (Mn, Pb, Fe and V) in the dissolved fraction of the water column in both collection campaigns.	151
Figure 7 – Flow of trace elements (Al, Ba, Cr and Fe) in the particulate fraction of the water column in both collection campaigns.	152
Figure 8 - Flow of trace elements (Mn, Ti, V and Zn) in the particulate fraction in the water column in both collection campaigns.....	153
Figure 9 – Principal component analysis (PCA) between the trace elements and the physicochemical parameters determined in this study and its relationship with the two collection campaigns.	154

LISTA DE TABELAS

Capítulo 1

Table 1 - The Kaiser-Meyer-Olkin and Bartlett's Test Result.	42
--	----

Capítulo 2

Table 1 – Accuracy statistics of ARMA models.	82
Table 2 – Accuracy measures of ARIMA models for both temporal approaches.	83
Table 3 - SARIMA accuracy measures	84
Table 4 – MLP accuracy measures.....	85
Table 5 – Accuracy measures linear regression.	86

LISTA DE ANEXOS

Capítulo 1

Table S2 - Flow and average rainfall values in each sub-region of the Doce River Basin.	47
Table S3 – Principal components (PCs) statistics for the parameters used in this study.	50
Figure S1 – Linear regression analyzing the relationship between As concentrations and precipitation and flow.....	48
Figure S2 – Linear regression analyzing the relationship between Pb concentrations and precipitation and flow.....	49

Capítulo 2

Table S1 – Descriptive statistics of the data.	89
Table S2 – Hyperparameters used in the testing of neural networks.	90

Capítulo 3

Table S1 - Analytical procedure validation using Nist Standard Reference Material® 1646a from estuarine sediments (mg kg ⁻¹ dry weight), N = 3. Data are presented as mean ± SD.....	155
Table S1 - Dissolved flows – Rainy.....	156
Table S2 – Dissolved Flows – Dry.....	157
Table S3 – Particulate Flows – Rainy.....	158
Table S4 - Particulate Flows – Dry.	159
Table S5 – Correlation values (r) and p from the April collection.....	160

Table S6 - Correlation values (r) and p from the September collection.....	161
Table S8 - Table of the distribution of river and estuarine loads.....	162
Table S9 -Distribution coefficient (Kd).....	163

RESUMO

Estudar bacias de drenagem é crucial para monitorar os impactos das atividades antrópicas e fornecer informações relevantes para uma gestão eficiente dos ecossistemas aquáticos. O objetivo do estudo foi avaliar o fluxo de elementos traço em duas bacias de drenagem: (i) a bacia do rio Doce (Minas Gerais) e a bacia do rio Serinhaém (Bahia); e a exportação dos mesmos para o Oceano Atlântico. Para a bacia do rio Doce, foi montado um banco de dados com as concentrações de arsênio (As) e chumbo (Pb) dissolvidos presentes em estudos de 2009 a 2019, enquanto na bacia do rio Serinhaém foram avaliados a partição de elementos traço na coluna d'água e seus respectivos fluxos ao longo do estuário no ano de 2019. Os resultados mostram que a contaminação existente na bacia do rio Doce é proveniente das atividades de mineração existentes na região, e que existe uma forte ligação entre As e Pb e as concentrações de Fe e Mn. Ainda, o acidente com a barragem de Fundão em 2015 maximizou a dispersão desses dois elementos ao longo da bacia, levando-os até o estuário em Regência (Espírito Santo). No estuário do rio Serinhaém, além do fluxo de elementos traço, foi realizado um estudo complementar para analisar a série temporal de 53 anos de vazão do rio, para avaliar se a seca do ano de 2012 teria influência na vazão e, com isso, estimar os valores de vazão do estuário, devido à falta dessas informações na literatura. De fato, foi observado que a seca de 2012 não influenciou nos valores de vazão e que o fluxo de todos os elementos analisados ocorre de forma constante em direção ao Oceano Atlântico. Além disso, o transporte dos elementos traço foi majoritariamente relacionado à fração particulada, e também que há uma clara relação entre os processos de remoção e liberação de elementos (floculação, dessorção, adsorção) com os parâmetros físico-químicos e os elementos analisados. Por fim, todos os elementos apresentaram concentrações mais baixas do que as preconizadas por órgãos ambientais, confirmando a hipótese inicial de que realmente se trata de uma área conservada. Esse estudo fornece informações relevantes sobre o uso de ferramentas específicas para o monitoramento de elementos traço ao longo de bacias de drenagem e apresenta informações sobre as concentrações dos mesmos.

Palavras-Chave: bacias de drenagem; rio Doce; estuário de Serinhaém; elementos traço; Oceano Atlântico; fluxo de elementos.

ABSTRACT

Studying drainage basins is crucial to monitor the impacts of human activities and provide relevant information for an efficient management of aquatic ecosystems. The objective of the study was to evaluate the flow of trace elements in two drainage basins: (i) the Doce River basin (Minas Gerais) and the Serinhaém River basin (Bahia); and exporting them to the Atlantic Ocean. For the Doce river basin, a database was set up with the dissolved arsenic (As) and lead (Pb) concentrations present in studies from 2009 to 2019, while in the Serinhaém river basin the partition of trace elements in the column was evaluated. of water and its respective flows along the estuary in 2019. The results show that the contamination in the Doce River basin comes from the mining activities in the region, and that there is a strong link between As and Pb and the concentrations of Fe and Mn. Also, the accident with the Fundão dam in 2015 maximized the dispersion of these two elements along the basin, taking them to the estuary in Regência (Espírito Santo). In the estuary of the Serinhaém River, in addition to the flow of trace elements, a complementary study was carried out to analyze the time series of 53 years of river flow, to assess whether the drought in the year of would have an influence on the flow and, with that, estimate estuary flow values, due to the lack of this information in the literature. In fact, it was observed that the 2012 drought did not influence the flow values and that the flow of all analyzed elements occurs constantly towards the Atlantic Ocean. In addition, the transport of trace elements was mostly related to the particulate fraction, and also that there is a clear relationship between the processes of removal and release of elements (flocculation, desorption, adsorption) with the physicochemical parameters and the analyzed elements. Finally, all the elements showed lower concentrations than those recommended by environmental agencies, confirming the initial hypothesis that it really is a conserved area. This study provides relevant information on the use of specific tools for monitoring trace elements along drainage basins and presents information on their concentrations.

Keywords: drainage basins; Doce River; estuary of Serinhaém; trace elements; Atlantic Ocean; elements flow.

ESTRUTURA DA TESE

Essa tese é dividida em:

- 1- **Introdução geral** - na qual é abordada a escassez de água e os cuidados necessários que devem ser tomados nas bacias de drenagem, além da especiação dos elementos traço ocorridas nos ecossistemas aquáticos e algumas ferramentas que podem ser utilizadas para o monitoramento eficiente dos recursos hídricos;
- 2- **Três capítulos em formatos de artigos científicos** - onde são apresentados os dados de elementos traços em duas bacias de drenagem diferentes e métodos estatísticos para estimar esses dados, quando houve a indisponibilidade dos mesmos. Todos os três capítulos apresentam resumo, introdução, resultados, discussão, conclusão e referências próprios.
- 3- **Uma discussão geral** - que apresenta uma sumarização dos resultados encontrados nos três capítulos anteriores, abordando-os de forma mais ampla e geral;
- 4- **Uma conclusão geral** - em que são expostas as lacunas existentes e soluções para estudos futuros que abordem o mesmo tema.

Introdução Geral

Nas últimas décadas, a escassez de água se tornou um tema recorrente na política mundial, devido a urbanização desenfreada e o aumento do despejo de efluentes domésticos e industriais nos corpos d'água (Gleick & Cooley, 2021). As bacias de drenagem representam uma área continental no qual toda água contida nela escoar para o mesmo destino. A manutenção das bacias de drenagem é vista como um fator importante para a conservação dos recursos hídricos. Entretanto, os programas de gestão das bacias de drenagem são complexos por demandar uma união dos objetivos econômicos, sociais e ambientais e demandam apoio político e articulação entre os tomadores de decisão (Santos et al., 2020).

Assim, a conservação dos recursos hídricos exige uma abordagem que seja eficiente na gestão dos recursos naturais nas bacias de drenagem. No Brasil a partir da Política Nacional de Recursos Hídricos, houve a necessidade de uma gestão integrada dos recursos das bacias de drenagem, realizada por meio dos Planos de Bacia Hidrográfica, que são importantes instrumentos de planejamento e funcionam com um procedimento similar aos planos conhecidos por “abordagem da bacia de drenagem” (Cohen & Davidson, 2011; Santos et al., 2020).

A “abordagem da bacia de drenagem” para governança dos recursos hídricos é apontada como uma das mais eficientes - nela são definidas estruturas políticas que usam as bacias de drenagem como unidades de governança (Cohen & Davidson, 2011b). Para isso, os setores públicos e privados são envolvidos em conjunto numa estrutura de manejo ambiental que inclui a definição de áreas geográficas com enfoque em priorizar majoritariamente os problemas hidrológicos levando em consideração os sistemas naturais e socioeconômicos (Gönenc et al., 2007).

Uma forma de realizar essa gestão integralizada é unir também as ferramentas utilizadas de forma interativa, para proporcionar resultados atrativos para os tomadores de decisões, estimulando a colaboração entre a população, setores públicos e privados e, conseqüentemente, aumentando a disseminação de conhecimento, dados e métodos com o intuito do uso sustentável dos recursos hídricos (Gönenc et al., 2007).

A disponibilidade de água potável reflete na economia mundial, tamanha sua relevância para a manutenção da vida. As atividades agrícolas, industriais, urbanas e recreativas dependem de uma fonte segura de água não contaminada, ironicamente, a maior parte das contaminações por elementos traço são oriundas dessas atividades (Chowdhary et al., 2020). O crescimento mundial e o avanço nas tecnologias têm ameaçado as fontes naturais de água potável. De acordo com (Elimelech, 2006), um sexto da população mundial sofre com escassez de água própria pra consumo. A disponibilidade de elementos traço pode ser proveniente de fontes tanto naturais, quanto antropogênicas e podem ser denominadas como pontuais e/ou não pontuais partindo dos rios para os oceanos.

A qualidade das águas fluviais reflete todas as alterações exercidas ao longo da extensão das bacias de drenagem, essas alterações influenciam na qualidade das águas estuarinas e, conseqüentemente, no aumento da exportação de elementos traço para os oceanos. Dessa forma, o uso da terra nas bacias de drenagem (e.g., agricultura, urbanização, industrialização e mineração) altera as propriedades geoquímicas (e.g., elementos dissolvidos, matéria orgânica, complexação) dos elementos traço, podendo levar a algum tipo de contaminação (Das et al., 2009). O escoamento superficial e a deposição seca são fontes importantes de elementos para os ecossistemas aquáticos inseridos nas bacias de drenagem. Em conjunto com a precipitação, esses processos são relevantes no transporte de elementos através do continente para os ecossistemas aquáticos (Li et al., 2009).

Dentre os ecossistemas aquáticos, os estuários agem como o principal elo de transporte de todo o material lixiviado e erodido nas bacias de drenagem para os oceanos, através de mudanças graduais nas propriedades da coluna d'água que criam um ambiente único (Bianchi, 2007; Samanta et al., 2018). Os elementos traço dissolvidos, presentes em estuários poluídos, originam complexos orgânicos e inorgânicos, enquanto que na forma particulada os elementos traço estão contidos, principalmente, adsorvidos nas partículas de argila, coloides e nanopartículas naturais, servindo como principal suporte geoquímico para o transporte de elementos traço (Kretzschmar & Schafer, 2005; Plathe et al., 2013; Tepe & Bau, 2014). Já em estuários não poluídos a maior parte dos

elementos traço estará associada à fração detrítica e pouco móvel das partículas (Salomons & Förstner, 1980).

Em locais de clima quente e úmido, como as regiões tropicais, a erosão dos solos é maximizada devido ao aumento das chuvas (Goudie & Viles, 2012; Macdonald et al., 2019). Nesse contexto, os rios tropicais contribuem de forma relevante com contaminantes para os oceanos, em razão do aumento das condições energéticas que diminuem o tempo de residência das partículas na coluna d'água (Prabakaran et al., 2020; Sultan et al., 2011). A presença de orgânicos dissolvidos torna as águas fluviais mais ácidas, aumentando a erosão e resultando na criação de dissolvidos, particulados e complexos orgânicos contendo contaminantes. (Gaillardet et al., 2014; Oliver et al., 1983; Walther, 1996).

A especiação de alguns elementos traço, como mercúrio, arsênio e chumbo, regula sua destinação e grau de toxicidade para os organismos. Essa especiação é altamente dependente dos parâmetros físico-químicos e biológicos da água, que são controlados de forma natural (*e.g.*, precipitação, geologia local) e de forma antrópica através das interações humanas e suas atividades. Atividades agrícolas são conhecidas por aumentarem as concentrações de nutrientes como fósforo (P) e nitrogênio (N) nos solos e, conseqüentemente, nos corpos d'água adjacentes em decorrência do uso desenfreado de fertilizantes (Kim et al., 2006; Yan et al., 2017). Além disso, atividades agrícolas aceleram o desmatamento local, aumentando a carga de solutos que atingem os rios. As atividades industriais e mineradoras são conhecidas por intensificar a quantidade de elementos traço (como arsênio (As), bário (Ba), cádmio (Cd) e chumbo (Pb)) nos ecossistemas terrestres e aquáticos, através da produção de seus respectivos resíduos (Chen et al., 2019; Yang et al., 2015).

A falta de fiscalização dessas atividades faz com que resíduos sejam despejados de forma incorreta no meio ambiente. Esses resíduos, quando sólidos, aumentam a quantidade de partículas transportadas para os rios e, conseqüentemente, alteram parâmetros como a turbidez, temperatura e a carga de material particulado em suspensão (MPS). A depender da origem desses resíduos, as partículas oriundas podem alterar o pH da água e aumentar a disponibilidade de elementos traço para a biota. A diminuição no valor do pH, ocasiona em uma acidificação da coluna d'água, levando a uma liberação

dos elementos que estão fracamente ligados às partículas, aumentando o potencial desses elementos de se tornarem biodisponíveis (Gäbler, 1997; Riba et al., 2004). O aumento no aporte de partículas ocasiona o assoreamento dos rios, diminuindo sua profundidade e acarretando na diminuição do habitat de organismos dependentes dessa característica. Além disso, o assoreamento dos rios pode levar a formação de locais de deposição e diminuição do fluxo fluvial. Uma das maneiras de resolver esse problema é através da dragagem, que também leva a consequências graves, como a ressuspensão de sedimentos contaminados, e a disponibilização de elementos contaminantes que se encontravam imobilizados nos sedimentos para a coluna d'água (Ip et al., 2007; Jia et al., 2021; Machado et al., 2016).

Os elementos traço são transportados majoritariamente ligados ao MPS, quer seja associado aos minerais na fração detrítica ou ainda através de processos como floculação, adsorção e/ou complexação (Fan et al., 2021; Sinclair et al., 1989). As partículas em suspensão podem ser divididas em quatro componentes que controlam suas composições: i) a composição litogênica que é formada pelo material inorgânico originado da erosão dos minerais que compõem a geologia local (e.g., quartzo, feldspatos e minerais silicatos); ii) o componente hidrogenado, proveniente dos processos químicos que ocorrem ligados ao material de origem mineral ou materiais em fases discretas (e.g., óxidos de Fe e Mn, carbonatos, sulfetos e agregados húmicos); iii) o componente biológico o qual é originado por processos locais ou externos realizados por microorganismos, plânctons, restos orgânicos, matéria fecal e restos de origem vegetal, esse componente também tem origem bioquímica oriundos das proteínas, carboidratos, lipídios e pigmentos; iv) o componente antrópico, esse abrange os efluentes domésticos e industriais, plásticos, solventes, surfactantes, rejeitos minerais, entre outros. Esse componente pode se originar como partículas discretas, ou em fases líquidas não aquosas aderidas na matriz particular (Fettweis & Lee, 2017; Ho et al., 2022; Turner & Millward, 2002).

No ecossistema aquático, existem dois tipos em geral de partículas: as entidades biogênicas, formadas por organismos (e.g., plânctons, bactérias e invertebrados), que são partículas que fornecem a principal fonte alimentar dos organismos em suspensão, são de baixa mobilidade e sua densidade é próxima à da água, o que faz com que sua

abundância e distribuição seja controlada pela produtividade primária e com a sazonalidade local; e os sedimentos em suspensão, formadas por um agregado complexo de materiais minerais, biológicos e antrópicos, com densidade maior que a da água e essas partículas estão sujeitas aos ciclos constantes de deposição e ressuspensão. Essas partículas propiciam uma linha relevante e regular de químicos entre a fase líquida, de suspensão e deposição (Bibi et al., 2021; Hecky & Kilham, 1988; Turner & Millward, 2002).

Sendo assim, a reatividade das partículas é dependente das fases e organismos a que estão submetidas (e.g., filme orgânico, microrganismos e material das fases hidrogênica e biológica). Dentre as partículas, os óxidos de Fe e Mn apresentam reatividade a íons inorgânicos, ocasionado pela grande área superficial e sítios reativos de hidroxila. Já a matéria orgânica, é um eficiente solvente para os componentes químicos orgânicos hidrofóbicos. Por último, os microrganismos são ferramentas importantes na especiação e disponibilidade dos elementos traço adsorvidos às partículas, devido ao controle que exercem na quebra da matéria orgânica particulada e também na sua habilidade em catalisar as reações redox (Perret et al., 2000; Turner & Millward, 2002).

Um fator determinante para o tempo de residência e as características de deposição das partículas são suas propriedades físicas, propriedades que também determinam os impactos das mesmas nos ciclos biológicos e químicos. As interações ocorridas entre as partículas em suspensão e os constituintes químicos resultam de vários processos, como: físico-químicos e biológicos. Dentre os quais estão a agregação coloidal, troca iônica, adsorção-dessorção, absorção, precipitação-dissolução, ligação hidrofóbica, atividade microbiológica e degradação da matéria orgânica particulada (Mosley & Liss, 2020; Turner & Millward, 2002).

Existem vários processos que controlam as concentrações e mobilidade dos elementos traço nos ecossistemas aquáticos, os principais envolvem a oxidação, redução, sulfato-redução, alcalinos e sorção (G. Lee et al., 2002; M. K. Lee & Saunders, 2003; Upping et al., 1986). Os processos de sorção, mais comuns em solos e sedimentos, são a adsorção, quimissorção e a troca iônica (Almeida et al., 2018; S. Lee et al., 2019). Quando há adsorção física, as ligações que acontecem nas superfícies das partículas

são de Van Der Waals, que conhecidamente são ligações relativamente fracas. A adsorção química ocorre com as associações entre íons e/ou moléculas em suspensão e a superfície das partículas. A troca iônica se inclui nesse tipo, e ocorre quando as cargas presentes na estrutura mineral (e.g., positivas ou negativas) são neutralizadas por íons de cargas opostas. Os íons presentes nas camadas internas das estruturas minerais são então trocados por íons presentes no meio (Salomons & Förstner, 1984).

Os parâmetros físico-químicos, além dos processos físicos, controlam os processos de remoção e liberação de contaminantes relativos às partículas em suspensão (Turner & Millward, 2002; Violante et al., 2010). A variação do pH influencia as interações entre as partículas sólidas e os complexos orgânicos metálicos, a especiação e também altera as características superficiais das partículas (Eg. carga das superfícies e o potencial) (Salomons & Förstner, 1984; Shimizu et al., 1992). As partículas em suspensão são então a forma majoritária de transporte de elementos nos ecossistemas aquáticos.

A floculação é um dos processos mais importantes que acontecem nos estuários. Esse processo controla a modificação dos elementos traço da fase dissolvida para a particulada (Boyle et al., 1977; Manning et al., 2010; Thill et al., 2001). Assim, a floculação altera o balanço de massas químico entre os rios e oceanos (Millward, 1995). A floculação é diretamente afetada por parâmetros como estabilidade coloidal, condutividade elétrica, pH, carbono orgânico dissolvido, oxigênio dissolvido, salinidade, ácidos húmicos e características superficiais os quais influenciam diretamente nas características físicas das partículas como, velocidade, densidade, área superficial e taxa de deposição (Salomons & Förstner, 1984). Durante a mistura estuarina, uma parte dos elementos presentes na fração dissolvida passa para a fase particulada (Karbassi & Ayaz, 2007; Sholkovitz, 1976; Thill et al., 2001).

Existem vários tipos ferramentas usados no estudo dos ecossistemas aquáticos, a depender do objetivo do estudo em questão. Pougnet et al., (2022), usou o cálculo de balanço de massas e outras ferramentas para estudar o transporte e retenção de Cd através da transição continente/oceano do estuário de Gironde na França. Os autores usaram dados de Cd dissolvido e particulado disponíveis desde de 1990, para afirmar que as médias dos fluxos anuais desse elemento se comparam às estimativas globais

feitas anteriormente, através de sensoriamento remoto e estudos de sedimentação, e que desde os anos 2000, o estuário de Gironde encontra-se em um equilíbrio sedimentar. No estuário de Gironde o teor de Cd biodisponível vem decaindo ao longo dos anos. Contudo, os sedimentos locais funcionam tanto como fontes, quanto como sumidouros desse elemento para a coluna d'água, dependendo da quantidade de Cd fornecida pela bacia de drenagem. Além disso, os autores também observaram que os fluxos de Cd particulado representam aproximadamente 20% do total dos fluxos desse elemento.

Rani et al., (2021) usou técnicas de interpolação (Krigagem Ordinária) e estatísticas multivariadas (PCA e Análise de Cluster) para inferir acerca das contaminações de elementos traço existentes na região costeira de Bangladesh, Índia. Os autores observaram concentrações acima das permitidas pela legislação local (Cr, Pb, As e Zn); provavelmente, ocasionadas pelas atividades antrópicas exercidas em cada local de coleta, e recomendaram um monitoramento constante dessas concentrações. González-Ortegón et al., (2019) estudaram a composição elementar na bacia do Golfo de Cádiz, Espanha, utilizando técnicas de cálculo de balanço de massas e análises estatísticas (regressão linear e correlação de Pearson), além de análises de interpolação. Essa região possui evidente histórico de impactos provocados pela mineração e atividades agrícolas ali presentes. Através desse estudo, com o uso dos fluxos dissolvidos e as outras ferramentas, o autor constatou contribuições relevantes de elementos traço fluviais para o Mar Mediterrâneo.

Nos últimos anos ferramentas de inteligência artificial vêm sendo muito utilizadas para o estudo de parâmetros ambientais (pH, alcalinidade, vazão, condutividade e MPS), concentrações de contaminantes, nutrientes (DOC, TN) e etc. Essas ferramentas apresentam um poder grande na avaliação ambiental, por utilizarem anos de dados já produzidos de anos anteriores (Guillou & Chapalain, 2021; Kang et al., 2020). Uma dessas ferramentas são as redes neurais artificiais que modelam sistemas complexos e incertos. A vantagem dessas ferramentas é que elas não precisam de modelos anteriores, elas são “treinadas” utilizando os próprios dados (Guillou & Chapalain, 2021; Kang et al., 2020; Yaseen, 2021). Além disso, essas ferramentas levam em consideração a sazonalidade local ao fazer as inferências (Guillou & Chapalain, 2021; Kang et al., 2020; Yaseen, 2021).

Dentro dessa perspectiva, o objetivo geral dessa tese foi o de avaliar os fluxos de elementos em duas bacias de drenagem brasileiras. Com esse propósito, a tese foi dividida em três capítulos, apresentados no formato de artigos científicos.

O primeiro capítulo teve como objetivo estimar os fluxos dissolvidos de As e Pb na bacia do rio Doce, MG; com a criação de um banco de dados contendo todas as informações encontradas em trabalhos publicados nos últimos anos e por fim inferir sobre as variações sazonais e a relação das concentrações de ambos os elementos e os parâmetros ambientais coletados nesses trabalhos. A hipótese desse capítulo foi que (I) a bacia do rio Doce, MG é fortemente impactada pelas atividades antrópicas exercidas na região, principalmente a mineração, que promove um incremento nas concentrações de elementos traço e pela variação sazonal da região. Esse último fator gera uma maior dispersão dos elementos ao longo de toda bacia durante os meses de maior pluviosidade, promovendo contaminações em regiões onde não há a presença de atividades com potencial poluidor.

O capítulo dois objetivou a utilização dos dados hidrológicos (vazão e precipitação) do estuário de Serinhaém, BA, com o intuito de comparar os métodos de inteligência artificial (ARIMA, SARIMA e ANN) para inferir acerca da eficiência de cada método para a predição dos valores de vazão dessa região, além de comparar duas divisões de subset, com o intuito de compreender se ocorre uma melhora no desempenho dos modelos. A principal hipótese desse capítulo foi de que o método de rede neural seria o mais eficiente para prever a vazão da região de estudo, como já foi observado em outros trabalhos que utilizaram os mesmos métodos (Wagena et al., 2020).

O capítulo três teve como objetivo o estudo do fluxo dissolvido e particulado de elementos traço no Estuário de Serinhaém, BA com o intuito de avaliar o impacto das atividades existentes dentro da APA do Pratigi, BA. A principal hipótese desse capítulo (III) era de que os anos de atividades antrópicas presentes na região como, a pecuária e a agricultura, realizadas na bacia de drenagem dos rios que desembocam no estuário, além das diferenças causadas pelas estações de seca e de chuva, promovem uma contaminação ambiental difusa no estuário do rio Serinhaém, BA.

CAPÍTULO 1

**Seasonal variation, environmental parameters and their importance for
the control of As and Pb concentrations: A case study**

Abstract

The Doce River Basin suffers from mining and its consequences, in addition to being a very urbanized region with many industries. In this review we have built a database with information about As and Pb Doce River contamination found in the literature, with the objective of observing how the flows of both elements occur in the entire extension of the basin, how they behaved along the seasonal variations, and which parameters control their concentrations. For this, statistical techniques were performed, such as interpolations of flows through the rivers of the basin, ANOVA to differentiate these flows during the different seasonal seasons and multivariate statistics (regression and PCR) to infer about the controlling parameters of the concentrations of both elements. As and Pb fluxes showed a clear seasonal difference, with the highest fluxes found in the wettest season, related to soil leaching, rock erosion and sediment resuspension. An important change that took place in the Doce River Basin was caused by the accident that occurred in 2015, with the rupture of the Fundão dam, which stored iron mining tailings. This fact increased both the fluxes of the elements, their concentrations present in the basin and promoted a greater export of As and Pb to the Atlantic Ocean. The concentrations of both elements are much more related to the presence of iron and manganese oxides and hydroxides, and the presence of sulfates, than to precipitation. Because this region presents a great mineral wealth, and is very much used, it is necessary to have constant monitoring programs, so that accidents like the one in 2015, which generates consequences until today, are avoided. Furthermore, it was observed that the Doce River presents a great potential for exporting contaminants in general to the Atlantic Ocean, becoming a source of pollution for other ecosystems.

Keywords: Doce River Basin; Drainage basin; River flow; Anthropic activities; Arsenic, Lead

1. Introduction

The water quality of rivers and their physical-chemical and biological characteristics are controlled by processes that occur in the drainage basin, such as dams, anthropic emissions and unrestrained urbanization, promoting increase

in the transport of trace elements by surface and underground runoff (Chang, 2008; Valle Junior et al., 2015). These trace elements are originated, in most cases, by the dissolution of rocks through natural weathering in the drainage basin (Gardes et al., 2020; Siwek et al., 2009).

An important parameter that acts in the regulation of the dissolved element concentrations is precipitation, which acts directly on the erosion and leaking of minerals from rocks and hence the release and transport elements contained in these rocks into rivers (Heinen De Carlo and Anthony, 2002; Rumsey et al., 2017; Wu et al., 2018). Besides acting on the erosion process, the precipitation is responsible for the transport of chemical elements in aerosol form to the continent through the wet deposition (Khatri and Tyagi, 2015; Négrel and Roy, 1998; Rastegari Mehr et al., 2019).

The changes in the concentrations of trace elements are given by variations in physical-chemical and biological parameters, in addition to anthropogenic inputs. The solubility of the trace elements is related to parameters such as pH, temperature and redox potential. Decreases in pH may lead to the release of elements that are adsorbed onto surfaces of the particles (Hong et al., 2011; Tipping, 1984). The decrease in pH can also result in a dissolution of the metal-carbonate complexes, causing release of metal ions into the water column (Papafilippaki et al., 2008).

The redox processes (oxidation and reduction) are known for their importance in the composition and chemical reactivity of the elements, by influencing chemical speciation, mobility, availability and biogeochemical cycles, in addition to altering their toxicity and the behavior of sulfates and oxy-hydroxides of Fe and Mn (Borch et al., 2010; Lee et al., 2019; Violante et al., 2010). In anoxia conditions, the redox potential presents low values, leading to changes in the composition of the metal complexes and, consequently, releasing ions into the water column (Iwashita and Shimamura, 2003; Papafilippaki et al., 2008; Shiller, 1997).

Changes in water temperature directly affect aquatic metabolism, leading to changes in photosynthetic rate, in the growth of aquatic organisms, microbial activity, in oxygen solubility and also make organisms more sensitive to diseases,

parasites and contaminants. In situations of high temperatures, there is an increase in the speed of growth and death of plants, resulting in a higher content of organic matter to be decomposed and there is a consequent release of trace elements to the water column (Huang et al., 2017; Iwashita and Shimamura, 2003).

The river flows affect the concentration of trace elements in aquatic environments by seasonal variation (Iwashita and Shimamura, 2003; Neal et al., 2000; Olías et al., 2004). When surface runoff occurs, the pH tends to increase and the concentrations of sulphates and trace elements decrease. On the other hand, in dry season runoff decreases and the concentrations of trace elements return to the values observed before the dilution, reaching maximum values due to the oxidation of sulfides through the increase in the activity of bacteria. In these conditions the concentrations of elements are affected due to evaporation (Olías et al., 2004).

The transport and concentration of trace elements in drainage basins are regulated by a combination of natural factors (rainfall, physical-chemical interactions and erosion) and anthropogenic factors (burning of fossil fuels, urban and industrial effluents) (Dean et al., 2005; Germer et al., 2009; Mouri et al., 2011). The combination of these factors is known to be an important agent in the regulation of the quality of river waters and also to govern the seasonal variation of the concentrations of the elements found in several studies carried out in drainage basins (Huang et al., 2014; Kerr et al., 2008).

The river flow of dissolved trace elements suffers strong contribution of the elements from the runoff of drainage basins and is one of the main processes in the global cycle of these elements (Dowling et al., 2003). The flow can be used to assist in the planning of environmental protection policies within the drainage basins so that there is a sustainable use of the area. However, estimating the flow of trace elements from drainage basins to the oceans is a costly and complex process, due to the large sampling effort and the size of most of the basins (Chichakly et al., 2013; Costanza et al., 2002; Lu et al., 2020).

Drainage basins are commonly defined by topographically delimited areas in which all the water that falls migrates towards a river. This water has chemical

changes in its composition resulting from the path taken to the rivers. Therefore, it can be said that drainage basins act as complex biogeochemical reactors and, consequently, are important in controlling the cycling of the elements (Lane et al., 2018). The Doce River Basin has been impacted since the end of the 17th century by different anthropic activities (e.g., mining, industry and agriculture) and has suffered over the years with the consequences by these processes, such as the dumping of waste, the degradation of soils adjacent to rivers and the removal of riparian forest (ANA, 2013; Oliveira and Quaresma, 2017a; Rhodes, 2010).

The higher concentrations of trace elements in the basin have been observed in the last years by several studies and the release of elements is directly associated with the dumping of tailings from mining activity and by industrial activities (Oliveira, 2016; Silva et al., 2018; Varejão et al., 2011). The aims of this study are to (1) analyze the seasonal variation of As and Pb along the basin, (2) assess the processes involving in the release of As and Pb in the Doce River Basin, (3) estimate the mass balance of those two elements and their exportation to the Atlantic Ocean and (4) analyze the changes caused by the accident with the Fundão dam in 2015 in the concentrations of As and Pb.

2. Data processing and analysis

2.1 Study Area

The Doce River Basin is located in the Southeast region Brazil, in the states of Minas Gerais and Espírito Santo (19° 38 ' to 19° 45 ' S, 39° 45 ' to 39° 55 ' W) and has a drainage area of 86.715 km² (**Figure 1**). According to Köppen's climatological classification, the predominant climates in the basin are Aw—tropical monsoon zone and Cwa—humid subtropical zone, which is characterized by a dry winter and hot summer, and Cwb – humid subtropical zone, which is characterized by a dry winter and temperate summer (Alvares et al., 2013), with average annual precipitation around 1200 mm (Lima et al., 2019). The average annual temperature ranges from 24°C to 26°C and the average annual rainfall is around 145 mm (Bernardino et al., 2019).

The Doce River is formed by the meeting of the waters of the Piranga and Carmo rivers, whose springs are located on the slopes of the mountains of Mantiqueira and Espinhaço, with altitudes reaching around 1,200 m. The Doce

River has a length of 853 km and its main tributaries are: the left bank of the Piracicaba, Santo Antonio and Suaçuí Grande, in Minas Gerais, Pancas and São José, in Espírito Santo; on the right bank of the Casca, Matipó, Caratinga-Cuieté and Manhuaçu Rivers, in Minas Gerais, and Guandu, in Espírito Santo (Euclides, 2021).

The Doce River basin is subdivided into 6 administrative planning and management units, to facilitate the management of local water resources, called Water Resources Management Units (UGRHs). The units are known as, to UGRH1 Piranga, UGRH2 Piracicaba, UGRH3 Santo Antônio, UGRH4 Suaçuí, UGRH5 Caratinga, and UGRH6 Manhuaçu (ANA, 2013). In order to facilitate, the part of the Rio Doce located in Espírito Santo was named ES01 (**Figure 1**).

2.2 Database used

Bibliographic searches were carried out in three databases, *Google Scholar*, *Science Direct* and *Web of Science*, using the keywords: "Metals", "Doce River Basin" and "Brazil". A total of 31 articles were found, 5 reports from Mining Institute of Water Management (IGAM), 4 reports from the Renova Foundation (ES) and 4 reports from Mineral Resources Research Company (CPRM), in addition to an Excel file from the database data, 3 monographs, 22 dissertations and 7 theses (**Supplementary Figure S1**). The information extracted from these documents were: concentrations of As and Pb in the dissolved fraction of the water, from studies that used cellulose acetate filters with 0.45 μm porosity, geographical coordinates and date of collection. Subsequently, information was extracted from the *Hydro* software of the National Water Agency (ANA), used to extract the flow and rainfall values for each point. The rain gauges and fluviometers closest to the sampled points were selected, with the help of Google Earth and using the map of the ANA at the link:

<http://www.snirh.gov.br/hidroweb/mapa>.

2.2.1 Analysis methods used

Information from 28 pluviometric stations was used to calculate average rainfall and 31 fluviometric stations to extract the flow data used in the flow calculations (**Supplementary Table S1**). The coordinates found in maps were extracted using the *MapInfo* software and the concentrations entered in graphs

extracted with the aid of the *WebDigitalizer* software. To carry out the calculation of the average rainfall in the catchment area of each subregion of the Doce River Basin, the Thiessen polygon (Voronoi diagram) method was used. To avoid overestimation in rainfall, 4 stations were used in each subregion.

2.2.2 Average rainfall

The method of the Thiessen polygon uses the rainfall observed in the available rain gauges and assigns a weight to each available station according to the area of influence exerted. Then polygons are drawn defining the area of influence of the rain gauge in relation to the basin, thus, the average precipitation is calculated by weighting the values obtained at each station and their areas of influence (da Paz, 2004; Pruski et al., 2004). Average rainfall can be expressed by:

Where:
$$P_m = \frac{\sum_{i=1}^n (P_i A_i)}{\sum_{i=1}^n A_i}$$

P_m - average rainfall in the basin (mm);

P_i - rainfall in each season (mm);

A_i - area of influence of P_i (km²);

n - number of rain gauges considered.

2.2.3 Flow estimation

The concentrations of As and Pb were organized by year in *Excel* together with the geographic coordinates, flow rate of the nearest point and sampling date. Subsequently, the flows of As and Pb in the water were calculated using the following formula:

Where: $F = [M] \times V \text{ (mg} \cdot \text{s}^{-1}\text{)}$

M - Element concentration (mg L);

V – River Flow (m³ s).

2.2.4 Preparation of geochemical maps

Interpolation maps were made to estimate the points close to those sampled and to facilitate the visualization of data over the years studied (2009 to 2019). The maps were made using interpolation methods according to the interpolation premises (mean and standard deviation within normality). The Kriging method was used when the data needed to be adjusted in order to attend the premises, being transformed to a logarithmic scale. When there was no need to adjust the data, the maps were made using IDW (Inverse Distance Weighting) (Ahrens, 1954; Albanese et al., 2007; Bai et al., 2010; Yamamoto and Landim, 2013). The data were evaluated using semiovariograms, histograms and normality graphs, using the *ArcGis*® 10.5 software.

2.3 Statistical analyses

Statistical analyzes were performed using R software (R Core Team, 2020). To differentiate seasonality and spatial heterogeneity, ANOVA tests were performed (aov function, base package, [R Core Team 2020](#)), followed by the Tukey test. The transformations were indicated in the figure's legends. For the purpose of analyze the relationship between flow and precipitation with As and Pb concentrations, linear regressions were made to investigate whether these parameters influenced the concentrations of these elements. In addition, principal component analyzes (PCA) were performed to ascertain the associations between the elements and the environmental parameters (Kassambara, Alboukadel Mundt, 2020; Lê and J & Husson, 2008). To handle missing values were used the function *imputePCA* of the package *missMDA* in the software R (Josse and Husson, 2016). The data used in the general linear models were transformed, when necessary, in order to achieve the assumptions of the models (linearity, normality and homoscedasticity of the residues) through the maximum likelihood function (boxcox function, MASS package, (Venables and Ripley, 2002). error assumed a priori was type 1 (α), 0.05 for the hypothesis in all tests.

3. Results and Discussion

3.1 – Seasonal variation of As an Pb along the Doce River Basin

In general, the flows of As and Pb were higher in the rainy season, except in 2010, probably relatedly to a historical drought that happens between August

to October of this year (**Figures 2 and 3**) (Climanálise, 2010) . Since 2015, environmental contamination by toxic elements was associated with the accident with the Fundão dam, which caused a disturbance in the sedimentary compartment of rivers, already known to have high concentrations of As and Pb derived from the historical mining and presence industrial and agricultural activities (Maia, 2017; Reis, 2020; Renova, 2017). Much of the mud tailings from the accident was retained in the drainage basin soils and whenever there is a precipitation event, there is leaching of these soils. This process makes available elements contained in this tailings mud to the adjacent rivers (Mahiques et al., 2016; Queiroz et al., 2018; Renova, 2018a).

Only the years of 2012, 2015, 2016 and 2018 showed statistical difference for both elements. From 2015 there is an increase in the numbers of surveys carried out in the region due to the accident with the Fundão dam (**Figures 2 and 3**). According to the study of (Oliveira and Quaresma, 2017), the year of 2012 exhibit a higher streamflow when compared with others years (2011 and 2013), which could explain the statistical differences observed. In both seasons, Pb concentrations were higher in the HPP Risoleta Neves dam, explained by the fact that dams are preferred areas of sedimentation and known to alter the flow of sediments, in addition to concentrating elements by deposition (Gao et al., 2018; Guo et al., 2020; Queiroz, 2017).

The chemical analysis of the waters of the Piranga River (DO1) indicated lower concentrations of the elements analyzed in dry season, being attributed to the seasonal differences found such as the association of rainfall with the supply of elements to the river water. However, Goulart, (2008) found higher values of As and Pb in sediments in the dry season, showing that precipitation is not the only mechanism responsible for releasing elements associated with sediments in this region. This release may be related to local characteristics, such as point sources of contamination and the reduction of the river's dilution (Bancon-Montigny et al., 2019; Oliveira and Quaresma, 2017b). In addition, the DO1 region has the presence of hydroelectric power plants, responsible for the river dam (ANA, 2013).

The report by the Renova Foundation of May 2017 confirms the results found **Figures 2 and 3**. In which, in most years, the concentrations of As and Pb

were higher in the rainy season, showing the increase in transport of trace elements, the presence of non-point sources, thus demonstrating a drop in water quality in this season, caused by the resuspension of sediments and by greater runoff. Additionally, according to this report, the deterioration in the water quality of the Doce River is not only caused by the rupture of the Fundão dam, but also by the influence of seasonal factors observed in the basin, such as the flow (Renova, 2017).

3.2 - Controlling parameters of As and Pb concentrations in the Doce River Basin

Based on the knowledge that precipitation and river flow control erosion and others process driving the removal or release of elements, it was hypothesized whether there was a relationship between the concentrations of As and Pb in the drainage basin of the Doce River with precipitation and river flow (**Supplementary Figures S2 and S3**). There were no influences of precipitation and river discharge on As concentrations in the Doce River Basin, based on the low R^2 found in the models ($R^2 = 0.025$, $p = 0.00019$, $R^2 = 0.045$, $p = 5e^{-07}$, respectively) (**Supplementary Figure S2**). Probably the concentrations found in this basin are linked directly to the Fe and Au mining activities as previously discussed, besides As concentration relies mostly on the local geochemical conditions as the presence of iron hydroxides (Battistel et al., 2021; Smedley and Kinniburgh, 2002). These results are different from those found by [Sankar et al., \(2019\)](#), who observed an increase in As concentrations with increasing precipitation.

Analyzing the relationship between Pb concentrations with discharge and rainfall, it was observed that there is a small influence caused by both parameters on the concentrations of this element ($R^2 = 0.13$, $p = 3e^{-16}$ and $R^2 = 0.23$, $p < 2, 2e^{-16}$) (**Supplementary Figure S2**). Concentrations of Pb usually are related to domestic and/or industrial waste, in addition to, the use of fungicides and pesticides in agricultural areas (Islam et al., 2020; Mil-Homens et al., 2013). Moodley et al., (2016), when analyzing three hydrographic basins, observed a clear relationship between precipitation and river discharge with increasing concentrations of elements in the water column.

Elements immobilized in the sedimentary compartment can be remobilized to the water column through various processes. Change in ionic composition with decreased pH leads to ionic exchange processes in the sediment grains, where electrostatic forces are weak and in elements co-precipitated with carbonates (Kim et al., 2020; Marin et al., 1997). The discharge of urban-industrial effluents can also result in the release of elements, as a result of changes in physical-chemical parameters (Kim et al., 2018). Elements linked to oxide-hydroxides of Fe and Mn undergo remobilization when the environment becomes more reducing (Shaike et al., 2014). Finally, environments where physical resuspension of sediments occurs by dredging, heavy rains and winds, there is also the remobilization of elements present in the sedimentary compartment to the water column (Morgan et al., 2012).

When dealing with multivariate data, the PCA is very important as it helps to reduce the size of data and simplify the understanding of the factors that control them (Kumar et al., 2019; Shil and Singh, 2019; Wang et al., 2017). For PCA to be performed, two tests must be performed, the Kaiser-Meyer-Olkin Sampling Adequacy Measure (KMO) and the Bartlett Sphericity Test. The objective of both is to understand if the count variable and the sample size allow the application of PCA or not. If the sphericity test shows high significance, it indicates that at least one correlation between the variables is significant. The recommended value for the KMO test is greater than 0.50. The values found in both tests are shown in **Table 1**.

The data matrix used in the PCA of As from 2009 to 2014 (1) was composed of 18 variables and 112 observations, while the data matrix of As from 2015 to 2019 (2) was composed of 18 variables and 440 observations. The size of the Pb data matrix from 2009 to 2014 (3) was 18 variables and 146 observations, whereas the PCA composed of the Pb from 2015 to 2019 (4) had 18 variables and 324 observations. In this study, only the first three principal components (PCs) were considered to describe 56.26% of the total variance of data in PCA 1 and 64.79% of the total variance of data in PCA 2. For PCA's referring to Pb, they were also considered the first three PCs to describe 57.22% of the total variation of data in PCA 3 and 62.70% of the total variation of data in PCA 4 (**Supplementary Table S2**).

In PCA 1 28.65% of the total data variance was explained by PC1, 17.25% by PC2 and 10.36% by PC3. In PCA 2 41.8% of the total variation of the data was explained by PC1, 16.90 by PC2 and 6.08 by PC3. In PCA 3 31.12% of the data was explained by PC1, 16.08 by PC2 and 10.03 by PC3. In PCA 4 37.53% of the total data variation was explained by PC1, 18.49 by PC2 and 6.68 by PC3. In this study, only the first two PCs of each PCA were explained. PCA 1 considered the first two PCs whose data variance was 45.90% and in PCA 2 the data variance analyzed on the first two PCs was 58.71%. PCA's 3 and 4 showed variances in the first two PCs of 47.20% and 56.03%, respectively.

The PCA 1 performed between the As concentrations and the parameters found in the various studies used in this review showed a relationship between the As concentrations and Mn ($r^2 = 0.26$, $p = 5.61e^{-03}$). The association of As with Mn is related to Mn oxides and hydroxides, which have strong attraction for trace elements and are known to promote the removal of ions from the dissolved fraction of the water column (Lafferty et al., 2011) (**Figure 4**). This association is reported on several studies as responsible for element immobilization on sediments, however, episodes of sediment resuspension, changes in pH and the action of bacteria can mobilize these elements to the water column (Du Laing et al., 2009; Salomons et al., 1987). Mn oxides and hydroxides have a negatively charged surface and large surface area, which increases the affinity for metals (Hem, 1978; Lee et al., 2002; Sánchez-España and Yusta, 2019; Xu et al., 2013). In addition, As showed a strong relationship with the flux ($r^2 = 0.52$, $p = 3.32e^{-09}$), which is probably related to the greater transport of this element when there is a higher flux.

PCA 2 exhibited an association of As with sulphates (SO_4^{2-}), DO, Fe and Mn ($r^2 = 0.60$, $p = 4.44e^{-16}$; $r^2 = -0.52$, $p = 4.44e^{-16}$; $r^2 = 0.51$, $p = 8.88e^{-16}$) (**Figure 4**). The observed association is related to the processes of Fe and Mn oxide/hydroxyl formation, As(III) oxidation and redox reactions (Gorny et al., 2015). Under redox conditions, the oxyanions of As tend to experience an increase in mobility, especially in reducing conditions, and become a relevant environmental problem (Du Laing et al., 2009). Thus, the main controlling factors of As speciation in aquatic environments are pH and redox potential. Studies report that reducing acidic conditions favor the precipitation of some minerals and

co-precipitation of minerals containing As, and in situations where reduced sulfur concentration occurs, the dissolved arsenic sulfide species can be significant. Therefore, it is not expected that there will be high concentrations of As in places where there are concentrations of free sulfides (Moore et al., 1988; Smedley and Kinniburgh, 2002). Although redox conditions are determinant in speciation of As, these processes occur slowly. Thus, many times the two forms are found in aquatic ecosystems occurring together, As (III) and As (V) in oxidizing conditions or reducing (Masscheleyn et al., 1991). The coexistence of the two As species affects its effect and behavior (Sarkar et al., 2008).

In PCA 3 Pb exhibited an association with Prec, Total Dissolved Solids (TDS), Fe, pH e Mg^{+2} ($r^2 = 0.41$, $p = 3.69e^{-07}$; $r^2 = 0.27$, $p = 9.16e^{-04}$; $r^2 = 0.27$, $p = 1.05e^{-03}$; $r^2 = -0.30$, $p = 2.27e^{-04}$; $r^2 = -0.31$, $p = 1.06e^{-04}$, respectively) (**Figure 5**). Studies show that Pb has a strong association with the solid phase, and has a low solubility in waters in pH above 8.0, furthermore, Pb has a tendency to form stable complexes with organic matter (Bubb et al., 1991; Guéguen et al., 2011). Pb association with iron may be related to the formation of iron oxides and hydroxides (Schaidler et al., 2014). The positive correlation between Pb and rainfall can be explained by the transport of this element by rain from non-point sources of contamination, as the leaching of agricultural soils. PCA 4 shows an association between Pb, pH, Precipitation (Prec) and Mg^{+2} , as seen before ($r^2 = -0.36$, $p = 2.44e^{-11}$; $r^2 = 0.27$, $p = 8.09e^{-07}$; $r^2 = 0.11$, $p = 4.60e^{-02}$), and also with alkalinity, Cl^- and K ($r^2 = -0.33$, $p = 7.35e^{-10}$; $r^2 = 0.19$, $p = 4.72e^{-04}$; $r^2 = 0.38$, $p = 2.29e^{-12}$) (**Figure 5**). The fact that Pb maintains the same associations before and after the Samarco's accident shows that the sources of this element have not changed and are related to the release of sewage (Cheung et al., 2003), industrial effluents (Nyamangara et al., 2008) and even natural sources (Karar and Gupta, 2007), which were not directly impacted by the tailings plume.

3.3 – As and Pb Fluxes along the Doce River Basin and export to the Atlantic Ocean

In the years before the accident, As concentrations were attributed to natural sources (geological and soil leaching) and to the processing of Au, which contributed to its availability in the environment (Nascimento et al., 2018; Neto et al., 2016; Rhodes, 2010) (**Figure 6**). It is evident from **Figure 6** that the largest

As fluxes were found in the mining-related subregions of the Rio Doce basin (DO1 and DO2). The years 2012 and 2013 show a small dispersion of the flows of both elements. This can be explained by hydrological factors that occurred in these two years. In 2012, the flow of the Doce River was higher than in 2013, in contrast to 2013, which had higher rainfall (Oliveira and Quaresma, 2017c). These two hydrological factors contribute to soil leaching and As transport. From 2015, with the Fundão accident, the As flows showed higher values close to the estuary in Regência, ES, probably related to the passage of tailings mud, which transported many contaminants towards the Atlantic Ocean (Hatje et al., 2017).

In order to assess the impacts resulted by the accident with the Fundão dam, Hatje (2017) analyzed sediment and water samples from the Doce River Basin. The concentrations of As observed by the author at points not impacted by the tailings, show the contamination that occurred in these areas, which are directly related to the years of gold mining carried out in the DO1 region (Figure 1). The concentrations of elements found in the portion of the basin affected by the accident show contamination directly associated with what happened. However, the patterns observed in the study in question demonstrate the contribution exerted by the anthropic activities present in the basin (e.g., dumping of domestic and industrial effluents and agricultural activities) corroborating with past studies (Costa et al., 2015; Queiroz, 2017).

The concentrations of Pb were related to the steel industries present in the Doce River Basin and agricultural activities through the use of fertilizers and insecticides in the years of 2009, 2011 and 2014 (IGAM, 2009) (Figure 7). However, Pb concentrations already gone associated with mining activities due to the high positive correlation found between iron (Fe) and Pb (Rodrigues et al., 2015). In addition, Pb can be found in calcophilic minerals related to gold mining, may also be responsible for the presence of this element in aquatic ecosystems (Costa et al., 2003; Hatje et al., 2017). In 2010 Pb fluxes showed higher values near the estuary in Regência, ES. There was a drought that year during the months of August and October, this fact probably led to the opening of the floodgates of the hydroelectric plants along the Doce River, thus increasing the transport of this element towards the Atlantic Ocean. Figure 7 shows a concentration of Pb fluxes in the same region observed in Figure 6 for As, in

addition to the hydrological factors discussed above, this is a region that has the presence of many hydroelectric plants and the water dams in these regions, causes the concentration of elements (ANA, 2013). After 2015 the Pb fluxes exhibited the expected behavior, with higher flows being observed near the estuary in Regência, ES.

One of the consequences of the Samarco's accident was the release of a large amount of Fe in the basin (Viana et al., 2020). The increase of Fe concentration can lead to an increment in As toxicity leading to a higher risk of contamination by organisms in aquatic ecosystems, especially in environments that are naturally enriched by Fe, as is the case of the rivers present in the Iron Quadrilateral (Sales, 2013). Despite the detectable concentrations of As found in the dissolved fraction in the Doce River Basin, there is no risk of contamination by ingestion of contaminated aquatic organisms due to the low concentrations found in drinking water in areas close to the Au mining area (Bidone et al., 2016). Another risk to increased iron concentrations is the formation of oxides and hydroxides, which are known to remove trace elements from the water column. This may have increased Pb transport along the Rio Doce towards the Atlantic Ocean (Ram et al., 2021).

Along the Doce River Basin most studies have observed that As concentrations are related to years of gold mining (Costa et al., 2010). Furthermore, there is a high association between clay particles and high concentrations of As. Clay particles are transported in suspension through river and are deposited in the floodplains. The sediments in these areas can therefore exhibit a history of contamination over the years. In these flood areas, As is probably adsorbed to oxide-hydroxides of Fe and clay minerals after the oxidation of arsenopyrite minerals, and can be carried for long distances downstream from the points of contamination (Costa et al., 2010). In addition, clay particles are known to bind to the most varied trace elements, including Pb, transporting them over long distances and/or depositing them in sediments (Ip et al., 2007).

The distribution of total and reactive As in the coastal area of the mouth of the Doce River demonstrated that its contribution comes from continental sediments, indicated by sedimentation rates, attributed to an increase in As concentrations at depths between 120 cm and 40 cm. The concentrations found

at depths above 40 cm showed a decrease, related to the decrease in Au mining in the 19th century. On the other hand, the As concentrations in the first 20 cm of depth were attributed to the mining of Fe in the Doce River Basin in the last 60 years, due to the fact that As is present in sulfides, arsenic sulfides and arsenates, which occur together with rich rocks in Fe ore (Cagnin et al., 2017). High concentrations of As were also found by (Mirlean et al., 2013) in points along the coast of Espírito Santo, showing a exportation of As to the coastal areas and to the Atlantic Ocean.

The Pb concentrations present in sediment cores collected at the mouth of the Doce River, near the city of Linhares, were related to anthropogenic activities occurring in the watershed, related the deepest and oldest part of the sedimentary testimony (Licínio et al., 2015). The concentrations of this element found in the portion of the sediment relative to the time between the years 2008 and 2013 were attributed to the construction of a hydroelectric plant along the course of the Doce River, and may also be related to the discharge of domestic and industrial effluents from the city of Linhares (Licínio et al., 2015).

Studies have investigated the dispersion of the sediment load caused by the tailings mud from the accident with the Fundão dam, from the mouth of the Doce River to the Atlantic Ocean, through satellite images measuring the turbidity of the river water (Magris et al., 2019; Marta-Almeida et al., 2016; Rudorff et al., 2018). Despite the increase in the sediment load from the Doce River after the accident, during 2015 a severe drought in this region had direct influence on the river discharge, decreasing the dispersion of sediments in the Atlantic Ocean (**Supplementary Table S1**) (Jesus et al., 2020). In precipitation events, sediments deposited in the basin are carried to the river, producing a new supply of elements immobilized in that compartment. In addition, winds are an important dispersing agent in the Doce River, especially in spring and summer (Magris et al., 2019b; Marta-Almeida et al., 2016; Rudorff et al., 2018).

The increase in the load and the change in the composition of the sediments after the accident resulted in a change in the flocculation process, modifying the deposition behavior of the particles and increasing their residence time in the water column, making them more prone to dispersion by current and waves through the water column (Grilo et al., 2018). Corroborating the finding of

the presence of As and Pb fluxes along the entire length of the Doce River Basin after 2015 found in this review, which can also cause possible long-term changes in the sediments of the continental shelf.

The impacts generated by the accident caused the contamination of water and sediments in the Doce River Basin, with potential ecological risks for the biota associated with the sediment and for the populations that use this water. According to several authors, due to the large quantity of materials transported along the basin to the Atlantic Ocean, the need to carry out monitoring with greater frequency in the Doce River Basin is reiterated (Bernardino et al., 2019; de Carvalho et al., 2018; Gabriel et al., 2020).

IGAM has been monitoring water quality in the Doce River Basin since 1977 and reports indicate that for the period from 2009 to 2018 there is a relationship between the concentrations of As in the Carmo River (DO1 region) and the mining activities that took place in that area (**Figure 1**). The Pb concentrations shown in the reports have always been attributed to industrial steel and textile effluents, the use of agrochemicals and diffuse loads present throughout the basin. Despite the reports showing the presence of toxic elements in the Doce River Basin, according to IGAM these concentrations were not of concern to the population and local biota as they are within the values recommended by Brazilian legislation (IGAM, 2018, 2015).

However, several studies carried out from 2009 to 2019 cited throughout this review, made in the waters and sediments of the Doce River Basin after the year 2015 show that the concentrations of As and Pb even though linked to these anthropic activities and the local geology must be considered due to the high toxicity presented by these two elements, as well as their possible release, if changes occur in the physical-chemical parameters of the waters (Renova, 2019, 2018b). The monitoring of pH values and redox potential in these regions allows that if occur changes in these parameters, mitigation measures to be carried out and, thus, public health problems related to the ingestion of these elements are avoided. In these areas, there is the discharge of domestic and industrial effluents, whose release in natura can lead to changes in the physical-chemical parameters of the water (Costa et al., 2015).

4. Further considerations and suggestions for future studies

The rainy season presented higher flows of As and Pb along the basin, showing that the rains exert a certain control on the concentrations of elements in the basin, related only to the resuspension of sediments, due to the lack of relationship observed between these parameters. The seasonal variation in the Doce River Basin was already relevant for the increase and transport of elements, after the 2015 accident, this relevance increased due to the retention of a large part of the tailings in the soils of the Doce River Basin, which are carried to the rivers when there are episodes of rain.

Seasonal variations can lead to greater contamination and greater supply of trace elements to the Atlantic Ocean, making it necessary to create monitoring programs that take into account all the characteristics of the basin, including the physical ones. Most studies do not take into account the other factors that affect the availability of elements, such as winds, tides, the construction of hydroelectric plants and rainfall.

The PCA's clearly showed that the concentrations of As and Pb in the Doce River Basin are influenced by the physical-chemical parameters and the presence of other elements in the water column. Knowing that the anthropic activities carried out in this basin alter both the physical-chemical parameters and the availability of elements, it is essential to inspect and monitor these activities, so that future environmental disasters in this region can be avoided.

As and Pb concentrations in the Doce River Basin have always been associated with human activities present in the region, especially mining. The 2015 accident showed this direct relationship between the increase in the concentrations of elements in the region and the activities present in the basin. In regions not affected by the accident, As and Pb concentrations were related to years of mining, whereas concentrations in regions affected by the accident were directly associated with it and also with anthropic activities, like dumping of urban and industrial effluents.

5. Acknowledgements

This study was financed in part by the Coordenação de Aperfeiçoamento de Pessoal de Nível Superior – Brazil (CAPES) – Finance Code 001.

6. Conflict of interest

The authors declared that they have no conflicts of interest to this work. We declare that we do not have any commercial or associative interest that represents a conflict of interest in connection with the work submitted.

7. Data Availability

The datasets generated and analysed during this study are available in our GitHub repository:

<https://github.com/Luisamsv/AsPbFlow.git>

8. References

- Ahrens, L.H., 1954. The lognormal distribution of the elements (A fundamental law of geochemistry and its subsidiary). *Geochim Cosmochim Acta*.
- Albanese, S., De Vivo, B., Lima, A., Cicchella, D., 2007. Geochemical background and baseline values of toxic elements in stream sediments of Campania region (Italy). *J Geochem Explor* 93, 21–34. <https://doi.org/10.1016/j.gexplo.2006.07.006>
- Alvares, C.A., Stape, J.L., Sentelhas, P.C., Gonçalves, J.L.D.M., Sparovek, G., 2013. Köppen's climate classification map for Brazil. *Meteorologische Zeitschrift* 22, 711–728. <https://doi.org/10.1127/0941-2948/2013/0507>
- ANA, A.N. das Á., 2013. Plano Intergrado de Recursos Hídricos da Bacia Hidrográfica do Rio Doce. Brasília, Brazil.
- Bai, J., Porwal, A., Hart, C., Ford, A., Yu, L., 2010. Mapping geochemical singularity using multifractal analysis: Application to anomaly definition on stream sediments data from Funin Sheet, Yunnan, China. *J Geochem Explor* 104, 1–11. <https://doi.org/10.1016/j.gexplo.2009.09.002>
- Bancon-Montigny, C., Gonzalez, C., Delpoux, S., Avenzac, M., Spinelli, S., Mhadhbi, T., Mejri, K., Hlaili, A.S., Pringault, O., 2019. Seasonal changes of chemical contamination in coastal waters during sediment resuspension. *Chemosphere* 235, 651–661. <https://doi.org/10.1016/j.chemosphere.2019.06.213>
- Battistel, M., Stolze, L., Muniruzzaman, M., Rolle, M., 2021. Arsenic release and transport during oxidative dissolution of spatially-distributed sulfide minerals. *J Hazard Mater* 409, 124651. <https://doi.org/10.1016/j.jhazmat.2020.124651>

- Bernardino, A.F., Pais, F.S., Oliveira, L.S., Gabriel, F.A., Ferreira, T.O., Queiroz, H.M., Mazzuco, A.C.A., 2019. Chronic trace metals effects of mine tailings on estuarine assemblages revealed by environmental DNA. *PeerJ* 2019, 1–18. <https://doi.org/10.7717/peerj.8042>
- Bidone, E., Castilhos, Z., Cesar, R., Santos, M.C., Sierpe, R., Ferreira, M., 2016. Hydrogeochemistry of arsenic pollution in watersheds influenced by gold mining activities in Paracatu (Minas Gerais State, Brazil). *Environmental Science and Pollution Research* 23, 8546–8555. <https://doi.org/10.1007/s11356-016-6089-3>
- Borch, T., Kretzschmar, R., Skappeler, A., Van Cappellen, P., Ginder-Vogel, M., Voegelin, A., Campbell, K., 2010. Biogeochemical redox processes and their impact on contaminant dynamics. *Environ Sci Technol* 44, 15–23. <https://doi.org/10.1021/es9026248>
- Bubb, J., Rudd, T., Lester, J., 1991. Distribution of Heavy Metals in the River Yare and its Associated Broads III. Lead and Zinc. *Sci Total Environ* 102, 189–208.
- Cagnin, R.C., Quaresma, V.S., Chaillou, G., Franco, T., Bastos, A.C., 2017. Arsenic enrichment in sediment on the eastern continental shelf of Brazil. *Science of the Total Environment* 607–608, 304–316. <https://doi.org/10.1016/j.scitotenv.2017.06.162>
- Chang, H., 2008. Spatial analysis of water quality trends in the Han River basin, South Korea. *Water Res* 42, 3285–3304. <https://doi.org/10.1016/j.watres.2008.04.006>
- Cheung, K.C., Poon, B.H.T., Lan, C.Y., Wong, M.H., 2003. Assessment of metal and nutrient concentrations in river water and sediment collected from the cities in the Pearl River Delta, South China. *Chemosphere* 52, 1431–1440. [https://doi.org/10.1016/S0045-6535\(03\)00479-X](https://doi.org/10.1016/S0045-6535(03)00479-X)
- Chichakly, K.J., Bowden, W.B., Eppstein, M.J., 2013. Minimization of cost, sediment load, and sensitivity to climate change in a watershed management application. *Environmental Modelling and Software* 50, 158–168. <https://doi.org/10.1016/j.envsoft.2013.09.009>
- Climanálise, 2010. Boletim de Monitoramento e Análise Climática. Cachoeira Paulista - SP.
- Costa, A.T., Naline Jr, H.A., Castro, P. de T.A., Tatum, S.H., 2010. Análise estratigráfica e distribuição do arsênio em depósitos sedimentares quaternários da porção sudeste do Quadrilátero Ferrífero, bacia do Ribeirão do Carmo, MG. *REM: R. Esc. Minas* 63, 703–714.
- Costa, A.T., Nalini, H.A., De Lena, J.C., Friese, K., Mages, M., 2003. Surface water quality and sediment geochemistry in the Gualaxo do Norte basin, eastern Quadrilátero Ferrífero, Minas Gerais, Brazil. *Environmental Geology* 45, 226–235. <https://doi.org/10.1007/s00254-003-0870-6>
- Costanza, R., Voinov, A., Boumans, R., Maxwell, T., Villa, F., Wainger, L., Voinov, H., 2002. Integrated Ecological Economic Modeling of the Patuxent River Watershed

, Maryland. *Ecological Monographs* 72, 203–231. [https://doi.org/10.1890/0012-9615\(2002\)072\[0203:IEEMOT\]2.0.CO;2](https://doi.org/10.1890/0012-9615(2002)072[0203:IEEMOT]2.0.CO;2)

da Paz, A.R., 2004. *Hidrologia Aplicada*. Caxias do Sul.

de Carvalho, G.O., Pinheiro, A. de A., de Sousa, D.M., Padilha, J. de A., Souza, J.S., Galvão, P.M., Paiva, T. de C., Freire, A.S., Santelli, R.E., Malm, O., Torres, J.P.M., 2018. Metals and arsenic in water supply for riverine communities affected by the largest environmental disaster in Brazil: The dam collapse on Doce river. *Orbital* 10, 299–307. <https://doi.org/10.17807/orbital.v10i4.1081>

Dean, C.M., Sansalone, J.J., Cartledge, F.K., Pardue, J.H., 2005. Influence of Hydrology on Rainfall-Runoff Metal Element Speciation. *Journal of Environmental Engineering* 131, 632–642. [https://doi.org/10.1061/\(asce\)0733-9372\(2005\)131:4\(632\)](https://doi.org/10.1061/(asce)0733-9372(2005)131:4(632))

Dowling, C.B., Poreda, R.J., Basu, A.R., 2003. The groundwater geochemistry of the Bengal Basin: Weathering, chemisorption, and trace metal flux to the oceans. *Geochim Cosmochim Acta* 67, 2117–2136. [https://doi.org/10.1016/S0016-7037\(02\)01306-6](https://doi.org/10.1016/S0016-7037(02)01306-6)

Du Laing, G., Rinklebe, J., Vandecasteele, B., Meers, E., Tack, F.M.G., 2009. Trace metal behaviour in estuarine and riverine floodplain soils and sediments: A review. *Science of the Total Environment* 407, 3972–3985. <https://doi.org/10.1016/j.scitotenv.2008.07.025>

Euclides, H.P., 2021. Atlas Digital das Águas de Minas; uma ferramenta para o planejamento e gestão dos recursos hídricos [WWW Document]. URL <http://www.atlasdasaguas.ufv.br/home.html> (accessed 1.25.21).

Gabriel, F.A., Silva, A.G., Queiroz, H.M., Ferreira, T.O., Hauser-Davis, R.A., Bernardino, A.F., 2020. Ecological Risks of Metal and Metalloid Contamination in the Rio Doce Estuary. *Integr Environ Assess Manag* 00, 1–6. <https://doi.org/10.1002/ieam.4250>

Gao, J.H., Jia, J., Kettner, A.J., Xing, F., Wang, Y.P., Li, J., Bai, F., Zou, X., Gao, S., 2018. Reservoir-induced changes to fluvial fluxes and their downstream impacts on sedimentary processes: The Changjiang (Yangtze) River, China. *Quaternary International* 493, 187–197. <https://doi.org/10.1016/j.quaint.2015.03.015>

Gardes, T., Debret, M., Copard, Y., Coynel, A., Deloffre, J., Fournier, M., Revillon, S., Nizou, J., Develle, A.L., Sabatier, P., Marcotte, S., Patault, E., Faivre, Q., Portet-Koltalo, F., 2020. Flux estimation, temporal trends and source determination of trace metal contamination in a major tributary of the Seine estuary, France. *Science of the Total Environment* 724, 138249. <https://doi.org/10.1016/j.scitotenv.2020.138249>

Germer, S., Neill, C., Vetter, T., Chaves, J., Krusche, A. V., Elsenbeer, H., 2009. Implications of long-term land-use change for the hydrology and solute budgets of small catchments in Amazonia. *J Hydrol (Amst)* 364, 349–363. <https://doi.org/10.1016/j.jhydrol.2008.11.013>

- Gorny, J., Billon, G., Lesven, L., Dumoulin, D., Madé, B., Noiriél, C., 2015. Arsenic behavior in river sediments under redox gradient: A review. *Science of the Total Environment* 505, 423–434. <https://doi.org/10.1016/j.scitotenv.2014.10.011>
- Goulart, R. de M., 2008. ANÁLISE DA QUALIDADE DA ÁGUA E DOS SEDIMENTOS DO ALTO RIO PIRANGA. Universidade Federal de Ouro Preto.
- Grilo, C.F., Quaresma, V. da S., Amorim, G.F.L., Bastos, A.C., 2018. Changes in flocculation patterns of cohesive sediments after an iron ore mining dam failure. *Mar Geol* 400, 1–11. <https://doi.org/10.1016/j.margeo.2018.03.004>
- Guéguen, C., Clarisse, O., Perroud, A., McDonald, A., 2011. Chemical speciation and partitioning of trace metals (Cd, Co, Cu, Ni, Pb) in the lower Athabasca river and its tributaries (Alberta, Canada). *Journal of Environmental Monitoring* 13, 2865–2872. <https://doi.org/10.1039/c1em10563a>
- Guo, C., Jin, Z., Guo, L., Lu, J., Ren, S., Zhou, Y., 2020. On the cumulative dam impact in the upper Changjiang River: Streamflow and sediment load changes. *Catena (Amst)* 184, 104250. <https://doi.org/10.1016/j.catena.2019.104250>
- Hatje, V., Pedreira, R.M.A., De Rezende, C.E., Schettini, C.A.F., De Souza, G.C., Marin, D.C., Hackspacher, P.C., 2017. The environmental impacts of one of the largest tailing dam failures worldwide. *Sci Rep* 7, 1–13. <https://doi.org/10.1038/s41598-017-11143-x>
- Heinen De Carlo, E., Anthony, S.S., 2002. Spatial and temporal variability of trace element concentrations in an urban subtropical watershed, Honolulu, Hawaii. *Applied Geochemistry* 17, 475–492. [https://doi.org/10.1016/S0883-2927\(01\)00114-7](https://doi.org/10.1016/S0883-2927(01)00114-7)
- Hem, J.D., 1978. Redox processes at surfaces of manganese oxide and their effects on aqueous metal ions. *Chem Geol* 21, 199–218. [https://doi.org/10.1016/0009-2541\(78\)90045-1](https://doi.org/10.1016/0009-2541(78)90045-1)
- Hong, Y.S., Kinney, K.A., Reible, D.D., 2011. Effects of cyclic changes in pH and salinity on metals release from sediments. *Environ Toxicol Chem* 30, 1775–1784. <https://doi.org/10.1002/etc.584>
- Huang, J., Huang, Y., Zhang, Z., 2014. Coupled effects of natural and anthropogenic controls on seasonal and spatial variations of river water quality during baseflow in a coastal watershed of Southeast China. *PLoS One* 9. <https://doi.org/10.1371/journal.pone.0091528>
- Huang, Y., Zhang, D., Xu, Z., Yuan, S., Li, Y., Wang, L., 2017. Effect of overlying water pH, dissolved oxygen and temperature on heavy metal release from river sediments under laboratory conditions. *Archives of Environmental Protection* 43, 28–36. <https://doi.org/10.1515/aep-2017-0014>
- IGAM, I.M. de G. das Á., 2018. Qualidade das águas do Rio Doce após 3 anos do rompimento da Barragem de Fundão.

- IGAM, I.M. de G. das Á., 2015. Monitoramento da qualidade das águas superficiais no estado de Minas Gerais.
- IGAM, I.M. de G. das Á., 2009. MONITORAMENTO DA QUALIDADE DAS ÁGUAS SUPERFICIAIS NO ESTADO DE MINAS GERAIS, Secretaria de Estado de. Belo Horizonte.
- Ip, C.C.M., Li, X.-D., Zhang, G., Wai, O.W.H., Li, Y.-S., 2007. Trace metal distribution in sediments of the Pearl River Estuary and the surrounding coastal area, South China. *Environmental Pollution* 147, 311–323. <https://doi.org/10.1016/j.envpol.2006.06.028>
- Islam, M.S., Ahmed, M.K., Al-Mamun, M.H., Eaton, D.W., 2020. Human and ecological risks of metals in soils under different land-use types in an urban environment of Bangladesh. *Pedosphere* 30, 201–213. [https://doi.org/10.1016/S1002-0160\(17\)60395-3](https://doi.org/10.1016/S1002-0160(17)60395-3)
- Iwashita, M., Shimamura, T., 2003. Long-term variations in dissolved trace elements in the Sagami River and its tributaries (upstream area), Japan. *Science of the Total Environment* 312, 167–179. [https://doi.org/10.1016/S0048-9697\(03\)00251-1](https://doi.org/10.1016/S0048-9697(03)00251-1)
- Jesus, E.T., Amorim, J. da S., Junqueira, R., Viola, M.R., de Mello, C.R., 2020. Meteorological and hydrological drought from 1987 to 2017 in doce river basin, Southeastern Brazil. *Revista Brasileira de Recursos Hídricos* 25, 1–10. <https://doi.org/10.1590/2318-0331.252020190181>
- Josse, J., Husson, F., 2016. missMDA: A Package for Handling Missing Values in Multivariate Data Analysis. *J Stat Softw* 70, 1–31. <https://doi.org/10.18637/jss.v070.i01>
- Karar, K., Gupta, A.K., 2007. Source apportionment of PM10 at residential and industrial sites of an urban region of Kolkata, India. *Atmos Res* 84, 30–41. <https://doi.org/10.1016/j.atmosres.2006.05.001>
- Kassambara, Alboukadel Mundt, F., 2020. factoextra: Extract and Visualize the Results of Multivariate Data Analyses, in: *Practical Guide To Principal Component Methods in R: PCA, M(CA), FAMD, MFA, HCPC, Factoextra*. pp. 42–82.
- Kerr, S.C., Shafer, M.M., Overdier, J., Armstrong, D.E., 2008. Hydrologic and biogeochemical controls on trace element export from northern Wisconsin wetlands. *Biogeochemistry* 89, 273–294. <https://doi.org/10.1007/s10533-008-9219-2>
- Khatri, N., Tyagi, S., 2015. Influences of natural and anthropogenic factors on surface and groundwater quality in rural and urban areas. *Front Life Sci* 8, 23–39. <https://doi.org/10.1080/21553769.2014.933716>
- Kim, B.S.M., Angeli, J.L.F., Ferreira, P.A.L., de Mahiques, M.M., Figueira, R.C.L., 2018. Critical evaluation of different methods to calculate the Geoaccumulation Index for environmental studies: A new approach for Baixada Santista –

Southeastern Brazil. Mar Pollut Bull 127, 548–552.
<https://doi.org/10.1016/j.marpolbul.2017.12.049>

Kim, B.S.M., Ferreira, P.A. de L., Angeli, J.L.F., Tramonte, K.M., de Mahiques, M.M., Figueira, R.C.L., 2020. Geochemical behavior and remobilization potential of trace elements in surface sediments from the baixada santista industrial area, Southeastern Brazilian coast. *Journal of Sedimentary Environments* 5, 505–518.
<https://doi.org/10.1007/s43217-020-00032-5>

Kumar, B., Singh, U.K., Ojha, S.N., 2019. Evaluation of geochemical data of Yamuna River using WQI and multivariate statistical analyses: a case study. *International Journal of River Basin Management* 17, 143–155.
<https://doi.org/10.1080/15715124.2018.1437743>

Lafferty, B.J., Ginder-Vogel, M., Sparks, D.L., 2011. Arsenite oxidation by a poorly-crystalline manganese oxide. 3. Arsenic and manganese desorption. *Environ Sci Technol* 45, 9218–9223. <https://doi.org/10.1021/es201281u>

Lane, C.R., Leibowitz, S.G., Autrey, B.C., LeDuc, S.D., Alexander, L.C., 2018. Hydrological, Physical, and Chemical Functions and Connectivity of Non-Floodplain Wetlands to Downstream Waters: A Review. *J Am Water Resour Assoc* 54, 346–371. <https://doi.org/10.1111/1752-1688.12633>

Lê, S., J & Husson, F., 2008. FactoMineR: An R Package for Multivariate Analysis. *J Stat Softw* 25, 1–18.

Lee, G., Bigham, J.M., Faure, G., 2002. Removal of trace metals by coprecipitation with Fe, Al and Mn from natural waters contaminated with acid mine drainage in the Ducktown Mining District, Tennessee. *Applied Geochemistry* 17, 569–581.
[https://doi.org/10.1016/S0883-2927\(01\)00125-1](https://doi.org/10.1016/S0883-2927(01)00125-1)

Lee, S., Roh, Y., Koh, D.C., 2019. Oxidation and reduction of redox-sensitive elements in the presence of humic substances in subsurface environments: A review. *Chemosphere* 220, 86–97.
<https://doi.org/10.1016/j.chemosphere.2018.11.143>

Licínio, M.V.V.J., Leão, R.T., Gaudereto, F.G., Costa-Gonçalves, A., Patchneelan, S.R., Vidal, M.S.M., Carneiro, M.T.W.D., Freitas, A.C., Evangelista, H.S., Ribeiro, J.N., Pereira, M.G., Ribeiro, A.V.F.N., 2015. Historical Trends in Sedimentation Rates and Trace Elements Accumulation in Doce River, Espírito Santo State, Brazil. *Cadernos de Geociências* 12, 13–24.

Lima, R.P.C., Silva, D.D. da, Pereira, S.B., Moreira, M.C., Passos, J.B.M.C., Coelho, C.D., Elesbon, A.A.A., 2019. Development of an annual drought classification system based on drought severity indexes. *An Acad Bras Cienc* 91.
<https://doi.org/10.1590/0001-3765201920180188>

Lu, Y., Gao, Y., Yang, T., 2020. A review of mass flux monitoring and estimation methods for biogeochemical interface processes in watersheds. *Journal of Geographical Sciences* 30, 881–907. <https://doi.org/10.1007/s11442-020-1760-5>

- Magris, R.A., Marta-Almeida, M., Monteiro, J.A.F., Ban, N.C., 2019. A modelling approach to assess the impact of land mining on marine biodiversity: Assessment in coastal catchments experiencing catastrophic events (SW Brazil). *Science of the Total Environment* 659, 828–840. <https://doi.org/10.1016/j.scitotenv.2018.12.238>
- Mahiques, M.M., Hanebuth, T.J.J., Martins, C.C., Montoya-Montes, I., Alcántara-Carrió, J., Figueira, R.C.L., Bicego, M.C., 2016. Mud depocentres on the continental shelf: a neglected sink for anthropogenic contaminants from the coastal zone. *Environ Earth Sci* 75, 1–12. <https://doi.org/10.1007/s12665-015-4782-z>
- Maia, F.F., 2017. Elementos traços em sedimentos e qualidade da água de rios afetados pelo rompimento da Barragem de Fundão, em Mariana, MG. Universidade Federal de Viçosa.
- Marin, B., Valladon, M., Polve, M., Monaco, A., 1997. Reproducibility testing of a sequential extraction scheme for the determination of trace metal speciation in a marine reference sediment by inductively coupled plasma-mass spectrometry. *Anal Chim Acta* 342, 91–112. [https://doi.org/10.1016/S0003-2670\(96\)00580-6](https://doi.org/10.1016/S0003-2670(96)00580-6)
- Marta-Almeida, M., Mendes, R., Amorim, F.N., Cirano, M., Dias, J.M., 2016. Fundão Dam collapse: Oceanic dispersion of River Doce after the greatest Brazilian environmental accident. *Mar Pollut Bull* 112, 359–364. <https://doi.org/10.1016/j.marpolbul.2016.07.039>
- Masscheleyn, P.H., Delaune, R.D., Patrick, W.H., 1991. Effect of Redox Potential and pH on Arsenic Speciation and Solubility in a Contaminated Soil. *Environ Sci Technol* 25, 1414–1419. <https://doi.org/10.1021/es00020a008>
- Mil-Homens, M., Costa, A.M., Fonseca, S., Trancoso, M.A., Lopes, C., Serrano, R., Sousa, R., 2013. Characterization of heavy-metal contamination in surface sediments of the minho river estuary by way of factor analysis. *Arch Environ Contam Toxicol* 64, 617–631. <https://doi.org/10.1007/s00244-012-9861-5>
- Mirlean, N., Garcia, F., Baisch, P., Quintana, G.C., Agnes, F., 2013. Sandy beaches contamination by arsenic, a result of nearshore sediment diagenesis and transport (Brazilian coastline). *Estuar Coast Shelf Sci* 135, 241–247. <https://doi.org/10.1016/j.ecss.2013.10.020>
- Moodley, K., Pillay, S., Pather, K., Ballabh, H., 2016. Seasonal discharge and chemical flux variations of rivers flowing into the Bayhead canal of Durban Harbour, South Africa. *Acta Geochimica* 35, 340–353. <https://doi.org/10.1007/s11631-016-0100-z>
- Moore, J.N., Ficklin, W.H., Johns, C., 1988. Partitioning of Arsenic and Metals in Reducing Sulfidic Sediments. *Environ Sci Technol* 22, 432–437. <https://doi.org/10.1021/es00169a011>
- Morgan, B., Rate, A.W., Burton, E.D., 2012. Water chemistry and nutrient release during the resuspension of FeS-rich sediments in a eutrophic estuarine system.

Science of the Total Environment 432, 47–56.
<https://doi.org/10.1016/j.scitotenv.2012.05.065>

- Mouri, G., Takizawa, S., Oki, T., 2011. Spatial and temporal variation in nutrient parameters in stream water in a rural-urban catchment, Shikoku, Japan: Effects of land cover and human impact. *J Environ Manage* 92, 1837–1848.
<https://doi.org/10.1016/j.jenvman.2011.03.005>
- Nascimento, L.P., Reis, D.A., Roeser, H.M.P., Santiago, A. da F., 2018. Geochemical assessment of metals in fluvial systems affected by anthropogenic activities in the iron quadrangl. *Engenharia Sanitaria e Ambiental* 23, 767–778.
<https://doi.org/10.1590/s1413-41522018165852>
- Neal, C., Williams, R.J., Neal, M., Bhardwaj, L.C., Wickham, H., Harrow, M., Hill, L.K., 2000. The water quality of the River Thames at a rural site downstream of Oxford. *Science of the Total Environment* 251–252, 441–457.
[https://doi.org/10.1016/S0048-9697\(00\)00398-3](https://doi.org/10.1016/S0048-9697(00)00398-3)
- Négre, P., Roy, S., 1998. Chemistry of rainwater in the Massif Central (France): A strontium isotope and major element study. *Applied Geochemistry* 13, 941–952.
[https://doi.org/10.1016/S0883-2927\(98\)00029-8](https://doi.org/10.1016/S0883-2927(98)00029-8)
- Neto, J.O. de A., Cota, G.E.M., Mendes, L.C., Magalhães, A.P., Felipe, M.F., 2016. Considerações sobre o ano hidrológico 2013- 2014 e os seus reflexos nos caudais fluviais da bacia do rio {Doce}. *Revista Geografias* 0, 26–45.
- Nyamangara, J., Bangira, C., Taruvinga, T., Masona, C., Nyemba, A., Ndlovu, D., 2008. Effects of sewage and industrial effluent on the concentration of Zn, Cu, Pb and Cd in water and sediments along Waterfalls stream and lower Mukuvisi River in Harare, Zimbabwe. *Physics and Chemistry of the Earth* 33, 708–713.
<https://doi.org/10.1016/j.pce.2008.06.053>
- Olías, M., Nieto, J.M., Sarmiento, A.M., Cerón, J.C., Cánovas, C.R., 2004. Seasonal water quality variations in a river affected by acid mine drainage: The Odiel River (South West Spain). *Science of the Total Environment* 333, 267–281.
<https://doi.org/10.1016/j.scitotenv.2004.05.012>
- Oliveira, E.G., 2016. CONTRIBUIÇÕES PARA O DIAGNÓSTICO AMBIENTAL DA BACIA HIDROGRÁFICA DO RIO DOCE, ESTUDO DE CASO: SUB-BACIA DO RIO PIRANGA Mestrando: Universidade Federal de Ouro Preto.
- Oliveira, K.S.S., Quaresma, V. da S., 2017a. Temporal variability in the suspended sediment load and streamflow of the Doce River. *J South Am Earth Sci* 78, 101–115. <https://doi.org/10.1016/j.jsames.2017.06.009>
- Oliveira, K.S.S., Quaresma, V. da S., 2017b. Temporal variability in the suspended sediment load and streamflow of the Doce River. *J South Am Earth Sci* 78, 101–115. <https://doi.org/10.1016/j.jsames.2017.06.009>
- Oliveira, K.S.S., Quaresma, V. da S., 2017c. Temporal variability in the suspended sediment load and streamflow of the Doce River. *J South Am Earth Sci* 78, 101–115. <https://doi.org/10.1016/j.jsames.2017.06.009>

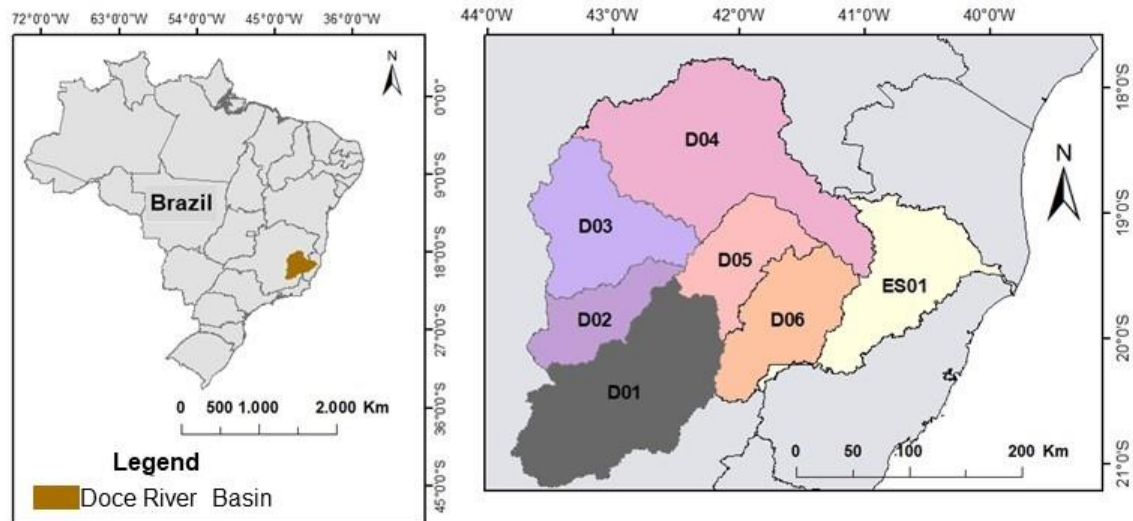
- Papafilippaki, A.K., Kotti, M.E., Stavroulakis, G.G., 2008. Seasonal variations in dissolved heavy metals in the Keritis River, Chania, Greece. *Global Nest Journal* 10, 320–325. <https://doi.org/10.30955/gnj.000528>
- Pruski, F.F., Pereira, S.B., Novaes, L.F. De, Silva, D.D., Ramos, M.M., 2004. Precipitação média anual e vazão específica média de longa duração, na Bacia do São Francisco. *Revista Brasileira de Engenharia Agrícola e Ambiental* 8, 247–253. <https://doi.org/10.1590/S1415-43662004000200013>
- Queiroz, H.M., Nóbrega, G.N., Ferreira, T.O., Almeida, L.S., Romero, T.B., Santaella, S.T., Bernardino, A.F., Otero, X.L., 2018. The Samarco mine tailing disaster: A possible time-bomb for heavy metals contamination? *Science of the Total Environment* 637–638, 498–506. <https://doi.org/10.1016/j.scitotenv.2018.04.370>
- Queiroz, M.T.A., 2017. AVALIAÇÃO DA QUALIDADE DA ÁGUA DA SUB-BACIA DO RIO PIRACICABA E DA SUA ÁREA DE INFLUÊNCIA NO RESERVATÓRIO DA USINA HIDRELÉTRICA DE SÁ CARVALHO, ANTÔNIO DIAS, MG, BRASIL. Universidade Federal de Minas Gerais. <https://doi.org/10.21450/rahis.v0i2.782>
- R Core Team, P., 2020. R: A language and environment for statistical computing. R Foundation for Statistical Computing.
- Ram, R., Morrisroe, L., Etschmann, B., Vaughan, J., Brugger, J., 2021. Lead (Pb) sorption and co-precipitation on natural sulfide, sulfate and oxide minerals under environmental conditions. *Miner Eng* 163. <https://doi.org/10.1016/j.mineng.2021.106801>
- Rastegari Mehr, M., Keshavarzi, B., Sorooshian, A., 2019. Influence of natural and urban emissions on rainwater chemistry at a southwestern Iran coastal site. *Science of the Total Environment* 668, 1213–1221. <https://doi.org/10.1016/j.scitotenv.2019.03.082>
- Reis, D.A., 2020. Environmental impacts at the bottom sediments in a Doce River tributary after the Fundão dam rupture Impacto. *Research, Society and Development* 9, 22.
- Renova, F., 2019. Programa de Monitoramento Quali-Quantitativo Sistemático de Água e Sedimentos – PMQQS Relatório - 2019.
- Renova, F., 2018a. Avaliação dos Resultados de Qualidade de Água e Sedimento do Rio Doce – Atualização de Fevereiro de 2018.
- Renova, F., 2018b. Programa de Monitoramento Quali-Quantitativo Quali-Quantitativo Sistemático de Água e Sedimentos – PMQQS - 2018.
- Renova, F., 2017. Qualidade da Água e do Sedimento na Zona Costeira Próxima à Foz do Rio Doce e na APA Costa das Algas - Atualização de Maio/2017.
- Rhodes, V., 2010. Distribuição de mercúrio e arsênio nos sedimentos da área afetada por garimpo de ouro–Rio Gualaxo do Norte, Mariana, MG. Universidade Federal de Ouro Preto.

- Rodrigues, A.S. de L., Nalini Junior, H.A., Costa, A.T., Malafaia, G., 2015. Construção de mapas geoquímicos a partir de sedimentos ativos de margens oriundos do Rio Gualaxo do Norte, MG, Brasil. *Multi-Science Journal* 1, 70. <https://doi.org/10.33837/msj.v1i1.50>
- Rudorff, N., Rudorff, C.M., Kampel, M., Ortiz, G., 2018. Remote sensing monitoring of the impact of a major mining wastewater disaster on the turbidity of the Doce River plume off the eastern Brazilian coast. *ISPRS Journal of Photogrammetry and Remote Sensing* 145, 349–361. <https://doi.org/10.1016/j.isprsjprs.2018.02.013>
- Rumsey, C.A., Miller, M.P., Schwarz, G.E., Hirsch, R.M., Susong, D.D., 2017. The role of baseflow in dissolved solids delivery to streams in the Upper Colorado River Basin. *Hydrol Process* 31, 4705–4718. <https://doi.org/10.1002/hyp.11390>
- Sales, S.C.M., 2013. AVALIAÇÃO ECOTOXICOLÓGICA DE IMPACTOS DA CONTAMINAÇÃO POR METAIS E ARSÊNIO EM ÁREAS DE MINERAÇÃO E BENEFICIAMENTO DE OURO EM MINAS GERAIS SUELLEN. Universidade Federal de Minas Gerais Instituto.
- Salomons, W., Rooji, M.N., Kerdijk, H., Bril, J., 1987. Sediments as a source for contaminants? *Hydrobiologia* 149, 13–30.
- Sánchez-España, J., Yusta, I., 2019. Coprecipitation of Co^{2+} , Ni^{2+} and Zn^{2+} with Mn(III/IV) oxides formed in metal-rich mine waters. *Minerals* 9, 1–22. <https://doi.org/10.3390/min9040226>
- Sarkar, S., Blaney, L.M., Gupta, A., Ghosh, D., Sengupta, A.K., 2008. Arsenic removal from groundwater and its safe containment in a rural environment: Validation of a sustainable approach. *Environ Sci Technol* 42, 4268–4273. <https://doi.org/10.1021/es702556t>
- Schaider, L.A., Senn, D.B., Estes, E.R., Brabander, D.J., Shine, J.P., 2014. Sources and fates of heavy metals in a mining-impacted stream: Temporal variability and the role of iron oxides. *Science of the Total Environment* 490, 456–466. <https://doi.org/10.1016/j.scitotenv.2014.04.126>
- Shaikh, M.M., Nath, B., Birch, G.F., 2014. Partitioning of trace elements in contaminated estuarine sediments: The role of environmental settings. *Ecotoxicol Environ Saf* 110, 246–253. <https://doi.org/10.1016/j.ecoenv.2014.09.007>
- Shil, S., Singh, U.K., 2019. Health risk assessment and spatial variations of dissolved heavy metals and metalloids in a tropical river basin system. *Ecol Indic* 106, 105455. <https://doi.org/10.1016/j.ecolind.2019.105455>
- Shiller, A.M., 1997. Dissolved trace elements in the Mississippi River: Seasonal, interannual, and decadal variability. *Geochim Cosmochim Acta* 61, 4321–4330. [https://doi.org/10.1016/S0016-7037\(97\)00245-7](https://doi.org/10.1016/S0016-7037(97)00245-7)
- Silva, D. de C., Bellato, C.R., Neto, J. de O.M., Fontes, M.P.F., 2018. TRACE ELEMENTS IN RIVER WATERS AND SEDIMENTS BEFORE AND AFTER A

- MINING DAM BREACH (BENTO RODRIGUES, BRAZIL). *Quim Nova* 41, 857–866. <https://doi.org/10.21577/0100-4042.20170252>
- Siwek, W., Zelazny, M., Chelmicki, J., 2009. THE INFLUENCE OF WATER CIRCULATION ON STREAM WATER ELECTRICAL CONDUCTIVITY IN CATCHMENTS WITH DIFFERENT LAND USE DURING FLOOD PERIODS (THE CARPATHIAN FOOTHILLS, POLAND). *Hydrological extremes in small basins* 84, 75–80.
- Smedley, P.L., Kinniburgh, D.G., 2002. A review of the source, behaviour and distribution of arsenic in natural waters. *Applied Geochemistry* 17, 517–568. [https://doi.org/10.1016/S0883-2927\(02\)00018-5](https://doi.org/10.1016/S0883-2927(02)00018-5)
- Tipping, E., 1984. Temperature dependence of Mn(II) oxidation in lakewaters: a test of biological involvement. *Geochim Cosmochim Acta* 48, 1353–1356. [https://doi.org/10.1016/0016-7037\(84\)90069-3](https://doi.org/10.1016/0016-7037(84)90069-3)
- Valle Junior, R.F., Varandas, S.G.P., Pacheco, F.A.L., Pereira, V.R., Santos, C.F., Cortes, R.M.V., Sanches Fernandes, L.F., 2015. Impacts of land use conflicts on riverine ecosystems. *Land use policy* 43, 48–62. <https://doi.org/10.1016/j.landusepol.2014.10.015>
- Varejão, E.V.V., Bellato, C.R., Fontes, M.P.F., Mello, J.W.V., 2011. Arsenic and trace metals in river water and sediments from the southeast portion of the Iron Quadrangle, Brazil. *Environ Monit Assess* 172, 631–642. <https://doi.org/10.1007/s10661-010-1361-3>
- Venables, W.N., Ripley, B.D., 2002. *Modern Applied Statistics with S*, Fourth. ed. Springer, New York.
- Viana, L.M. de S., Pestana, I.A., Carvalho, C.E.V., Salomão, M.S.M.B., 2020. Doce River Estuary: Geochemical Changes Following the Largest Tailing Spill in South America. *Arch Environ Contam Toxicol* 79, 343–353. <https://doi.org/10.1007/s00244-020-00766-3>
- Violante, A., Cozzolino, V., Perelomov, L., Caporale, A.G., Pigna, M., 2010. Mobility and bioavailability of heavy metals and metalloids in soil environments. *J Soil Sci Plant Nutr* 10, 268–292. <https://doi.org/10.4067/S0718-95162010000100005>
- Wang, Q., Zhang, Q., Wu, Y., Wang, X.C., 2017. Chemosphere Physicochemical conditions and properties of particles in urban runoff and rivers : Implications for runoff pollution. *Chemosphere* 173, 318–325. <https://doi.org/10.1016/j.chemosphere.2017.01.066>
- Wu, Y., Ouyang, W., Hao, Z., Lin, C., Liu, H., Wang, Y., 2018. Assessment of soil erosion characteristics in response to temperature and precipitation in a freeze-thaw watershed. *Geoderma* 328, 56–65. <https://doi.org/10.1016/j.geoderma.2018.05.007>
- Xu, M., Wang, H., Lei, D., Qu, D., Zhai, Y., Wang, Y., 2013. Removal of Pb(II) from aqueous solution by hydrous manganese dioxide: Adsorption behavior and

mechanism. *J Environ Sci (China)* 25, 479–486. [https://doi.org/10.1016/S1001-0742\(12\)60100-4](https://doi.org/10.1016/S1001-0742(12)60100-4)

Yamamoto, J.K., Landim, P.M.B., 2013. *GEOESTATISTICA conceitos e aplicações*, 1st ed. Oficina de textos, São Paulo.



Coordinate System: GCS_WGS_1984
 DATUM: D_WGS_1984
 Source: ANA, IGAM, IBGE
 Organizer: Luisa Viana

Sub-Regions and Its Main Tributaries						
D01	D02	D03	D04	D05	D06	ES01
Piranga River	Piracicaba River	Passa Sete Stream	Corrente Grande River	Doce River	Doce River	Santa Joana River
Camo River	Santa Bárbara River	Água Santa Stream	Doce River	Caratinga River	Manhuaçu River	Santa Maria do River Doce River
Casca River	Peixe River (D02)	Santo Antônio River (D03)	Suaçuí Grande River	Ribeirão Traíras	São Mateus River (D06)	Guandu River
Matipó River	Doce River	Preto do Itambé River	Suaçuí Pequeno River	Piã Stream	José Pedro River	Doce River Mouth
Ribeirão do Sacramento	Prata River (D02)	Peixe River (D03)	Urupuca River	Preto River (D05)		Pancas River
Turvo River	Maquiné River	Tanque River	Itambacuri River			
Xopotó River		Guanhães River	Eme River			
Doce River						
Gualaxo do Norte River						

Figure 1 - Division of the watershed of the Doce River in sub-regions. The ES01 region was assigned by the author due to the lack of an official nomenclature.

1

2

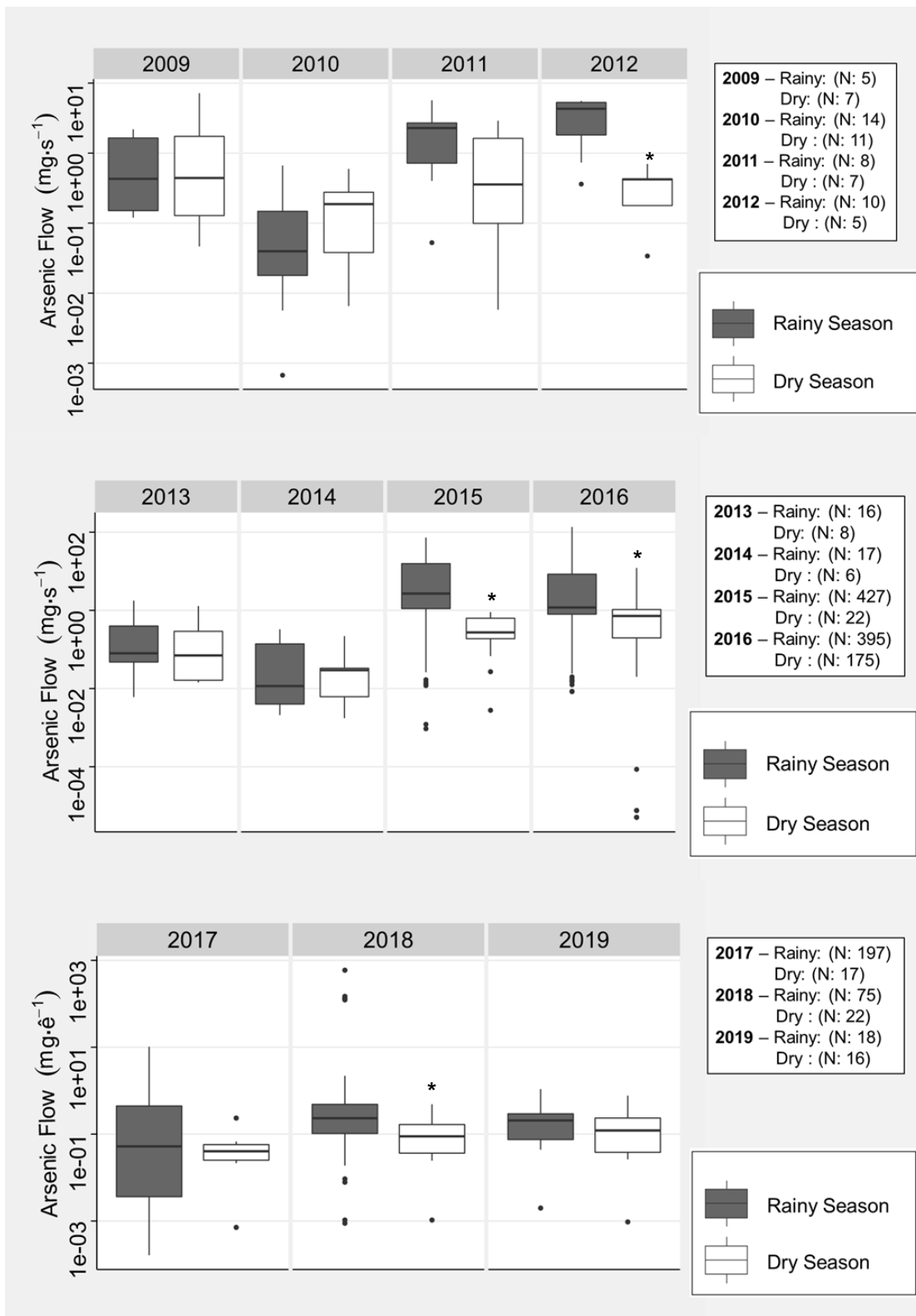


Figure 2 - Seasonal differences in the flows of As. Asterisks indicate statistical difference. Values of p: 2012 p = 0.0009765, 2015 p = 2.401e-10, 2016 p < 2.2e-16, 2018 p = 0.012399. The y-axis is logarithmic to facilitate understanding. The values were transformed to meet the assumptions of ANOVA. N: number of samples.

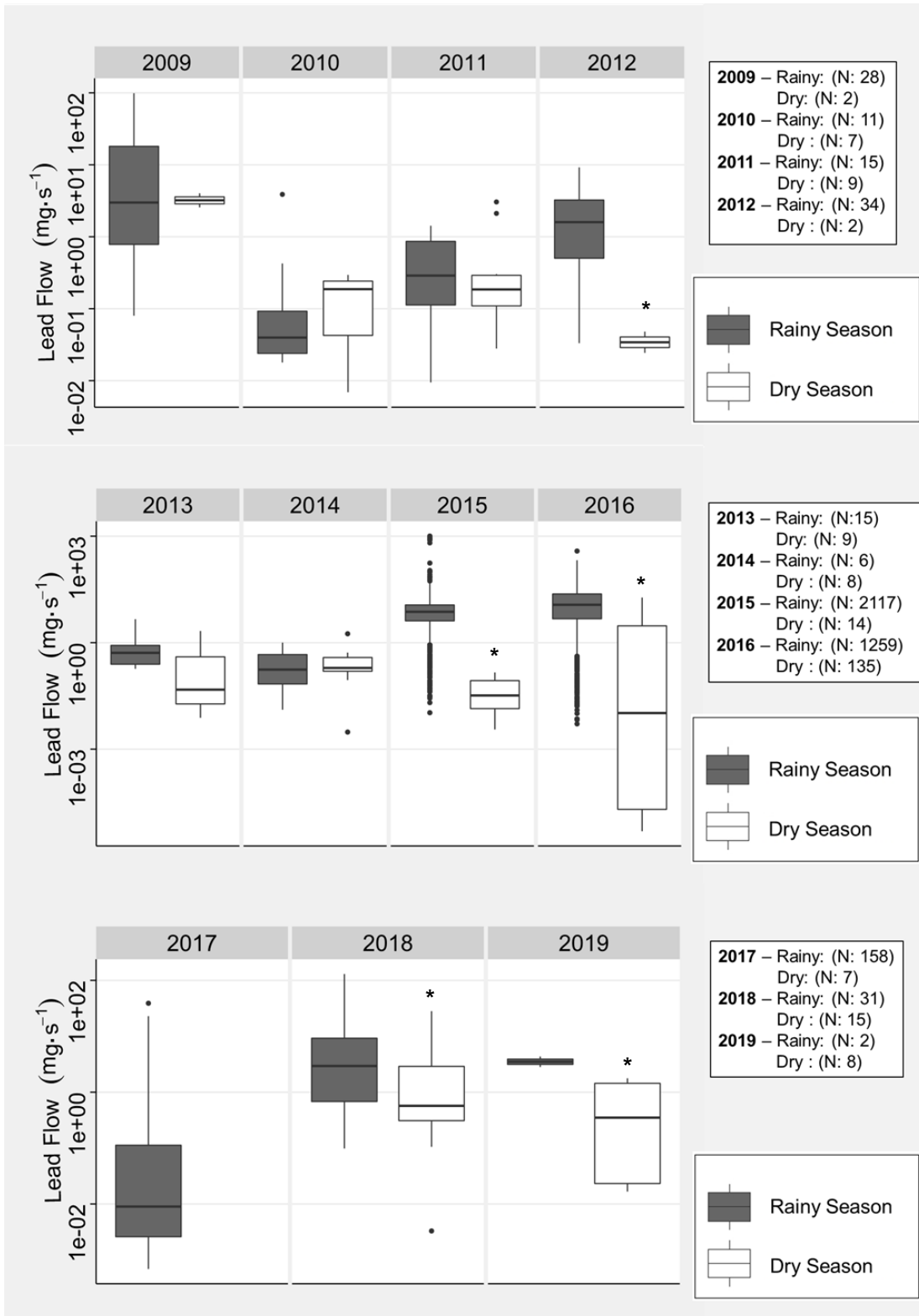


Figure 3 - Seasonal differences in Pb flows. The year 2017 only presented data on the rainy season. Asterisks indicate statistical difference. Values of p: 2012 $p = 0.000542$, 2015 $p = 2.401e-10$, 2016 $p < 2.261e-16$, 2018 $p = 0.0578667$, 2019 $p = 0.0145725$. The y-axis is logarithmic to facilitate understanding. The values were transformed to meet the assumptions of ANOVA. N: number of samples.

41 **Table 1** - The Kaiser-Meyer-Olkin and Bartlett's Test Result.

42

		As	As	Pb	Pb
		(2009 - 2014)	(2015-2019)	(2009 - 2014)	(2015-2019)
Kaiser-Meyer-Olkin Measure of Sampling Adequacy		0.70485	0.85594	0.77507	0.79547
Approx. ChiSquare		1168.2	6931.3	1542.6	4986.6
Bartlett's Test of Sphericity	df	153	153	153	153
	Sig.	8,26E-156	0,000	5,39E-224	0,000

43

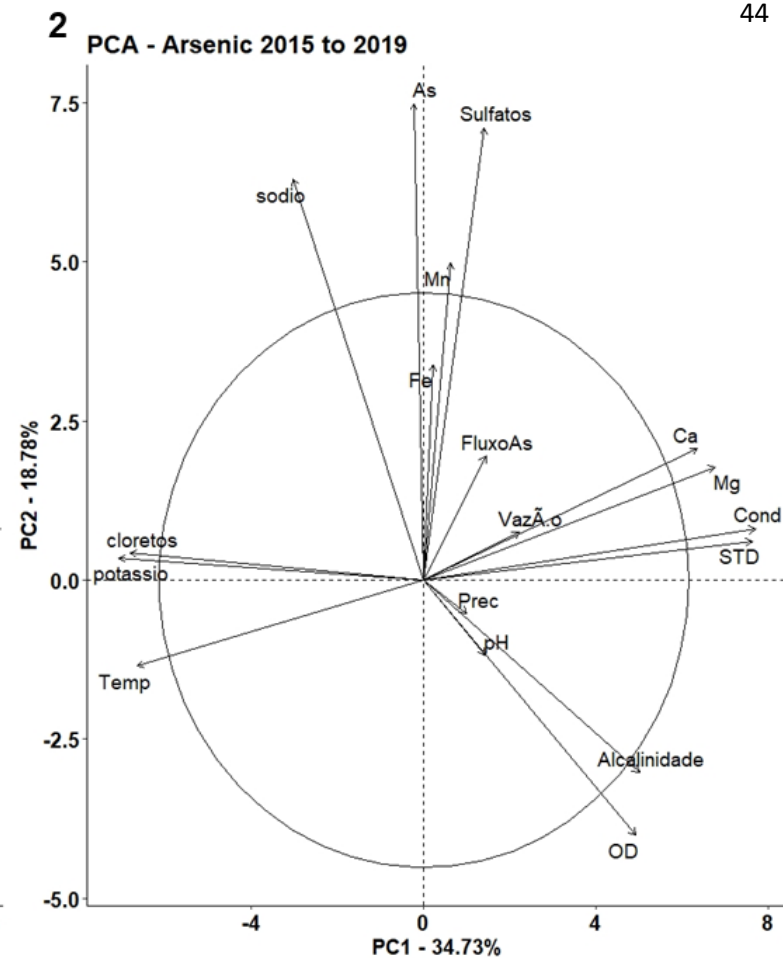
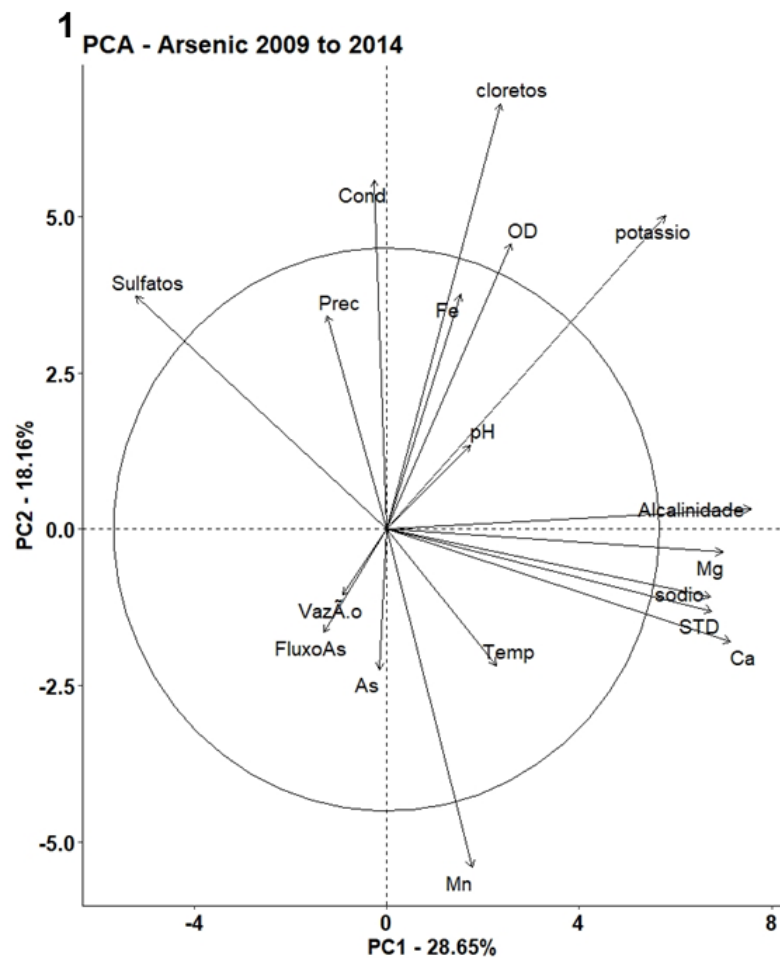


Figure 4 - PCA between As concentrations and environmental parameters found in the reviewed studies. Mg- Magnesium, Fe - Iron, K - Potassium, Cl- - Chlorides, STD - Total Dissolved Solids, T - Temperature, Mn - Manganese, Alc - Alkalinity, EC - Electrical Conductivity, Ca^{2+} - Calcium, Na^{+} - Sodium, SO_4^{-2} - Sulfates, As - Arsenic, Alt - Altitude, OD - Dissolved Oxygen and pH - Hydrogenionic Potential.

59

60

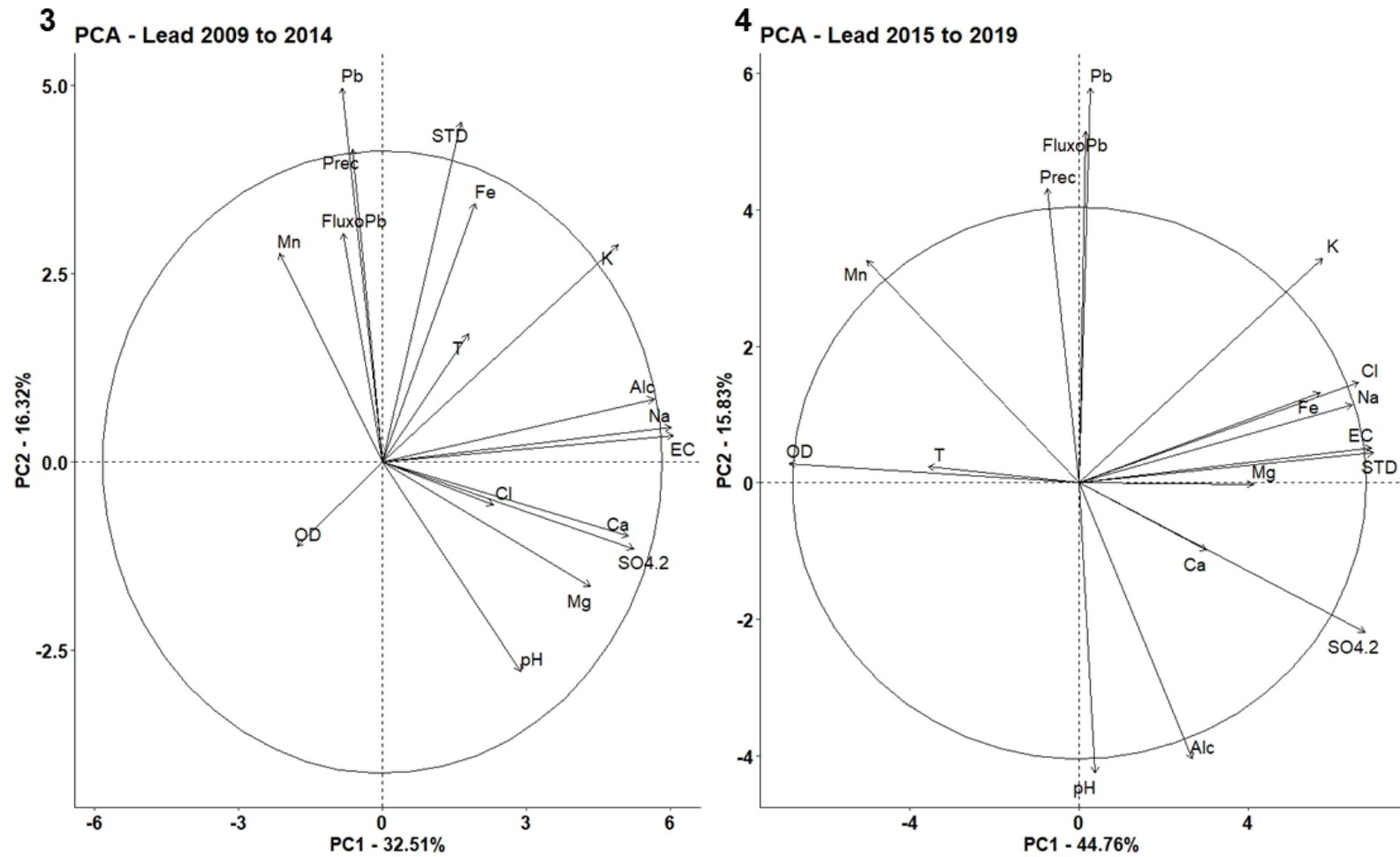


Figure 5 - PCA between Pb concentrations and environmental parameters found in the reviewed studies. Mg - Magnesium, Fe - Iron, K - Potassium, Cl- Chlorides, STD - Total Dissolved Solids, T - Temperature, Mn - Manganese, Alc - Alkalinity, EC - Electrical Conductivity, Ca+2 - Calcium, Na + - Sodium, SO4- 2 - Sulfates, As - Arsenic, Alt - Altitude, OD - Dissolved Oxygen and pH - Hydrogenionic Potential.

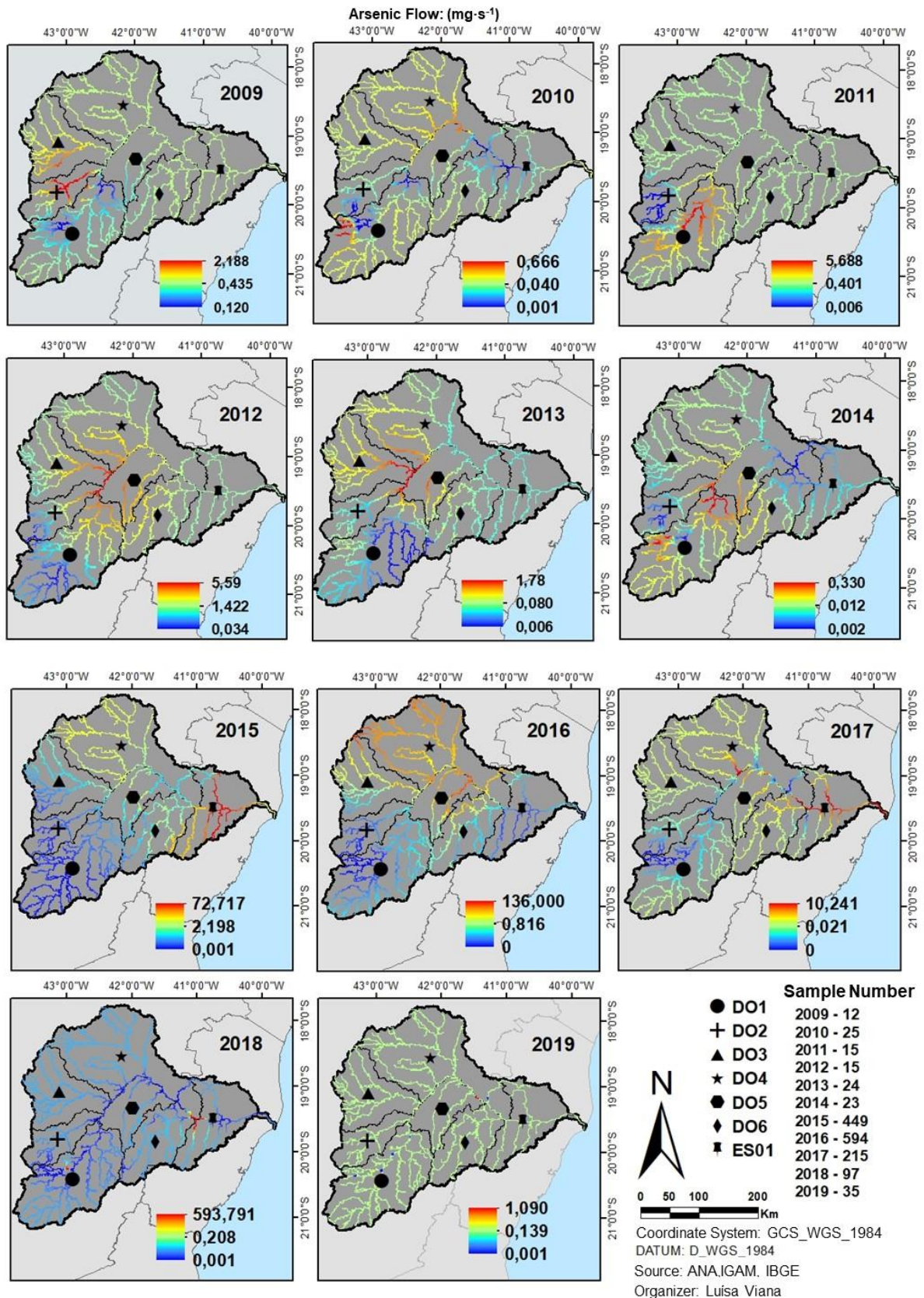


Figure 6 - As flow in the dissolved fraction of the water column (mg s⁻¹) calculated for the years 2009 to 2019. The maps were plotted by Kriging interpolation, except for the year 2014.

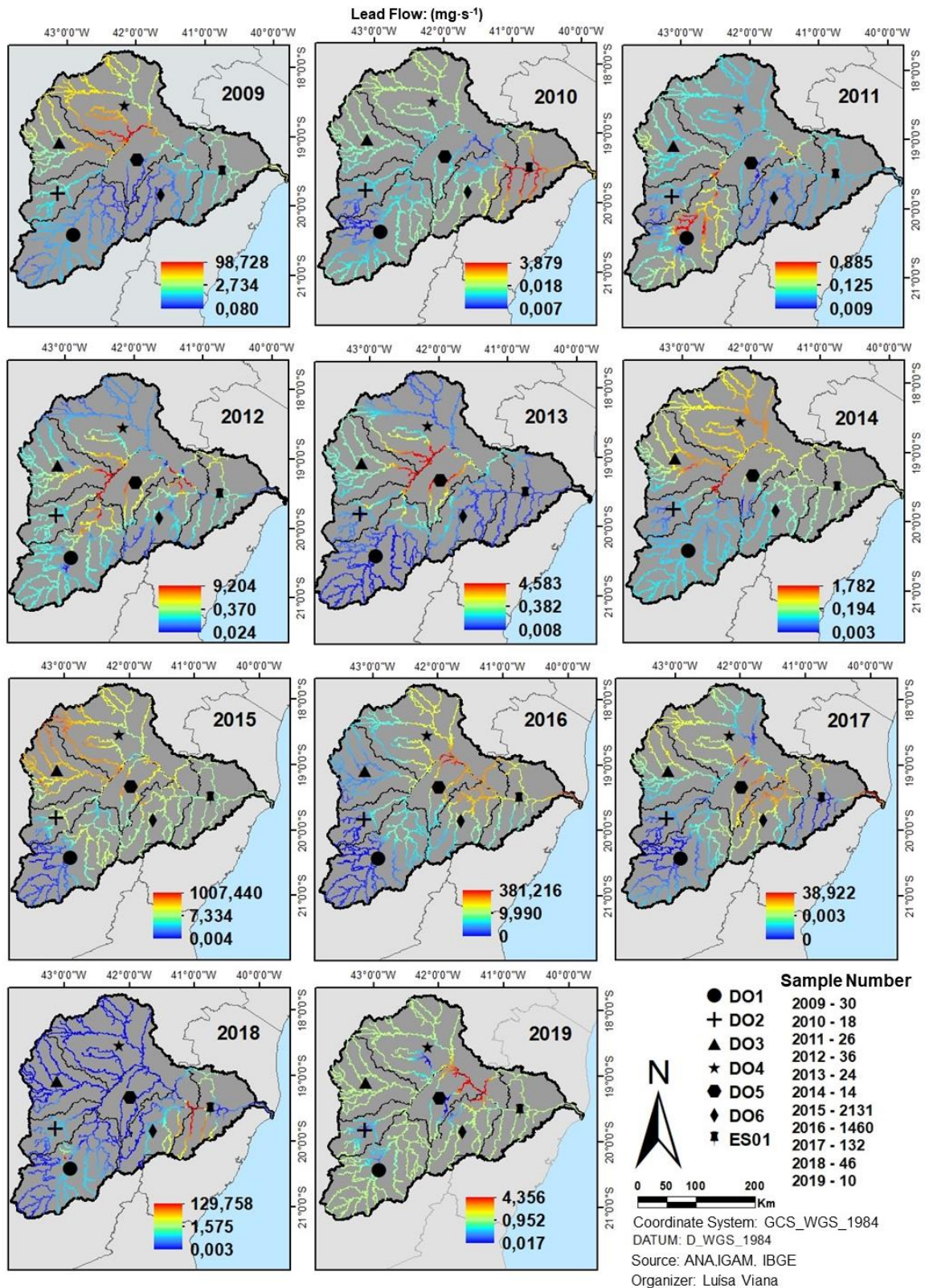


Figure 7 - Pb flow in the dissolved fraction of the water column (mg s⁻¹) calculated for the years 2009 to. The maps were plotted by Kriging interpolation, except for the years 2011, 2012, 2013, 2014 and 2018.

Supplementary Material

Table S1 - Flow and average rainfall values in each sub-region of the Doce River Basin.

Sub-Region	2009	2010	2011	2012	2013	2014	2015	2016	2017	2018	2019	
DO1	1488	1254	1662	1142	1278	717	990	1294	964	1213	861	Rainfall (mm)
DO2	1899	1247	1650	1036	1630	2917	990	1409	988	1443	992	
DO3	1534	1310	1529	1044	1310	889	939	1431	1119	1541	1035	
DO4	1342	1052	1179	940	1360	599	667	1119	777	1093	641	
DO5	1308	1176	1115	760	1406	642	628	1022	810	1140	675	
DO6	1377	1123	1309	873	1521	651	700	1139	903	1292	816	
ES01	1356	1168	1294	582	1498	918	549	1012	921	1277	704	
Sub-Region	2009	2010	2011	2012	2013	2014	2015	2016	2017	2018	2019	
DO1	1182	757	986	953	657	380	393	516	331	514	403	Flow (m³ s)
DO2	3238	1828	2696	2391	1995	1164	935	1591	1048	1891	1382	
DO3	828	536	746	727	535	299	255	370	231	407	201	
DO4	524	212	301	296	270	215	102	135	123	203	106	
DO5	727	531	674	549	482	281	167	244	250	376	180	
DO6	1005	659	971	689	661	395	192	312	307	540	252	
ES01	764	403	638	480	478	359	92	178	215	395	239	

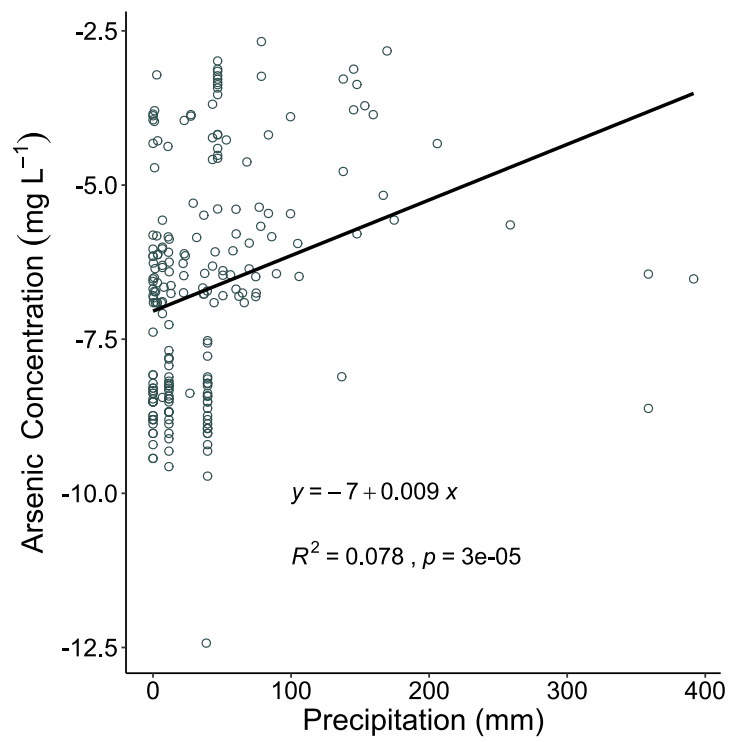
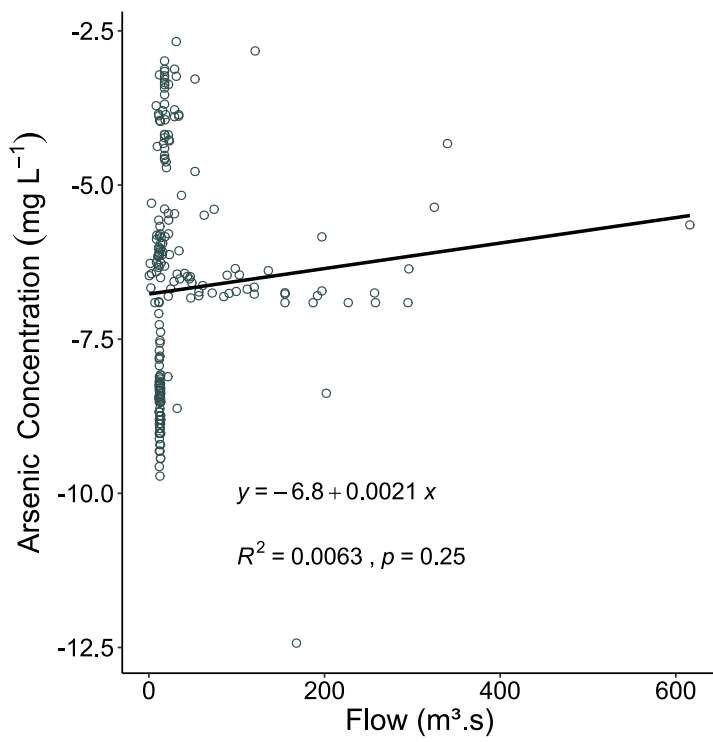


Figure S1 – Linear regression analyzing the relationship between As concentrations and precipitation and flow.

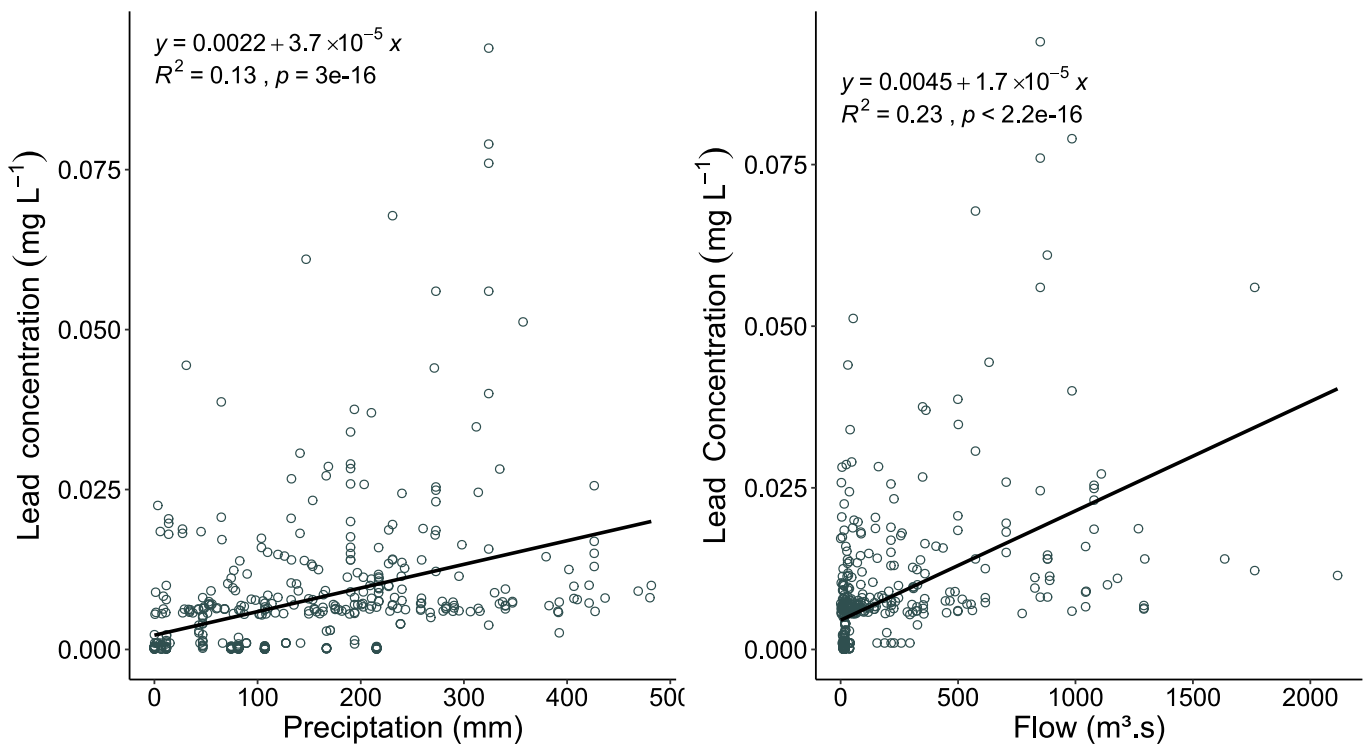


Figure S2 – Linear regression analyzing the relationship between Pb concentrations and precipitation and flow.

Table S2 – Principal components (PCs) statistics for the parameters used in this study.

	Variance PCA 1			name	Loading PCA 1				
	eigenvalue	percentage of variance	cumulative percentage of variance		Dim.1	Dim.2	coord	cos2	contrib
comp 1	5.16	28.65	28.65	As	-0.29	-0.20	0.12	0.12	1.45
comp 2	3.11	17.25	45.9	FluxoAs	-0.55	-0.11	0.32	0.32	3.84
comp 3	1.87	10.36	56.26	Vazão	-0.33	-0.08	0.11	0.11	1.36
comp 4	1.34	7.43	63.7	Prec	-0.46	0.46	0.42	0.42	5.10
comp 5	1.18	6.57	70.27	pH	0.31	0.23	0.15	0.15	1.86
comp 6	1	5.57	75.84	Cond	0.11	0.67	0.46	0.46	5.53
comp 7	0.75	4.18	80.02	Temp	0.11	-0.15	0.03	0.03	0.40
comp 8	0.65	3.6	83.62	STD	0.67	-0.15	0.47	0.47	5.69
comp 9	0.6	3.32	86.94	Alcalinidade	0.83	0.16	0.72	0.72	8.72
comp 10	0.55	3.04	89.98	OD	-0.45	0.33	0.31	0.31	3.76
comp 11	0.41	2.28	92.26	Sulfatos	0.65	-0.36	0.55	0.55	6.66
comp 12	0.34	1.89	94.15	cloretos	0.22	0.85	0.77	0.77	9.26
comp 13	0.31	1.75	95.9	Ca	0.89	-0.12	0.81	0.81	9.85
comp 14	0.28	1.56	97.46	Mg	0.81	0.00	0.65	0.65	7.90
comp 15	0.17	0.92	98.38	Fe	-0.01	0.45	0.20	0.20	2.43
comp 16	0.12	0.66	99.04	potassio	0.52	0.77	0.87	0.87	10.56
comp 17	0.1	0.55	99.59	sodio	0.88	-0.10	0.78	0.78	9.44
comp 18	0.07	0.41	100	Mn	0.15	-0.70	0.51	0.51	6.20

Variance PCA 2				Loading PCA 2					
	eigenvalue	percentage of variance	cumulative percentage of variance	name	Dim.1	Dim.2	coord	cos2	contrib
comp 1	7.52	41.8	41.8	As	0.63	0.19	0.44	0.44	4.15
comp 2	3.04	16.9	58.71	AsFlux	-0.08	0.87	0.77	0.77	7.30
comp 3	1.09	6.08	64.79	Discharge	-0.24	0.86	0.81	0.81	7.63
comp 4	0.98	5.46	70.25	Prec	-0.22	0.57	0.37	0.37	3.54
comp 5	0.85	4.73	74.98	pH	-0.18	-0.36	0.16	0.16	1.54
comp 6	0.8	4.43	79.41	Cond	-0.87	0.15	0.78	0.78	7.43
comp 7	0.7	3.87	83.29	Temp	-0.44	0.47	0.42	0.42	3.94
comp 8	0.65	3.62	86.9	STD	-0.87	0.13	0.77	0.77	7.31
comp 9	0.56	3.11	90.01	Alcalinity	-0.71	-0.24	0.55	0.55	5.25
comp 10	0.49	2.7	92.71	OD	-0.73	-0.34	0.65	0.65	6.14
comp 11	0.31	1.73	94.44	SO4-2	0.89	-0.19	0.83	0.83	7.88
comp 12	0.27	1.5	95.94	Cl	0.63	0.20	0.43	0.43	4.10
comp 13	0.23	1.26	97.2	Ca	0.87	-0.10	0.76	0.76	7.19
comp 14	0.22	1.2	98.4	Mg	0.84	-0.03	0.71	0.71	6.76
comp 15	0.11	0.63	99.03	Fe	-0.44	0.25	0.26	0.26	2.44
comp 16	0.08	0.45	99.49	K	0.49	0.62	0.62	0.62	5.88
comp 17	0.07	0.41	99.9	Na	0.88	0.08	0.79	0.79	7.47
comp 18	0.02	0.1	100	Mn	0.61	0.25	0.43	0.43	4.07

Variance PCA 3				Loading PCA 3					
	eigenvalue	percentage of variance	cumulative percentage of variance	name	Dim.1	Dim.2	coord	cos2	contrib
comp 1	5.6	31.12	31.12	Discharge	-0.005	0.507	0.257	0.257	2.551
comp 2	2.89	16.08	47.2	Pb	0.005	0.752	0.565	0.565	5.606
comp 3	1.8	10.03	57.22	PbFlux	0.006	0.791	0.625	0.625	6.200
comp 4	1.29	7.17	64.39	Prec	-0.086	0.526	0.284	0.284	2.813
comp 5	1.03	5.74	70.13	pH	0.070	-0.513	0.268	0.268	2.662
comp 6	0.91	5.04	75.18	Cond	0.899	0.047	0.811	0.811	8.037
comp 7	0.8	4.43	79.61	Temp	-0.359	0.116	0.143	0.143	1.414
comp 8	0.63	3.5	83.11	STD	0.919	0.048	0.847	0.847	8.400
comp 9	0.59	3.28	86.4	Alcalinity	0.407	-0.485	0.401	0.401	3.971
comp 10	0.55	3.03	89.43	OD	-0.934	0.012	0.872	0.872	8.643
comp 11	0.51	2.81	92.24	SO4-2	0.905	-0.281	0.899	0.899	8.910
comp 12	0.4	2.25	94.48	Cl	0.715	0.315	0.610	0.610	6.053
comp 13	0.3	1.64	96.12	Ca	0.894	-0.006	0.799	0.799	7.923
comp 14	0.21	1.17	97.3	Mg	0.873	0.073	0.767	0.767	7.603
comp 15	0.15	0.85	98.15	Fe	-0.625	0.106	0.402	0.402	3.990
comp 16	0.14	0.77	98.92	K	0.149	0.683	0.488	0.488	4.840
comp 17	0.12	0.64	99.56	Na	0.784	0.162	0.641	0.641	6.354
comp 18	0.08	0.44	100	Mn	0.076	0.633	0.406	0.406	4.030

Variance PCA 4				Loading PCA 4					
	eigenvalue	percentage of variance	cumulative percentage of variance	name	Dim.1	Dim.2	coord	cos2	contrib
comp 1	6.76	37.53	37.53	Discharge	-0.19	0.55	0.33	0.33	3.92
comp 2	3.33	18.49	56.03	Pb	-0.15	0.78	0.63	0.63	7.44
comp 3	1.2	6.68	62.7	PbFlux	-0.17	0.65	0.45	0.45	5.35
comp 4	1.16	6.46	69.16	Prec	-0.12	0.64	0.42	0.42	4.98
comp 5	1.04	5.79	74.95	pH	0.39	-0.29	0.24	0.24	2.77
comp 6	0.81	4.48	79.43	Cond	0.93	0.06	0.87	0.87	10.22
comp 7	0.75	4.16	83.59	Temp	0.22	0.37	0.19	0.19	2.22
comp 8	0.58	3.21	86.8	STD	0.37	0.56	0.44	0.44	5.23
comp 9	0.51	2.81	89.61	Alcalinity	0.90	0.09	0.82	0.82	9.63
comp 10	0.39	2.15	91.76	OD	-0.10	-0.18	0.04	0.04	0.49
comp 11	0.37	2.03	93.79	SO4-2	0.81	0.00	0.66	0.66	7.76
comp 12	0.35	1.93	95.71	Cl	0.36	-0.15	0.15	0.15	1.77
comp 13	0.24	1.32	97.04	Ca	0.76	-0.13	0.59	0.59	6.93
comp 14	0.18	1	98.03	Mg	0.73	-0.30	0.62	0.62	7.28
comp 15	0.15	0.84	98.88	Fe	0.29	0.50	0.33	0.33	3.88
comp 16	0.12	0.64	99.52	K	0.80	0.33	0.75	0.75	8.87
comp 17	0.08	0.43	99.95	Na	0.91	0.09	0.84	0.84	9.94
comp 18	0.01	0.05	100	Mn	-0.15	0.30	0.11	0.11	1.33

Variance PCA 3				Loading PCA 3					
	eigenvalue	percentage of variance	cumulative percentage of variance	name	Dim.1	Dim.2	coord	cos2	contrib
comp 1	5.6	31.12	31.12	Discharge	-0.005	0.507	0.257	0.257	2.551
comp 2	2.89	16.08	47.2	Pb	0.005	0.752	0.565	0.565	5.606
comp 3	1.8	10.03	57.22	PbFlux	0.006	0.791	0.625	0.625	6.200
comp 4	1.29	7.17	64.39	Prec	-0.086	0.526	0.284	0.284	2.813
comp 5	1.03	5.74	70.13	pH	0.070	-0.513	0.268	0.268	2.662
comp 6	0.91	5.04	75.18	Cond	0.899	0.047	0.811	0.811	8.037
comp 7	0.8	4.43	79.61	Temp	-0.359	0.116	0.143	0.143	1.414
comp 8	0.63	3.5	83.11	STD	0.919	0.048	0.847	0.847	8.400
comp 9	0.59	3.28	86.4	Alcalinity	0.407	-0.485	0.401	0.401	3.971
comp 10	0.55	3.03	89.43	OD	-0.934	0.012	0.872	0.872	8.643
comp 11	0.51	2.81	92.24	SO4-2	0.905	-0.281	0.899	0.899	8.910
comp 12	0.4	2.25	94.48	Cl	0.715	0.315	0.610	0.610	6.053
comp 13	0.3	1.64	96.12	Ca	0.894	-0.006	0.799	0.799	7.923
comp 14	0.21	1.17	97.3	Mg	0.873	0.073	0.767	0.767	7.603
comp 15	0.15	0.85	98.15	Fe	-0.625	0.106	0.402	0.402	3.990
comp 16	0.14	0.77	98.92	K	0.149	0.683	0.488	0.488	4.840
comp 17	0.12	0.64	99.56	Na	0.784	0.162	0.641	0.641	6.354
comp 18	0.08	0.44	100	Mn	0.076	0.633	0.406	0.406	4.030

Variance PCA 4				Loading PCA 4					
	eigenvalue	percentage of variance	cumulative percentage of variance	name	Dim.1	Dim.2	coord	cos2	contrib
comp 1	6.76	37.53	37.53	Discharge	-0.19	0.55	0.33	0.33	3.92
comp 2	3.33	18.49	56.03	Pb	-0.15	0.78	0.63	0.63	7.44
comp 3	1.2	6.68	62.7	PbFlux	-0.17	0.65	0.45	0.45	5.35
comp 4	1.16	6.46	69.16	Prec	-0.12	0.64	0.42	0.42	4.98
comp 5	1.04	5.79	74.95	pH	0.39	-0.29	0.24	0.24	2.77
comp 6	0.81	4.48	79.43	Cond	0.93	0.06	0.87	0.87	10.22
comp 7	0.75	4.16	83.59	Temp	0.22	0.37	0.19	0.19	2.22
comp 8	0.58	3.21	86.8	STD	0.37	0.56	0.44	0.44	5.23
comp 9	0.51	2.81	89.61	Alcalinity	0.90	0.09	0.82	0.82	9.63
comp 10	0.39	2.15	91.76	OD	-0.10	-0.18	0.04	0.04	0.49
comp 11	0.37	2.03	93.79	SO4-2	0.81	0.00	0.66	0.66	7.76
comp 12	0.35	1.93	95.71	Cl	0.36	-0.15	0.15	0.15	1.77
comp 13	0.24	1.32	97.04	Ca	0.76	-0.13	0.59	0.59	6.93
comp 14	0.18	1	98.03	Mg	0.73	-0.30	0.62	0.62	7.28
comp 15	0.15	0.84	98.88	Fe	0.29	0.50	0.33	0.33	3.88
comp 16	0.12	0.64	99.52	K	0.80	0.33	0.75	0.75	8.87
comp 17	0.08	0.43	99.95	Na	0.91	0.09	0.84	0.84	9.94
comp 18	0.01	0.05	100	Mn	-0.15	0.30	0.11	0.11	1.33

CAPÍTULO 2

Comparison of stochastic and machine learning models in streamflow forecasting of a small basin in northeast Brazil

Abstract

Brazil has a great abundance of aquatic ecosystems, although, it does not have many monitoring programs, causing failures to produce basic information such as flow and precipitation values. Thus, the objective of this study was to compare prediction methods and choose the one that best fits two temporal situations, establishing a path for future studies that run into the same difficulties. The time series of flow and precipitation of the estuary of Serinhaém, BA, whose flowmeter was discontinued by ANA, were used and from there, the linear regression models, ARMA, ARIMA, SARIMA and MLP were tested and compared. The series were separated into T1 and T2 to observe which dataset subdivision was sufficient to promote differences in the flow forecast. The linear regression models presented the worst performances for the prediction of flow values in both time intervals. Among the autoregressive models, it was observed that the SARIMA models for the T1 interval presented the most reliable results. For the MLP models, the interval with the highest reliability in the prediction was also T1, indicating that for this region increasing the amount of data in the training subset did not cause differences for the prediction of the data. Among the autoregressive models and the MLP models, the last ones were the ones that presented the best performances during the prediction of the flow values, being therefore, the indicated in this study for presenting more robustness and reliability.

Keywords: Stochastic models, Neural network, Linear models, Estuary, Hydrological variables.

1. Introduction

Water resources are part of a multitude of essential processes for civilizations, both for survival and for carrying out various activities (e.g., irrigation of agricultural areas, energy generation and navigation). Therefore, proper planning for the use and conservation of these resources becomes of paramount importance (Adamowski et al., 2012; Vieira et al., 2020).

A planned management of water resources needs information about environmental variables of aquatic ecosystems, such as precipitation, water temperature, indices that measure water quality and flow (Alkasassbeh, 2013;

Biswas, 2004). The forecast of these parameters and the scenarios derived from these forecasts plays an important role in the greater efficiency of resource management, with a plan about which measures should be taken for each foreseen scenario. Therefore, estimating the flow values of river systems serves to predict and mitigate possible damage in flood events, water shortages and also assist in planning food production and animal husbandry (Alsmadi, 2017).

Therefore, the use of techniques to estimate the variables related to water quality has been widely used in recent years. In addition to reducing the costs of proper management of water resources, the modeling techniques of environmental parameters are reliable and efficient, capable of determining the future values of variables related to water quality (Martin-Ortega et al., 2011; Rajaei et al., 2020).

Data-driven models are less complex as they depend only on a historical series of the variable used, aiming to produce results that can estimate the variable of interest. Examples of these types of models are Linear Regression (LR) and Autoregressive Integrated Moving Average Models (ARIMA). Because they are models that use linear approaches end up failing to capture non-linear dynamics of the data (Nourani and Komasi, 2013; Nur Adli Zakaria et al., 2021).

From this perspective, in the last two decades, machine learning models have been extensively studied because they have the advantage of dealing with large amounts of data and the ability to model nonlinear dynamics (Nayak et al., 2005). An important example of this type of model is artificial neural networks (ANN), models inspired by human neural networks, that have an adaptive capacity to produce the expected result when enough training samples are used (Mosavi et al., 2018; Rajaei et al., 2020). The comparison of the accuracy of linear models with non-linear models is well studied in the literature, and it is observed that the ANN have greater precision to estimate the parameters of water quality (Danandeh Mehr et al., 2015; Khairuddin et al., 2019; Rajaei et al., 2020; Yaseen et al., 2016).

LR models are generally expressed by a simple linear function of a response variable being predicted by one or more predictor variables and an error term (**Eq.1**) (Hyndman and Athanasopoulos, 2018). When more than one

predictor is present, the regression is called Multiple Linear Regression (MLR) (Bangdiwala, 2018). Making use of metrics to compare the accuracy of tested models is one of the main advantages of these methods of predicting values, as they are easy and simple to implement (Adamowski and Karapataki, 2010).

$$Y = \alpha_0 + \alpha_i X + \varepsilon \quad (\text{Eq.1})$$

In which:

α_0 : *intercept*;

α_i : *slope*;

ε : *random error term*;

X : *predictor variable*;

Y : *value to be predicted*.

The ANN models are based on artificial intelligence and when comparing them with the LR it was observed, in most studies, that the ANN have greater accuracy for predicting water quality variables (Alp and Cigizoglu, 2007). However, the major obstacle in the prediction of hydrological and environmental processes lies in the non-linear relationship between these processes in aquatic ecosystems, making the accuracy of these estimates difficult (Rajaei et al., 2020).

1.1 Autoregressive Moving Average Models

Autoregressive moving average models (ARMA) are used to model univariate and stationary time series, being more effective in linear time series (Box et al., 1977). These models are derived from autoregressive models and pure moving average models (Adamowski and Karapataki, 2010; Zhang and Moore, 2015) and its main limitation is assuming that the series are linear and follow a normal distribution (Irvine and Eberhardt, 1992; Zhang, 2003).

The composition of ARMA models has two components, the autoregressive (AR) and the moving averages (MA). The AR component estimates values for the dependent variable based on previous values using the regression function (Irvine and Eberhardt, 1992; Tealab, 2018), while the MA

component is related to past random fluctuations which are contained in the time series (Tealab, 2018). The junction of the two components in the ARMA model statistically represents the time series in a parsimonious model, whose objective is to estimate fewer parameters. Furthermore, the combination of these models provides the necessary flexibility to predict the results from the interaction between seasonal components and random fluctuations, which are contained in the time series of hydrological variables (Irvine and Eberhardt, 1992).

1.1 Autoregressive Integrated Moving Average Models

ARIMA models are extremely flexible and can be used to model a wide range of univariate time series, such as series that contain seasonal components, unlike ARMA models (Zhang, 2003). The major disadvantage of ARIMA models is the impossibility of dealing with non-linear patterns. Thus, in these models it is assumed that the values to be predicted are a linear function of the previous observations together with random errors (Mehrmolaei and Keyvanpour, 2016; Zhang, 2003).

These models are expressed as ARIMA (p,d,q), in which “p” is the parameter of the AR component, the “q” is the parameter of the MA component and the parameter “d” is the degree of differentiation involved (Wang et al., 2015). According to the methodology proposed by Box-Jenkins, there are three steps to correctly identify the model, to predict the parameters and to check the residuals. Furthermore, it is known that time series from ARIMA processes contain theoretical autocorrelation properties (Zhang, 2003).

Thus, to identify the probable models for the time series, the autocorrelation and partial autocorrelation functions are used. However, before that, it is necessary that the data be transformed if they are not stationary. In this case, power and differentiation transformations are performed to remove the trend and make the data homoscedastic to fit the model (Adamowski and Karapataki, 2010).

A stationary time series is one whose mean and autocorrelation remain constant over time, this characteristic is extremely important to estimate future values in time series. Finally, errors are checked to assess whether the model is correctly fitted, using diagnostic statistics and residual plots. To choose the model

that best fits, a comparison is usually performed between the statistics that measure the model's accuracy, and the one with the lowest value of the used statistic is chosen to estimate the unknown values (Mehrmolaei and Keyvanpour, 2016; Zhang, 2003).

1.2 Artificial Neural Network

ANN are flexible statistical models that have the ability to identify non-linear relationships and patterns between input data and output data, with the ability to estimate output values from training and learning processes (Antanasijević et al., 2013; Heddami, 2014). These models were based on the structures of biological neurons, their connections and the transmission of information, presenting three components: (1) nodes or neurons, (2) weights (connection strength) and (3) an activation function (transfer) (Damian, 2019; Dogan et al., 2009). ANNs can be organized in several architectures, the simplest are composed of two layers, one for input (predictors) and one for output (predictions), other architectures contain an intermediate layer called hidden neurons, such as MLP networks (*multilayer perceptron*) (Damian, 2019; Hyndman and Athanasopoulos, 2018). Each predictor is accompanied by a coefficient known as a weight and these weights are selected through a learning algorithm whose objective is to minimize the costs of the function (Hyndman and Athanasopoulos, 2018).

MLP networks are formed by a simple input layer of neurons (perceptron), one or several hidden layers and an output layer, are the most used for hydrological modeling (Oyebode and Stretch, 2019; Zadeh et al., 2010). There are several types of activation functions, linear or not (linear, gaussian, logistic, sigmoid), and they depend on the type of network, the learning algorithm and the method used (Bennett et al., 2013). In most studies of hydrological data, the activation function commonly used is the sigmoid, which is a feedforward function, that is, it presents positive propagation (Maier and Dandy, 2000).

1.3 Statistical comparison

There are a variety of precision measures to compare statistical methods of time series analysis (*e.g.*, RMSE, MSE, MAE, MAPE, MASE, AIC and BIC). To be a good accuracy validator, the measurement used must be informative and

clearly summarize the distribution of errors (Chen et al., 2017). In addition, it must also validate the construction, include computational complexity, be scale independent, be sensitive to change and interpretability (Chen et al., 2017).

Absolute error measures are known as dependent scale, so they can only be used for data of the same scale. In addition, they are very sensitive to outliers, providing conservative values. The RMSE and MSE measurements may present different results depending on the fraction of the data used, thus being unreliable (Hyndman and Koehler, 2006; Koutsandreas et al., 2021; Shcherbakov et al., 2013).

Measurements based on error percentages have some disadvantages such as apparent division by zero when the value is less than the actual value. Outliers influence the results, especially when they are greater than the maximum value of the expected cases. In this way, these error measures become biased, which can lead to incorrect evaluations of the performance of the models (Hyndman and Koehler, 2006; Koutsandreas et al., 2021; Shcherbakov et al., 2013).

The scale error measures are symmetric and little influenced by outliers, containing only two disadvantages, division by zero can happen in specific cases, such as when the horizon of real values to be predicted are equal to each other and in analogous experiments, in which it is possible to observe a weak bias (Hyndman and Koehler, 2006; Koutsandreas et al., 2021; Shcherbakov et al., 2013).

In this way, choosing only one precision measure to evaluate the performance of the models is almost impossible, since all of them have some disadvantages, requiring a combination of precision measures to reduce the chance of error when choosing the best prediction model (Chen et al., 2017; Hyndman and Koehler, 2006; Koutsandreas et al., 2021; Shcherbakov et al., 2013).

1.4 Case Study

The data used in the statistical models were applied in a case study, in order to compare the accuracy of the stochastic, linear regression and neural

network models, to evaluate which would be the best to predict the flow values of the study region. In addition, two percentages of dataset division were tested to assess which would be the most effective in adjusting the data, given that many studies point to an increase in accuracy when there is an increase in the amount of data used in the training dataset. Monthly monitoring was carried out by the National Water Agency (ANA), with the aid of a flowmeter installed in the city of Ituberá, BA (-13.78, -39.17), which was discontinued in April 2019. The beginning of flow data is from 1966 and data validation is guaranteed by periodic calibration of the equipment.

The estuary of the Serinhaém River is part of the Pratigi Environmental Protection Area (EPA), forming part of the Camamu Bay, the second largest basin present in the state of Bahia (**Figure 1**). This area has great tourist potential and, as it is an estuarine system, it is characterized by being a very rich environment, with remnants of forests, mangroves and sandbanks, making it prone to suffering anthropogenic impacts related to tourism. This aquatic ecosystem presents a huge gap in information, since it is a poorly studied area. Another characteristic that should be highlighted in this environment is the absence of a marked seasonality, with the presence of rain throughout the year. Despite this, the month of July is pointed out as the wettest and the month of September as the driest (Carneiro et al., 2021; Da Silva Santos and Nolasco, 2017; de Amorim et al., 2015).

2. Methodology

The rainfall samples used for the linear regression were extracted from the rain gauge located in Camamu, BA (-13.93, -39.16). The total number of samples is 660, from 1966 to 2020, however, only data from 1966 to 2019 (637) were used in this study, to be equal to the fluviometric data range.

The total number of samples extracted from the fluviometer was 637, totaling 53 years (1966-2019) of sampling. The dataset was divided into two subsets, calibration and validation. In addition, two-time intervals were used in the data set, the first (T1) refers to 75% of the data set, as is usually done in most studies - totaling 476 samples (1966 to 2005). In the validation set of the models, the remaining 166 samples were used, corresponding to 25% of the data set

(2005 to 2019). The second time interval (T2) (1966 to 2011) is related to 85% of the data set, totaling 589 data in the calibration set and 53 in the validation set that refers to the last 4 years of samples. The data were normalized according to the minimum and maximum method (**Eq.2**), which linearizes the original data to improve the training convergence rate (Han et al., 2012; Wang et al., 2021).

$$\frac{x'_i = (x_i - \min(x))}{(\max(x) - \min(x))} \quad (\text{Eq. 2})$$

The models were compared with each other, and the one whose error statistic was the lowest was chosen. **Table S1** presents the descriptive statistics values of the data.

2.1 Stationarity

Stationarity must be measured to assess the effect of seasonality and trend in the time series, whose presence affects the mean and variance of the series over time. Traditional methods of time series analysis require some kind of stationarity to work, so stationarity must be measured before choosing method structures. There are several methods for measuring stationarity, also known as the unit root test. Two tests were used in this study: the augmented Dickey Fuller test (ADF) and the Kwiatkowski–Phillips–Schmidt–Shin test (KPSS). The ADF has the null hypothesis of the existence of a unit root, therefore, non-stationary, and the alternative hypothesis that it is stationary (**Eq.3**) (Adamowski and Karapataki, 2010).

$$H_0 : \pi = 0, \text{non - stationary series}; \quad (\text{Eq.3})$$

$$H_1 : \pi < 0, \text{stationary series}.$$

The KPSS test assumes the premise that the null hypothesis predicts that the series is stationary, that is, that there is no unit root (**Eq.4**) (Dickey and Fuller, 1979; Hyndman and Athanasopoulos, 2018; Kwiatkowski et al., 1992; Mocanu-Vargancsik and Tudor, 2020).

$$H_0 : \text{stationary series}; \quad (\text{Eq.4})$$

$$H_1 : \text{non - stationary series}.$$

2.2 Development of ARMA and ARIMA models

The structural hyperparameters (p, d, q) and (P, D, Q) of the ARMA and ARIMA models were determined before training, as described above, with the help of graphs of autocorrelation function (ACF) and partial autocorrelation function (PACF) which are shown in **Figure 2**. The presence of seasonality is observed with a 12-month cycle. The lags of the ACF graph decay exponentially indicating that there is no trend in the data (**Figure 2**).

Altogether, 28 ARMA models, 44 ARIMA models and 325 autoregressive seasonal moving averages (SARIMA) models were performed for the T1 interval and 27 ARMA, 55 ARIMA and 299 SARIMA models for the T2 interval. The models were optimized by the least square algorithm and the residuals tested for normality and independence. The performance of the models was evaluated by the AICc in both training and test datasets. And they were used for comparison with other statistical methods (ANN and Regression) and prediction of flow values.

The ACF plot shows high and significant lag at seasonal 12 (**Figure 2**) and non-significant after these. Therefore, the value of the hyperparameter “ q ” was tested and specified in $\{0,1,3\}$. The values of parameters “ p ” and “ P ” according to the PACF graph were tested and specified in $\{1,2,3\}$.

2.3 Development of ANN models

The feedforward neural network had its parameters determined and trained to choose the model. 96 models were tested, for both time intervals (T1 and T2), with the hidden layer (hidden nodes) ranging from 1 to 16. The tested lags were from 1 to 24, the learning rate was from 0.001 to 0.03 and the activation functions for the Logistic Sigmoid and Hyperbolic Tangent (tahn) and the one whose MSE presented the lowest value was chosen (**Table S2**).

3. Results and Discussion

3.1 Performance evaluation of ARMA, ARIMA and SARIMA models

The models were tested by trial and error after defining the maximum hyperparameter value shown in the ACF and PACF graphs (**Figure 2**). When

evaluating the first-time interval (T1), the model that best fitted was ARMA (2,0,2) (RMSE 1.4554; NRMSE 0.6731; MAE 1.0677; MASE 0.4622). For the second time interval (T2), the ARMA model that best fitted the data was ARMA (3,0,3) (RMSE 1.5503; NRMSE 0.5104; MAE 1.2138; MASE 0.4325). When comparing both models, it is possible to observe that the errors in the validation periods are close, but in some error measures (NRMSE and MASE) the second temporal approach seems to fit better in the data adjustment (**Table 1**).

However, a large difference in errors is not observed, as previously found in other studies that also compare temporal approaches (Aghelpour and Varshavian, 2020). According to Sun et al., (2019), despite the wide use of traditional ARMA models for the prediction of hydrological models, they present flaws in their performance in areas where there is a weak correlation between river flow data and where the frequency of extreme events is high, as is the case in the study region.

Regarding the ARIMA models, the model that presented the lowest statistics in the T1 approach was ARIMA (5,1,3) (RMSE 1.4387; NRMSE 0.6654; MAE 1.0618; MASE 0.4596). When comparing this model with the ARMA model (2,0,2), chosen for the same time interval, the ARIMA model presented the lowest error statistics, except for the value of MASE and NRMSE, demonstrating that the presence of the parameter (d), whose objective is to make the series stationary, not promoting a great improvement in the fit of the data, as expected (Valipour et al., 2012).

Among the models of the second approach (T2), the one that presented the lowest statistics was the ARIMA model (0.1.0) (RMSE 1.5955; NRMSE 0.5253; MAE 1.2203; MASE 0.4348) (**Table 2**). Analyzing the error measures of the T2 approach for both statistical models (ARMA and ARIMA), an increase in the performance of the models was also not observed, indicating that perhaps splitting the data set by 85% did not cause a difference in the modeling of the data of the study area.

ARIMA models with seasonal differentiation, that is, SARIMA models, when compared for both temporal approaches (T1 and T2), exhibited the statistical behavior already observed in previous models, with the T1 model,

SARIMA (1,1,2) (1.0.0) (RMSE 1.4666; NRMSE 0.5762; MAE 1.0927; MASE 0.4730) showing at least one error statistic lower than those of the T2 SARIMA model (2,1,1) (0,0,2) (RMSE 1.6910; NRMSE 0.5567; MAE 1.2721; MASE 0.4533) (**Table 3**). Despite small differences between the two temporal approaches, there was no significant gain in the performance of the models in the fit of the data, as seen in the previous models. However, previous studies pointed to the reliability of SARIMA models to predict long periods of time. Thus, among the stochastic models, the one that would bring more reliable flow results would be the SARIMA model of the T1 temporal approach (Alonso Brito et al., 2021). Furthermore, Yazar, (2014), found similar results when using SARIMA models to estimate flow values in the Sakarya basin, Turkey.

Bazrafshan et al., (2015), tested the ARIMA and SARIMA models to discuss a probable difference between monthly flow values and at different seasonal times. The authors observed that for the studied area (Karkheh Basin in west of the Iran), the seasonal models did not present a good performance when compared to the monthly prediction models, as observed in this study. Unlike other studies, the increase in the autoregressive parameters and moving average did not provide a decrease in the errors of the ARMA and SARIMA models (Aghelpour et al., 2021; Valipour et al., 2013, 2012). In this study, an opposite behavior was observed, with an increase in the error measurements of these two models along with the increase in the parameters (Aghelpour et al., 2021; Valipour et al., 2013, 2012).

When comparing the stochastic models (ARMA, ARIMA and SARIMA) for the time interval T1, the ARIMA model (5,1,3) presented the best performance. On the other hand, for the T2 interval, the best performance was that of the ARMA model (2,0,2), however, without a significant gain in performance. Errors did not show very different values.

3.2 Performance evaluation of MLP models

The structure of the MLP models was chosen through trial and error. When comparing the T1 models, the best fit was the 5-5-1 with the tangential activation function and the learning rate of 0.01 (RMSE 0.08328; MAE 0.05741; MASE 0.02424). For the T2 models, the structure that best fitted the data was the 5-5-

1, with a tangential activation function and a learning rate of 0.001 (RMSE 1.0054; NRMSE 0.3950; MAE 0.9046; MASE 0.3340) (**Table 4**). Contrary to the models seen previously, in the case of MLP, the model of the time interval T2 presented all the error statistics greater than those of the interval T1, showing that increasing the amount of data in the training dataset did not lead to big differences for the prediction of the data. Contrary to the findings of other studies, which claim that increasing the amount of data used for calibration and validation of models helps to increase their performance in the forecasting phase (Mourad et al., 2005).

3.3 Performance evaluation of Linear Regression models

Linear regression models were made with the actual values of precipitation and flow for both time intervals (T1 and T2). Comparing both temporal intervals, it is observed that the T1 interval presented a better performance than the T2. This behavior was seen in previous models, corroborating the fact that for the study area, the increase in the amount of data with the division by 85% did not influence the statistical models used to predict the flow values. When observing the error statistics referring to the data validation dataset, it is clear that regression is not the ideal statistical approach to predict flow values, despite presenting similar statistics with the other models (**Table 5**). However, linear regression performed well in predicting future data on variables in other studies, such as for water temperature (Graf et al., 2019), river flow (Patel et al., 2016) and precipitation (Swain et al., 2017).

Rezaeianzadeh et al., (2014), compared linear regression models and neural networks with different selections of data used to predict river flow from Khosrow Shirin watershed, located in the Fars Province of Iran. The authors observed values similar to those obtained in this study, in models in which the data used were the real precipitation data, showing that tests with other data intervals should perhaps be performed. However, other factors influence the performance of linear regressions, such as the correlations between variables and time interval (Wang, 2006), which may be responsible for the low accuracy of the model. In addition, the study area does not have well-demarcated seasonal seasons, which may have caused this low performance of the model.

4. Statistical comparison between the performance of the approached models

The performances of the models in relation to the coefficient of determination (R^2) are shown in the scatter plots (**Figure 3**). The R^2 value confirms that the linear regression presented the worst performances for the flow prediction for both time intervals ($R^2= 6.33\%$; $R^2= 20.69\%$, respectively). The low performance of linear regression models may be related to the fact that in this basin, in particular, the precipitation values are not enough to describe the flow phenomena and that, probably, the inclusion of other variables would increase the accuracy of the models (Swain et al., 2017; Tabari et al., 2010).

The ARMA autoregressive models ($R^2= 54.49\%$; $R^2= 58.13\%$), ARIMA ($R^2= 59.07\%$; $R^2= 58.94\%$) and SARIMA ($R^2= 54.02\%$; $R^2= 49, 28\%$) showed similar performances to predict future flow values for both temporal approaches, T1 and T2, respectively, according to the values of R^2 . However, the R^2 values for T1 were slightly higher than the T2 values, except for the ARMA model, demonstrating that the models of the first temporal approach fit better than those of the second, probably related to the increase in variance and bias, which may have occurred in the T2 interval (Šafránková et al., 2010). Unlike the other models, the two MLP exhibited a different performance in relation to the two-time intervals, with the model of the second temporal approach (T2) presenting a better fit than the T1 model. In addition, the values found are higher than the values considered optimal for these models ($R^2 \geq 60\%$), ($R^2= 81,36\%$; $R^2= 96,41\%$, respectively) (Aghelpour and Varshavian, 2020).

Time series plots display the relationship between observed values and predicted values for both time intervals (**Figure 4**). When analyzing the figure, it is evident that the fit of the linear regression models is poor for both intervals (T1 and T2). These models were not able to represent all time series variations in any of the time intervals, showing a low overlap, with the highest predicted values being $8.79 \text{ m}^3\cdot\text{s}$ and $6.97\text{m}^3\cdot\text{s}$ and the lowest $3.33 \text{ m}^3\cdot\text{s}$ and $3.67 \text{ m}^3\cdot\text{s}$ for T1 and T2, respectively. These values are different from the observed data, in which the highest value was $13.92 \text{ m}^3\cdot\text{s}$ and the lowest was $0.48 \text{ m}^3\cdot\text{s}$, corroborated by the scatter plots and the low R^2 value (**Figure 4**).

The stochastic models (ARMA, ARIMA and SARIMA) showed a good fit, with the predicted series almost overlapping the observed series. However, the MLP models showed an almost perfect fit for the T2 interval, while for the T1 interval the overlap seems perfect, which may be related to the fact that the coefficient of variation of the T1 interval is smaller than the coefficient of variation of the T2 interval. It is known that the lower the coefficient of variation, the greater the uniformity of the data, causing an increase in the accuracy of the prediction (**Figure 4, Table S1**) (Abyaneh, 2014). Therefore, these four models seem to efficiently record the existing variations in river flow, with flow peaks and minimums, in addition to dependence on previous values, as observed in other studies (Londhe and Charhate, 2010).

Most studies that approach stochastic models observe a good performance to estimate future values of short time scales (e.g., one month ahead). However, for longer scales, these models begin to show a decrease in the accuracy in estimating the values (Bazrafshan et al., 2015; Mishra and Desai, 2006). Despite this, studies involving some type of prediction model (ARIMA, LR, SARIMA) report that when comparing the final results, the models that present the best performances are the MLP models, as observed in this study (Adamowski and Karapataki, 2010; Ghorbani et al., 2016; Graf et al., 2019).

Although the scatter plots and the flow series plots show that the stochastic models would be as good as the MLP models for estimating the flow values of the Serinhaém River estuary, the error statistics show that the MLP model for the interval T1 is the one that best fits the data and the one that presents the best performance in estimating the values (**Table 4**). In addition, the data prove that the division of the data, whose interval T2 refers, does not cause significant alterations in the estimated flow values. Thus, the suggested interval to estimate the flow values in this area would be T1, whose period of values encompasses the largest amount of data.

5. Conclusion

The prediction models must take into account the factors that influence the parameter to be estimated. In the case of the Serinhaém River estuary, BA, the flow time series, as it is extremely uniform, does not seem to be influenced by

other environmental factors in the region. The division of the data in the interval T2, of 85%, did not cause differences in the hydrological data of the study area and therefore, the complete time series presented greater robustness and explanation in the prediction of the data. Thus, only the linear regression did not present a good fit of the data.

Although some studies point out great differences in the error measures when comparing temporal approaches, this was not observed in this study, probably related to the few changes suffered in the physical characteristics of the basin in question. The lack of sudden changes that could alter the stationarity of the model demonstrated that the addition of the parameter “d” did not promote an improvement in the fit of the data. In addition, it was also observed that the increase in autoregressive parameters and moving averages did not improve the performance of the model.

The stochastic models presented a good performance and fit in the data and can be used to predict the flow values of the area. However, the MLP models exhibited a greater robustness in the fit of the data and smaller errors associated with the model. Thus, although stochastic models are simpler and easier to use, MLP neural networks are the most suitable for predicting the flow in this region because they provide greater data reliability.

Acknowledgements

This study was financed in part by the Coordenação de Aperfeiçoamento de Pessoal de Nível Superior – Brazil (CAPES) – Finance Code 001.

Conflict of interest

The authors declared that they have no conflicts of interest to this work. We declare that we do not have any commercial or associative interest that represents a conflict of interest in connection with the work submitted.

Data Availability

The datasets generated and analysed during this study are available in our GitHub repository:

<https://github.com/Luisamsv/Serinha-mdata>

7. References

Abyaneh, H.Z., 2014. Evaluation of multivariate linear regression and artificial neural networks in prediction of water quality parameters. *J Environ Health Sci Eng* 12, 6–13. <https://doi.org/10.1186/2052-336X-12-40>

Adamowski, J., Fung Chan, H., Prasher, S.O., Ozga-Zielinski, B., Sliusarieva, A., 2012. Comparison of multiple linear and nonlinear regression, autoregressive integrated moving average, artificial neural network, and wavelet artificial neural network methods for urban water demand forecasting in Montreal, Canada. *Water Resour Res* 48, 1–14. <https://doi.org/10.1029/2010WR009945>

Adamowski, J., Karapataki, C., 2010. Comparison of Multivariate Regression and Artificial Neural Networks for Peak Urban Water-Demand Forecasting: Evaluation of Different ANN Learning Algorithms. *J Hydrol Eng* 15, 729–743. [https://doi.org/10.1061/\(asce\)he.1943-5584.0000245](https://doi.org/10.1061/(asce)he.1943-5584.0000245)

Aghelpour, P., Bahrami-Pichaghchi, H., Varshavian, V., 2021. Hydrological drought forecasting using multi-scalar streamflow drought index, stochastic models and machine learning approaches, in northern Iran. *Stochastic Environmental Research and Risk Assessment* 35, 1615–1635. <https://doi.org/10.1007/s00477-020-01949-z>

Aghelpour, P., Varshavian, V., 2020. Evaluation of stochastic and artificial intelligence models in modeling and predicting of river daily flow time series. *Stochastic Environmental Research and Risk Assessment* 34, 33–50. <https://doi.org/10.1007/s00477-019-01761-4>

Alkasassbeh, M., 2013. Predicting of Surface Ozone Using Artificial Neural Networks and Support Vector Machines. *International Journal of Advanced Science and Technology* 55, 1–12.

Alonso Brito, G.R., Rivero Villaverde, A., Lau Quan, A., Ruíz Pérez, M.E., 2021. Comparison between SARIMA and Holt–Winters models for forecasting monthly streamflow in the western region of Cuba. *SN Appl Sci* 3. <https://doi.org/10.1007/s42452-021-04667-5>

Alp, M., Cigizoglu, H.K., 2007. Suspended sediment load simulation by two artificial neural network methods using hydrometeorological data. *Environmental Modelling and Software* 22, 2–13. <https://doi.org/10.1016/j.envsoft.2005.09.009>

Alsmadi, M.K., 2017. Forecasting river flow in the USA using a hybrid metaheuristic algorithm with back-propagation algorithm. *Scientific Journal of King Faisal University* 18, 13–24.

Antanasijević, D., Pocajt, V., Povrenović, D., Perić-Grujić, A., Ristić, M., 2013. Modelling of dissolved oxygen content using artificial neural networks: Danube River, North Serbia, case study. *Environmental Science and Pollution Research* 20, 9006–9013. <https://doi.org/10.1007/s11356-013-1876-6>

Bangdiwala, S.I., 2018. Regression: simple linear. *Int J Inj Contr Saf Promot* 25, 113–115. <https://doi.org/10.1080/17457300.2018.1426702>

Bazrafshan, O., Salajegheh, A., Bazrafshan, J., Mahdavi, M., Fatehi Maraj, A., 2015. Hydrological Drought Forecasting using ARIMA Models (Case Study: Karkheh Basin) *TT - Mdrsjrns* 3, 1099–1117.

Bennett, C., Stewart, R.A., Beal, C.D., 2013. ANN-based residential water end-use demand forecasting model. *Expert Syst Appl* 40, 1014–1023. <https://doi.org/10.1016/j.eswa.2012.08.012>

Biswas, A.K., 2004. Integrated water resources management: A reassessment: A water forum contribution. *Water Int* 29, 248–256. <https://doi.org/10.1080/02508060408691775>

Box, G.E.P., Jenkins, G.M., Reinsel, G.C., 1977. Time Series Analysis: Forecasting and Control. *Journal of Marketing Research* 14, 269. <https://doi.org/10.2307/3150485>

Carneiro, L.M., Dourado, G.B., de Carvalho, C.E.V., da Silva Júnior, J.B., de Jesus, T.B., Hadlich, G.M., 2021. Evaluation of the concentrations of elements at trace level in the Serinhaem River estuary, Bahia, Brazil, using chemometric tools. *Mar Pollut Bull* 163, 111953. <https://doi.org/10.1016/j.marpolbul.2020.111953>

Chen, C., Twycross, J., Garibaldi, J.M., 2017. A new accuracy measure based on bounded relative error for time series forecasting. *PLoS One* 12, 1–23. <https://doi.org/10.1371/journal.pone.0174202>

Da Silva Santos, I., Nolasco, M., 2017. Modelagem de Fundo do Estuário do Serinhaém – Ba: Morfologia e Granulometria / Modeling of the bottom of Serinhaém's estuary, BA: Morphology and Granulometry. *Caderno de Geografia* 27, 247. <https://doi.org/10.5752/p.2318-2962.2017v27n49p247>

Damian, D.C., 2019. A Critical Review on Artificial Intelligence Models in Hydrological Forecasting How Reliable are Artificial Intelligence Models. *International Journal of Engineering Research and* V8. <https://doi.org/10.17577/ijertv8is070123>

Danandeh Mehr, A., Kahya, E., Şahin, A., Nazemosadat, M.J., 2015. Successive-station monthly streamflow prediction using different artificial neural network algorithms. *International Journal of Environmental Science and Technology* 12, 2191–2200. <https://doi.org/10.1007/s13762-014-0613-0>

de Amorim, F.N., Rezende, L.F., Cirano, M., Lessa, G.C., Hajte, V., da Silva, P.M. da C.A., 2015. Oceanographic characteristics of camamu bay (14°s, Brazil) during dry and wet conditions. *Revista Brasileira de Geofísica* 33, 637–650. <https://doi.org/10.22564/rbgf.v33i4.764>

Dickey, D.A., Fuller, W.A., 1979. Distribution of the Estimators for Autoregressive Time Series With a Unit Root. *J Am Stat Assoc* 74, 37–41. <https://doi.org/10.1080/01621459.1979.10482531>

Dogan, E., Sengorur, B., Koklu, R., 2009. Modeling biological oxygen demand of the Melen River in Turkey using an artificial neural network technique. *J Environ Manage* 90, 1229–1235. <https://doi.org/10.1016/j.jenvman.2008.06.004>

Ghorbani, M.A., Zadeh, H.A., Isazadeh, M., Terzi, O., 2016. A comparative study of artificial neural network (MLP, RBF) and support vector machine models for river flow prediction. *Environ Earth Sci* 75, 1–14. <https://doi.org/10.1007/s12665-015-5096-x>

Graf, R., Zhu, S., Sivakumar, B., 2019. Forecasting river water temperature time series using a wavelet–neural network hybrid modelling approach. *J Hydrol (Amst)* 578, 124115. <https://doi.org/10.1016/j.jhydrol.2019.124115>

Han, J., Kamber, M., Pei, J., 2012. *Data Mining: Concepts and Techniques*. Elsevier.

Heddam, S., 2014. Generalized regression neural network-based approach for modelling hourly dissolved oxygen concentration in the Upper Klamath River, Oregon, USA. *Environmental Technology (United Kingdom)* 35, 1650–1657. <https://doi.org/10.1080/09593330.2013.878396>

Hyndman, R.J., Athanasopoulos, G., 2018. *Forecasting : principles and practice*, 2nd ed. OTexts, Melbourne, Australia.

Hyndman, R.J., Koehler, A.B., 2006. Another look at measures of forecast accuracy. *Int J Forecast* 22, 679–688. <https://doi.org/10.1016/j.ijforecast.2006.03.001>

Irvine, K.N., Eberhardt, A.J., 1992. Multiplicative, seasonal ARIMA models for Lake Erie and Lake Ontario water levels. *Water Resources Bulletin* 28, 385–396.

Khairuddin, N., Aris, A.Z., Elshafie, A., Sheikhy Narany, T., Ishak, M.Y., Isa, N.M., 2019. Efficient forecasting model technique for river stream flow in tropical environment. *Urban Water J* 16, 183–192. <https://doi.org/10.1080/1573062X.2019.1637906>

Koutsandreas, D., Spiliotis, E., Petropoulos, F., Assimakopoulos, V., 2021. On the selection of forecasting accuracy measures. *Journal of the Operational Research Society* 0, 1–18. <https://doi.org/10.1080/01605682.2021.1892464>

Kwiatkowski, D., Phillips, P.C.B., Schmidt, P., Shin, Y., 1992. Testing the null hypothesis of stationarity against the alternative of a unit root. How sure are we that economic time series have a unit root? *J Econom* 54, 159–178. [https://doi.org/10.1016/0304-4076\(92\)90104-Y](https://doi.org/10.1016/0304-4076(92)90104-Y)

Londhe, S., Charhate, S., 2010. Comparaison de techniques de modélisation conditionnée par les données pour la prévision des débits fluviaux. *Hydrological Sciences Journal* 55, 1163–1174. <https://doi.org/10.1080/02626667.2010.512867>

Maier, H.R., Dandy, G.C., 2000. Neural networks for the prediction and forecasting of water resources variables: A review of modelling issues and applications. *Environmental Modelling and Software* 15, 101–124. [https://doi.org/10.1016/S1364-8152\(99\)00007-9](https://doi.org/10.1016/S1364-8152(99)00007-9)

Martin-Ortega, J., Giannoccaro, G., Berbel, J., 2011. Environmental and Resource Costs Under Water Scarcity Conditions: An Estimation in the Context of the European Water Framework Directive. *Water Resources Management* 25, 1615–1633. <https://doi.org/10.1007/s11269-010-9764-z>

Mehrmolaei, S., Keyvanpour, M.R., 2016. Time series forecasting using improved ARIMA. *2016 Artificial Intelligence and Robotics, IRANOPEN 2016* 92–97. <https://doi.org/10.1109/RIOS.2016.7529496>

Mishra, A.K., Desai, V.R., 2006. Drought forecasting using feed-forward recursive neural network. *Ecol Modell* 198, 127–138. <https://doi.org/10.1016/j.ecolmodel.2006.04.017>

Mocanu-Vargancsik, C., Tudor, G., 2020. On the linear trends of a water discharge data under temporal variation. Case study: The upper sector of the Buzău river (Romania). *Forum Geografic* 19, 37–44. <https://doi.org/10.5775/FG.2020.041.I>

Mosavi, A., Ozturk, P., Chau, K.W., 2018. Flood prediction using machine learning models: Literature review. *Water (Switzerland)* 10, 1–40. <https://doi.org/10.3390/w10111536>

Mourad, M., Bertrand-Krajewski, J.L., Chebbo, G., 2005. Calibration and validation of multiple regression models for stormwater quality prediction: Data partitioning, effect of dataset size and characteristics. *Water Science and Technology* 52, 45–52. <https://doi.org/10.2166/wst.2005.0060>

Nayak, P.C., Sudheer, K.P., Rangan, D.M., Ramasastri, K.S., 2005. Short-term flood forecasting with a neurofuzzy model. *Water Resour Res* 41, 1–16. <https://doi.org/10.1029/2004WR003562>

Nourani, V., Komasi, M., 2013. A geomorphology-based ANFIS model for multi-station modeling of rainfall-runoff process. *J Hydrol (Amst)* 490, 41–55. <https://doi.org/10.1016/j.jhydrol.2013.03.024>

Nur Adli Zakaria, M., Abdul Malek, M., Zolkepli, M., Najah Ahmed, A., 2021. Application of artificial intelligence algorithms for hourly river level forecast: A case study of Muda River, Malaysia. *Alexandria Engineering Journal* 60, 4015–4028. <https://doi.org/10.1016/j.aej.2021.02.046>

Oyebode, O., Stretch, D., 2019. Neural network modeling of hydrological systems: A review of implementation techniques. *Nat Resour Model* 32. <https://doi.org/10.1111/nrm.12189>

Patel, S., Hardaha, M.K., Seetpal, M.K., Madankar, K.K., 2016. Multiple Linear Regression Model for Stream Flow Estimation of Wainganga River. *American Journal of Water Science and Engineering* . <https://doi.org/10.11648/j.ajwse.20160201.11>

Rajaei, T., Khani, S., Ravansalar, M., 2020. Artificial intelligence-based single and hybrid models for prediction of water quality in rivers: A review. *Chemometrics and Intelligent Laboratory Systems* 200, 103978. <https://doi.org/10.1016/j.chemolab.2020.103978>

Rezaeianzadeh, M., Tabari, H., Arabi Yazdi, A., Isik, S., Kalin, L., 2014. Flood flow forecasting using ANN, ANFIS and regression models. *Neural Comput Appl* 25, 25–37. <https://doi.org/10.1007/s00521-013-1443-6>

Šafránková, J., Annual Conference of Doctoral Students (19 2010.06.01-04 Prague), WDS'10 (19 2010.06.01-04 Prague), Week of Doctoral Students 2010 (19 2010.06.01-04 Prague), 2010. Data Splitting. Matfyzpress.

Shcherbakov, M.V., Brebels, A., Shcherbakova, N.L., Tyukov, A.P., Janovsky, T.A., Kamaev, V.A. evich, 2013. A survey of forecast error measures. *World Appl Sci J* 24, 171–176. <https://doi.org/10.5829/idosi.wasj.2013.24.itmies.80032>

Sun, Y., Niu, J., Sivakumar, B., 2019. A comparative study of models for short-term streamflow forecasting with emphasis on wavelet-based approach. *Stochastic Environmental Research and Risk Assessment* 33, 1875–1891. <https://doi.org/10.1007/s00477-019-01734-7>

Swain, S., Patel, P., Nandi, S., 2017. A multiple linear regression model for precipitation forecasting over Cuttack district, Odisha, India. 2017 2nd International Conference for Convergence in Technology, I2CT 2017 2017-Janua, 355–357. <https://doi.org/10.1109/I2CT.2017.8226150>

Tabari, H., Marofi, S., Sabziparvar, A.A., 2010. Estimation of daily pan evaporation using artificial neural network and multivariate non-linear regression. *Irrig Sci* 28, 399–406. <https://doi.org/10.1007/s00271-009-0201-0>

Tealab, A., 2018. Time series forecasting using artificial neural networks methodologies: A systematic review. *Future Computing and Informatics Journal* 3, 334–340. <https://doi.org/10.1016/j.fcij.2018.10.003>

Valipour, M., Banihabib, M.E., Behbahani, S.M.R., 2013. Comparison of the ARMA, ARIMA, and the autoregressive artificial neural network models in forecasting the monthly inflow of Dez dam reservoir. *J Hydrol (Amst)* 476, 433–441. <https://doi.org/10.1016/j.jhydrol.2012.11.017>

Valipour, M., Banihabib, M.E., Behbahani, S.M.R., 2012. Parameters estimate of autoregressive moving average and autoregressive integrated moving average models and compare their ability for inflow forecasting. *J Math Stat* 8, 330–338. <https://doi.org/10.3844/jmssp.2012.330.338>

Vieira, O.E., Sandoval-Solis, S., Pedrosa, A.V., Ortiz-Partida, J.P., 2020. *Integrated Water Resource Management, Integrated Water Resource Management*. Springer. https://doi.org/10.1007/978-3-030-16565-9_3

Wang, W., 2006. *Stochasticity, Nonlinearity and Forecasting of Streamflow Processes*. IOS Press, Amsterdam, Netherlands.

Wang, X., Tian, W., Liao, Z., 2021. Statistical comparison between SARIMA and ANN's performance for surface water quality time series prediction. *Environmental Science and Pollution Research* 28, 33531–33544. <https://doi.org/10.1007/s11356-021-13086-3>

Wang, Z., Wang, Y., Zhao, P., Chen, L., Yan, C., Yan, Y., Chi, Q., 2015. Metal release from contaminated coastal sediments under changing pH conditions: Implications for metal mobilization in acidified oceans. *Mar Pollut Bull* 101, 707–715. <https://doi.org/10.1016/j.marpolbul.2015.10.026>

Yarar, A., 2014. A Hybrid Wavelet and Neuro-Fuzzy Model for Forecasting the Monthly Streamflow Data. *Water Resources Management* 28, 553–565. <https://doi.org/10.1007/s11269-013-0502-1>

Yaseen, Z.M., Jaafar, O., Deo, R.C., Kisi, O., Adamowski, J., Quilty, J., El-Shafie, A., 2016. Stream-flow forecasting using extreme learning machines: A case study in a semi-arid region in Iraq. *J Hydrol (Amst)* 542, 603–614. <https://doi.org/10.1016/j.jhydrol.2016.09.035>

Zadeh, M.R., Amin, S., Khalili, D., Singh, V.P., 2010. Daily Outflow Prediction by Multi Layer Perceptron with Logistic Sigmoid and Tangent Sigmoid Activation Functions. *Water Resources Management* 24, 2673–2688. <https://doi.org/10.1007/s11269-009-9573-4>

Zhang, P.G., 2003. Time series forecasting using a hybrid ARIMA and neural network model. *Neurocomputing* 50, 159–175. [https://doi.org/10.1016/S0925-2312\(01\)00702-0](https://doi.org/10.1016/S0925-2312(01)00702-0)

Zhang, Z., Moore, J.C., 2015. Autoregressive Moving Average Models. *Mathematical and Physical Fundamentals of Climate Change* 239–290. <https://doi.org/10.1016/b978-0-12-800066-3.00008-5>

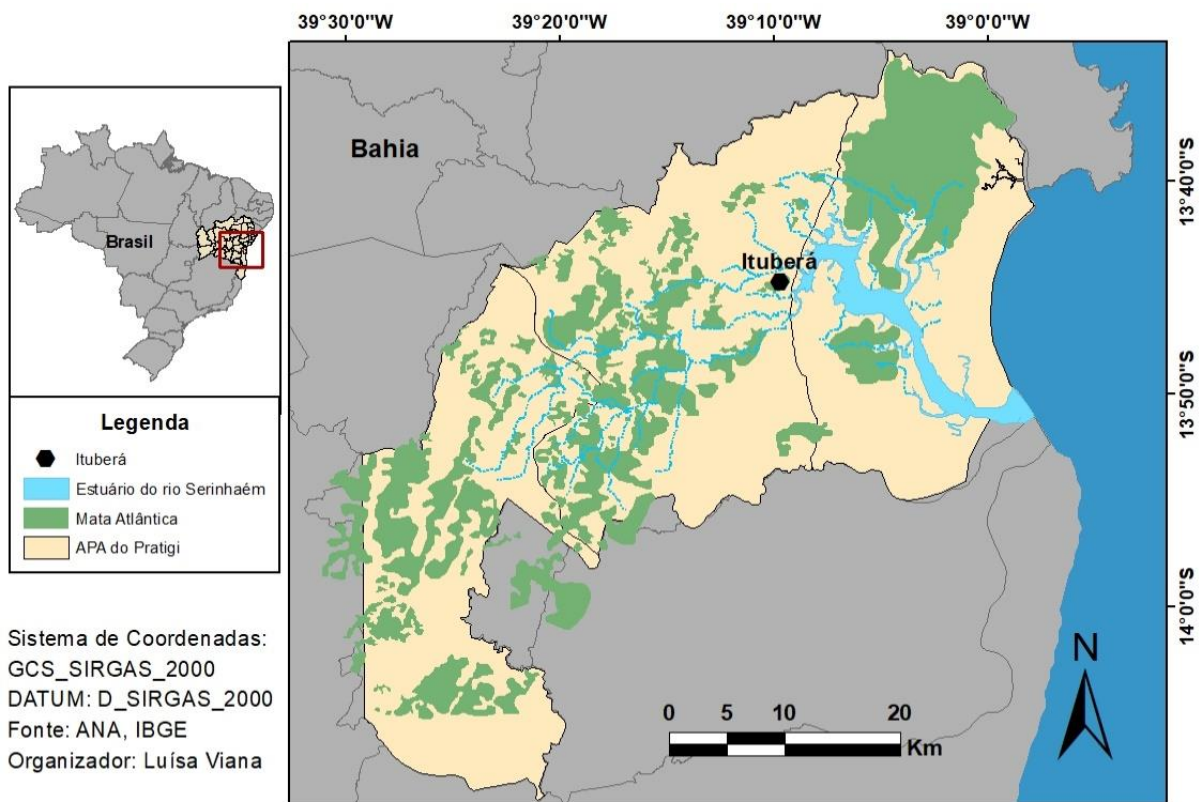


Figure 1 – Study area.

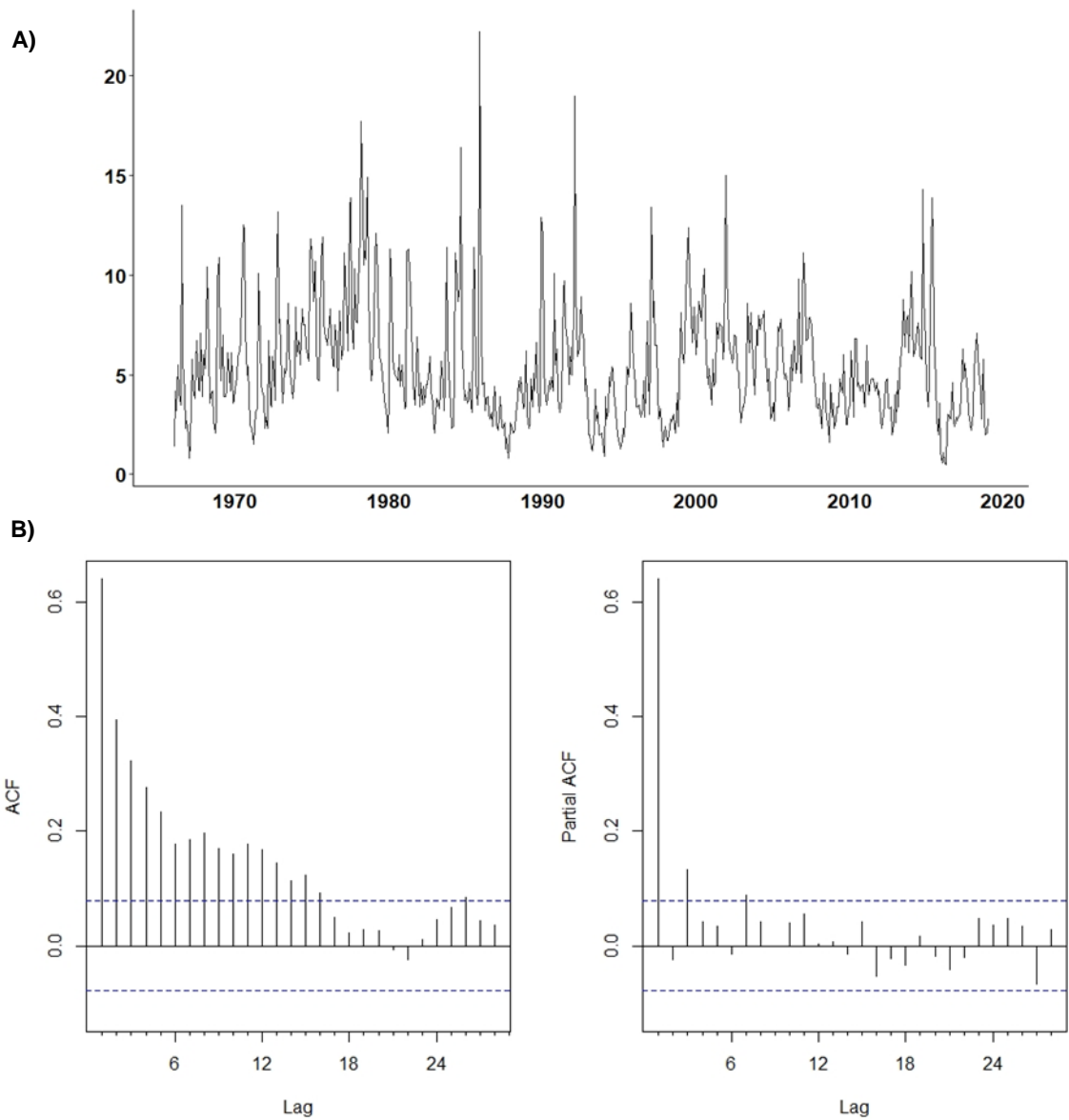


Figure 2 – A) Time series of the flow of the Serinhaém estuary, BA from 1966 to 2019; B) ACF and C) PACF graphics.

Table 1 – Accuracy statistics of ARMA models.

Calibration							Validation					
Models (T1)	R ²	MSE	RMSE	NRMSE	MAE	MASE	R ²	MSE	RMSE	NRMSE	MAE	MASE
ARMA (1,0,2)	0.3992	5.5211	2.3497	0.7735	1.5395	0.5398	0.5437	2.13	1.46	0.67	1.07	0.46
ARMA (3,0,0)	0.3987	5.4999	2.3452	0.7721	1.5320	0.5372	0.5423	2.12	1.46	0.67	1.07	0.46
ARMA (1,0,1)	0.3808	5.6753	2.3823	0.7843	1.5539	0.5449	0.5351	2.16	1.47	0.68	1.09	0.47
ARMA (2,0,1)	0.3882	5.6206	2.3708	0.7805	1.5359	0.5386	0.5390	2.14	1.46	0.68	1.08	0.47
ARMA (2,0,2)	0.3988	5.4996	2.3451	0.7720	1.5302	0.5366	0.5436	2.12	1.46	0.67	1.07	0.46
ARMA (1,0,3)	0.3983	5.5295	2.3515	0.7741	1.5401	0.5400	0.5436	2.13	1.46	0.68	1.07	0.47
ARMA (3,0,1)	0.3980	5.5066	2.3466	0.7725	1.5304	0.5366	0.5419	2.12	1.46	0.67	1.07	0.46
ARMA (1,0,0)	0.3809	5.6731	2.3818	0.7841	1.5552	0.5453	0.5274	2.19	1.48	0.68	1.09	0.47
ARMA (4,0,0)	0.3977	5.4965	2.3445	0.7718	1.5248	0.5347	0.5415	2.13	1.46	0.67	1.07	0.46
ARMA (2,0,0)	0.3809	5.6715	2.3815	0.7840	1.5479	0.5428	0.5324	2.16	1.47	0.68	1.08	0.47

Calibration							Validation					
Models (T2)	R ²	MSE	RMSE	NRMSE	MAE	MASE	R ²	MSE	RMSE	NRMSE	MAE	MASE
ARMA (2,0,0)	0.3905	5.1584	2.2712	0.7477	1.4770	0.5453	0.5736	2.5179	1.5868	0.5224	1.2456	0.4438
ARMA (1,0,1)	0.3905	5.1590	2.2713	0.7477	1.4770	0.5453	0.5781	2.4914	1.5784	0.5196	1.2300	0.4382
ARMA (1,0,0)	0.3905	5.1583	2.2712	0.7477	1.4768	0.5452	0.5709	2.5336	1.5917	0.5240	1.2439	0.4432
ARMA (0,0,3)	0.3670	5.3578	2.3147	0.7620	1.5144	0.5591	0.5700	2.5389	1.5934	0.5246	1.2411	0.4422
ARMA (3,0,0)	0.4097	4.9963	2.2352	0.7359	1.4591	0.5387	0.5774	2.4952	1.5796	0.5200	1.2301	0.4383
ARMA (2,0,1)	0.3978	5.0972	2.2577	0.7433	1.4680	0.5420	0.5782	2.4905	1.5781	0.5195	1.2296	0.4381
ARMA (1,0,2)	0.4100	4.9940	2.2347	0.7357	1.4579	0.5382	0.5782	2.4903	1.5781	0.5195	1.2296	0.4381
ARMA (0,0,4)	0.3820	5.2303	2.2870	0.7529	1.4852	0.5483	0.5765	2.5007	1.5814	0.5206	1.2473	0.4444
ARMA (1,0,3)	0.4085	5.0061	2.2374	0.7366	1.4605	0.5392	0.5785	2.4891	1.5777	0.5194	1.2297	0.4382
ARMA (3,0,3)	0.4057	5.0300	2.2428	0.7383	1.4632	0.5402	0.5930	2.4033	1.5503	0.5104	1.2138	0.4325

Table 2 – Accuracy measures of ARIMA models for both temporal approaches.

Calibration							Validation					
Models (T1)	R ²	MSE	RMSE	NRMSE	MAE	MASE	R ²	MSE	RMSE	NRMSE	MAE	MASE
ARIMA(1,1,2)	0.3933	5.5570	2.3573	0.7761	1.5596	0.5469	0.5369	2.1660	1.4717	0.6806	1.0922	0.4728
ARIMA(0,1,2)	0.3945	5.6050	2.3675	0.7794	1.5929	0.5586	0.5217	2.2210	1.4903	0.6892	1.1120	0.4813
ARIMA(0,1,3)	0.3987	5.5591	2.3578	0.7762	1.5688	0.5501	0.5283	2.1913	1.4803	0.6846	1.1085	0.4799
ARIMA(1,1,3)	0.4002	5.5553	2.3570	0.7759	1.5587	0.5466	0.5457	2.1681	1.4725	0.6810	1.0908	0.4722
ARIMA(0,1,4)	0.4000	5.5481	2.3554	0.7754	1.5543	0.5450	0.5291	2.1889	1.4795	0.6842	1.1096	0.4803
ARIMA(2,1,1)	0.3909	5.5907	2.3645	0.7784	1.5398	0.5399	0.5341	2.1602	1.4698	0.6797	1.0577	0.4579
ARIMA(2,1,2)	0.3987	5.5389	2.3535	0.7748	1.5341	0.5379	0.5408	2.2200	1.4900	0.6891	1.0618	0.4596
ARIMA(0,1,5)	0.3988	5.5535	2.3566	0.7758	1.5461	0.5421	0.5303	2.1881	1.4792	0.6841	1.1135	0.4820
ARIMA(1,1,4)	0.4008	5.5279	2.3512	0.7740	1.5476	0.5427	0.5460	2.2175	1.4891	0.6887	1.0569	0.4575
ARIMA(5,1,3)	0.4151	5.2699	2.2956	0.7557	1.4980	0.5253	0.5900	2.0698	1.4387	0.6654	1.0618	0.4596

Calibration							Validation					
Models (T2)	R ²	MSE	RMSE	NRMSE	MAE	MASE	R ²	MSE	RMSE	NRMSE	MAE	MASE
ARIMA(0,1,4)	0.4103	4.9911	2.2341	0.7355	1.4723	0.5436	0.5192	2.8392	1.6850	0.5547	1.2794	0.4559
ARIMA(0,1,6)	0.4153	4.9485	2.2245	0.7323	1.4600	0.5390	0.5107	2.8891	1.6997	0.5596	1.3075	0.4659
ARIMA(0,1,3)	0.4102	4.9915	2.2342	0.7355	1.4857	0.5485	0.5008	2.9476	1.7169	0.5652	1.2944	0.4612
ARIMA(2,1,1)	0.4002	5.0762	2.2530	0.7417	1.4680	0.5420	0.5131	2.8752	1.6956	0.5582	1.2708	0.4528
ARIMA(1,1,6)	0.4136	4.9632	2.2278	0.7334	1.4605	0.5392	0.5171	2.8515	1.6887	0.5559	1.3036	0.4645
ARIMA(3,1,1)	0.4111	4.9844	2.2326	0.7350	1.4580	0.5383	0.5153	2.8619	1.6917	0.5569	1.2761	0.4547
ARIMA(0,1,0)	0.2490	6.3561	2.5211	0.8300	1.6377	0.6046	0.5689	2.5458	1.5955	0.5253	1.2203	0.4348
ARIMA(0,1,2)	0.4066	5.7045	2.3884	0.7863	1.5928	0.5881	0.4868	2.5302	1.5907	0.5237	1.2001	0.4276
ARIMA(4,1,0)	0.3812	5.2377	2.2886	0.7534	1.5354	0.5668	0.5434	2.6959	1.6419	0.5405	1.2306	0.4385
ARIMA(4,1,3)	0.4109	4.9860	2.2329	0.7351	1.4595	0.5388	0.5258	2.8000	1.6733	0.5509	1.3011	0.4636

Table 5 - SARIMA accuracy measures

Models (T1)	Calibration						Validation					
	R ²	MSE	RMSE	NRMSE	MAE	MASE	R ²	MSE	RMSE	NRMSE	MAE	MASE
SARIMA (1,1,2)(1,0,0)	0.393	5.5938	2.3651	0.7786	1.5399	0.5399	0.538	2.1509	1.4666	0.5762	1.0927	0.473
SARIMA (1,1,2)(0,0,1)	0.393	5.592	2.3647	0.7785	1.5403	0.5401	0.538	2.1517	1.4669	0.5763	1.0927	0.473
SARIMA (0,1,2)(1,0,0)	0.394	5.5778	2.3617	0.7775	1.5874	0.5566	0.521	2.2245	1.4915	0.586	1.1118	0.4813
SARIMA (0,1,2)(0,0,1)	0.394	5.5773	2.3616	0.7775	1.5876	0.5567	0.521	2.225	1.4916	0.5861	1.1118	0.4813
SARIMA (0,1,3)(1,0,0)	0.399	5.5361	2.3529	0.7746	1.5662	0.5492	0.528	2.1924	1.4807	0.5818	1.1101	0.4805
SARIMA (0,1,3)(0,0,1)	0.399	5.5361	2.3529	0.7746	1.5663	0.5492	0.528	2.1929	1.4808	0.5818	1.1101	0.4806
SARIMA (2,1,1)(1,0,0)	0.391	5.6118	2.3689	0.7799	1.5401	0.54	0.535	2.1609	1.47	0.5776	1.0966	0.4747
SARIMA (2,1,1)(0,0,1)	0.391	5.6103	2.3686	0.7798	1.5395	0.5398	0.535	2.1618	1.4703	0.5777	1.0964	0.4746
SARIMA (1,1,2)(1,0,1)	0.394	5.5758	2.3613	0.7774	1.5339	0.5378	0.538	2.1528	1.4673	0.5765	1.0931	0.4732
SARIMA (1,1,2)(0,0,2)	0.39	5.6184	2.3703	0.7803	1.5385	0.5395	0.538	2.1532	1.4674	0.5765	1.0931	0.4732
Models (T2)	Calibration						Validation					
R ²	MSE	RMSE	NRMSE	MAE	MASE	R ²	MSE	RMSE	NRMSE	MAE	MASE	
SARIMA (0,1,4)(1,0,0)	0.41	4.9936	2.2346	0.7357	1.4697	0.5426	0.519	2.8423	1.6859	0.555	1.2765	0.4548
SARIMA (0,1,4)(0,0,1)	0.41	4.993	2.2345	0.7356	1.4699	0.5427	0.519	2.842	1.6858	0.555	1.2771	0.455
SARIMA (0,1,4)(2,0,0)	0.409	5.0013	2.2364	0.7362	1.4714	0.5432	0.409	2.8652	1.6927	0.5573	1.2628	0.4499
SARIMA (0,1,4)(0,0,2)	0.409	5.0025	2.2366	0.7363	1.4716	0.5433	0.514	2.8698	1.694	0.5577	1.2633	0.4501
SARIMA (2,1,1)(0,0,2)	0.397	5.1074	2.26	0.744	1.4623	0.5399	0.516	2.8595	1.691	0.5567	1.2721	0.4533
SARIMA (2,1,1)(2,0,0)	0.431	4.8184	2.1951	0.7226	1.3983	0.5162	0.516	2.1948	1.4815	0.4877	0.8973	0.3197
SARIMA (0,1,4)(1,0,1)	0.417	4.9367	2.2219	0.7315	1.4535	0.5366	0.519	2.84	1.6852	0.5548	1.28	0.4561
SARIMA (4,1,0)(2,0,0)	0.38	5.2451	2.2902	0.754	1.5344	0.5665	0.498	2.9631	1.7214	0.5667	1.2737	0.4538
SARIMA (4,1,3)(1,0,0)	0.409	5.0049	2.2372	0.7365	1.4442	0.5332	0.581	2.4762	1.5736	0.518	1.236	0.4404
SARIMA (4,1,0)(0,0,2)	0.38	5.2473	2.2907	0.7541	1.5345	0.5665	0.498	2.9641	1.7217	0.5668	1.2713	0.453

Table 3 – MLP accuracy measures.

Models (T1)	Structure	Function	Learning Rate	Calibration						Validation					
				R ²	MSE	RMSE	NRMSE	MAE	MASE	R ²	MSE	RMSE	NRMSE	MAE	MASE
1	(5-5-1)	Logistic	0.001	0.7927	0.5219	0.7224	0.2378	0.8529	0.1813	0.7987	0.0176	0.1326	0.0521	0.0954	0.0403
2	(5-5-1)	Tanh	0.001	0.7458	0.7723	0.8788	0.2893	1.0898	0.2114	0.7673	0.0100	0.1003	0.0394	0.0695	0.0293
3	(5-5-1)	Logistic	0.003	0.7949	0.5783	0.7605	0.2504	0.7479	0.1935	0.7624	0.0146	0.1208	0.0475	0.0861	0.0364
4	(5-5-1)	Tanh	0.003	0.7753	0.7083	0.8416	0.2771	1.1200	0.2039	0.7610	0.0146	0.1208	0.0475	0.0861	0.0364
5	(5-5-1)	Logistic	0.010	0.8057	0.5491	0.7410	0.2439	0.8497	0.1933	0.7809	0.0217	0.1472	0.0578	0.1046	0.0442
6	(5-5-1)	Tanh	0.010	0.7722	0.6956	0.8340	0.2746	1.0898	0.2109	0.8136	0.0069	0.0833	0.0327	0.0574	0.0242
7	(5-5-1)	Logistic	0.030	0.6565	0.6136	0.7833	0.2579	0.6442	0.1978	0.7732	0.0140	0.1181	0.0464	0.0837	0.0354
8	(5-5-1)	Tanh	0.030	0.7713	0.7067	0.8407	0.2768	0.9144	0.2174	0.7620	0.0075	0.0865	0.0340	0.0612	0.0258

Models (T2)	Structure	Function	Learning Rate	Calibration						Validation					
				R ²	MSE	RMSE	NRMSE	MAE	MASE	R ²	MSE	RMSE	NRMSE	MAE	MASE
1	(5-1)	Logistic	0.001	0.5211	2.9809	1.7265	0.6026	1.1670	0.4192	0.8351	0.0002	1.6147	0.6344	1.4835	0.5477
2	(5-5-1)	Tanh	0.001	0.7080	2.4813	1.5752	0.5498	1.0950	0.3988	0.9641	0.0002	1.0054	0.3950	0.9046	0.3340
3	(5-1)	Logistic	0.003	0.6199	3.0863	1.7568	0.6132	1.1950	0.4292	0.8437	0.0003	1.8089	0.7107	1.6536	0.6105
4	(5-4-1)	Tanh	0.003	0.7108	2.6342	1.6230	0.5665	1.1366	0.4140	0.8994	0.0002	1.2845	0.5047	1.1215	0.4141
5	(5-1)	Logistic	0.010	0.6226	3.1522	1.7754	0.6197	1.2027	0.4320	0.8570	0.0004	1.9274	0.7573	1.7932	0.6621
6	(5-3-1)	Tanh	0.010	0.6744	2.1125	1.4535	0.5073	1.0483	0.3765	0.8797	0.0003	1.3161	0.5171	1.1744	0.4336
7	(5-1)	Logistic	0.030	0.6139	3.0670	1.7513	0.6113	1.1875	0.4265	0.8457	0.0004	1.7511	0.6880	1.5418	0.5692
8	(4-5-1)	Tanh	0.030	0.5436	2.7837	1.6685	0.5824	1.1596	0.4165	0.8649	0.0002	1.5017	0.5900	1.3552	0.5003

Table4 – Accuracy measures linear regression.

Linear Regression	Calibration						Validation					
	R ²	MSE	RMSE	NRMSE	MAE	MASE	R ²	MSE	RMSE	NRMSE	MAE	MASE
T1	0.2092	6.9551	2.6372	1.0362	1.9908	0.6043	0.0633	4.7403	2.1772	1.0069	1.6763	1.3858
T2	0.2168	6.8253	2.6125	0.9119	1.9235	0.6026	0.2069	7.6299	2.7622	0.9093	2.043	1.5632

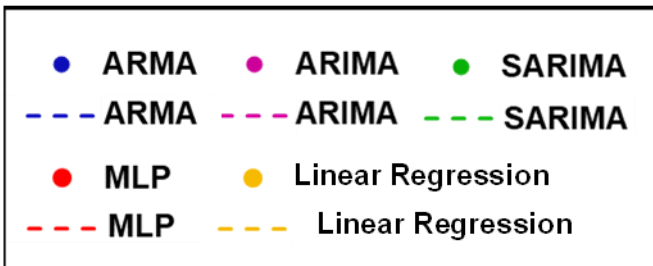
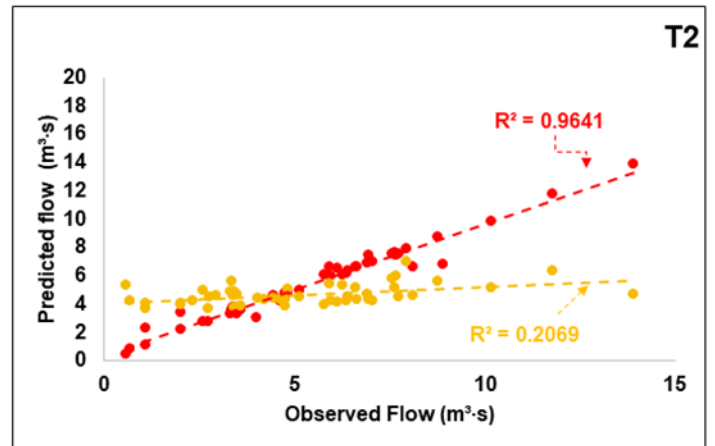
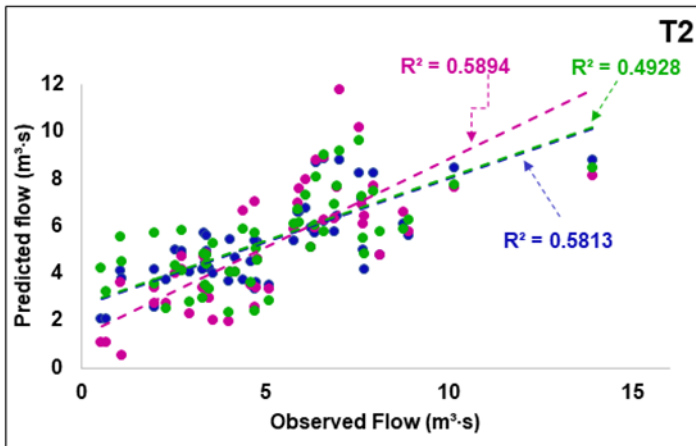
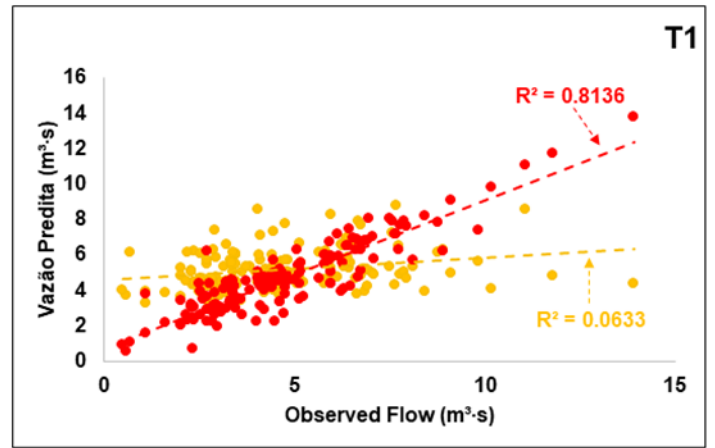
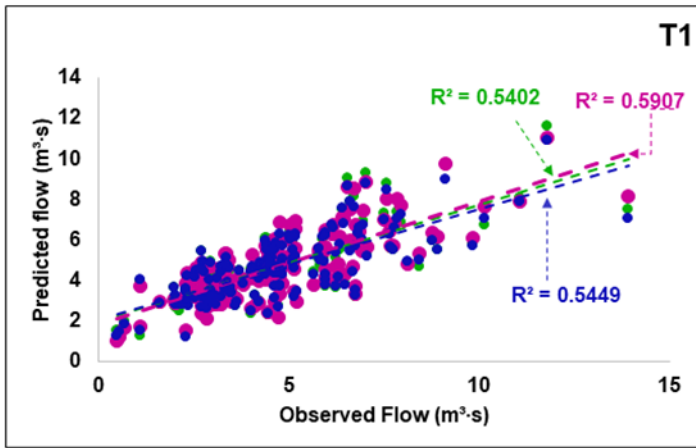


Figure 3 – Scatter plot of model regressions in both time intervals (T1 and T2).

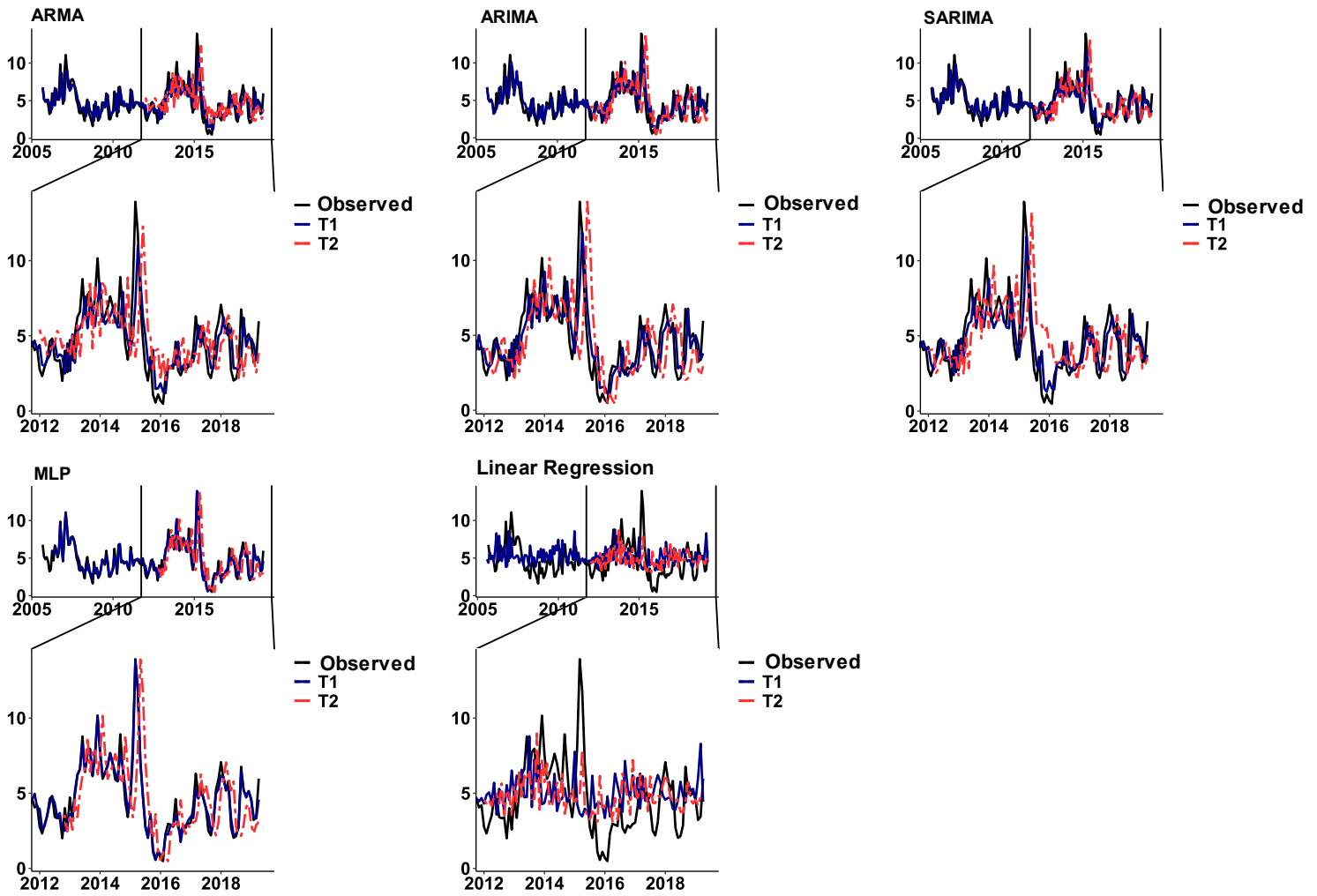


Figure 4 – Flow series predicted by the models used.

Supplementary Material

Table S1 (Page 10).

Table S5 – Descriptive statistics of the data.

	Precipitation	Flow	T1	T2
Mean	156.5	5.4	4.76	4.57
Median	143.2	4.8	4.57	4.08
Standard deviation	90.1	2.9	2.16	2.44
Minimum	0.0	0.5	0.48	0.48
Maximum	654.5	22.2	13.92	13.92
Coefficient of variation	0.57	0.53	0.45	0.53

* Descriptive statistics for intervals T1 (September 2005 to April 2019) and T2 (January 2012 to April 2019) refer to the validation time interval.

Table S2 (Page 12).

Table S6 – Hyperparameters used in the testing of neural networks.

Hyperparameters	Implications	Tested Value
frequency	Time series frequency	12
hidden nodes	hidden layers	1,2,3,4,5,6,7,8,9,10,11,12,13,14,15,16
difforder	Degree of differentiation in Lags	1
act.funct	Activation Function	sigmóide logística e tanh, reLU
lags	Lags used as inputs	1,2,3,4,5,6,7,8,9,10,11,12,13,14,15,16,17,18,19,20,21,22,23 e 24
learning rate	Learning Rate	0,003, 0,001, 0,03 e 0,01

CAPÍTULO 3

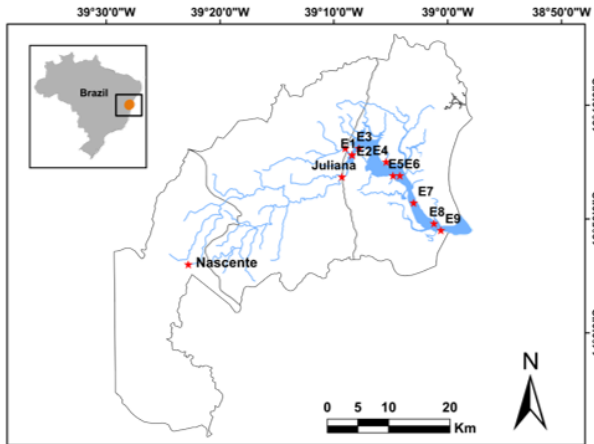
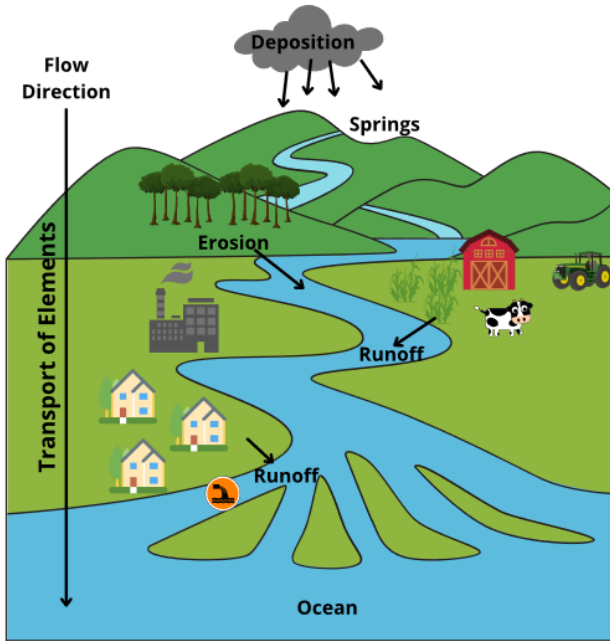
Seasonal variation, contribution and dynamics of trace elements in the drainage basin and estuary of the Serinhaém river, BA

Abstract

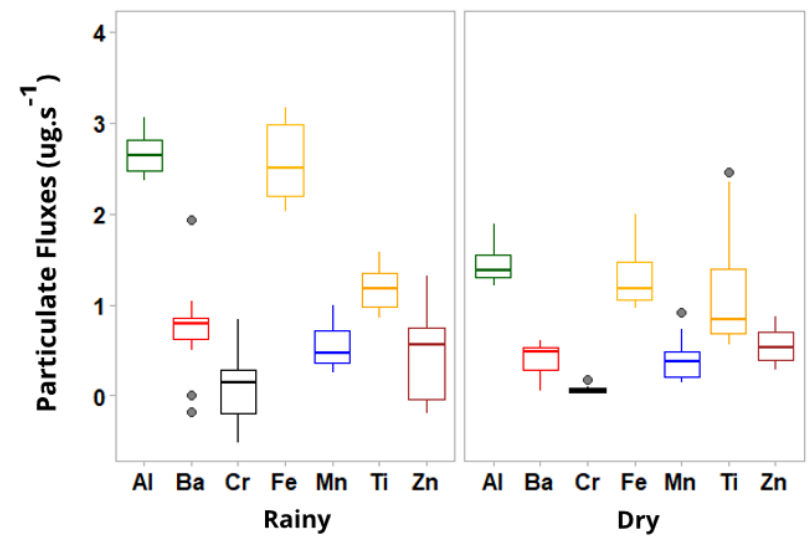
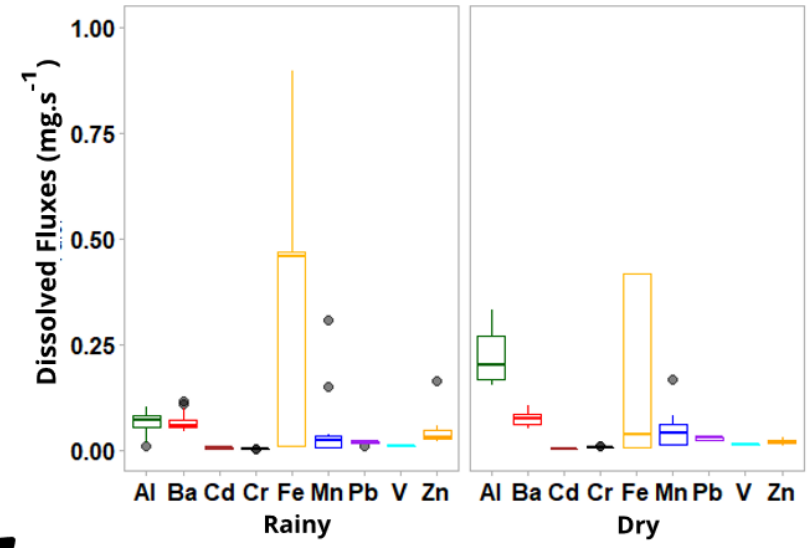
In this study, the mass balance calculation was used to quantify the fluxes of trace elements (Al, Ba, Cd, Cr, Cu, Fe, Mn, Pb, Ti, V e Zn) in the particulate and dissolved fractions of the water column, which are exported from the estuary of the Serinhaém - BA river to the Atlantic Ocean. The export of the elements in the dissolved fraction followed a uniform distribution in both campaigns, while in the particulate fraction all elements showed higher fluxes in the sampling campaign 1 towards the estuarine mouth, showing a greater export of these to the Atlantic Ocean at this season. The physical-chemical parameters varied according to the collections, with the first sampling campaign showing the highest values. This variation resulted in different behaviors of trace elements in fluvial and estuarine ecosystems, which underwent processes of removal and addition of the water column, causing changes in the distribution coefficient and in flows to the Atlantic Ocean. Thus, the trace elements present in the EPA of Pratigi, BA are controlled by the variation of environmental parameters (physical-chemical, flow and precipitation), however, despite this, the aquatic ecosystems present in the EPA, exhibit a water quality in compliance with the legislation Brazilian. As it is an Environmental Protection Area (EPA), which has the presence of economic activities and increasing urbanization, it is necessary that management and monitoring programs are constantly carried out in these areas in order to avoid contamination and an increase in exports of contaminants to the Atlantic Ocean.

Keywords: Estuary; Trace elements; Atlantic Ocean; Environmental Protection Area; Brazil.

Graphical Abstract



Flow of Elements



1. Introduction

Rivers play a key role in continental erosion, as well as being the main responsible for transporting materials from the continent to the oceans (Araujo et al., 2014; Carvalho et al., 2002; Horan et al., 2019). Erosion products, both solid and liquid, are transported from drainage basins to the oceans through estuaries, and can arrive in their original forms and/or altered by natural and anthropic processes (e.g. soil erosion, urbanization and industrial effluents) (E. Boyle et al., 1974; Kara et al., 2017). In recent years, geochemical studies that evaluated the changes suffered by trace elements on the way to the oceans have been the focus of lots of research, in order to understand the consequences for aquatic ecosystems on a regional and global scale (Kara et al., 2017).

Through studies carried out in fluvial areas, it is known that the chemistry of the waters in these was related, for the most part, to compounds from the erosion of the rocks in the drainage basins, being considered of natural origin (Azam et al., 2018; Friedrich et al., 2006). However, current studies show that the origin of chemical elements is directly related to human activities carried out in drainage basins, which alter the point and non-point sources of these elements (Azam et al., 2018; Cidu and Biddau, 2007).

In aquatic ecosystems, the particulate fraction is considered the most important tool to assess the transport of trace elements in the water column, while the dissolved fraction is relevant to analyze the bioavailability of these elements for aquatic organisms (Burger et al., 2002; Constantino et al., 2019; Constantino et al., 2022; Eggleton and Thomas, 2004). The particulate fraction presents a great binding affinity between the trace elements and the suspended particles, which are considered one of the main geochemical supports in the transport of these elements (Constantino et al., 2019; Constantino et al., 2022). In this way, each fraction provides relevant information about the geochemical signatures, transport, deposition and origin of trace elements (Friedrich et al., 2006; Lindsay et al., 1996). Also, that evaluating environmental parameters along with contaminants in both fractions (dissolved and particulate) increases the understanding of the factors influencing water quality and the interference caused by human activities in the aquatic ecosystem in question (Azam et al., 2018; V. Hatje et al., 2003a; Mosley and Liss, 2020; Richards et al., 2018).

Several tools have been used to study drainage basins over the last few years (Boongaling et al., 2018; Liu et al., 2019; Srinivas et al., 2020). However, many of them come up against the lack of hydrological information on the regions and the lack of financial stimulus, in addition to the difficulty of sampling in very large basins. Monitoring aquatic ecosystems has been much discussed in recent years, given the growing concern about the lack of water on the planet (Bunke et al., 2019; Jones and van Vliet, 2018; Ma et al., 2020). Therefore, monitoring becomes relevant for the sustainable use of ecological services.

The Mass Balance Calculation (MBC) has been used to infer about trace elements fluxes along the drainage basins in order to assist the water quality monitoring programs in region of Pratigi EPA, BA (Bidone et al., 2018; González-ortegón et al., 2019). Thus, this work aims to evaluate the partitioning of trace elements in two fractions of the water column (dissolved and particulate fractions) and the effects of physicochemical parameters on their concentrations. In addition, the fluxes of trace elements in both fractions and their exports to the Atlantic Ocean were calculated. We predicted that trace element partitioning in the Pratigi EPA would be controlled by environmental variations, mainly in the estuarine region, with transport and retention dependent on higher SPM concentration and salinity. However, we expected that the concentrations would be low or non-existent because it is an environmental protection area.

2. Materials e Methods

2.1. Study Area

The Pratigi Environmental Protection Area (EPA) is located in the south center of the state of Bahia and is part of five cities, with a total area of 859km². The hydrography of the EPA is composed mainly by the Juliana River, which flows into the Serinhaém estuary and has a drainage area of approximately 473.68 km² (MMA, 2004). The Serinhaém River estuary (**Figure 1**) has two types of tidal regime: syzygy tides with very high and low high tides; and quadrature tides with very low high tides and higher low tides. In the region, the climate is classified as Tropical Rainy Forest, with no well-demarcated sampling campaign 2, with average monthly rainfall greater than 60 mm and annual rainfall greater than 1500 mm (CRA, 2004). Pratigi EPA is part of the Central Corridor of the Atlantic Forest and has a great diversity of species of

birds, mammals, reptiles, invertebrates and amphibians. The EPA area presents a great anthropogenic pressure and, therefore, is inserted in the regions of maximum priority of biodiversity conservation (CRA, 2004).

2.2. Sampling

Two collection campaigns were carried out, one in April/2019 and one in September/2019 to incorporate the climatic variability of the region. In the region, there is no well-defined dry and flood season, it rains all year round, due to this samplings campaigns were called sampling 1 and sampling 2. According to, the information extracted from the rain gauge located in Camamu - BA (-13.93, -39.16), precipitation annual averages varying from 126 mm (February to July) to 80 mm (August to January). The flow values were calculated from a time series of 53 years of flow data from the fluvimeter located in the city of Ituberá - BA (-13.78, -39.18), using a *multilayer perceptron* (5-5-1), with 0.01 learning rate and tanh activation function (Viana et al., in preparation) (4.40 and 4.84 m³. s⁻¹, respectively). Samplings were carried out during high tide.

In total, 12 samples of surface water (40 cm) were collected, with the aid of a bucket where the sample was rinsed and then collected at each point, in a previously demarcated transect, which covers two areas of this EPA: one in a fluvial area (Juliana, Serinhaém Rivers and Nascente) and one in the Serinhaém river estuary (**Figure 1**). The samples collected were stored in 5L polyethylene bottles, previously rinsed with the sample, identified and taken to the laboratory. The physicochemical parameters of the water column (pH, electrical conductivity, dissolved oxygen and salinity) were determined *in situ* using a multiparameter probe (U-50 series, Horiba, Japan).

2.3. Analytical procedures

2.3.1. Sampling filtration

Cellulose acetate filters were used for trace elements analysis and SPM and GF/F filters were used to DOC and TN analysis, both filters were dried in an oven at 60 °C for approximately 48 hours and weighed on a digital scale accurate to four decimal places. Of the raw samples, 120 mL were vacuum filtered through glass fiber filters (Whatman® GF/F) with a porosity of 0.7 µm, and 40 mL aliquots taken in triplicate were used for analysis of dissolved organic carbon (DOC) and stored in amber flasks with 0.40 mL of phosphoric acid (H₃PO₄).

Another 600 mL of the raw sample was filtered using cellulose acetate membranes with 0.45 µm porosity, and 200 mL aliquots taken in triplicate were used for metal analysis, where later the average concentration of SPM was determined gravimetrically, according to the equation 1. Each aliquot was acidified to pH = 1 with nitric acid (HNO₃) suprapur and kept under refrigeration until chemical determinations were carried out. Water analyzes were performed in accordance with USEPA 3015a.

$$(1) \frac{SPM = (\text{filter weight with sample in mg}) - (\text{filter weight in mg})}{\text{filtered volume in L}}$$

2.3.2. Trace Elements Fluxes

(2) The gross fluxes of trace elements in the dissolved and particulate fractions were calculated using the following formulas (**Equation 2 and 3**). The distribution of river and estuarine loads was calculated from the sum of the total loads of each ecosystem. $Dissolved\ flux_{(\mu g/day)} = [M]_{(\mu g \cdot L^{-1})} \times River\ flow_{(m^3 \cdot s^{-1})}$

$$(3) Particulate\ flux_{(\mu g/day)} = [M]_{(\mu g \cdot g^{-1})} \times River\ flow_{(m^3 \cdot s^{-1})} \times [SPM]_{(mg \cdot L^{-1})}$$

2.4. Analytical procedures

2.4.1. Determination of Dissolved Organic Carbon (DOC) and Total Nitrogen (TN)

DOC and TN concentrations were determined on a TOC – VCPH analyzer (Shimadzu, Japan) by catalytic oxidation at high temperature, after acidification and purging with ultrapure air.

2.4.2. Sample solubilization

The total concentrations of aluminum (Al), cadmium (Cd), chromium (Cr), copper (Co), iron (Fe), lead (Pb), manganese (Mn), nickel (Ni), vanadium (V) and zinc (Zn) were determined in the particulate (SPM) and dissolved fractions. The extraction of the elements (pseudo-total) in the SPM for determination was performed after drying in an oven at 60° C, weighing and digestion of the filters (0.45 µm). The filters were placed in teflon tubes with 8 mL of aqua regia (HCl: HNO₃ – 3:1 (v/v)) and taken to microwave digestion (Mars Xpress, CEM, model 907501, United States). Digestion time was 80 min under the following conditions: ramp time 10 min, digestion 40 min at

180°C and cooling for 30 min. After cooling, the final extracts were filtered through Whatman® 40 paper and brought to a final volume of 20 mL in a volumetric flask.

2.4.3. Determination of trace elements and quality control

The determination of trace elements was performed in the ICP-OES equipment (Varian Liberty Series II, Australia). All analyzes were performed using three analytical blanks. The dissolved samples were analyzed in triplicate, whereas the particulate samples were analyzed using a composite sample of the filters, due to lack of sufficient weight (0.05g). Recovery values that validate the method are available in the supplement material (**Table S2**). The ICP-OES detection limits, for both matrices, are presented in the **Table S1**.

2.5. Statistical analysis

Statistical analyzes were performed in the R program ([R Core Team, 2022](#)). An ANOVA was used to compare the mean concentrations of trace elements between river and estuarine points, followed by a Tukey test. An ANOVA was also used to evaluate the influence of seasonality on the concentrations of trace elements and on the flow. Data were adjusted using a maximum likelihood function, when necessary, to meet the basic assumptions of ANOVA (normality, homoscedasticity and linearity). In addition, Principal Component Analysis (PCA) and Pearson Correlation were performed to investigate the associations between the elements and environmental parameters (Harrel Jr, 2022; Kassambara, Alboukadel Mundt, 2020; Lê and J & Husson, 2008; Wei and Simko, 2021). The tests were finally validated from the analysis of diagnostic graphs (Altman and Krzywinski, 2016). In all cases, an a priori type 1 error of 5% ($\alpha = 0.05$) was assumed. Interpolated maps were made by *Kriging* in *Arcgis* 10.5 software.

3. Results and Discussion

3.1. Environmental parameters

The physical-chemical parameters varied with distance to point 1 (Nascente) and also between seasons (**Figure 2**). Seasonally, pH, salinity, electrical conductivity and temperature were higher in the sampling campaign 1 (April) (**Figure 2**). The highest temperature values observed in the sampling campaign 1 are probably related to a greater inflow of warm water from the tributaries present in the drainage basin (Fatema et al., 2014). In addition, in tropical aquatic ecosystems, temperature has a proportional relationship with salinity, referring to the intensification of evaporation,

caused by the increase in temperature, which raises salinity levels (Fatema et al., 2014; Wolanski, 1986). From the third point (Serinhaém), there is a gradient of increase in salinity and electrical conductivity in both sampling periods, due to the greater marine influence (Rathnayake et al., 2017; I. V. Telesh and Khlebovich, 2010).

The SPM load was higher at estuarine points when compared to river points in both collections (**Figure 2**). SPM values ranged from 2.2 mg L⁻¹ to 35.6 mg L⁻¹ and 8.7 mg L⁻¹ to 21.5 mg L⁻¹ in the wet and sampling campaign 2s, respectively. The higher SPM load observed at the estuarine points may be related to the resuspension of sediments caused by the entry of denser saline water, since the collection was carried out at high tide. In addition, the intense turbidity near the estuarine mouth can also intensify the process of resuspension of the surface layer of sediments (Suzumura, 2004). When comparing the SPM concentrations of the two collections, a decrease in the values in the estuarine points is observed, being mainly related to the lower amount of rainfall in the sampling campaign 2, leading to a lower drag of particles from adjacent soils into the bodies of water (Dias et al., 2016).

Spatially, DO values were always higher at river points when compared to estuarine points, probably related to different types of metabolism in these ecosystems. At river points, there is the presence of agricultural areas, which can intensify photosynthetic rates (Wang et al., 2003). At estuarine points, low DO concentrations may be related to mangrove metabolism, which is known to promote a high respiratory rate, decreasing DO concentrations (Mattone and Sheaves, 2017). Another factor that influences DO concentrations are high temperatures, which reduce DO solubility, leading to decreased DO concentrations (Caccia and Boyer, 2005).

Seasonally, DO concentrations were higher in the sampling campaign 2 (**Figure 2**) ($p = 0,000032640$), being mainly influenced by an increase in primary productivity, facilitated by the decrease in turbidity and increase in water transparency in periods with less rainfall and, with this, there is a greater range of luminosity in the water column, favoring greater photosynthetic activity (Almeida et al., 2007; Constantino et al., 2019). The lowest DO values were found at points 1 and 6 (Nascente and E3) (4.1 mg L⁻¹ and 4.7 mg L⁻¹, respectively) of the sampling campaign 1. These low values can be explained by the greater input of effluents, from point sources, richer in organic matter, whose consequence is to increase the depletion of dissolved oxygen (O'Boyle et al., 2009; Radwan et al., 2003). In addition, environments with high temperatures

decrease the solubility of dissolved oxygen, as observed in these two sampling points (Bello et al., 2017). According to CONAMA resolution 357/2005, DO values must not be less than 6 mg L⁻¹ for freshwater ecosystems. Thus, the water quality at these two points can be considered as low (CONAMA, 2005).

Following the same direction, DOC concentrations showed the same trends as DO concentrations, with the highest values found in the sampling campaign 2 ($p = 0.0000208$), and were lower than those found in other locations in Brazil, for example: Caeté River - PA (Dittmar et al., 2001) e Sepetiba Bay - RJ (Rezende et al., 2007). Seasonal differences occur due to increased dilution in periods of higher flow in the sampling campaign 1, which carries a greater proportion of river water poorer in DOC and a lower period of residence of the waters in the estuary (Ray et al., 2018). The spatial oscillations found in the concentrations between the river and estuarine points showed an increase in relation to the transect – River Source → Serinhaém River. According to CONAMA, DOC values for saline waters should be below 3 mg L⁻¹ and, thus, the concentrations measured in the estuary of the Serinhaém River are within the recommended range (**Figure 2**) (CONAMA, 2005).

The oscillations in DOC concentrations may be related to the proximity of the points to the mangrove, as this is more evident in the estuary. In addition, this behavior has already been observed by other authors in estuarine regions with the presence of mangroves (Bouillon et al., 2007; Dittmar et al., 2001; Ray et al., 2018; Romigh et al., 2006). The increase in DOC in points close to the mangrove is probably due to its production from the mangrove vegetation, known to increase these concentrations from the production of humic substances and the leaching of sediments from these regions (Ray et al., 2018; Richard et al., 2000). Furthermore, this variation demonstrates that under these conditions, DOC entry is directly related to the metabolism of mangroves, which are known to export large amounts of DOC to adjacent oceans (Kristensen et al., 2008).

For TN, the concentrations showed significant differences between sampling campaigns ($p = 0.02713$). The third point (Serinhaém) presented the highest concentration in the sampling campaign 1 (0.59 mg L⁻¹). The seasonal differences observed in TN concentrations can be explained by the increased capture of this element in aquatic ecosystems, through photosynthetic assimilation by phytoplanktonic organisms (Damashek and Francis, 2018) and by the increase in

denitrification rates observed during the sampling campaign 1 (Alexander et al., 2009; Mulholland et al., 2008; Peterson et al., 2001). In addition to these, soil leaching and seasonal biochemical changes that occur in vegetation and through soil microorganisms associated with certain water sources, such as riparian zones and mangroves, are factors that influence TN concentrations (Arheimer et al., 1996; Burns et al., 2009; Holloway and Dahlgren, 2001; Molenat et al., 2008; Ocampo et al., 2006).

3.2. Trace elements

3.2.1 - Essentials trace elements

The essential trace elements are those whose presents importance to physiological process, mostly in cells functioning, having a crucial role as cofactors or mediator of enzymes in biochemical processes and in the production of proteins and enzymes (Shayganfard, 2022).

In this study, Fe ($p = 0.4961$), V ($p = 0.000000195$) and Cr ($p = 0.000000000193$) showed different behavior in the dissolved fraction of the water column with the higher concentration being found in the sampling campaign 2, unlike Zn ($p = 0.0056$) and Cu ($p = 0.4279$) that exhibit higher concentrations in the sampling campaign 1. Mn concentrations were high in sampling campaign 2 in almost every sampling point as the others elements, excepting the river points Nascente and Juliana. In the particulate fraction, all trace elements showed higher concentrations in the sampling campaign 1 (Figure 4). In this fraction, Al ($p = 0.000000003$), Ba ($p = 0.000001$), Cr ($p = 0.000004$), Fe ($p = 0.00001$), Mn ($p = 0.000001$), Ti ($p = 0.000000004$), V ($p = 0.00065$) and Zn ($p = 0.00042$) exhibited significant differences between the different collection campaigns.

1. Iron (Fe)

Iron plays a crucial role in metabolic processes (e.g. photosynthesis, electron transfer, nitrogen fixation, nitrate reduction) and is thus an essential element that regulates the growth of all organisms. The higher concentration of Fe in the dissolved fraction was observed in the sampling campaign 2, which may be related to a low dilution power of the river observed during the period of lower discharge (Saputro et al., 2014; Shiller and Boyle, 1987) (Figure 3). According to, (Laglera and van den Berg, 2009) most of the dissolved iron in rivers is complexed with humic substances (humic acids and fulvic acids) and transported through them.

The lack of dissolved iron from E2 point in the sampling campaign 1 can be explained for the formation of precipitates, since salinity values were higher at this seasonal time (Figure 3). In estuaries, most of the Fe in the dissolved fraction usually precipitates and coagulated in brackish zones occasioned by high salinities, that neutralize surface charges on colloidal particles. Although this happens, some of the Fe in this fraction remains available to phytoplankton in the form of organic complexes (Gustafsson et al., 2000; Kendall et al., 2012; Krachler et al., 2010; Kranzler et al., 2011; Morrissey and Bowler, 2012).

The oceans are poor in Fe and therefore biological productivity is limited. The majority of Fe that is transported to the oceans from the continents is usually in the form of oxyhydroxides, that are known as more stable forms (Kappler et al., 2021; Kendall et al., 2012). The variability exhibit in the river points (Nascente, Juliana and Serinhaém) on the sampling campaign 2, can be related to the removal of the dissolved iron from the solution to the particulate form, by precipitated in oxyhydroxide forms (Figures 3 and 4) (Kappler et al., 2021). Besides that, the non-conservative behavior of dissolved iron in the estuaries are well documented, mostly in estuarine mixing (Boyle et al., 1974; Boyle et al., 1977; Mayer, 1982; Edward R. Sholkovitz, 1978). As expected, was observed a removal process of dissolved Fe to the particulate fraction, mostly in the sampling campaign 1, intermediated by high salinity (Sholkovitz, 1978) (Figures 3 and 4).

Finally, Fe colloids originated from the fluvial waters suffers aggregations in the estuarine region due to interaction with cations as Mg^{2+} and Ca^{2+} from seawater. Furthermore, the distribution of dissolved Fe in estuaries suffers influences of the physical-chemical parameters and of adsorption and desorption process. A part of this dissolved iron is deposited in the sediments of the continental shelf, becoming unavailable (Raiswell, 2011). In the sampling campaign 2, the constant presence of iron was observed in both fractions (dissolved and particulate), probably related to the processes of removal (adsorption, flocculation, complexation and aggregation) and addition (desorption, dissolution and resuspension) of this element in the column of water, caused by the variation of physical-chemical parameters, as salinity, DOC and pH (Daneshvar, 2015).

1. Vanadium (V)

Vanadium (V) plays an important role in various metabolic processes such as chlorophyll synthesis (Wilhelm and Wild, 1984), cell division (Meisch and Benzschawel, 1978) and cell motility and photosynthesis (Gilmour et al., 1985). It is an essential element for prokaryote biochemistry (Schlesinger et al., 2017), macroalgae (Johnson et al., 2015; Wever et al., 1991) and other organisms (Wang and Sañudo Wilhelmy, 2009). In addition to being present in enzymes (Wever et al., 1991), and nitrogen fixation on plants (Bellenger et al., 2014; Darnajoux et al., 2017; Zhang et al., 2016). Despite being essential for some organisms, V is toxic for humans and others organisms (Gummow, 2011; Schiffer and Liber, 2017).

At this study V concentrations was higher in the sampling campaign 2 (Figures 3 and 4) in both the dissolved and particulate fractions, probably related to low dilution power with the lower water discharge. The presence of V in the dissolved fraction at points in the river may be related to the types of rocks being weathering or the nature of the weathering process, oil combustion or pollution and could be related to inputs from reducing sources in the drainage area (Biwa and Sugiyama, 1989; Shiller, 1997; Shiller and Mao, 2000).

The behavior of V in the estuaries are known to be conservative, but some studies point to a deviation of conservative during estuary mixing, caused by adsorption and desorption process with particulate matter and Fe and Mn oxyhydroxides (Dellwig et al., 2007; Joung and Shiller, 2016; Strady et al., 2009). V concentration in both fractions suffers process of removal in the estuary, since concentrations at some sampled points (E1 to E5) in the sampling campaign 1 was below detection limit, demonstrated biological uptake (Figures 3 and 4) (Shiller and Boyle, 1987). After point E5, the concentrations of V showed a desorption process in both seasons, caused by the increase in salinity, as observed by Strady et al., (2009) in Girond estuary, France.

2. Chromium (Cr)

Animals and plants need chromium (Cr) to carry out essential metabolic processes (e.g. glucose metabolism and cholesterol and fatty acid metabolism) (Richard and Bourg, 1991). In high levels, Cr becomes toxic and can cause serious disease as, lung cancer, skin ulcerations and nausea (Richard and Bourg, 1991; Saputro et al., 2014). Cr occurs naturally in rocks and sediments and its solubility in

water depends on the redox conditions (Gurumurthy et al., 2014; Saputro et al., 2014). The Cr concentrations observed in the dissolved fraction in the sampling campaign 1 were lower than in the sampling campaign 2, due to changes in pH range. In the sampling campaign 1, the pH values were alkaline, while in the sampling campaign 2 the values were neutral (Figures 3 and 4). Also, it is also related to the low dilution power of the rivers observed during the period of lower discharge (Saputro et al., 2014; Sherrell and Boyle, 1988).

According to Richard and Bourg, (1991) Cr dissolved in alkaline pH undergoes precipitation, being removed from the dissolved fraction to the particulate fraction, although, some species of Cr can be oxidized by dissolved oxygen and manganese oxides. Furthermore, Saputro et al., (2014) observed a maximum rate of adsorption in pH range of 6 to 9, as seen in this study in the river points, with dissolved concentrations decreasing while concentrations in the particulate fraction increase (Figures 3 and 4).

The speciation of Cr in waters, especially redox reactions, is highly dependent of pH (Gorny et al., 2016), dissolved oxygen (Goring-Harford et al., 2020), particulate organic matter (Wittbrodt and Palmer, 1997), phytoplankton (Semeniuk et al., 2016) and the concentrations of Fe and Mn (Gorny et al., 2016). According to Campbell and Yeats, (1984) constant dissociated Cr concentrations in the St. Lawrence estuary (Canadá) as was seen in this study, and a decrease in concentration caused by turbidity maximum zone together with an increase in the concentrations of SPM and salinity as seen in point E7 (Figures 3 and 4).

The increases in Cr concentrations in the particulate fraction in the estuary (Figures 3 and 4) could be related to removal from dissolved fraction by phytoplankton activities, also plankton and organic matter can influence the presence and reduction of Cr forms in SPM. Moreover, Cr concentrations in SPM are also be related to anthropogenic disturbances and natural processes (Forero López et al., 2021).

3. Zinc (Zn)

Zinc (Zn) is an essential element for being part of a variety of metalloenzymes in organisms and is a cofactor in enzymes as carbonic anhydrase, responsible for regulating the activity of specific zinc-dependent enzymes involved in crustaceans ecdysis (Gerpe et al., 2002). Zn concentrations are mostly related to the

erosion of the rocks in the drainage area, as observed in this study in which the highest concentrations were found in the fluvial area, mainly in the sampling campaign 1 (Elderfield et al., 1979). In more alkaline waters Zn suffers removal from precipitation or sorption reactions, corroborating the highest concentrations observed in the estuary in the particulate fraction (Figures 3 and 4) (Elderfield et al., 1979).

According to some authors, the behavior of Zn in the estuaries is conservatively during much of the estuarine mixing process (Chiffoleau et al., 1994a; Elderfield et al., 1979). However, studies point to a reactivity of Zn, related to the association with Fe and Mn in estuaries, demonstrating the occurrence of removal of this element from the dissolved fraction to the particulate, as observed in our results. In addition, the increase in Zn concentrations in the particulate fraction is indicated by several studies to occur due to the resuspension of surface sediments (Chiffoleau et al., 1994a; V Hatje et al., 2003). Thus, the increase in Zn concentrations, observed in the sampling campaign 1, may be related to the higher concentrations of SPM.

In addition, Zn may undergo desorption processes from suspended particles in saline environments, caused by the increase in inorganic complexation with marine anions (Cl⁻) and by the increase in the charge of particles in the water column, due to events of resuspension of sediments caused by higher river discharges in times of high water and also by tides (Ackroyd et al., 1986; Araújo et al., 2019; Pearson et al., 2017; Schäfer et al., 2009). Elements such as Zn and Cu are generally related to freshwater environments, as they undergo complexation when in the presence of ligands (organic matter and chlorides) that have the ability to complex these two divalent cations (Luoma and Davis, 1983).

4. Cooper (Cu)

Copper (Cu) is an element capable of changing its oxidation states, which makes it relevant for eukaryotic cells, because it is able to act as an electron donor or acceptor (Cruces-Sande et al., 2019; Stern, 2010). Like other essential elements, Cu acts as a cofactor for important enzymes and as a structural component of various proteins (Cruces-Sande et al., 2019). However, at high concentrations, Cu has the potential to interact with hydrogen peroxides and form reactive and unstable radicals, which cause negative effects on macromolecules (Cruces-Sande et al., 2019; Montes et al., 2014).

Cu is extremely toxic to aquatic organisms and, therefore, its release in the river systems is a concern (Apte, 2008; Lee et al., 2010). Cu speciation depends mainly on physical-chemical properties of the water, leading to Cu complexation on inorganic ligands or organic ligands (Waeles et al., 2005). The concentrations of Cu in the dissolved fraction were higher in the sampling campaign 1, mostly in the river points, that exhibit the higher concentrations in both seasons. Cu is generally related to effluent releases, surface runoff and atmospheric deposition. Therefore, a greater concentration of it is expected at the time of greater fluvial discharge and precipitation, as observed in this study (Wang et al., 2012; Zhang et al., 2014) (Figures 3 and 4).

In the estuary, Cu concentrations in the dissolved fraction were constant in several points (E1 to E4), showing a peak from point E5 to E9, in both seasons. The increase in Cu concentrations from point E5 to E9 could be related to release by phytoplankton, resuspension of sediments and desorption from suspended particles caused by salinity (Waeles et al., 2005). According to several authors, Cu behavior varies depending on the estuary. (Boyle et al., 1982), observed a conservatively behavior of Cu in the mixing zone of Amazon Estuary. Release behavior from suspended particles was seen in southeastern of U.S. estuaries by Windom et al, 1983, and a removal from solution in the estuaries of Rhine and San Francisco by Duinker and Nolting, (1976) and Eaton, (1979).

Unlike Monbet, (2004), who studied the seasonal behavior of Cu in the Morlaix river estuary in Brittany (FRA) no strong seasonal variation of Cu was observed in the Serinhaém river estuary (BA). Particulate Cu concentrations was not observed in this study in any season, probably caused by an increase in desorption process. According to Monbet, (2004), the particulate Cu concentration in the estuary is controlled by desorption and adsorption process complexation in organic ligands, can also be the cause of the lack of Cu in the particulate, since this element has a great complexation capacity (van den Berg et al., 1987).

5. Manganese (Mn)

Manganese (Mn) is an importante trace element in aquatic ecosystem and in organisms. In humans Mn is responsible for various process, as syntheses and activation of enzymes, metabolism of glucose and lipids, improve of immune system and others (Li and Yang, 2018). In aquatic ecosystems Mn is highly biogeochemically active, responds to changes in environmental conditions quickly, undergoing transfer

between the fractions of the water column and the sediment (Evans et al., 1977). Concentrations of Mn in the dissolved fraction were higher in the river points in both seasons. The control of Mn concentrations in this fraction is related to reductive processes, which may be biologically mediated or photochemically induced processes. In addition, Mn concentrations can also be controlled by physical-chemical parameters, mainly by pH, which can lead to desorption and adsorption processes. Bourg et al., (2000) observed the same trend in dissolved Mn concentrations in the Lot River in southwestern France. The author observed that as the pH increased, Mn concentrations decreased, as seen in this study at river points, during the sampling campaign 2. Also, the behavior Mn in river points, can be explained by the formation of oxides and hydroxides, since the soils in this region have high concentrations of these compounds (Complementary Material 1) (Gurumurthy et al., 2014; Mascarenhas, 2018) .

In the particulate fraction, Mn concentrations were higher in the sampling campaign 2 when compared to the sampling campaign 1 in the river points. Mn exhibits a non-conservative behavior, the lower salinity observed in the sampling campaign 2 in the initial points of the estuary (E1, E2 and E3) does not leads to a removal process of these element from the dissolved fraction to the particulate as expected. Instead, we observed high concentrations of these element on those points (Morris et al., 1982; Yan et al., 1990). Sediments can be a source of Mn to the water column, if reducing conditions occur, the manganese oxides, present in the particles, undergo reduction and release the soluble ion Mn^{2+} (Evans et al., 1977; Klinkhammer and Mcmanus, 2001). Also, in the initial points of the estuary (E1 to E4) a desorption process seems to occur, with the concentration in the particulate concentration decreasing and the concentration in the dissolved fraction increasing, contrary to what happens from point E5, where an adsorption process seems to occur, since the opposite process succeeds (Yang and Sañudo-Wilhelmy, 1998). The Mn removed from suspended particles through exchanges with the cations present in seawater (Mg^{+2} , Ca^{+2} , Na^{+}) (Wilke and Dayal, 1982).

3.2.2 Non-Essentials trace elements

6. Lead (Pb)

Non-essentials trace elements have no recognized role in organisms and even in lower concentrations are toxic (Lockitch, 1993; Papanikolaou et al., 2005). Lead (Pb) is a toxic persistent trace element in environment and their concentrations can progressively increase in water, sediments and biological tissues (Fernández Severini et al., 2011). The bioavailability of Pb is controlled mainly by pH decrease (Stouthart et al., 1994) and its main to the aquatic environment are related to anthropogenic activities, such as industrial emissions (Monbet, 2006).

Pb concentrations were higher in the sampling campaign 2 and were related to DOC (**Complementary Material 1**). According to Samani et al., (2014), there is a relationship between Pb, DOC and salinity, that promotes flocculation, explaining the decrease in concentrations of this element in the sampling campaign 1, which despite having the highest salinities exhibited lower DOC values than the seen in the sampling campaign 2. The elements in the dissolved fraction that present a positive relationship with DOC (Al, Cr, Pb and V), demonstrate a probable connection with the complexation of organic compounds (Complementary Material 1) (Gurumurthy et al., 2014). In addition, some authors discuss the role of DOC in flocculation processes in estuarine environments along with salinity, DO, and electrical conductivity (Chenar et al., 2013; Samani et al., 2014).

Many estuaries in the world have Pb concentrations above what is considered acceptable and these ecosystems are considered polluted. In contrast to this, the Serinhaém River estuary has concentrations in the dissolved fraction below acceptable levels by Brazilian legislation and no concentration in the particulate fraction (Fianko et al., 2007; Monbet, 2006; Udechukwu et al., 2015; Yan et al., 2020).

7. Aluminum (Al)

Aluminum (Al) is a non-essential trace element for organisms, however, is the third most abundant element in the Earth's crust (Jones and Ryan, 2016). Despite that, Al accumulates in humans and animal organisms, but without any role in metabolism (Exley, 2003). Al in plants exhibit toxicity for roots growth, becoming a challenge for farmers, since at low pH values mineral dissolution in soils increase and Al becomes soluble (Jones and Ryan, 2016). Human recent studies point to Al toxicity in the central nervous system, causing neurotoxicity and possibly inducing neurological disorders, such as dementia and cognitive impairment (Alasfar and Isaifan, 2021;

Exley and House, 2011; Niu, 2018). In the natural environment, Al is released from weathering of rocks in soils to aquatic ecosystems (Bezak-Mazur et al., 2001). The anthropic sources of Al are related to industrial and mineral activities (Botté et al., 2022). Al concentrations in the dissolved fraction were higher in the sampling campaign 2, mostly in river points, probably related to the weathering of rocks in the drainage area and to the low power of dilution of the river (Rotteveel and Sterling, 2020) (Rotteveel and Sterling, 2019; Botté et al., 2022). According to studies, Al in alkaline environments is found in anionic forms, in neutral Al occurs in the form of inactive aluminum hydroxide and in acidic environments in cationic forms season (Igbokwe et al., 2020; Krupińska, 2020). In this study, Al probably was found in the form of aluminum hydroxide in the sampling campaign 2 and in anionic forms in the rainy (Figures 3 and 4). In the particulate fraction, Al concentrations vary according to point sample, but despite that, the higher concentrations are found mainly in the river points (Figures 3 and 4). Senze et al., (2021) observed that the highest concentrations of Al were related to the highest surface runoff, which occurred after the season with the highest river discharge caused by the rains.

In the estuary, Al behaves non-conservatively depending on pH and salinity (Hydes' and Liss, 1977; Upadhyay, 2008), and its sources are mainly related to resuspension of the sediments, fluvial input and effluent discharges (Takayanagi and Gobeil, 2000; Wang et al., 2013; Zhou et al., 2018). The variation observed in the particulate fraction are related to the resuspension of the sediments, at the points where there is addition of Al in the solution and removal by biological uptake at the points where there is a decrease in concentrations (Brown and Bruland, 2009; Hydes' and Liss, 1977; Mackin and Aller, 1984). According to Wei-Wang et al., 2015, the process of Al adsorption to the dissolved fraction is influenced by high turbidity and salinity, which may lead to an increase in its removal from this fraction. Despite that, the high removals by salinity-induced flocculation and adsorption to SPM, observed by the author in the Huanghe Estuary in China, was not observed in this study

8. Cadmium (Cd)

Cadmium (Cd) presents toxicity to plant growth, can cause the formation of reactive oxygen species in the human organism (Benavides et al., 2005), renal damage (Rani et al., 2014), problems in the cardiovascular system (Fagerberg et al., 2012) and others, being so a non-essential trace element. Sources of Cd are related

to anthropogenic activities such as industries, domestic effluent and atmospheric deposition, it has a high solubility in water and a high toxicity for organisms (Benavides et al., 2005; Pinto et al., 2004).

The concentration of in the dissolved fraction were higher in the sampling campaign 1 of the Serinhaém Estuary, probably related to the increase in discharge in this season (Audry et al., 2004). Also, the higher concentrations were found in the river points, possible related to the input from agricultural activities present in this region (Monbet, 2004). Bourg et al., (2000) observed a inversely relation between Cd and pH and high concentrations of Cd in the sampling campaign 2, related to an increase in runoff in the Lot River in France, these trends were not observed in this study. Metzger et al., (2007) studied the dynamics of Cd dissolved in the Lagoon of Thau in the south of France. The authors noted that sediments can act as a sink for particulate Cd from the water column. This process probably occurred at river points in the study area, explaining the lack of Cd concentrations in the particulate fraction in this study.

Cd concentrations were not observed in the particulate fraction (Figures 3 and 4). Cd in estuaries behavior mostly non-conservatively with addition and removal process to the solution (Waeles et al., 2008). The lack of Cd concentrations in this fraction could be related to release of Cd from clay surfaces in the estuaries caused by higher ionic strength, formation of metal sulfides (Hao et al., 2020) and also Cd can be adsorbed in Fe- and Mn oxides and undergo deposition in sediments (Turner et al., 2008; Wen et al., 2008). Particulate Cd in the Serinhaém Estuary probably was adsorbed in Fe- Mn oxides and immobilized in the estuary induced by salinity (Turner et al., 2008).

Also, according to Waeles et al., (2004), Cd can be rapidly be desorbed from particles and be remobilized in the water column. Moreover, as it is an extremely active element during estuarine mixing, Cd is most often released from the particulate fraction and/or the colloidal phase (Dai Ap' et al., 1995; Guieu et al., 1998). Finally, Cd in the dissolved fraction can be absorbed by filtering organisms, such as oysters, since according to some studies the main source of Cd for these organisms is the dissolved fraction, and is thus removed from the water column (Denton and Burdon-Jones, 1981; Frazier', n.d.; Lekhi et al., 2008).

9. Barium (Ba)

Barium (Ba) sources to aquatic environmental are the weathering of rocks and minerals and from anthropogenic releases. Ba is a non-essential element, very toxic to animals, humans and plants and its toxicity depends on their solubility. On humans Ba free ions are absorbed by the lung or the gastrointestinal tract, and can cause renal intoxication, hypertension and cardiac malfunction (Bhoelan et al., 2014; Kravchenko et al., 2014; Oskarsson, 2015). In plants Ba can inhibit potassium uptake, photosynthetic activity and plant growth (Raghu, 2001; Sleimi et al., 2021).

In the river points, Ba concentrations in the dissolved fraction were in the sampling campaign 1, unlike the estuarine points whose highest concentrations were in the sampling campaign 2 (Figures 3 and 4). In the particulate fraction, concentrations varied according to the sample points in both seasons (Figures 3 and 4). In the Ganges-Brahmaputra River, India, Moore, (1997), observed high concentrations of Ba in the dissolved fraction occurring in the low discharge season in the mixing zone of the river, related to desorption of Ba from the sediments, contrary to this study. The concentrations of Ba may be associated with the presence of barite ore in the soils of this region and in the Camamu Bay, to which the Serinhaém estuary belongs, which can lead to high concentrations of this element in the water column due to higher drag of particles enriched by this element from adjacent soils in rainy periods (Carneiro et al., 2021; de Oliveira et al., 2009; Hatje et al., 2008).

In the estuary points, Ba concentrations in the dissolved fraction was higher in the sampling campaign 2, showing that the desorption expected induced by salinity it is not the main process responsible for the variation in Ba concentrations in the estuary of the Serinhaém River (Coffey et al., 1997). The behavior observed usually for barium in estuaries is non-conservative, with desorption from clays, however, the behavior depends on seasonality (Jeffrey S Hanor and Chan, 1977; Joung and Shiller, 2014). The distribution of Ba in this ecosystem could be affect by other process, as such, seasonal productivity-related depletion and removal by co-precipitation in Fe oxyhydroxides with subsequent flocculation (Coffey et al., 1997a; Guay and Kenison Falkner, 1998; Hilmar A Stecher and Kogut, 1999). Also, benthic inputs are extremely important in the distribution of Ba in the estuaries, by dissolution of marine barite or from desorption of the river sediments deposited in high discharge on mangroves (Carroll et al., 1993; Colbert and McManus, 2005; Dehairs et al., 1980; Falkner et al., 1993

The concentrations in the dissolved fraction in the sampling campaign 2, could be related to a kinetic/hydrodynamic mechanism. According to (Dion, 1983), at low discharge the suspended particle has the ability to be transported across the salinity gradient for greater distances until it has caused desorption, resulting in a greater maximum desorption gradient. This fact can explain the higher concentrations of dissolved Ba in estuarine points at sampling campaign 2 in the Serinhaém estuary (Figures 3 and 4). The variation observed in the particulate fraction of Ba in the estuary is related to sedimentation occurring in the mixture of river water with saltwater and to the desorption process of Ba (Bridgestock et al., 2021; Colbert and McManus, 2005).

Most of the trace elements present in suspended particles can be released through degradation of organic matter and/or diagenesis of Fe and Mn oxides/hydroxides at times of low flow (Duan et al., 2019; Thibault de Chanvalon et al., 2016). These compounds are also crucial components in the removal of trace elements from the dissolved fraction of the water column to the particulate fraction, through the sorption processes of transition metals (Turner et al., 2004; Young and Harvey, 1992).

The distribution coefficient (K_d) is widely used to describe the affinity of trace elements between particulate and dissolved phases (Table S9). The common calculation used is: K_d (L/Kg) = trace element concentration in the particulate fraction (mg/kg) / trace element concentration in the dissolved fraction (mg/L) (Boyer et al., 2018; Chiffolleau et al., 1994; Tomczak et al., 2019). K_d was calculated for each element in both collections and in each ecosystem. For the river points in the sampling campaign 1, the distribution was Al>Cr>Fe>V>Mn>Ba>Zn and in the sampling campaign 2 Al>Fe>Zn>Cr>V>Mn>Ba. The estuarine points exhibited the follow distribution, rainy: Fe>Al>Mn>Cr>Ba>Zn>V and dry: Fe>Al>Zn>Mn>Cr>Ba>V.

The distribution of estuarine points followed that observed in other studies according to the increase in the saline gradient (V. Hatje et al., 2003b; Koukina et al., 2021). The K_d of the river points evidenced the formation processes of Fe and Mn oxides in the MPS, in the complexation by the organic matter and in the formation of colloids from the variation of the environmental parameters (Barreto et al., 2011; Veselyâ et al., n.d.).

Al, Zn, V and Cr exhibited the highest K_d values in the sampling campaign 1, corroborating the greater affinity of the elements for the particulate fraction during the period of greater river discharge (Benoit and Rozan, 1999; Prabakaran et al., 2020;

Salomão et al., 2001). Fe and Mn showed the highest K_d values in the river points for the sampling campaign 2 and in the estuarine points in the sampling campaign 1. This behavior during the period of lower river flow, indicates a greater formation of Fe and Mn oxyhydroxides in this region, since the behavior observed in the estuarine points is related to the greater transport of particles in the period of greater precipitation and river discharge (Benoit and Rozan, 1999; Duc et al., 2013).

Ba exhibited a higher K_d at river points and lower at estuarine points during the sampling campaign 1, a behavior explained by the desorption processes that Ba undergoes with the increase in salinity in estuarine environments, being removed from the particulate fraction to the dissolved fraction (Coffey et al., 1997a). This behavior is corroborated by the fact that the K_d of Ba at the estuarine points is higher in the sampling campaign 2, when the salinity is lower, than in the flood season.

3.3. Relationship between physical-chemical parameters and trace elements

The data matrix used in the PCA (**Figure 5**) was composed of 25 variables and 24 observations. In this study, only the first three principal components (PCs) were considered to describe 81.51% of the total variance of the data in the PCA. In total, 44.49% of the total variance of the data was explained by PC1, 29.71% by PC2 and 7.31% by PC3. Only the first two PCs are shown, whose data variance was 74.20%.

The PCA performed between the concentrations of trace elements and the physical-chemical parameters showed a separation between the two components, PC1 related to the physical-chemical parameters and PC2 related to the different sources. The PCA shows that the river points varied between seasons with a direct relation to the behavior of the trace elements in those periods, while the estuarine points were more influenced by the physical-chemical parameters (Figure 5). Al, Cr, Pb and V in the dissolved fraction and the DO and DOC correlated among themselves, and also with the campaign of the sampling campaign 2 (all elements presented values of $p < 0.05$, except Pb x V ($p = 0.16$), and positive correlations above 42%) (Tables S6 and SY). Cu and Cd in the dissolved fraction, all trace elements found in the particulate fraction of the water column and all environmental parameter, except DOC and DO, were related to the sampling campaign 1 campaign (all with p values < 0.05 , except Zn x Cu (dissolved); TN x Zn (particulate) and TN x Cr (particulate), and positive

correlations above 40%, except for Cd and Pb, which showed inverse correlations) (Tables S6 and S7).

The behavior of trace elements largely depends on the source of these elements and on what parameters govern their speciation across aquatic ecosystems. The fact that river points vary between seasons according to the behavior of trace elements corroborates this. The trace elements that presented greater relationships with the sampling campaign 2 and the river points, demonstrate that their sources are related to the erosion of the rocks of the drainage basin, anthropic emissions and are elements, whose speciation is influenced by the variation of DOC, pH and redox conditions (Botté et al., 2022; Monbet, 2006; Shiller and Mao, 2000; Stouthart et al., 1994). All these factors were correlated with each other according to the PCA (Figure 5, Tables S6 and S7).

The relationship observed between the physicochemical parameters and the estuarine points was expected, due to the formation of the saline gradient when salt water mixes with river water (Telesh and Khlebovich, 2010). The formation of this gradient is known to influence the conservative or non-conservative behavior of trace elements within estuarine ecosystems and which processes they are more likely to undergo (addition or removal) (de Souza Machado et al., 2016). Consequently, this gradient directly influences the speciation and transport of most trace elements within estuaries (de Souza Machado et al., 2016; Millward, 1995).

Salinity and SPM load were correlated with each other, this is explained by the increase in flocculation caused by the increase in salinity, which leads to a change in hydrodynamic conditions and an increase in ionic strength (Thill et al., 2001). In addition, the entry of saline water, with different density from the river water, promotes the occurrence of zones of maximum turbidity, due to the resuspension of surface sediments (Eisma, 1986; Jiang et al., 2013). Suspended particles generally have a negatively charged surface and the change in ionic strength leads to a reduction in the repulsion existing between the particles. These, which when in contact with the salts in suspension, usually positive, brought by the entrance of sea water (Na^+ , Mg^{+2}), form larger flocs (salt-induced flocculation) (Eisma, 1986). In addition to generating more particles, this phenomenon is also known to cause an increase in their deposition near the mouths of rivers (Thill et al., 2001).

The correlation between the trace elements in the particulate fraction and the SPM load with the campaign of the sampling campaign 1 was expected due to the higher amount of rainfall and river flow in this period. In addition, SPM is the major carrier of trace elements along aquatic ecosystems. Elements bind to SPM through a variety of processes (*e.g.*, flocculation, adsorption, complexation) and can be transported over long distances to the oceans (Eckert and Sholkovitz, 1976). Also, they can also be inserted into the food chain through ingestion by the biota (Kolarova and Napiórkowski, 2021) and, finally, they can suffer deposition in surface sediments, contaminating this other compartment (Thill et al., 2001).

PCA also shows that there is a direct relationship between the concentrations of Ba, Fe and Mn in the dissolved fraction, which is probably related to the oxides/hydroxides of Fe and Mn. The Fe and Mn flocculation processes that occur in the first portions of the estuaries, whose salinity is low, provide a favorable surface for the reversible adsorption of Ba, which, when in contact with salinities ≥ 24 and with concentrations of Mg^{+2} and Ca^{2+} undergo desorption (Samanta and Dalai, 2016; Hilmar A. Stecher and Kogut, 1999). On the other hand, as observed in PCA, the correlation of Fe with Ba and Mn is weak and did not present significant p values ($r^2 = 0.45$ and 0.39 ; $p = 0.06$ and 0.12 , respectively).

In the estuary of the Serinhaém River, the Ba was probably removed from Mn oxides/hydroxides, since these two elements showed a significant correlation above 50% ($r^2 = 0.62$; $p = 0.001$). Some studies point to the relationship between these two compounds and the removal of Ba in estuaries (Coffey et al., 1997b; Samanta and Dalai, 2016). When analyzing the Hooghly estuary (India), Samanta e Dalai, (2016) also observed a positive correlation between Ba and Mn which, according to the authors, points to the probable cycling of Ba with the oxides/hydroxides of Fe and Mn.

3.4. Export of trace elements to the Atlantic Ocean

3.4.1. Export via dissolved flux

The flow of trace elements in the dissolved fraction ($mg\ s^{-1}$) is illustrated in Figures 6 and 7. Seasonally, all elements analyzed exhibited a similar behavior in both campaigns, except Al, which presented a flux present throughout the transect in the sampling campaign 1 and the highest flux values in the final portion estuary in the sampling campaign 2 (**Figure 6**). Cr, Pb and V presented higher flow values from the

middle portion of the estuary towards the Atlantic Ocean, while Ba, Cd, Cu, Mn, Fe and Zn presented flows very close to the minimum values shown on the scale.

During the sampling campaign 1 90.87% of the dissolved Al load is of estuarine origin, and 9.13% of fluvial origin. In the sampling campaign 2, however, the discrepancy between loads decreases, 30.36% of the Al load is of river origin and 69.64% of estuarine origin. This behavior is observed in Figures 6 and 7 and in Table S8. In the dissolved Al fluxes at river points during the sampling campaign 1 were related to rock erosion, mainly at the Nascent point. From the Serinhaém point, fluxes exhibited an increase, showing an export of dissolved Al to the Atlantic Ocean. Al suffers influences from pH and salinity, probably this element underwent processes of desorption of particles, corroborated by the decrease in particulate concentrations (Figures 3 and 4) (Wang et al., 2016).

In the sampling campaign 2, Al fluxes in the river points is probably related to rock erosion. Contrary to the sampling campaign 1, in the sampling campaign 2, there was probably a greater absorption of Al by the biota, thus reducing the export of this element to the Atlantic Ocean, consequently, decreasing the estuarine source of the dissolved Al load (Chou and Wollast, 1997; Stoffyn and Mackenzie, 1982) (Figure 6).

Dissolved Ba loads during the sampling campaign 1 showed a fluvial origin of 40% and 60% of estuarine origin, evidenced by the flow distribution shown in Figure 6 and table S8, whose dissolved Ba flow presents a higher concentration in the initial portion of the estuary. This Ba load is probably related to the desorption of the rocks of the local geology, the Pratigi APA, presents barite in the composition of the rocks of the basin (Carneiro et al., 2021). Dissolved Ba loads during the sampling campaign 2 presented the highest percentage from the estuary (29.05% and 70.95%, respectively). The low flow of the rivers leads to a greater inflow of saline water, explaining the high concentration of dissolved Ba flows in the initial portions of the estuary at this time, in the same way as observed during the sampling campaign 1. An increase in the concentrations of dissolved Ba is expected from the removal processes, which occurred in the particles of fluvial origin, induced by the increase in salinity caused by the entry of saline water.

Most of the Ba found in coastal waters comes from this source (Shaw et al., 1998). Colbert and McManus, (2005), when studying the estuary of Tillamook Bay, USA, observed that Ba flows are directly related to the increase in river flow, and that

the greatest Ba exportation occurs during the period of greatest flow. In addition, the authors found that most of the particles exported during this period are reduced by sedimentation, reducing the amount of Ba exported to the adjacent ocean. The same trends were observed for the Serinhaém River estuary in relation to the Ba flow. Gou et al., (2020), observed the same trend for flows from Ba into the Yellow River, China, with most of the export taking place at the time of greatest discharge.

Dissolved Mn flux showed mineral loads of fluvial origin during the sampling campaign 1 (78.09% and 21.91%, respectively) and a decrease in the load distribution during the sampling campaign 2 (54.59% and 45.41%, respectively) (Table S8). The higher fluvial contribution observed during the sampling campaign 1 in the dissolved flows of Mn, is related to the formation of particles of oxyhydroxides of Mn and to the greater transport in this way associated with the particles in suspension, as observed in figure 7, whose concentration of the flow of Mn is higher at the beginning of the estuary (Gurumurthy et al., 2014). Fluvial loads are related to the resuspension of fluvial sediments, resulting in the mobilization of Mn present in the interstitial water of the sediments (**Figure 7 and Table S2**) (Chiffolleau et al., 1994; Yeats, 1993). In addition, Mn oxides are more susceptible to solubilization from natural factors such as luminosity, pH, surface reactivity and organic matter (Briant et al., 2021). The decrease in fluvial contribution during the sampling campaign 2 is related to the removal and addition processes that occur with dissolved Mn in the estuarine ecosystem with the variation of physical-chemical parameters and salinity (Bourg et al., 2000). Despite the decrease in fluvial contributions, the highest fluxes of dissolved Mn in the sampling campaign 2 are observed in the initial points of the estuary, related to sediment resuspension and showing a retention of this dissolved element in the estuary (Figure 7).

Dissolved Cd loads were mostly of estuarine origin in both collection seasons (wet: 34.49% and 65.51%; dry: 25.45% and 74.55%, respectively) (**Figure 6, Table S3, Table S8**). Higher flux values of this element with salinity ≥ 22 in periods of high flow are attributed to the desorption process of this element that, previously, was adsorbed to the surface of suspended particles, caused in the mixing zone, due to the complexation of free Cd^{+2} ions in solution by Cl^- ions from seawater, concomitantly increasing the ionic strength (Comans and van Dijk, 1988; Shiller and Boyle, 1991).

The labile Cd forms are generally formed with salinity values between 0 and 12, suffering a decrease in Cd concentrations with increasing salinity (Waeles et al., 2004b). This corroborates the behavior observed in the Cd flow in the Serinhaém river estuary, in which there are no concentrations of this element with salinity values between 5 and 15, however, there is an increase in concentrations when salinity values exceed 22. In addition, the increase in Cd concentrations in these two parts of the estuary may also be associated with resuspension of the sediment, since the suspended particles are known to exchange among themselves when influenced by the mixing of water caused by the tides (Allen et al., 1977; Kraepiel et al., 1997).

Dissolved Cr fluxes showed higher estuarine loads than those of fluvial origin in both seasons (rainy: 26.86% and 73.14%; dry: 32.85% and 67.15%) (Table S8). The dissolved Cr flux exhibits higher values at the initial points of the estuary, indicating a possible retention of this element in this environment (Figure 6). Cr speciation is influenced by redox conditions and mainly by pH, but also by phytoplankton, particulate organic matter and salinity, these factors caused this difference in load distribution, due to the variation that occurs in these factors when there is a mixture of river and saline waters, leading to desorption processes (Campbell and Yeats, 1984; Gorny et al., 2016).

Dissolved Cu flux exhibited a higher load distribution for river points (54.37%) during the sampling campaign 1, related to effluent discharge and surface runoff, due to the proximity of these points to urban and agricultural areas (Wang et al., 2012; Zhang et al., 2014) (Table S8). During the sampling campaign 2, the distribution of Cu flux loads showed a source inversion, with estuarine loads being higher than fluvial loads (56.48%) (Table S8). This fact occurs due to the release of Cu by resuspension of sediments, phytoplankton and also by desorption of particles in suspension with the increase in salinity, corroborated by figure 6, which shows an increasing Cu flux along the estuary with increasing salinity (Waeles et al., 2005).

In both collection stations the flow of dissolved Fe presented a greater load, coming from fluvial origin (rainy: 99.07% and 0.93%; dry: 95.14% and 4.86%) (Table S8). Dissolved Fe of fluvial origin comes from complexes of humic substances and in the form of Fe oxides and hydroxides and is transported along rivers. This transport is evident in the sampling campaign 1, whose Fe flow exhibits a similar flow gradient along the entire estuary until it reaches the Atlantic Ocean (Figure 7). Part of this Fe is

immobilized in estuarine sediments and is not transported to the Ocean (Kappler et al., 2021; Laglera and van den Berg, 2009; Raiswell, 2011). This immobilization is clear in the Fe fluxes during the sampling campaign 2, whose concentration occurs in different ways along the estuary, with points showing low Fe fluxes (Figure 7).

At the two collection seasons, only Pb concentrations were observed in the dissolved fraction and in the estuarine points. When evaluating the flow and origin of the Pb loads, a majority origin was observed for the estuarine points (rainy: 6.37% and 93.63%; dry: 0 and 100%) (Table S8). Pb has a tendency to associate with Fe and Mn oxides, therefore, the presence of this element in estuarine points is due to the desorption of these oxides with the consequent release of this element in estuarine waters (Abdel-Moati, 1990). Furthermore, sediments resuspension is also a source of this element to the water column. Also, the concentration of Pb dissolved in the initial points of the estuary in the sampling campaign 1 may be related to the discharge of effluents, due to the proximity of these points to urbanized areas (Figure 7, Table S2).

Dissolved V fluxes showed a majority distribution of loads of estuarine origin (rainy: 24.17% and 75.83%; dry: 25.53% and 74.47%) in the two collection campaigns, indicating an increase in dissolved V from the desorption processes caused by the salinity (Shiller and Boyle, 1987; Strady et al., 2009) (Table S8). Dissolved V fluxes show a clear export of this element to the Atlantic Ocean in both campaigns with the increase of salinity gradient (Figure 7, Table S2). Dissolved Zn fluxes exhibit a fluvial contribution (70.22% and 29.73%) in the sampling campaign 1, with the highest dissolved fluxes being presented in the initial portion of the estuary (Figure 6, Table S8). In contrast to the sampling campaign 2, in which the highest flows were shown from the middle portion of the estuary, thus presenting a greater estuarine contribution (31,885 and 68.12%) (Figure 6, Table S8). The highest fluvial contributions in the sampling campaign 1 are related to Zn sources, which are geological, that is, from the erosion of rocks and the greater surface runoff occurring at that time (Elderfield et al., 1979). In saline environments, Zn undergoes desorption processes caused by complexation in marine anions, corroborating what was observed in figure 6, with the increase in the estuarine contribution to Zn fluxes (Araújo et al., 2019).

3.4.2 – Export via particulate fraction (SPM)

The flow of trace elements in the particulate fraction ($\mu\text{g s}^{-1}$) is illustrated in Figures 8 and 9. The trace elements in the particulate fraction of the water column

exhibited a behavior different from that observed in the dissolved fraction, as expected. Seasonally, all elements showed different behavior between collection campaigns (**Figures 8 and 9**). The flow values of all elements analyzed were higher in the sampling campaign 1, increasing towards the estuarine mouth, showing a possible export of these to the Atlantic Ocean. On the other hand, although the flow values were lower in the sampling campaign 2, which was expected due to the lower export capacity of the rivers in less rainy periods, the first points of the estuary (E1, E2 and E3) presented flow values higher, indicating that there is a storage of these elements in estuarine sediments during periods of low flow (**Supplementary Material 1**) (Alyazichi et al., 2017).

Particulate Al loads exhibit a contrary origin between collection stations. During the sampling campaign 2, the loads of particulate Al were mostly of estuarine origin (83.04%), indicating a transport of particles from the resuspension of surface sediments (Figure 8, Table S8). In the sampling campaign 1, 69.96% of the Al load came from the river points, while 30.04% of the particulate Al load came from the estuary, demonstrating that the decrease in the diluting power of the rivers at that time may be more relevant for the export of Al river (Figure 8, Table S8). Furthermore, at that time, rock erosion, surface runoff and the discharge of industrial effluents could be sources of Al into the Atlantic Ocean (Bezack-Mazur et al., 2001; Botté et al., 2022). The Al fluxes in both samplings show a retention of this element in the estuary through the deposition of particles. In the sampling campaign 2 this deposition occurs close to the mouth of the estuary and in the sampling campaign 1 the transport of particulate Al is reduced from the initial portions of the estuary (Figure 8).

The loads of particulate Ba during the sampling campaign 1 were mainly of estuarine origin (91.73%), related to the remobilization of Ba deposited in the sediments (Figure 8, Table S8). In the sampling campaign 2, the distribution of particulate Ba loads followed that observed in the dissolved fraction during the sampling campaign 1 (42.92% and 57.06%, respectively), due to the seasonality already observed by other authors for the behavior of Ba in estuaries and the gradient maximum desorption in times of lower river discharge (Colbert and McManus, 2005; Dion, 1983) (Table S8). In the Bay of Bengal, exported Ba is usually in the form of deposited particles, which undergo remobilization and consequently release Ba to the dissolved phase, becoming an important source of Ba for the Indian Ocean (Singh et

al., 2013). This process of remineralization of particulate Ba may be an important process for exporting Ba to the Atlantic Ocean from the Serinhaém estuary. Making it necessary to carry out future studies in the three compartments of the aquatic ecosystem (dissolved, particulate and sedimentary), so that this process of the Ba cycle can be corroborated.

According to Guo et al., (2020), the Ba particulate fluxes in the Yellow River, China, come from fluvial Ba adsorption in the SPM and the Ba isotopes exhibit strong seasonality, directly related to the higher SPM input during the highest river discharge. Contrary to what was observed in the Serinhaém estuary, where the greatest Ba flows occurred during the sampling campaign 2. However, the study area is located in a region where seasonality is not well defined and it rains all year round. Thus, it is necessary to carry out studies throughout the year, in order to confirm the greater exportation of Ba during the sampling campaign 2.

The Mn fluxes of the particulate fraction exhibited a load distribution mainly of estuarine origin during the sampling campaign 1 (13.86% and 86.14%, respectively) and an opposite distribution in the sampling campaign 2, with the loads of fluvial origin greater than those of estuarine origin (72.73% and 27.27%, respectively) (Table S8). The speciation of Mn is controlled by redox processes, and physical-chemical parameters, the variation of these factors can lead to the release of Mn from the sediments and to processes of adsorption and desorption of this element in the water column, causing a variation in the concentrations of the fractions dissolved and particulate and, consequently, a variation in the fluxes of this element (Evans et al., 1977; Klinkhammer and Mcmanus, 2001). This variation is observed in figure 9, whose Mn particulate flux is greater at the beginning of the estuary in the sampling campaign 2, related to the greater transport of fluvial Mn particles. And it presents peaks of high flows in the middle and end of the estuary, related to the increase of the estuarine contribution through the resuspending of the sediments and processes of removal of this element from the dissolved fraction.

The particulate Cr fluxes during the sampling campaign 1 (52.49% and 47.51%) and sampling campaign 2 (72.11% and 27.89%) showed a greater fluvial than estuarine origin (Table S8). The greater fluvial contribution of Cr flows is evident when observing Figure 8, in which, in the sampling campaign 2, the largest Cr flows are concentrated in the first points of the estuary. According to some authors, dissolved Cr

can precipitate in alkaline waters, thus increasing the concentration of particulate Cr (Richard and Bourg, 1991; Saputro et al., 2014). In addition, Cr can also be removed from the dissolved fraction through biological activity and is related to both local geology and anthropogenic sources (Forero López et al., 2021). The distribution of the Cr flux in the sampling campaign 1 shown in figure 8, corroborates the greater transport of this element through the suspended particles and the decrease in the distribution of contribution loads, corroborates the processes involved in the speciation of Cr in the estuaries.

Fe in the particulate fraction, exhibited a flow with higher loads of estuarine origin during the sampling campaign 1 (18.09% and 81.91%) and an opposite distribution during the sampling campaign 2 (88.45% and 11.95%) (Table S8). The variation observed in the fluxes of particulate Fe comes from the precipitation processes of Fe in oxyhydroxides at river points and removal and addition processes at estuarine points (Daneshvar, 2015; Kappler et al., 2021). The inversion of the distribution of particulate Fe loads is observed in figure 8. The flows of the sampling campaign 2, of greater fluvial origin are concentrated in the first estuarine points and the flows of the sampling campaign 1 from the middle of the estuary, related to the formation of the zone of maximum turbidity with the resuspension of the sediments.

The V fluxes in the particulate fraction exhibited an inverse charge distribution in the two collections. During the sampling campaign 1, the greater contribution was made by estuarine particles (37.09% and 62.91%), whereas during the sampling campaign 2, fluvial particles exhibited a greater contribution (77.61% and 22.39%) (Table S8). This distribution is evident when observing Figure 9, whose V input during the sampling campaign 2 is more prominent at the beginning of the estuary, as opposed to the sampling campaign 1, where the V distributions are displayed along the entire estuary.

This distinct behavior is related to the processes that V undergoes in aquatic ecosystems. During the period of lower river discharge, the low polluting power of rivers promotes an increase in dissolved concentrations of this element in river points (Shiller and Mao, 2000). Upon entering the estuaries, the V undergoes processes of particle desorption and also biological absorption, which explains the decrease in flow in the middle portion of the estuary (Figure 9) (Joung and Shiller, 2016; Shiller and Boyle,

1987). V undergoes adsorption processes of Fe and Mn oxyhydroxide particles, and thus is transported to the Atlantic Ocean, as observed in Figure 9 (Dellwig et al., 2007).

The Zn particulate fluxes presented a greater estuarine contribution than the fluvial one in the sampling campaign 1 (92.82% and 7.18%) (Table S8). During the sampling campaign 2, the greatest contribution became fluvial, however, with a close distribution between the two environments (50.11% and 49.89%) (Table S8). Zn can undergo processes of adsorption to particles in estuarine environments, and sediment resuspension can also occur by increasing concentrations in the particulate fraction (Chiffoleau et al., 1994a; V Hatje et al., 2003). Figure 9 shows an export of particulate Zn to the Atlantic Ocean, related to the transport of this element together with particulate matter in suspension.

The seasonal differences observed for Fe flow are probably related to the difference in river flow between the wet and sampling campaign 2s (Fu et al., 2013). In addition, in some estuaries around the world, Fe exhibits a non-conservative removal behavior through colloid aggregation mechanisms (E. Boyle et al., 1974; Fu et al., 2013; Hunter and Leonard, 1988; Sholkovitz, 1978b). The Fe concentrations in the dissolved fraction of the sampling campaign 1, which were below the detection limit of the device (**Figure 3**), are probably related to the Fe removal mechanisms from this fraction, since this element was found in the particulate fraction of the water column in the estuarine region in both collections. According to (Sanders et al., 2015), although much of the Fe that is adsorbed to the surface of suspended particles suffer deposition in estuaries, there is still a part that is exported to the oceans.

A relevant control for speciation and Fe flux in aquatic environments is the redox state of the water column (Mosley and Liss, 2020). It is known that the formation of Fe oxides/hydroxides promotes the removal of a wide variety of trace elements from the fraction dissolved under oxidizing conditions, in which the formation of sulfides occurs (Duan et al., 2019). However, the resuspension of sediments, which present iron sulfides (FeS), can cause the release of Fe and other trace elements, if it occurs under oxidizing conditions (Richards et al., 2018). Therefore, isotopic techniques that help in tracking the distribution of fluvial elements in estuarine sediments become relevant for future studies that address both the quality of estuarine water and the export of trace elements to the oceans (Reese et al., 2019).

All trace elements showed similar flux values in the particulate fraction, except Ba, which is known to have a close association with salinity, corroborated by PCA, whose inverse relationship between the element in the dissolved fraction and some physicochemical parameters (*e.g.*, salinity and electrical conductivity) are shown in **Figure 5**. The salinity in the sampling campaign 2 exhibited higher values from point 6 (E3), together with this increase, the concentrations of Ba also increased, consequently also the flux. On the other hand, in the sampling campaign 1 the salinity ranged from 30.5 to 37, showing similar values in the last points (E8: 34.1 and E9: 34.7), where it presented a slight decrease, when compared to point E7, which could also be observed in the Ba flow from this campaign. Ba can be removed from particles through ion exchanges with most of the larger ions (*e.g.*, magnesium [Mg] and potassium [K]) during the early mixing phases of fresh and salt water (Hanor & Chan, 1977; Samanta & Dalai, 2016).

The flux of trace elements in the sampling campaign 1 showed an increase from the middle portion of the estuary towards the Atlantic Ocean, probably related to the inflow of the tides, due to the resuspension of sediments in zones of maximum turbidity (Briant et al., 2021). The sedimentary compartment is extremely important in studies that address environmental contamination by pollutants in aquatic ecosystems, due to the fact that, ultimately, these pollutants settle and are trapped in this compartment, which can act as a secondary source of these pollutants by the resuspension of the particles to which these contaminants are adsorbed (Premier et al., 2019).

According to Salomão et al., 2001, the highest loads of trace elements are related to times of higher discharges and precipitation, that is, sampling campaign 1s and consequently to higher concentrations of PMS. This study corroborates what was observed in the Serinhaém estuary, with the highest element fluxes being found in the April/19 collection, whose SPM concentration was also higher, reinforcing that the transport of elements along aquatic ecosystems is done through the suspended particles.

4. Conclusions

The concentrations of all trace elements analyzed, in both fractions of the water column, were below the limits recommended by the current Brazilian legislation (CONAMA), providing an understanding of good water quality in this region, which presents little or no risk to human and wildlife.

The physical-chemical parameters, when analyzed together with the trace elements, demonstrate the clear relationship between the removal and release processes (flocculation, adsorption, desorption and deposition) with the trace elements of the water column. The behavior of these elements in the estuary in both fractions (dissolved and particulate) is governed by the salinity and also by the resuspension of the sediments, leading to the occurrence of mechanisms of release and/or removal of these elements from the water column.

The estuary of the Serinhaém river presents constant flows of all elements analyzed to the Atlantic Ocean. All these elements showed a higher transport affinity for the particulate fraction when compared to the same in the dissolved fraction, indicating a more efficient transport by the first matrix. The dissolved fluxes were mostly controlled by the seasonal variation of precipitation and flow and by the variation of the tides, which cause the resuspension of the surface layer of the sediments and, consequently, a higher contribution of these elements to the water column. On the other hand, the fluxes of elements present in the particulate fraction showed a different behavior, being more dependent of the concentrations of SPM.

The results presented here make clear the close association between trace elements and environmental parameters (physical-chemical, rain and tide). Thus, the behavior of these elements was governed, in most cases, by one or more of these parameters. Despite this, because it is an Environmental Protection Area that has the presence of economic activities and increasing urbanization, it is necessary that management and monitoring programs are constantly carried out in these environments in order to avoid future contamination of water and local biota.

Acknowledgements

This study was financed in part by the Coordenação de Aperfeiçoamento de Pessoal de Nível Superior – Brazil (CAPES) – Finance Code 001.

Conflict of interest

The authors declared that they have no conflicts of interest to this work. We declare that we do not have any commercial or associative interest that represents a conflict of interest in connection with the work submitted.

5. Referências

- Abdel-Moati, A.R., 1990. Behaviour and fluxes of Copper and Lead in the Nile River Estuary, *Estuarine, Coastal and Shelf Science*.
- Ackroyd, D.R., Bale, A.J., Howland, R.J.M., Knox, S., Millward, G.E., Morris, A.W., 1986. Distributions and behaviour of dissolved Cu, Zn and Mn in the Tamar estuary. *Estuar Coast Shelf Sci* 23, 621–640. [https://doi.org/10.1016/0272-7714\(86\)90103-4](https://doi.org/10.1016/0272-7714(86)90103-4)
- Alasfar, R.H., Isaifan, R.J., 2021. Aluminum environmental pollution: the silent killer. *Environmental Science and Pollution Research* 28, 44587–44597. <https://doi.org/10.1007/s11356-021-14700-0>
- Alexander, R.B., Böhlke, J.K., Boyer, E.W., David, M.B., Harvey, J.W., Mulholland, P.J., Seitzinger, S.P., Tobias, C.R., Tonitto, C., Wollheim, W.M., 2009. Dynamic modeling of nitrogen losses in river networks unravels the coupled effects of hydrological and biogeochemical processes. *Biogeochemistry* 93, 91–116. <https://doi.org/10.1007/s10533-008-9274-8>
- Allen, G.P., Sauzay, G., Castaing, P., Jouanneau, J.M., 1977. Transport and deposition of suspended sediment in the Gironde Estuary, France., in: *Estuarine Processes (Proc. Third Int. Estuarine Research Conf. Galveston, U.S.a.: Oct. 7-9, 1975)* Wiley, M. (Ed.). ACADEMIC PRESS, INC. <https://doi.org/10.1016/b978-0-12-751802-2.50013-8>
- Almeida, M.G., Rezende, C.E., Souza, C.M.M., 2007. VARIAÇÃO TEMPORAL , TRANSPORTE E PARTIÇÃO DE HG E CAR- BONO ORGÂNICO NAS FRAÇÕES PARTICULADA E DISSOLVIDA DA COLUNA D ' ÁGUA DA BACIA INFERIOR DO RIO PARAÍBA DO. *Geochimica Brasiliensis* 21, 111–128.
- Altman, N., Krzywinski, M., 2016. Points of Significance: Regression diagnostics. *Nat Methods* 13, 385–386. <https://doi.org/10.1038/nmeth.3854>
- Alyazichi, Y.M., Jones, B.G., McLean, E., Pease, J., Brown, H., 2017. Geochemical Assessment of Trace Element Pollution in Surface Sediments from the Georges River, Southern Sydney, Australia. *Arch Environ Contam Toxicol* 72, 247–259. <https://doi.org/10.1007/s00244-016-0343-z>
- Apte, S.C., 2008. Chapter 9 Biogeochemistry of Copper in the Fly River. *Developments in Earth and Environmental Sciences*. [https://doi.org/10.1016/S1571-9197\(08\)00409-6](https://doi.org/10.1016/S1571-9197(08)00409-6)
- Araújo, D.F., Ponzevera, E., Briant, N., Knoery, J., Sireau, T., Mojtahid, M., Metzger, E., Brach-Papa, C., 2019. Assessment of the metal contamination evolution in the Loire estuary using Cu and Zn stable isotopes and geochemical data in sediments. *Mar Pollut Bull* 143, 12–23. <https://doi.org/10.1016/j.marpolbul.2019.04.034>
- Araujo, M., Noriega, C., Lefèvre, N., 2014. Nutrients and carbon fluxes in the estuaries of major rivers flowing into the tropical Atlantic. *Front Mar Sci* 1, 1–16. <https://doi.org/10.3389/fmars.2014.00010>
- Arheimer, B., Andersson, L., Lepistö, A., 1996. Variation of nitrogen concentration in forest streams - Influences of flow, seasonality and catchment characteristics. *J Hydrol (Amst)* 179, 281–304. [https://doi.org/10.1016/0022-1694\(95\)02831-5](https://doi.org/10.1016/0022-1694(95)02831-5)

- Audry, S., Blanc, G., Schäfer, J., 2004. Cadmium transport in the Lot-Garonne River system (France) - Temporal variability and a model for flux estimation. *Science of the Total Environment* 319, 197–213. [https://doi.org/10.1016/S0048-9697\(03\)00405-4](https://doi.org/10.1016/S0048-9697(03)00405-4)
- Azam, M., Kumari, M., Maharana, C., Singh, A.K., Tripathi, J.K., 2018. Recent insights into the dissolved and particulate fluxes from the Himalayan tributaries to the Ganga River. *Environ Earth Sci* 77, 1–14. <https://doi.org/10.1007/s12665-018-7490-7>
- Barreto, S.R.G., Barreto, W.J., Deduch, E.M., 2011. Determination of Partition Coefficients of Metals in Natural Tropical Water. *Clean (Weinh)* 39, 362–367. <https://doi.org/10.1002/clen.201000271>
- Bellenger, J.P., Xu, Y., Zhang, X., Morel, F.M.M., Kraepiel, A.M.L., 2014. Possible contribution of alternative nitrogenases to nitrogen fixation by asymbiotic N₂-fixing bacteria in soils. *Soil Biol Biochem* 69, 413–420. <https://doi.org/10.1016/j.soilbio.2013.11.015>
- Bello, A.A.D., Hashim, N.B., Haniffah, M.R.M., 2017. Predicting impact of climate change on water temperature and dissolved oxygen in tropical rivers. *Climate* 5. <https://doi.org/10.3390/cli5030058>
- Benavides, M.P., Gallego, S.M., Tomaro, M.L., 2005. Cadmium toxicity in plants. *Brazilian Journal of Plant Physiology* 17, 21–34. <https://doi.org/10.1590/S1677-04202005000100003>
- Benoit, G., Rozan, T.F., 1999. The influence of size distribution on the particle concentration effect and trace metal partitioning in rivers.
- Bezak-Mazur, E., Widłak, M., Ciupa, T., 2001. A Speciation Analysis of Aluminium in the River Silnica, *Polish Journal of Environmental Studies*.
- Bhoelan, B.S., Stevering, C.H., van der Boog, A.T.J., van der Heyden, M.A.G., 2014. Barium toxicity and the role of the potassium inward rectifier current. *Clin Toxicol* 52, 584–593. <https://doi.org/10.3109/15563650.2014.923903>
- Bidone, E., Cesar, R., Santos, M.C., Sierpe, R., Silva-Filho, E.V., Kutter, V., Dias da Silva, L.I., Castilhos, Z., 2018. Mass balance of arsenic fluxes in rivers impacted by gold mining activities in Paracatu (Minas Gerais State, Brazil). *Environmental Science and Pollution Research* 25, 9085–9100. <https://doi.org/10.1007/s11356-018-1215-z>
- Biwa, I.L., Sugiyama, J.M., 1989. Seasonal variation of vanadium concentration, *Geochemical Journal*.
- Boongaling, C.G.K., Faustino-Eslava, D. V., Lansigan, F.P., 2018. Modeling land use change impacts on hydrology and the use of landscape metrics as tools for watershed management: The case of an ungauged catchment in the Philippines. *Land use policy* 72, 116–128. <https://doi.org/10.1016/j.landusepol.2017.12.042>
- Botté, A., Zaidi, M., Guery, J., Fichet, D., Leignel, V., 2022. Aluminium in aquatic environments: abundance and ecotoxicological impacts. *Aquat Ecol*. <https://doi.org/10.1007/s10452-021-09936-4>

- Bouillon, S., Middelburg, J.J., Dehairs, F., Borges, A. V., Abril, G., Flindt, M.R., Ulomi, S., Kristensen, E., 2007. Importance of intertidal sediment processes and porewater exchange on the water column biogeochemistry in a pristine mangrove creek (Ras Dege, Tanzania). *Biogeosciences* 4, 311–322. <https://doi.org/10.5194/bg-4-311-2007>
- Bourg, A.C.M., Kedziorek, M.A.M., Crouzet, C., 2000. Seasonal Cycles of Dissolved Cd, Mn and Zn in River Water Caused by Variations in pH Induced by Biological Activity, *Aquatic Geochemistry*.
- Boyer, P., Wells, C., Howard, B., 2018. Extended Kd distributions for freshwater environment. *J Environ Radioact* 192, 128–142. <https://doi.org/10.1016/j.jenvrad.2018.06.006>
- Boyle, E., Collier, R., Dengler, A.T., 1974. On the chemical mass- balance in estuaries. *Geochim. Cosmochim. Acta* 38, 1719–1728. [https://doi.org/10.1016/0016-7037\(74\)90188-4](https://doi.org/10.1016/0016-7037(74)90188-4)
- Boyle, E., Collier, R., Dengler, A.T., 1974. On the chemical mass- balance in estuaries. *Geochim. Cosmochim. Acta* 38, 1719–1728. [https://doi.org/10.1016/0016-7037\(74\)90188-4](https://doi.org/10.1016/0016-7037(74)90188-4)
- Boyle, E.A., Edmond, J.M., Sholkovitz, E.R., 1977. The mechanism of iron removal in estuaries, *Geochimica et Cosmochimica Acta*. Pergamon Press.
- Boyle, E.A., Husted, S.S., Grant, B., 1982. The chemical mass balance of the Amazon Plume II. Copper, nickel, and cadmium.
- Briant, N., Chiffolleau, J.F., Knoery, J., Araújo, D.F., Ponzevera, E., Crochet, S., Thomas, B., Brach-Papa, C., 2021. Seasonal trace metal distribution, partition and fluxes in the temperate macrotidal Loire Estuary (France). *Estuar Coast Shelf Sci* 262. <https://doi.org/10.1016/j.ecss.2021.107616>
- Bridgestock, L., Nathan, J., Paver, R., Hsieh, Y. te, Porcelli, D., Tanzil, J., Holdship, P., Carrasco, G., Annammala, K.V., Swarzenski, P.W., Henderson, G.M., 2021. Estuarine processes modify the isotope composition of dissolved riverine barium fluxes to the ocean. *Chem Geol* 579. <https://doi.org/10.1016/j.chemgeo.2021.120340>
- Brown, M.T., Bruland, K.W., 2009. Dissolved and particulate aluminum in the Columbia River and coastal waters of Oregon and Washington: Behavior in near-field and far-field plumes. *Estuar Coast Shelf Sci* 84, 171–185. <https://doi.org/10.1016/j.ecss.2009.05.031>
- Bunke, D., Moritz, S., Brack, W., Herráez, D.L., Posthuma, L., Nuss, M., 2019. Developments in society and implications for emerging pollutants in the aquatic environment. *Environ Sci Eur* 31. <https://doi.org/10.1186/s12302-019-0213-1>
- Burger, J., Gaines, K.F., Boring, C.S., Stephens, W.L., Snodgrass, J., Dixon, C., McMahon, M., Shukla, S., Shukla, T., Gochfeld, M., 2002. Metal Levels in Fish from the Savannah River: Potential Hazards to Fish and Other Receptors. *Environ Res* 89, 85–97. <https://doi.org/10.1006/enrs.2002.4330>

- Burns, D.A., Boyer, E.W., Elliott, E.M., Kendall, C., 2009. Sources and Transformations of Nitrate from Streams Draining Varying Land Uses: Evidence from Dual Isotope Analysis. *J Environ Qual* 38, 1149–1159. <https://doi.org/10.2134/jeq2008.0371>
- Caccia, V.G., Boyer, J.N., 2005. Spatial patterning of water quality in Biscayne Bay, Florida as a function of land use and water management. *Mar Pollut Bull* 50, 1416–1429. <https://doi.org/10.1016/j.marpolbul.2005.08.002>
- Campbell, J.A., Yeats, P.A., 1984. Dissolved Chromium in the St. Lawrence Estuary, Coastal and Shelf Science.
- Carneiro, L.M., Dourado, G.B., de Carvalho, C.E.V., da Silva Júnior, J.B., de Jesus, T.B., Hadlich, G.M., 2021. Evaluation of the concentrations of elements at trace level in the Serinhaem River estuary, Bahia, Brazil, using chemometric tools. *Mar Pollut Bull* 163, 111953. <https://doi.org/10.1016/j.marpolbul.2020.111953>
- Carroll, J., Kenison Falkner, K., Thorson Brown, E., Moore, W.S., 1993. The role of the Ganges-Brahmaputra mixing zone in supplying barium and ²²⁶Ra to the Bay of Bengal, *Geochimica et Cosmochimica Acta*.
- Carvalho, C.E. V, Salomão, M.S.M.B., Molisani, M.M., Rezende, C.E., Lacerda, L.D., 2002. Contribution of a medium-sized tropical river to the particulate heavy-metal load for the South Atlantic Ocean. *Science of the Total Environment* 284, 85–93. [https://doi.org/10.1016/S0048-9697\(01\)00869-5](https://doi.org/10.1016/S0048-9697(01)00869-5)
- Chenar, S.S., Karbassi, A., Zaker, N.H., Ghazban, F., 2013. Electroflocculation of metals during estuarine mixing (caspien sea). *J Coast Res* 29, 847–854. <https://doi.org/10.2112/JCOASTRES-D-11-00224.1>
- Chiffoleau, J.F., Cossa, D., Auger, D., Truquet, I., 1994a. Trace metal distribution, partition and fluxes in the Seine estuary (France) in low discharge regime. *Mar Chem* 47, 145–158. [https://doi.org/10.1016/0304-4203\(94\)90105-8](https://doi.org/10.1016/0304-4203(94)90105-8)
- Chou, L., Wollast, R., 1997. Biogeochemical behavior and mass balance of dissolved aluminum in the western Mediterranean Sea, *Ekvier Science Ltd*.
- Cidu, R., Biddau, R., 2007. Transport of trace elements under different seasonal conditions: Effects on the quality of river water in a Mediterranean area. *Applied Geochemistry* 22, 2777–2794. <https://doi.org/10.1016/j.apgeochem.2007.06.017>
- Coffey, M., Dehairs, F., Collette, O., Luther, G., Church, T., Jickells, T., 1997a. The Behaviour of Dissolved Barium in Estuaries. *Estuar Coast Shelf Sci* 45, 113–121.
- Colbert, D., McManus, J., 2005. Importance of seasonal variability and coastal processes on estuarine manganese and barium cycling in a Pacific Northwest estuary. *Cont Shelf Res* 25, 1395–1414. <https://doi.org/10.1016/j.csr.2005.02.003>
- Comans, N.J.R., van Dijk, P.J.C., 1988. Role of Complexation Process in Cadmium Mobilization During Estuarine Mixing. *Nature Publishing Group* 336, 151–154.
- CONAMA, C.N. do M.A., 2005. Resolução 357/2005. Brazil.
- Constantino, I., Teodoro, G., Moreira, A., Paschoal, F., Trindade, W., Bisinoti, M., 2019. Distribution of Metals in the Waters and Sediments of Rivers in Central Amazon

- Region, Brazil. *J Braz Chem Soc* 30, 1906–1915. <https://doi.org/10.21577/0103-5053.20190100>
- Constantino, I.C., Teodoro, G.C., Moreira, A.B., Paschoal, F.M.M., Trindade, W.G., Bisinoti, M.C., 2019. Distribution of metals in the waters and sediments of rivers in central amazon region, Brazil. *J Braz Chem Soc* 30, 1906–1915. <https://doi.org/10.21577/0103-5053.20190100>
- Constantino, W.D., Viana, L.M. de S., Luze, F.H.R., Tostes, E.C.L., Pestana, I.A., de Carvalho, C.E.V., 2022. Mercury levels in an environmentally protected estuarine area in Northeast Brazil: partitioning in the water column and transport to the ocean. *Environmental Science and Pollution Research*. <https://doi.org/10.1007/s11356-022-24400-y>
- CRA, C. de R.A., 2004. Síntese do plano de manejo da APA do Pratigi. Ituberá.
- Cruces-Sande, A., Rodríguez-Pérez, A.I., Herbello-Hermelo, P., Bermejo-Barrera, P., Méndez-Álvarez, E., Labandeira-García, J.L., Soto-Otero, R., 2019. Copper Increases Brain Oxidative Stress and Enhances the Ability of 6-Hydroxydopamine to Cause Dopaminergic Degeneration in a Rat Model of Parkinson's Disease. *Mol Neurobiol* 56, 2845–2854. <https://doi.org/10.1007/s12035-018-1274-7>
- Dai Ap', M., Martin, J.-M., Cauwet, G., 1995. The significant role of colloids in the transport and transformation of organic carbon and associated trace metals (Cd, Cu and Ni) in the Rh6ne delta (France), *Marine Chemistry*.
- Damashek, J., Francis, C.A., 2018. Microbial Nitrogen Cycling in Estuaries: From Genes to Ecosystem Processes. *Estuaries and Coasts*. <https://doi.org/10.1007/s12237-017-0306-2>
- Daneshvar, E., 2015. Dissolved Iron Behavior in the Ravenglass Estuary Waters, An Implication on the Early Diagenesis. *Universal Journal of Geoscience* 3, 1–12. <https://doi.org/10.13189/ujg.2015.030101>
- Darnajoux, R., Zhang, X., McRose, D.L., Miadlikowska, J., Lutzoni, F., Kraepiel, A.M.L., Bellenger, J.P., 2017. Biological nitrogen fixation by alternative nitrogenases in boreal cyanolichens: importance of molybdenum availability and implications for current biological nitrogen fixation estimates. *New Phytologist* 213, 680–689. <https://doi.org/10.1111/nph.14166>
- de Oliveira, O.M.C., Cruz, M.J.M., de Souza Queiroz, A.F., 2009. Comportamento geoquímico de metais em sedimentos de manguezal da Baía de Camamu-Bahia. *Brazilian Journal of Aquatic Science and Technology* 13, 1. <https://doi.org/10.14210/bjast.v13n2.p1-8>
- de Souza Machado, A.A., Spencer, K., Kloas, W., Toffolon, M., Zarfl, C., 2016. Metal fate and effects in estuaries: A review and conceptual model for better understanding of toxicity. *Science of The Total Environment* 541, 268–281. <https://doi.org/10.1016/j.scitotenv.2015.09.045>

- Dehairs, F., Chesselet, R., Jedwab, J., 1980. DISCRETE SUSPENDED PARTICLES OF BARITE AND THE BARIUM CYCLE IN THE OPEN OCEAN, *Earth and Planetary Science Letters*.
- Dellwig, O., Beck, M., Lemke, A., Lunau, M., Kolditz, K., Schnetger, B., Brumsack, H.J., 2007. Non-conservative behaviour of molybdenum in coastal waters: Coupling geochemical, biological, and sedimentological processes. *Geochim Cosmochim Acta* 71, 2745–2761. <https://doi.org/10.1016/j.gca.2007.03.014>
- Denton, G.R.W., Burdon-Jones, C., 1981. Influence of Temperature and Salinity on the Uptake, Distribution and Deputation of Mercury, Cadmium and Lead by the Black-lip Oyster *Saccostrea echinata*. *Mar Biol* 64, 317–326.
- Dias, F.J. da S., Castro, B.M., Lacerda, L.D., Miranda, L.B., Marins, R.V., 2016. Physical characteristics and discharges of suspended particulate matter at the continent-ocean interface in an estuary located in a semiarid region in northeastern Brazil. *Estuar Coast Shelf Sci* 180, 258–274. <https://doi.org/10.1016/j.ecss.2016.08.006>
- Dion, E.P., 1983. Trace elements and radionuclides in the Connecticut River and Amazon River Estuary (Dissertation). Yale University.
- Dittmar, T., Lara, R.J., Kattner, G., 2001. River or mangrove? Tracing major organic matter sources in tropical Brazilian coastal waters. *Mar Chem* 73, 253–271. [https://doi.org/10.1016/S0304-4203\(00\)00110-9](https://doi.org/10.1016/S0304-4203(00)00110-9)
- Duan, L., Song, J., Liang, X., Yin, M., Yuan, H., Li, X., Ren, C., Zhou, B., Kang, X., Yin, X., 2019. Dynamics and diagenesis of trace metals in sediments of the Changjiang Estuary. *Science of the Total Environment* 675, 247–259. <https://doi.org/10.1016/j.scitotenv.2019.04.190>
- Duc, T.A., Loi, V.D., Thao, T.T., 2013. Partition of heavy metals in a tropical river system impacted by municipal waste. *Environ Monit Assess* 185, 1907–1925. <https://doi.org/10.1007/s10661-012-2676-z>
- Duinker, J.C., Nolting, R.F., 1976. Distribution model for particulate trace metals in the rhine estuary, Southern Bight and Dutch Wadden Sea. *Netherlands Journal of Sea Research* 10, 71–102. [https://doi.org/10.1016/0077-7579\(76\)90005-3](https://doi.org/10.1016/0077-7579(76)90005-3)
- Eaton, A., 1979. Observations on the geochemistry of soluble copper, iron, nickel, and zinc in the San Francisco Bay estuary. *Environ Sci Technol* 13, 425–432. <https://doi.org/10.1021/es60152a003>
- Eckert, J.M., Sholkovitz, E.R., 1976. The flocculation of iron, aluminium and humates from river water by electrolytes. *Geochim Cosmochim Acta* 40, 847–848. [https://doi.org/10.1016/0016-7037\(76\)90036-3](https://doi.org/10.1016/0016-7037(76)90036-3)
- Eggleton, J., Thomas, K. v., 2004. A review of factors affecting the release and bioavailability of contaminants during sediment disturbance events. *Environ Int.* <https://doi.org/10.1016/j.envint.2004.03.001>
- Eisma, D., 1986. Flocculation and de-flocculation of suspended matter in estuaries. *Netherlands Journal of Sea Research* 20, 183–199.

- Elderfield, H., Hepworth, A., Edwards, P.N., Holliday, L.M., 1979. Zinc in the Conwy River and Estuary.
- Evans, D.W., Cutshall, N.H., Cross, F.A., Wolfi, D.A., 1977. Manganese Cycling in the Newport River Estuary, North Carolina.
- Exley, C., 2003. A biogeochemical cycle for aluminium?, in: *Journal of Inorganic Biochemistry*. Elsevier Inc., pp. 1–7. [https://doi.org/10.1016/S0162-0134\(03\)00274-5](https://doi.org/10.1016/S0162-0134(03)00274-5)
- Exley, C., House, E.R., 2011. Aluminium in the human brain. *Monatsh Chem.* <https://doi.org/10.1007/s00706-010-0417-y>
- Fagerberg, B., Bergström, G., Borén, J., Barregard, L., 2012. Cadmium exposure is accompanied by increased prevalence and future growth of atherosclerotic plaques in 64-year-old women. *J Intern Med* 272, 601–610. <https://doi.org/10.1111/j.1365-2796.2012.02578.x>
- Falkner, K.K., Klinkhammer, G.P., Bowers, ', T.S., Todd, J.F., Lewis, B.L., Landing, W.M., Edmond', J.M., n.d. NOAA, Office of Global Programs, 12th floor, 1100 Wayne Ave.
- Fatema, K., Maznah O, W.W., Mat Isa, M., 2014. Spatial and Temporal Variation of Physico-chemical Parameters in the. *Trop Life Sci Res* 25, 1–19.
- Fernández Severini, M.D., Botté, S.E., Hoffmeyer, M.S., Marcovecchio, J.E., 2011. Lead concentrations in zooplankton, water, and particulate matter of a southwestern Atlantic temperate estuary (Argentina). *Arch Environ Contam Toxicol* 61, 243–260. <https://doi.org/10.1007/s00244-010-9613-3>
- Fianko, J.R., Osaе, S., Adomako, D., Adotey, D.K., Serfor-Armah, Y., 2007. Assessment of heavy metal pollution of the Iture Estuary in the central region of Ghana. *Environ Monit Assess* 131, 467–473. <https://doi.org/10.1007/s10661-006-9492-2>
- Forero López, A.D., Villagran, D.M., Fernandez, E.M., Spetter, C. v., Buzzi, N.S., Fernández Severini, M.D., 2021. Chromium behavior in a highly urbanized coastal area (Bahía Blanca Estuary, Argentina). *Mar Pollut Bull* 165. <https://doi.org/10.1016/j.marpolbul.2021.112093>
- Frazier', J.M., n.d. Bioaccumulation of Cadmium in Marine Organisms, *Environmental Health Perspectives*.
- Friedrich, A.A.C., Niencheski, L.F., Santos, I.R., Friedrichf, A.C., Niencheskij, L.F., Santos, I.R., 2006. Dissolved and Particulate Metals in Mirim Lagoon , Brazil-Uruguayan Border. *Journal of Coastal Resear II*, 1036–1039.
- Fu, J., Tang, X.L., Zhang, J., Balzer, W., 2013. Estuarine modification of dissolved and particulate trace metals in major rivers of east-hainan, china. *Cont Shelf Res* 57, 59–72. <https://doi.org/10.1016/j.csr.2012.06.015>
- Gerpe, M., Rodríguez, D., Moreno, V.J., Bastida, R.O., Moreno, J.E., 2002. Accumulation of heavy metals in the franciscana (*pontoporia blainvillei*) from Buenos Aires Province, Argentina. *Latin American Journal of Aquatic Mammals* 1. <https://doi.org/10.5597/lajam00013>

- Gilmour, D.J., Kaaden, R., Gimmler, H., 1985. Vanadate Inhibition of ATPases of *Dunaliella parva* in vitro and in vivo. *J Plant Physiol* 118, 111–126. [https://doi.org/10.1016/S0176-1617\(85\)80140-1](https://doi.org/10.1016/S0176-1617(85)80140-1)
- González-ortegón, E., Laiz, I., Sánchez-quiles, D., Cobelo-garcia, A., Tovar-sánchez, A., 2019. Science of the Total Environment Trace metal characterization and fluxes from the Guadiana, Tinto-Odiel and Guadalquivir estuaries to the Gulf of Cadiz. *Science of the Total Environment* 650, 2454–2466. <https://doi.org/10.1016/j.scitotenv.2018.09.290>
- Goring-Harford, H.J., Klar, J.K., Donald, H.K., Pearce, C.R., Connelly, D.P., James, R.H., 2020. Behaviour of chromium and chromium isotopes during estuarine mixing in the Beaulieu Estuary, UK. *Earth Planet Sci Lett* 536, 116166. <https://doi.org/10.1016/j.epsl.2020.116166>
- Gorny, J., Billon, G., Noiriél, C., Dumoulin, D., Lesven, L., Madé, B., 2016. Chromium behavior in aquatic environments: a review. *Environmental Reviews* 24, 503–516. <https://doi.org/10.1139/er-2016-0012>
- Gou, L.F., Jin, Z., Galy, A., Gong, Y.Z., Nan, X.Y., Jin, C., Wang, X.D., Bouchez, J., Cai, H.M., Chen, J. bin, Yu, H.M., Huang, F., 2020. Seasonal riverine barium isotopic variation in the middle Yellow River: Sources and fractionation. *Earth Planet Sci Lett* 531. <https://doi.org/10.1016/j.epsl.2019.115990>
- Guay, C.K., Kenison Falkner, K., 1998. A survey of dissolved barium in the estuaries of major Arctic rivers and adjacent seas, *Continental Shelf Research*.
- Guieu, C., Martin, J.-M., Tankéré, S.P.C., Mousty, F., Trincherini, P., Bazot, M., Dai, M.H., 1998. On Trace Metal Geochemistry in the Danube River and Western Black Sea, *Estuarine, Coastal and Shelf Science*.
- Gummow, B., 2011. Vanadium: Environmental Pollution and Health Effects, in: *Encyclopedia of Environmental Health*. Elsevier, pp. 628–636. <https://doi.org/10.1016/B978-0-444-52272-6.00661-9>
- Gurumurthy, G.P., Balakrishna, K., Tripti, M., Audry, S., Riotte, J., Braun, J.J., Shankar, H.N.U., 2014. Geochemical behaviour of dissolved trace elements in a monsoon-dominated tropical river basin, Southwestern India. *Environmental Science and Pollution Research* 21, 5098–5120. <https://doi.org/10.1007/s11356-013-2462-7>
- Gustafsson, O., Widerlund, A., Andersson, P.S., Ingri, J., Ledin, A., 2000. Colloid dynamics and transport of major elements through a boreal river-brackish bay mixing zone, *Marine Chemistry*.
- Hanor, Jeffrey S., Chan, L.H., 1977. Non-conservative behavior of barium during mixing of Mississippi River and Gulf of Mexico waters. *Earth Planet Sci Lett* 37, 242–250. [https://doi.org/10.1016/0012-821X\(77\)90169-8](https://doi.org/10.1016/0012-821X(77)90169-8)
- Hanor, Jeffrey S., Chan, L.H., 1977. Non-conservative behavior of barium during mixing of Mississippi River and Gulf of Mexico waters. *Earth Planet Sci Lett* 37, 242–250. [https://doi.org/10.1016/0012-821X\(77\)90169-8](https://doi.org/10.1016/0012-821X(77)90169-8)

- Hao, W., Kashiwabara, T., Jin, R., Takahashi, Y., Gingras, M., Alessi, D.S., Konhauser, K.O., 2020. Clay minerals as a source of cadmium to estuaries. *Sci Rep* 10. <https://doi.org/10.1038/s41598-020-67279-w>
- Harrel Jr, F.E., 2022. Hmisc: Harrell Miscellaneous.
- Hatje, V., Apte, S.C., Hales, L.T., Birch, G.F., 2003. Dissolved trace metal distributions in Port Jackson estuary (Sydney Harbour), Australia. *Mar Pollut Bull* 46, 719–730. [https://doi.org/10.1016/S0025-326X\(03\)00061-4](https://doi.org/10.1016/S0025-326X(03)00061-4)
- Hatje, V., Barros, F., Magalhães, W., Riatto, B.V., Amorim, F.N., Figueiredo, M.B., Spanó, S., Cirano, M., 2008. Trace metals and benthic macrofauna distributions in Camamu Bay, Brazil: Sediment quality prior oil and gas exploration. *Mar Pollut Bull* 56, 359–363. <https://doi.org/10.1016/j.marpolbul.2007.10.028>
- Hatje, V., Payne, T.E., Hill, D.M., McOrist, G., Birch, G.F., Szymczak, R., 2003b. Kinetics of trace element uptake and release by particles in estuarine waters: Effects of pH, salinity, and particle loading. *Environ Int* 29, 619–629. [https://doi.org/10.1016/S0160-4120\(03\)00049-7](https://doi.org/10.1016/S0160-4120(03)00049-7)
- Holloway, J.A.M., Dahlgren, R.A., 2001. Seasonal and event-scale variations in solute chemistry for four Sierra Nevada catchments. *J Hydrol (Amst)* 250, 106–121. [https://doi.org/10.1016/S0022-1694\(01\)00424-3](https://doi.org/10.1016/S0022-1694(01)00424-3)
- Horan, K., Hilton, R.G., Dellinger, M., Tipper, E., Galy, V., Calmels, D., Selby, D., Gaillardet, J., Ottley, C.J., Parsons, D.R., Burton, K.W., 2019. Carbon dioxide emissions by rock organic carbon oxidation and the net geochemical carbon budget of the Mackenzie River Basin. *Am J Sci* 319, 473–499. <https://doi.org/10.2475/06.2019.02>
- Hunter, K.A., Leonard, M.W., 1988. Colloid stability and aggregation in estuaries: 1. Aggregation kinetics of riverine dissolved iron after mixing with seawater. *Geochim Cosmochim Acta* 52, 1123–1130. [https://doi.org/10.1016/0016-7037\(88\)90266-9](https://doi.org/10.1016/0016-7037(88)90266-9)
- Hydes, D.J., Liss, P.S., 1977. Estuarine and & .ttal Make S&??ue.
- Igbokwe, I.O., Igbokwe, E., Igbokwe, N.A., 2020. Aluminium toxicosis: A review of toxic actions and effects. *Interdiscip Toxicol* 12, 45–70. <https://doi.org/10.2478/intox-2019-0007>
- Jiang, X., Lu, B., He, Y., 2013. Response of the turbidity maximum zone to fluctuations in sediment discharge from river to estuary in the Changjiang Estuary (China). *Estuar Coast Shelf Sci* 131, 24–30. <https://doi.org/10.1016/j.ecss.2013.07.003>
- Johnson, T.L., Brahamsha, B., Palenik, B., Mühle, J., 2015. Halomethane production by vanadium-dependent bromoperoxidase in marine *Synechococcus*. *Limnol Oceanogr* 60, 1823–1835. <https://doi.org/10.1002/lno.10135>
- Jones, D.L., Ryan, P.R., 2016. Aluminum Toxicity, in: *Encyclopedia of Applied Plant Sciences*. Elsevier Inc., pp. 211–218. <https://doi.org/10.1016/B978-0-12-394807-6.00120-9>

- Jones, E., van Vliet, M.T.H., 2018. Drought impacts on river salinity in the southern US: Implications for water scarcity. *Science of the Total Environment* 644, 844–853. <https://doi.org/10.1016/j.scitotenv.2018.06.373>
- Joung, D., Shiller, A.M., 2014. Dissolved barium behavior in Louisiana Shelf waters affected by the Mississippi/Atchafalaya River mixing zone. *Geochim Cosmochim Acta* 141, 303–313. <https://doi.org/10.1016/j.gca.2014.06.021>
- Joung, D.J., Shiller, A.M., 2016. Temporal and spatial variations of dissolved and colloidal trace elements in Louisiana Shelf waters. *Mar Chem* 181, 25–43. <https://doi.org/10.1016/j.marchem.2016.03.003>
- Kappler, A., Bryce, C., Mansor, M., Lueder, U., Byrne, J.M., Swanner, E.D., 2021. An evolving view on biogeochemical cycling of iron. *Nat Rev Microbiol.* <https://doi.org/10.1038/s41579-020-00502-7>
- Kara, G.T., Kara, M., Bayram, A., Gündüz, O., 2017. Assessment of seasonal and spatial variations of physicochemical parameters and trace elements along a heavily polluted effluent-dominated stream. *Environ Monit Assess* 189. <https://doi.org/10.1007/s10661-017-6309-4>
- Kassambara, Alboukadel Mundt, F., 2020. factoextra: Extract and Visualize the Results of Multivariate Data Analyses, in: *Practical Guide To Principal Component Methods in R: PCA, M(CA), FAMD, MFA, HCPC, Factoextra*. pp. 42–82.
- Kendall, B., Anbarm Ariel, Kappler, A., Konhauser, K., 2012. *Fundamentals of Geobiology*. Wiley. <https://doi.org/10.1002/9781118280874>
- Klinkhammer, G.P., Mcmanus, J., 2001. Dissolved manganese in the Columbia River estuary: Production in the water column.
- Kolarova, N., Napiórkowski, P., 2021. Trace elements in aquatic environment. Origin, distribution, assessment and toxicity effect for the aquatic biota. *Ecohydrology and Hydrobiology* 21, 655–668. <https://doi.org/10.1016/j.ecohyd.2021.02.002>
- Koukina, S.E., Lobus, N. v., Shatravin, A. v., 2021. Multi-element signatures in solid and solution phases in a tropical mixing zone: A case study in the Cai River estuary, Vietnam. *Chemosphere* 280. <https://doi.org/10.1016/j.chemosphere.2021.130951>
- Krachler, R., Krachler, R.F., von der Kammer, F., Süphandag, A., Jirsa, F., Ayromlou, S., Hofmann, T., Keppler, B.K., 2010. Relevance of peat-draining rivers for the riverine input of dissolved iron into the ocean. *Science of the Total Environment* 408, 2402–2408. <https://doi.org/10.1016/j.scitotenv.2010.02.018>
- Kraepiel, A.M.L., Chiffolleau, J.F., Martin, J.M., Morel, F.M.M., 1997. Geochemistry of trace metals in the Gironde estuary. *Geochim Cosmochim Acta* 61, 1421–1436. [https://doi.org/10.1016/S0016-7037\(97\)00016-1](https://doi.org/10.1016/S0016-7037(97)00016-1)
- Kranzler, C., Lis, H., Shaked, Y., Keren, N., 2011. The role of reduction in iron uptake processes in a unicellular, planktonic cyanobacterium. *Environ Microbiol* 13, 2990–2999. <https://doi.org/10.1111/j.1462-2920.2011.02572.x>

- Kravchenko, J., Darrah, T.H., Miller, R.K., Lyerly, H.K., Vengosh, A., 2014. A review of the health impacts of barium from natural and anthropogenic exposure. *Environ Geochem Health* 36, 797–814. <https://doi.org/10.1007/s10653-014-9622-7>
- Kristensen, E., Bouillon, S., Dittmar, T., Marchand, C., 2008. Organic carbon dynamics in mangrove ecosystems: A review. *Aquat Bot* 89, 201–219. <https://doi.org/10.1016/j.aquabot.2007.12.005>
- Krupińska, I., 2020. Aluminium drinking water treatment residuals and their toxic impact on human health. *Molecules* 25. <https://doi.org/10.3390/molecules25030641>
- Laglera, L.M., van den Berg, C.M.G., 2009. Evidence for geochemical control of iron by humic substances in seawater. *Limnol Oceanogr* 54, 610–619. <https://doi.org/10.4319/lo.2009.54.2.0610>
- Lê, S., J & Husson, F., 2008. FactoMineR: An R Package for Multivariate Analysis. *J Stat Softw* 25, 1–18.
- Lee, J.A., Marsden, I.D., Glover, C.N., 2010. The influence of salinity on copper accumulation and its toxic effects in estuarine animals with differing osmoregulatory strategies. *Aquatic Toxicology* 99, 65–72. <https://doi.org/10.1016/j.aquatox.2010.04.006>
- Lekhi, P., Cassis, D., Pearce, C.M., Ebell, N., Maldonado, M.T., Orians, K.J., 2008. Role of dissolved and particulate cadmium in the accumulation of cadmium in cultured oysters (*Crassostrea gigas*). *Science of the Total Environment* 393, 309–325. <https://doi.org/10.1016/j.scitotenv.2007.12.004>
- Li, L., Yang, X., 2018. The essential element manganese, oxidative stress, and metabolic diseases: Links and interactions. *Oxid Med Cell Longev*. <https://doi.org/10.1155/2018/7580707>
- Lindsay, P., Balls, P.W., West, J.R., 1996. Influence of tidal range and river discharge on suspended particulate matter fluxes in the Forth estuary (Scotland). *Estuar Coast Shelf Sci* 42, 63–82. <https://doi.org/10.1006/ecss.1996.0006>
- Liu, Y., Guo, T., Wang, R., Engel, B.A., Flanagan, D.C., Li, S., Pijanowski, B.C., Collingsworth, P.D., Lee, J.G., Wallace, C.W., 2019. A SWAT-based optimization tool for obtaining cost-effective strategies for agricultural conservation practice implementation at watershed scales. *Science of the Total Environment* 691, 685–696. <https://doi.org/10.1016/j.scitotenv.2019.07.175>
- Lockitch, G., 1993. Perspectives on Lead Toxicity, *Clin Biochem*.
- Luoma, S.N., Davis, J.A., 1983. Requirements for modeling trace metal partitioning in oxidized estuarine sediments. *Mar Chem* 12, 159–181. [https://doi.org/10.1016/0304-4203\(83\)90078-6](https://doi.org/10.1016/0304-4203(83)90078-6)
- Ma, T., Sun, S., Fu, G., Hall, J.W., Ni, Y., He, L., Yi, J., Zhao, N., Du, Y., Pei, T., Cheng, W., Song, C., Fang, C., Zhou, C., 2020. Pollution exacerbates China's water scarcity and its regional inequality. *Nat Commun* 11, 1–9. <https://doi.org/10.1038/s41467-020-14532-5>

- Mackin, J.E., Aller, R.C., 1984. PROCESSES AFFECTING THE BEHAVIOR OF DISSOLVED ALUMINUM IN ESTUARINE WATERS, *Marine Chemistry*.
- Mascarenhas, R.B., 2018. Caracterização e determinação de Valores de Referência de Qualidade para metais traços em Latossolo, Argissolos e Espodossolo do Baixo Sul da Bahia FEIRA.
- Mattone, C., Sheaves, M., 2017. Patterns, drivers and implications of dissolved oxygen dynamics in tropical mangrove forests. *Estuar Coast Shelf Sci* 197, 205–213. <https://doi.org/10.1016/j.ecss.2017.08.028>
- Mayer, L.M., 1982. Retention of riverine iron in estuaries. *Geochim Cosmochim Acta* 46, 1003–1009. [https://doi.org/10.1016/0016-7037\(82\)90055-2](https://doi.org/10.1016/0016-7037(82)90055-2)
- Meisch, H.-U., Benzschawel, H., 1978. The Role of Vanadium in Green Plants III. Influence on Cell Division of *Chlorella*, *Arch. Microbiol.*
- Metzger, E., Simonucci, C., Viollier, E., Sarazin, G., Prévot, F., Elbaz-Poulichet, F., Seidel, J.L., Jézéquel, D., 2007. Influence of diagenetic processes in Thau lagoon on cadmium behavior and benthic fluxes. *Estuar Coast Shelf Sci* 72, 497–510. <https://doi.org/10.1016/j.ecss.2006.11.016>
- Millward, G.E., 1995. Processes Affecting Trace Element Speciation in Estuaries* A Review, *Analyst*.
- MMA, M. do M.A.-, 2004. Plano de Manejo - APA do Pratigi. Ituberá.
- Molenat, J., Gascuel-Oudou, C., Ruiz, L., Gruau, G., 2008. Role of water table dynamics on stream nitrate export and concentration in agricultural headwater catchment (France). *J Hydrol (Amst)* 348, 363–378. <https://doi.org/10.1016/j.jhydrol.2007.10.005>
- Monbet, P., 2006. Mass balance of lead through a small macrotidal estuary: The Morlaix River estuary (Brittany, France). *Mar Chem* 98, 59–80. <https://doi.org/10.1016/j.marchem.2005.08.003>
- Monbet, P., 2004. Dissolved and particulate fluxes of copper through the Morlaix river estuary (Brittany, France): Mass balance in a small estuary with strong agricultural catchment. *Mar Pollut Bull* 48, 78–86. [https://doi.org/10.1016/S0025-326X\(03\)00327-8](https://doi.org/10.1016/S0025-326X(03)00327-8)
- Montes, S., Rivera-Mancia, S., Diaz-Ruiz, A., Tristan-Lopez, L., Rios, C., 2014. Copper and copper proteins in Parkinson's disease. *Oxid Med Cell Longev*. <https://doi.org/10.1155/2014/147251>
- Moore, W.S., 1997. EPSL High fluxes of radium and barium from the mouth of the Ganges-Brahmaputra River during low river discharge suggest large groundwater source, *Earth and Planetary Science Letters*.
- Morris, A.W., Bale, A.J., Howland, R.J.M., 1982. The dynamics of estuarine manganese cycling. *Estuar Coast Shelf Sci* 14, 175–192. [https://doi.org/10.1016/S0302-3524\(82\)80044-3](https://doi.org/10.1016/S0302-3524(82)80044-3)
- Morrissey, J., Bowler, C., 2012. Iron utilization in marine cyanobacteria and eukaryotic algae. *Front Microbiol* 3. <https://doi.org/10.3389/fmicb.2012.00043>

- Mosley, L.M., Liss, P.S., 2020. Particle aggregation, pH changes and metal behaviour during estuarine mixing: Review and integration. *Mar Freshw Res* 71, 300–310. <https://doi.org/10.1071/MF19195>
- Mulholland, P.J., Helton, A.M., Poole, G.C., Hall, R.O., Hamilton, S.K., Peterson, B.J., Tank, J.L., Ashkenas, L.R., Cooper, L.W., Dahm, C.N., Dodds, W.K., Findlay, S.E.G., Gregory, S. V., Grimm, N.B., Johnson, S.L., McDowell, W.H., Meyer, J.L., Valett, H.M., Webster, J.R., Arango, C.P., Beaulieu, J.J., Bernot, M.J., Burgin, A.J., Crenshaw, C.L., Johnson, L.T., Niederlehner, B.R., O'Brien, J.M., Potter, J.D., Sheibley, R.W., Sobota, D.J., Thomas, S.M., 2008. Stream denitrification across biomes and its response to anthropogenic nitrate loading. *Nature* 452, 202–205. <https://doi.org/10.1038/nature06686>
- Niu, Q., 2018. Overview of the Relationship Between Aluminum Exposure and Health of Human Being, in: *Advances in Experimental Medicine and Biology*. Springer New York LLC, pp. 1–31. https://doi.org/10.1007/978-981-13-1370-7_1
- O'Boyle, S., McDermott, G., Wilkes, R., 2009. Dissolved oxygen levels in estuarine and coastal waters around Ireland. *Mar Pollut Bull* 58, 1657–1663. <https://doi.org/10.1016/j.marpolbul.2009.07.002>
- Ocampo, C.J., Sivapalan, M., Oldham, C.E., 2006. Field exploration of coupled hydrological and biogeochemical catchment responses and a unifying perceptual model. *Adv Water Resour* 29, 161–180. <https://doi.org/10.1016/j.advwatres.2005.02.014>
- Oskarsson, A., 2015. Barium, in: Nordberg, G.F., Fowler, B.A., Nordberg, M. (Eds.), *Handbook on the Toxicology of Metals Fourth Edition*. Academic Press, Boston, pp. 625–634.
- Papanikolaou, N.C., Hatzidaki, E.G., Belivanis, S., Tzanakakis, G.N., Tsatsakis, A.M., 2005. Lead toxicity update. A brief review RA.
- Pearson, H.B.C., Comber, S.D.W., Braungardt, C., Worsfold, P.J., 2017. Predicting Copper Speciation in Estuarine Waters - Is Dissolved Organic Carbon a Good Proxy for the Presence of Organic Ligands? *Environ Sci Technol* 51, 2206–2216. <https://doi.org/10.1021/acs.est.6b05510>
- Peterson, B.J., Wollheim, W.M., Mulholland, P.J., Webster, J.R., Meyer, J.L., Tank, J.L., Marti, E., Bowden, W.B., Valett, H.M., Hershey, A.E., McDowell, W.H., Dodds, W.K., Hamilton, S.K., Gregory, S., Morrall, D.D., 2001. Control of nitrogen export from watersheds by headwater streams. *Science* (1979) 292, 86–90. <https://doi.org/10.1126/science.1056874>
- Pinto, A.P., Mota, A.M., de Varennes, A., Pinto, F.C., 2004. Influence of organic matter on the uptake of cadmium, zinc, copper and iron by sorghum plants. *Science of the Total Environment* 326, 239–247. <https://doi.org/10.1016/j.scitotenv.2004.01.004>
- Prabakaran, K., Eswaramoorthi, S., Nagarajan, R., Anandkumar, A., Franco, F.M., 2020. Geochemical behaviour and risk assessment of trace elements in a tropical river, Northwest Borneo. *Chemosphere* 252, 126430. <https://doi.org/10.1016/j.chemosphere.2020.126430>

- Premier, V., Machado, A.A. de S., Mitchell, S., Zarfl, C., Spencer, K., Toffolon, M., 2019. A model-based analysis of metal fate in the thames estuary. *Estuaries and Coasts* 42, 1185–1201. <https://doi.org/10.1007/s12237-019-00544-y>
- Radwan, M., Willems, P., El-Sadek, A., Berlamont, J., 2003. Modelling of dissolved oxygen and biochemical oxygen demand in river water using a detailed and a simplified model. *International Journal of River Basin Management* 1, 97–103. <https://doi.org/10.1080/15715124.2003.9635196>
- Raghu, V., 2001. Accumulation of elements in plants and soils in and around Mangampeta and Vemula barite mining areas, Cuddapah District, Andhra Pradesh, India. *Environmental Geology* 40, 1265–1277. <https://doi.org/10.1007/s002540100308>
- Raiswell, R., 2011. Iron transport from the continents to the open ocean: The aging-rejuvenation cycle. *Elements* 7, 101–106. <https://doi.org/10.2113/gselements.7.2.101>
- Rani, A., Kumar, A., Lal, A., Pant, M., 2014. Cellular mechanisms of cadmium-induced toxicity: A review. *Int J Environ Health Res.* <https://doi.org/10.1080/09603123.2013.835032>
- Rathnayake, A.S., Dushyantha, N., De Silva, N., Somarsiri, H.P., Jayasekara, N.N., Weththasinghe, S.M., Samaradivakara, G.V.I., Vijitha, A.V.P., Ratnayake, N.P., 2017. Sediment and Physicochemical Characteristics in Madu-Ganga Sediment and Physicochemical Characteristics in Madu-Ganga Estuary, Southwest Sri Lanka. *Journal of Geological Society of Sri Lanka* Pp.43-52.
- Ray, R., Baum, A., Rixen, T., Gleixner, G., Jana, T.K., 2018. Exportation of dissolved (inorganic and organic) and particulate carbon from mangroves and its implication to the carbon budget in the Indian Sundarbans. *Science of the Total Environment* 621, 535–547. <https://doi.org/10.1016/j.scitotenv.2017.11.225>
- Reese, A., Zimmermann, T., Pröfrock, D., Irrgeher, J., 2019. Extreme spatial variation of Sr, Nd and Pb isotopic signatures and 48 element mass fractions in surface sediment of the Elbe River Estuary - Suitable tracers for processes in dynamic environments? *Science of the Total Environment* 668, 512–523. <https://doi.org/10.1016/j.scitotenv.2019.02.401>
- Rezende, C.E., Lacerda, L.D., Ovalle, A.R.C., Silva, L.F.F., 2007. Dial organic carbon fluctuations in a mangrove tidal creek in Sepetiba bay, Southeast Brazil. *Brazilian Journal of Biology* 67, 673–680. <https://doi.org/10.1590/S1519-69842007000400012>
- Richard, F.C., Bourg, A.C.M., 1991. Aqueous geochemistry of chromium: A review. *Water Res* 25, 807–816. [https://doi.org/10.1016/0043-1354\(91\)90160-R](https://doi.org/10.1016/0043-1354(91)90160-R)
- Richard, S., Galy-Lacaux, C., Arnoux, A., Cerdan, P., Delmas, R., François Dumestre, J., Gosse, P., Horeau, V., Labroue, L., Sissakian, C., 2000. Evolution of physico-chemical water quality and methane emissions in the tropical hydroelectric reservoir of Petit Saut (French Guiana). *SIL Proceedings, 1922-2010* 27, 1454–1458. <https://doi.org/10.1080/03680770.1998.11901478>
- Richards, C.M., van Puffelen, J.L., Pallud, C., 2018. Effects of sediment resuspension on the oxidation of acid-volatile sulfides and release of metals (iron, manganese, zinc) in

- Pescadero estuary (CA, USA). *Environ Toxicol Chem* 37, 993–1006. <https://doi.org/10.1002/etc.4047>
- Romigh, M.M., Davis, S.E., Rivera-Monroy, V.H., Twilley, R.R., 2006. Flux of organic carbon in a riverine mangrove wetland in the Florida Coastal Everglades. *Hydrobiologia* 569, 505–516. <https://doi.org/10.1007/s10750-006-0152-x>
- Rotteveel, L., Sterling, S.M., 2020. Five Aluminum Seasonality Regimes Identified in Chronically Acidified Rivers of Nova Scotia. *Environ Sci Technol* 54, 807–817. <https://doi.org/10.1021/acs.est.9b04872>
- Salomão, M.S.M.B., Molisani, M.M., Ovalle, A.R.C., Rezende, C.E., Lacerda, L.D., Carvalho, C.E.V., 2001. Particulate heavy metal transport in the lower Paraíba do Sul River basin, southeastern, Brazil. *Hydrol Process* 15, 587–593. <https://doi.org/10.1002/hyp.168>
- Samani, A.R.V., Karbassi, A.R., Fakhraee, M., Heidari, M., Vaezi, A.R., Valikhani, Z., 2014. Effect of dissolved organic carbon and salinity on flocculation process of heavy metals during mixing of the Navrud River water with Caspian Seawater. *Desalination Water Treat* 55, 926–934. <https://doi.org/10.1080/19443994.2014.920730>
- Samanta, S., Dalai, T.K., 2016. Dissolved and particulate Barium in the Ganga (Hooghly) River estuary, India: Solute-particle interactions and the enhanced dissolved flux to the oceans. *Geochim Cosmochim Acta* 195, 1–28. <https://doi.org/10.1016/j.gca.2016.09.005>
- Sanders, C.J., Santos, I.R., Maher, D.T., Sadat-Noori, M., Schnetger, B., Brumsack, H.J., 2015. Dissolved iron exports from an estuary surrounded by coastal wetlands: Can small estuaries be a significant source of Fe to the ocean? *Mar Chem* 176, 75–82. <https://doi.org/10.1016/j.marchem.2015.07.009>
- Saputro, S., Yoshimura, K., Matsuoka, S., Takehara, K., Narsito, Aizawa, J., Tennichi, Y., 2014. Speciation of dissolved chromium and the mechanisms controlling its concentration in natural water. *Chem Geol* 364, 33–41. <https://doi.org/10.1016/j.chemgeo.2013.11.024>
- Schäfer, J., Norra, S., Klein, D., Blanc, G., 2009. Mobility of trace metals associated with urban particles exposed to natural waters of various salinities from the Gironde Estuary, France. *J Soils Sediments* 9, 374–392. <https://doi.org/10.1007/s11368-009-0096-7>
- Schiffer, S., Liber, K., 2017. Toxicity of aqueous vanadium to zooplankton and phytoplankton species of relevance to the athabasca oil sands region. *Ecotoxicol Environ Saf* 137, 1–11. <https://doi.org/10.1016/j.ecoenv.2016.10.040>
- Schlesinger, W.H., Klein, E.M., Vengosh, A., 2017. Global biogeochemical cycle of vanadium. *Proc Natl Acad Sci U S A* 114, E11092–E11100. <https://doi.org/10.1073/pnas.1715500114>
- Semeniuk, D.M., Maldonado, M.T., Jaccard, S.L., 2016. Chromium uptake and adsorption in marine phytoplankton - Implications for the marine chromium cycle. *Geochim Cosmochim Acta* 184, 41–54. <https://doi.org/10.1016/j.gca.2016.04.021>

- Senze, M., Kowalska-Góralaska, M., Czyż, K., 2021. Availability of aluminum in river water supplying dam reservoirs in Lower Silesia considering the hydrochemical conditions. *Environ Nanotechnol Monit Manag* 16. <https://doi.org/10.1016/j.enmm.2021.100535>
- Shayganfard, M., 2022. Are Essential Trace Elements Effective in Modulation of Mental Disorders? Update and Perspectives. *Biol Trace Elem Res* 200, 1032–1059. <https://doi.org/10.1007/s12011-021-02733-y>
- Sherrell, R.M., Boyle, E.A., 1988. Zinc, chromium, vanadium and iron in the Mediterranean Sea. *Deep Sea Research Part A. Oceanographic Research Papers* 35, 1319–1334. [https://doi.org/10.1016/0198-0149\(88\)90085-4](https://doi.org/10.1016/0198-0149(88)90085-4)
- Shiller, A.M., 1997. Dissolved trace elements in the Mississippi River: Seasonal, interannual, and decadal variability. *Geochim Cosmochim Acta* 61, 4321–4330. [https://doi.org/10.1016/S0016-7037\(97\)00245-7](https://doi.org/10.1016/S0016-7037(97)00245-7)
- Shiller, A.M., Boyle, E.A., 1991. Trace elements in the Mississippi River Delta outflow region: Behavior at high discharge. *Geochim Cosmochim Acta* 55, 3241–3251. [https://doi.org/10.1016/0016-7037\(91\)90486-O](https://doi.org/10.1016/0016-7037(91)90486-O)
- Shiller, A.M., Boyle, E.A., 1987. Dissolved vanadium in rivers and estuaries. *Earth Planet Sci Lett* 86, 214–224. [https://doi.org/10.1016/0012-821X\(87\)90222-6](https://doi.org/10.1016/0012-821X(87)90222-6)
- Shiller, A.M., Mao, L., 2000. Dissolved vanadium in rivers: effects of silicate weathering, *Chemical Geology*.
- Sholkovitz, E.R., 1978a. The flocculation of dissolved Fe, Mn, Al, Cu, Ni, Co and Cd during estuarine mixing. *Earth Planet Sci Lett* 41, 77–86. [https://doi.org/10.1016/0012-821X\(78\)90043-2](https://doi.org/10.1016/0012-821X(78)90043-2)
- Sholkovitz, E.R., 1978b. The flocculation of dissolved Fe, Mn, Al, Cu, Ni, Co and Cd during estuarine mixing. *Earth Planet Sci Lett* 41, 77–86. [https://doi.org/10.1016/0012-821X\(78\)90043-2](https://doi.org/10.1016/0012-821X(78)90043-2)
- Singh, S.P., Singh, S.K., Bhushan, R., 2013. Internal cycling of dissolved barium in water column of the Bay of Bengal. *Mar Chem* 154, 12–23. <https://doi.org/10.1016/j.marchem.2013.04.013>
- Sleimi, N., Kouki, R., Hadj Ammar, M., Ferreira, R., Pérez-Clemente, R., 2021. Barium effect on germination, plant growth, and antioxidant enzymes in *Cucumis sativus* L. plants. *Food Sci Nutr* 9, 2086–2094. <https://doi.org/10.1002/fsn3.2177>
- Srinivas, R., Singh, A.P., Dhadse, K., Garg, C., 2020. An evidence based integrated watershed modelling system to assess the impact of non-point source pollution in the riverine ecosystem. *J Clean Prod* 246, 118963. <https://doi.org/10.1016/j.jclepro.2019.118963>
- Stecher, Hilmar A, Kogut, M.B., 1999. Rapid barium removal in the Delaware estuary. *Geochim Cosmochim Acta* 63, 1003–1012. [https://doi.org/10.1016/S0016-7037\(98\)00310-X](https://doi.org/10.1016/S0016-7037(98)00310-X)

- Stecher, Hilmar A., Kogut, M.B., 1999. Rapid barium removal in the Delaware estuary. *Geochim Cosmochim Acta* 63, 1003–1012. [https://doi.org/10.1016/S0016-7037\(98\)00310-X](https://doi.org/10.1016/S0016-7037(98)00310-X)
- Stern, B.R., 2010. Essentiality and toxicity in copper health risk assessment: Overview, update and regulatory considerations, in: *Journal of Toxicology and Environmental Health - Part A: Current Issues*. pp. 114–127. <https://doi.org/10.1080/15287390903337100>
- Stoffyn, M., Mackenzie, F.T., 1982. Fate of dissolved aluminum in the oceans, *Marine Chemistry*.
- Stouthart, A.J.H.X., Spanings, F.A.T., Lock, R.A.C., Wendelaar Bonga, S.E., 1994. Effects of low water pH on lead toxicity to early life stages of the common carp (*Cyprinus carpio*).
- Strady, E., Blanc, G., Schäfer, J., Coynel, A., Dabrin, A., 2009. Dissolved uranium, vanadium and molybdenum behaviours during contrasting freshwater discharges in the Gironde Estuary (SW France). *Estuar Coast Shelf Sci* 83, 550–560. <https://doi.org/10.1016/j.ecss.2009.05.006>
- Suzumura, M., 2004. Distribution and characteristics of suspended particulate matter in a heavily eutrophic estuary, Tokyo Bay, Japan 49, 496–503. <https://doi.org/10.1016/j.marpolbul.2004.03.002>
- Takayanagi, K., Gobeil, C., 2000. Dissolved Aluminum in the Upper St. Lawrence Estuary. *J Oceanogr* 56, 517–525. <https://doi.org/https://doi.org/10.1023/A:1011196826709>
- Telesh, I. V., Khlebovich, V. V., 2010. Principal processes within the estuarine salinity gradient: A review. *Mar Pollut Bull* 61, 149–155. <https://doi.org/10.1016/j.marpolbul.2010.02.008>
- Telesh, I. v., Khlebovich, V. v., 2010. Principal processes within the estuarine salinity gradient: A review. *Mar Pollut Bull* 61, 149–155. <https://doi.org/10.1016/j.marpolbul.2010.02.008>
- Thibault de Chanvalon, A., Mouret, A., Knoery, J., Geslin, E., Péron, O., Metzger, E., 2016. Manganese, iron and phosphorus cycling in an estuarine mudflat, Loire, France. *J Sea Res* 118, 92–102. <https://doi.org/10.1016/j.seares.2016.10.004>
- Thill, A., Moustier, S., Garnier, J.M., Estournel, C., Naudin, J.J., Bottero, J.Y., 2001. Evolution of particle size and concentration in the Rhône river mixing zone: Influence of salt flocculation. *Cont Shelf Res* 21, 2127–2140. [https://doi.org/10.1016/S0278-4343\(01\)00047-4](https://doi.org/10.1016/S0278-4343(01)00047-4)
- Tomczak, W., Boyer, P., Krimissa, M., Radakovitch, O., 2019. Kd distributions in freshwater systems as a function of material type, mass-volume ratio, dissolved organic carbon and pH. *Applied Geochemistry* 105, 68–77. <https://doi.org/10.1016/j.apgeochem.2019.04.003>
- Turner, A., le Roux, S.M., Millward, G.E., 2008. Adsorption of cadmium to iron and manganese oxides during estuarine mixing. *Mar Chem* 108, 77–84. <https://doi.org/10.1016/j.marchem.2007.10.004>

- Turner, A., Millward, G.E., Le Roux, S.M., 2004. Significance of oxides and particulate organic matter in controlling trace metal partitioning in a contaminated estuary. *Mar Chem* 88, 179–192. <https://doi.org/10.1016/j.marchem.2004.03.008>
- Udechukwu, B.E., Ismail, A., Zulkifli, S.Z., Omar, H., 2015. Distribution, mobility, and pollution assessment of Cd, Cu, Ni, Pb, Zn, and Fe in intertidal surface sediments of Sg. Puloh mangrove estuary, Malaysia. *Environmental Science and Pollution Research* 22, 4242–4255. <https://doi.org/10.1007/s11356-014-3663-4>
- Upadhyay, S., 2008. Sorption model for dissolved and particulate aluminium in the Conway estuary, UK. *Estuar Coast Shelf Sci* 76, 914–919. <https://doi.org/10.1016/j.ecss.2007.08.021>
- van den Berg, C.M.G., Merks, A.G.A., Duursma, E.K., 1987. Organic complexation and its control of the dissolved concentrations of copper and zinc in the Scheldt estuary. *Estuar Coast Shelf Sci* 24, 785–797. [https://doi.org/10.1016/0272-7714\(87\)90152-1](https://doi.org/10.1016/0272-7714(87)90152-1)
- Veselyâ, J., R Majer, V., Kuci Era, J., n.d. Solid±water partitioning of elements in Czech freshwaters.
- Waeles, M., Riso, R.D., le Corre, P., 2005. Seasonal variations of dissolved and particulate copper species in estuarine waters. *Estuar Coast Shelf Sci* 62, 313–323. <https://doi.org/10.1016/j.ecss.2004.09.019>
- Waeles, M., Riso, R.D., Maguer, J.F., Corre, P. le, 2004a. Distribution and chemical speciation of dissolved cadmium and copper in the Loire estuary and North Biscay continental shelf, France. *Estuar Coast Shelf Sci* 59, 49–57. <https://doi.org/10.1016/j.ecss.2003.07.009>
- Waeles, M., Riso, R.D., Maguer, J.F., Le Corre, P., 2004b. Distribution and chemical speciation of dissolved cadmium and copper in the Loire estuary and North Biscay continental shelf, France. *Estuar Coast Shelf Sci* 59, 49–57. <https://doi.org/10.1016/j.ecss.2003.07.009>
- Waeles, M., Tanguy, V., Lespes, G., Riso, R.D., 2008. Behaviour of colloidal trace metals (Cu, Pb and Cd) in estuarine waters: An approach using frontal ultrafiltration (UF) and stripping chronopotentiometric methods (SCP). *Estuar Coast Shelf Sci* 80, 538–544. <https://doi.org/10.1016/j.ecss.2008.09.010>
- Wang, D., He, Y., Liang, J., Liu, P., Zhuang, P., 2013. Distribution and source analysis of aluminum in rivers near Xi'an City, China. *Environ Monit Assess* 185, 1041–1053. <https://doi.org/10.1007/s10661-012-2612-2>
- Wang, D., Lin, W., Yang, X., Zhai, W., Dai, M., Chen, C.T.A., 2012. Occurrences of dissolved trace metals (Cu, Cd, and Mn) in the Pearl River Estuary (China), a large river-groundwater-estuary system. *Cont Shelf Res* 50–51, 54–63. <https://doi.org/10.1016/j.csr.2012.10.009>
- Wang, D., Sañudo Wilhelmy, S.A., 2009. Vanadium speciation and cycling in coastal waters. *Mar Chem* 117, 52–58. <https://doi.org/10.1016/j.marchem.2009.06.001>

- Wang, H., Hondzo, M., Xu, C., Poole, V., Spacie, A., 2003. Dissolved oxygen dynamics of streams draining an urbanized and an agricultural catchment. *Ecol Modell* 160, 145–161. [https://doi.org/10.1016/S0304-3800\(02\)00324-1](https://doi.org/10.1016/S0304-3800(02)00324-1)
- Wang, Z.-W., Ren, J.-L., Jiang, S., Liu, S.-M., Xuan, J.-L., Zhang, J., 2016. Geochemical behavior of dissolved manganese in the East China Sea: Seasonal variation, estuarine removal, and regeneration under suboxic conditions. *Geochemistry, Geophysics, Geosystems* 17, 282–299. <https://doi.org/10.1002/2015GC006128>
- Wei, T., Simko, V., 2021. R package “corrplot”: Visualization of a Correlation Matrix.
- Wen, L.S., Warnken, K.W., Santschi, P.H., 2008. The role of organic carbon, iron, and aluminium oxyhydroxides as trace metal carriers: Comparison between the Trinity River and the Trinity River Estuary (Galveston Bay, Texas). *Mar Chem* 112, 20–37. <https://doi.org/10.1016/j.marchem.2008.06.003>
- Wever, R., Tromp, M.G.M., Krenn, B.E., Marjani, A., van Tol, M., 1991. Brominating activity of the seaweed *Ascophyllum nodosum*: impact on the biosphere. *Environ Sci Technol* 25, 446–449. <https://doi.org/10.1021/es00015a010>
- Wilhelm, C., Wild, A., 1984. The Variability of the Photosynthetic Unit in *Chlorella* I. The Effect of Vanadium on Photosynthesis, Productivity, P-700 and Cytochrome f in Undiluted and Homocontinuous Cultures of *Chlorella*. *J Plant Physiol* 115, 115–124. [https://doi.org/10.1016/S0176-1617\(84\)80058-9](https://doi.org/10.1016/S0176-1617(84)80058-9)
- Wilke, R.J., Dayal, R., 1982. The behavior of iron, manganese and silicon in the Peconic River estuary, New York. *Estuar Coast Shelf Sci* 15, 577–586. [https://doi.org/10.1016/0272-7714\(82\)90009-9](https://doi.org/10.1016/0272-7714(82)90009-9)
- Wittbrodt, P.R., Palmer, C.D., 1997. Reduction of Cr(VI) by soil humic acids. *Eur J Soil Sci* 48, 151–162. <https://doi.org/10.1111/j.1365-2389.1997.tb00194.x>
- Wolanski, E., 1986. An evaporation-driven salinity maximum zone in Australian tropical estuaries. *Estuar Coast Shelf Sci* 22, 415–424. [https://doi.org/10.1016/0272-7714\(86\)90065-X](https://doi.org/10.1016/0272-7714(86)90065-X)
- Yan, L., Stallard, R.F., Key, R.M., Crerar, D.A., 1990. The chemical behavior of trace metals and ²²⁶Ra during estuarine mixing in the Mullica River estuary, New Jersey, U.S.A.: A comparison between field observation and equilibrium calculation, *Chemical Geology*. Elsevier Science Publishers B.V.
- Yan, Yu, Han, L., Yu, R. lian, Hu, G. ren, Zhang, W. fang, Cui, J. yong, Yan, Yan, Huang, H. bin, 2020. Background determination, pollution assessment and source analysis of heavy metals in estuarine sediments from Quanzhou Bay, southeast China. *Catena (Amst)* 187. <https://doi.org/10.1016/j.catena.2019.104322>
- Yang, M., Sañudo-Wilhelmy, S.A., 1998. Cadmium and manganese distributions in the Hudson River estuary: interannual and seasonal variability, *Earth and Planetary Science Letters*. [https://doi.org/https://doi.org/10.1016/S0012-821X\(98\)00100-9](https://doi.org/https://doi.org/10.1016/S0012-821X(98)00100-9)
- Yeats, P.A., 1993. Input of metals to the North Atlantic from two large Canadian estuaries. *Mar Chem* 201–209. [https://doi.org/10.1016/0304-4203\(93\)90225-D](https://doi.org/10.1016/0304-4203(93)90225-D)

- Young, L.B., Harvey, H.H., 1992. The relative importance of manganese and iron oxides and organic matter in the sorption of trace metals by surficial lake sediments. *Geochim Cosmochim Acta* 56, 1175–1186. [https://doi.org/10.1016/0016-7037\(92\)90055-N](https://doi.org/10.1016/0016-7037(92)90055-N)
- Zhang, C., Yu, Z., Zeng, G., Jiang, M., Yang, Z., Cui, F., Zhu, M., Shen, L., Hu, L., 2014. Effects of sediment geochemical properties on heavy metal bioavailability. *Environ Int* 73, 270–281. <https://doi.org/10.1016/j.envint.2014.08.010>
- Zhang, X., McRose, D.L., Darnajoux, R., Bellenger, J.P., Morel, F.M.M., Kraepiel, A.M.L., 2016. Alternative nitrogenase activity in the environment and nitrogen cycle implications. *Biogeochemistry*. <https://doi.org/10.1007/s10533-016-0188-6>
- Zhou, L., Tan, Y., Huang, L., Fortin, C., Campbell, P.G.C., 2018. Aluminum effects on marine phytoplankton: implications for a revised Iron Hypothesis (Iron–Aluminum Hypothesis). *Biogeochemistry*. <https://doi.org/10.1007/s10533-018-0458-6>

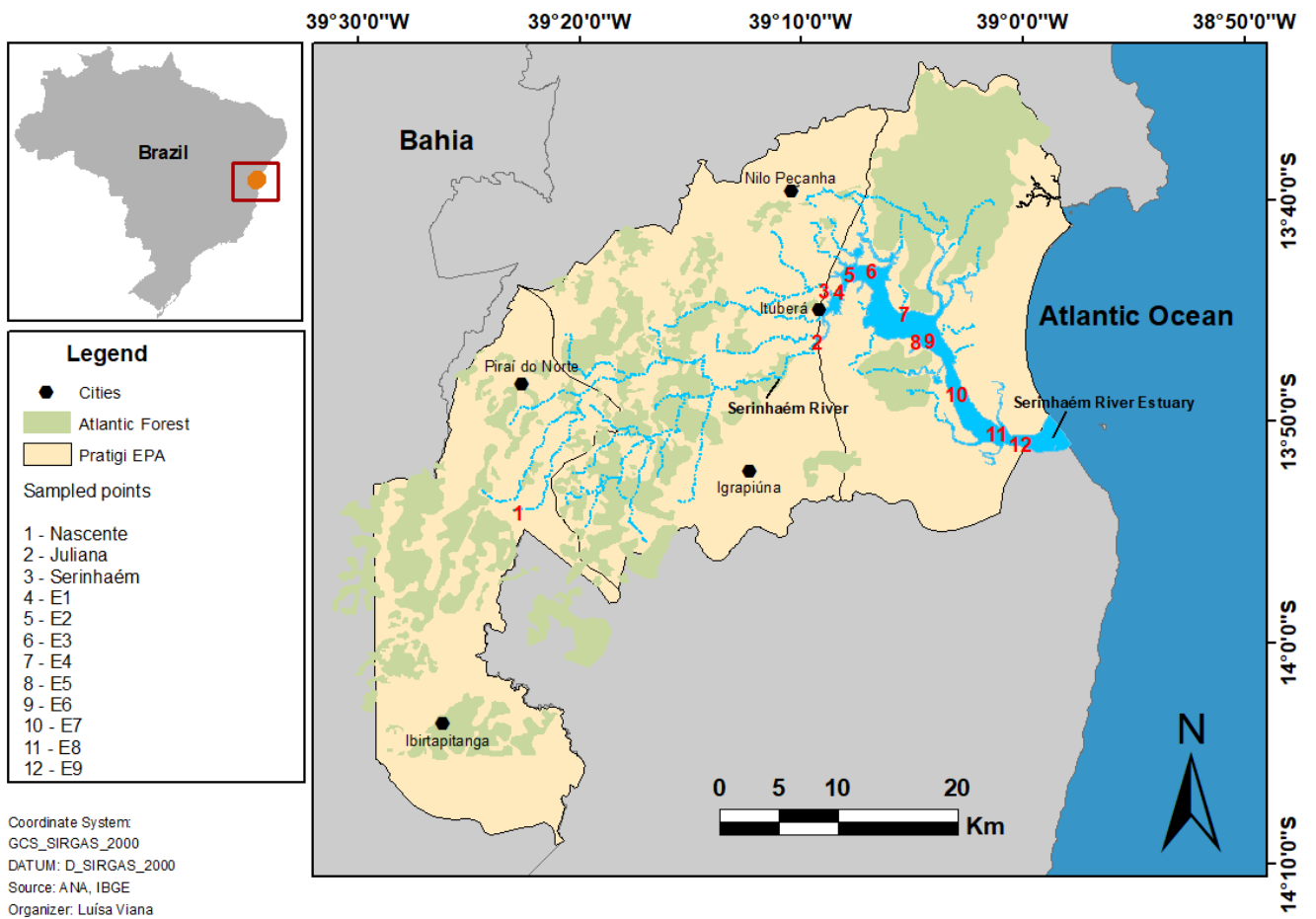


Figure 1 – Map of the Pratigi Environmental Protection Area (EPA), sampling points and main tributaries. The cities are represented by the black dots and the numbers refer to the sampling points.

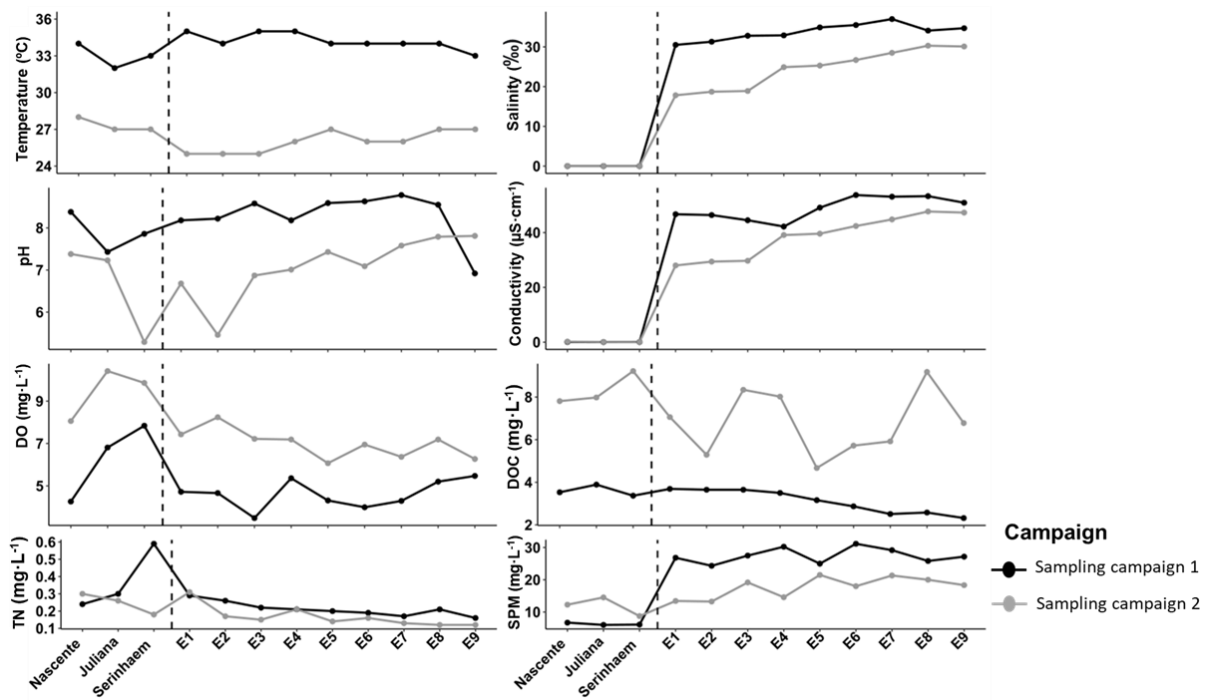


Figure 2 – Physico-chemical parameters of the water column in both campaigns.

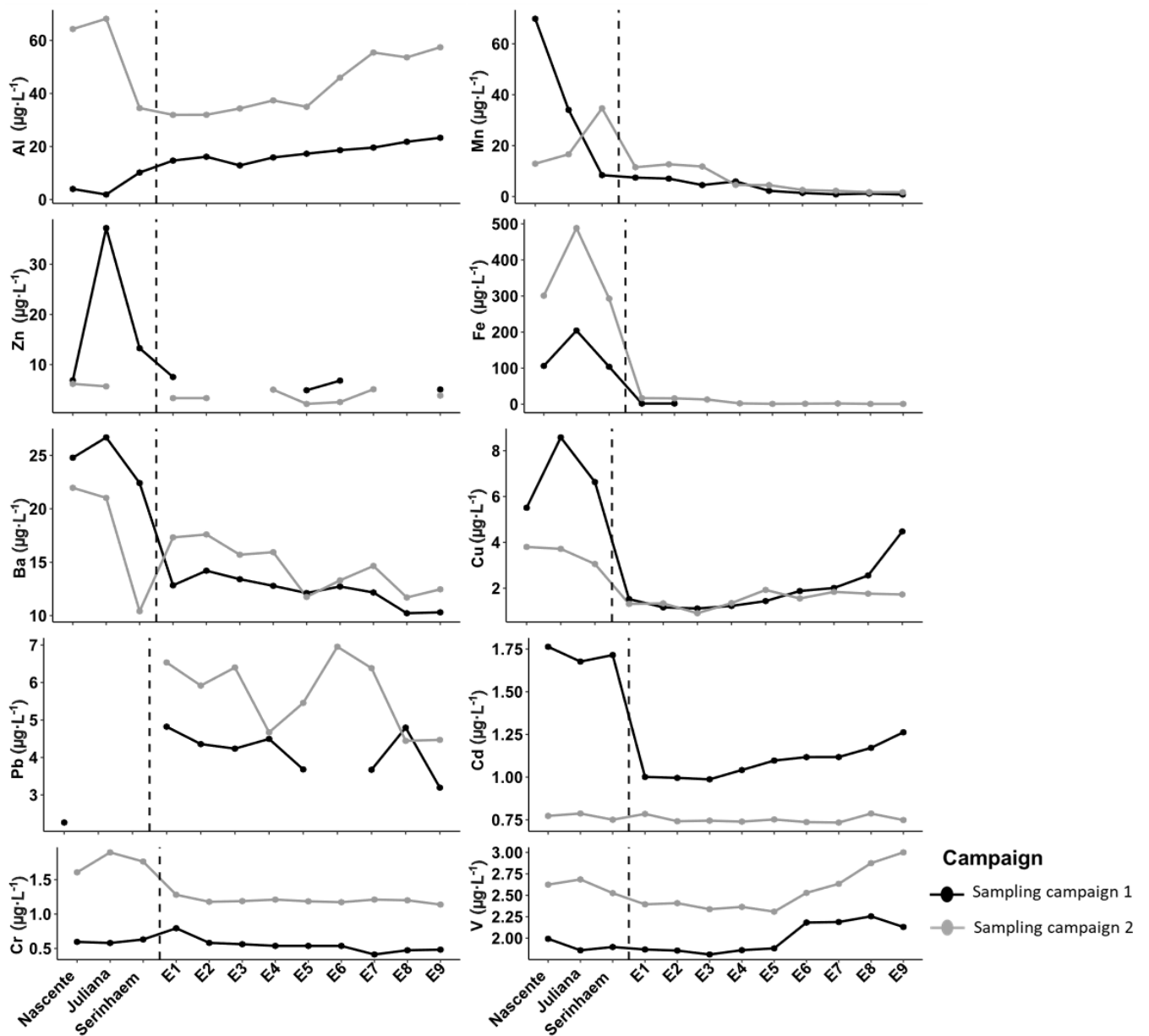


Figure 3 – Concentrations of trace elements (Al, Ba, Cd, Cr, Cu, Fe, Mn, Pb, V, Zn) in the dissolved fraction of the water column in the two collection campaigns. Missing values refer to concentrations below the limit of detection

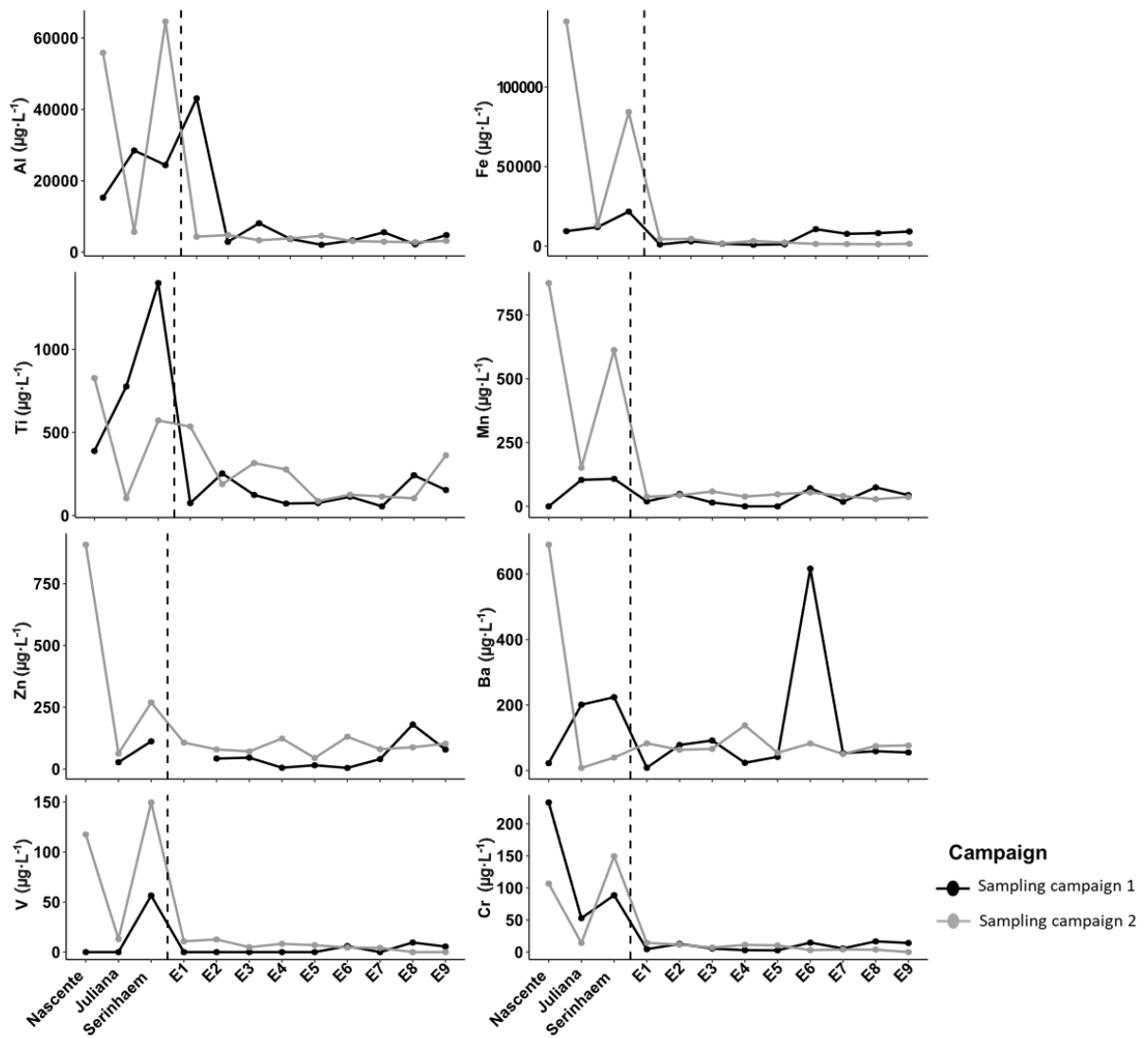


Figure 4 - Concentrations of trace elements (Al, Ba, Cr, Fe, Mn, Ti, V, Zn) in the particulate fraction of the water column in the two collection campaigns.

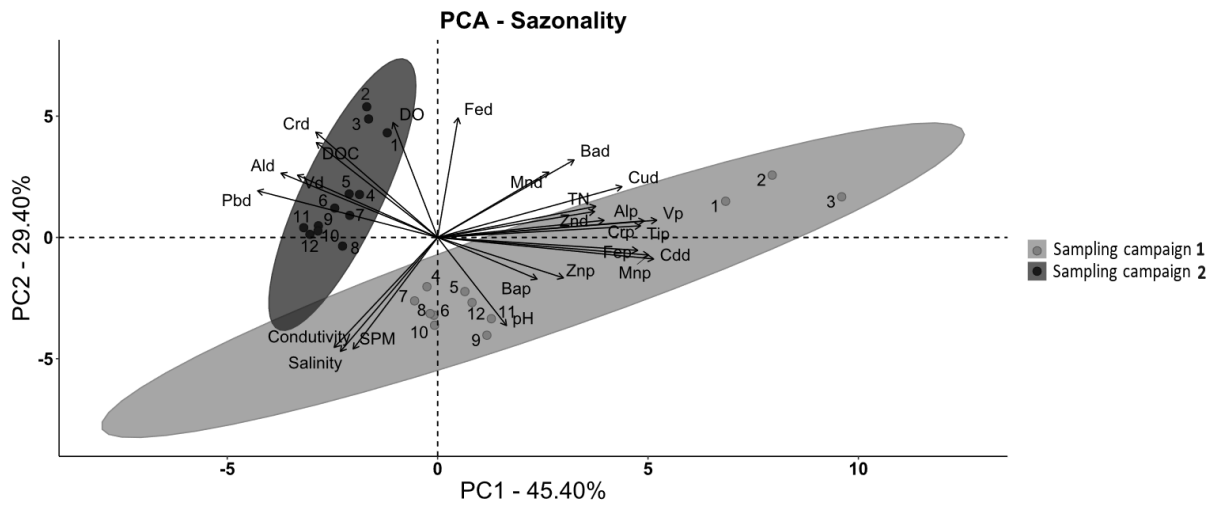


Figure 5 – Principal component analysis (PCA) between the trace elements and the physicochemical parameters determined in this study and its relationship with the two collection campaigns.

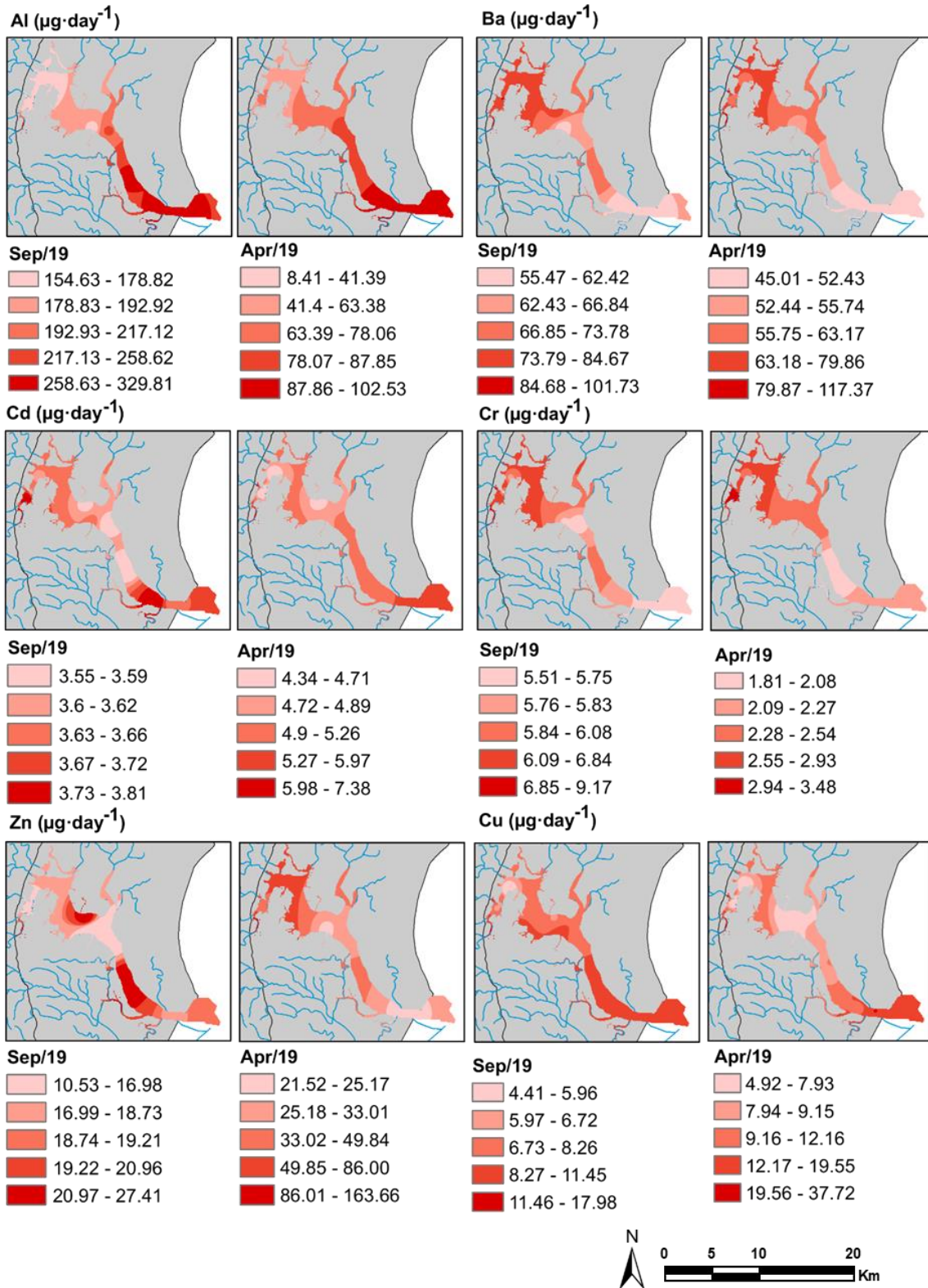


Figure 6 – Flow of trace elements (Al, Ba, Cd, Cr, Cu and Zn) in the dissolved fraction of the water column in both collection campaigns.

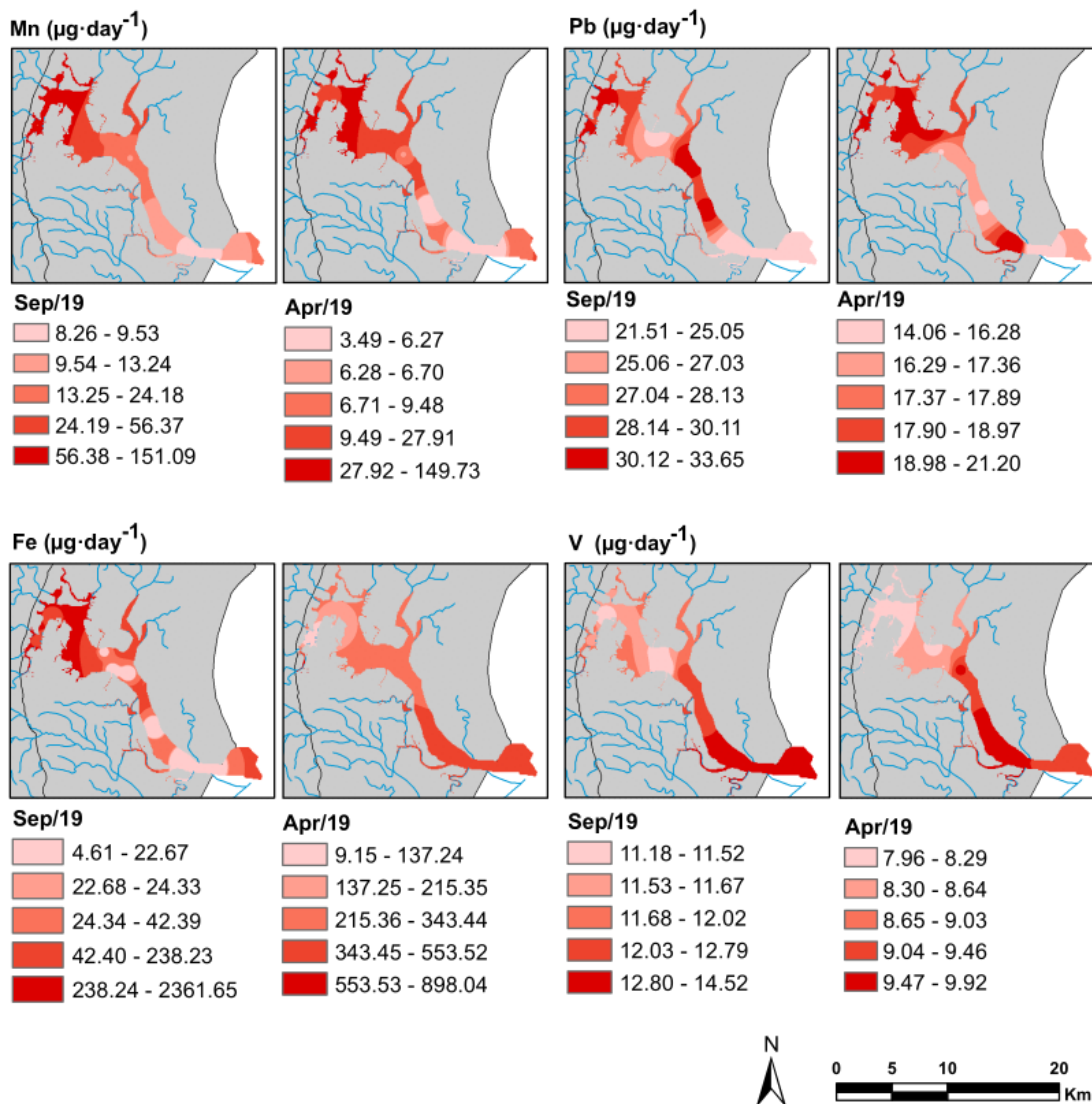


Figure 7 – Flow of trace elements (Mn, Pb, Fe and V) in the dissolved fraction of the water column in both collection campaigns.

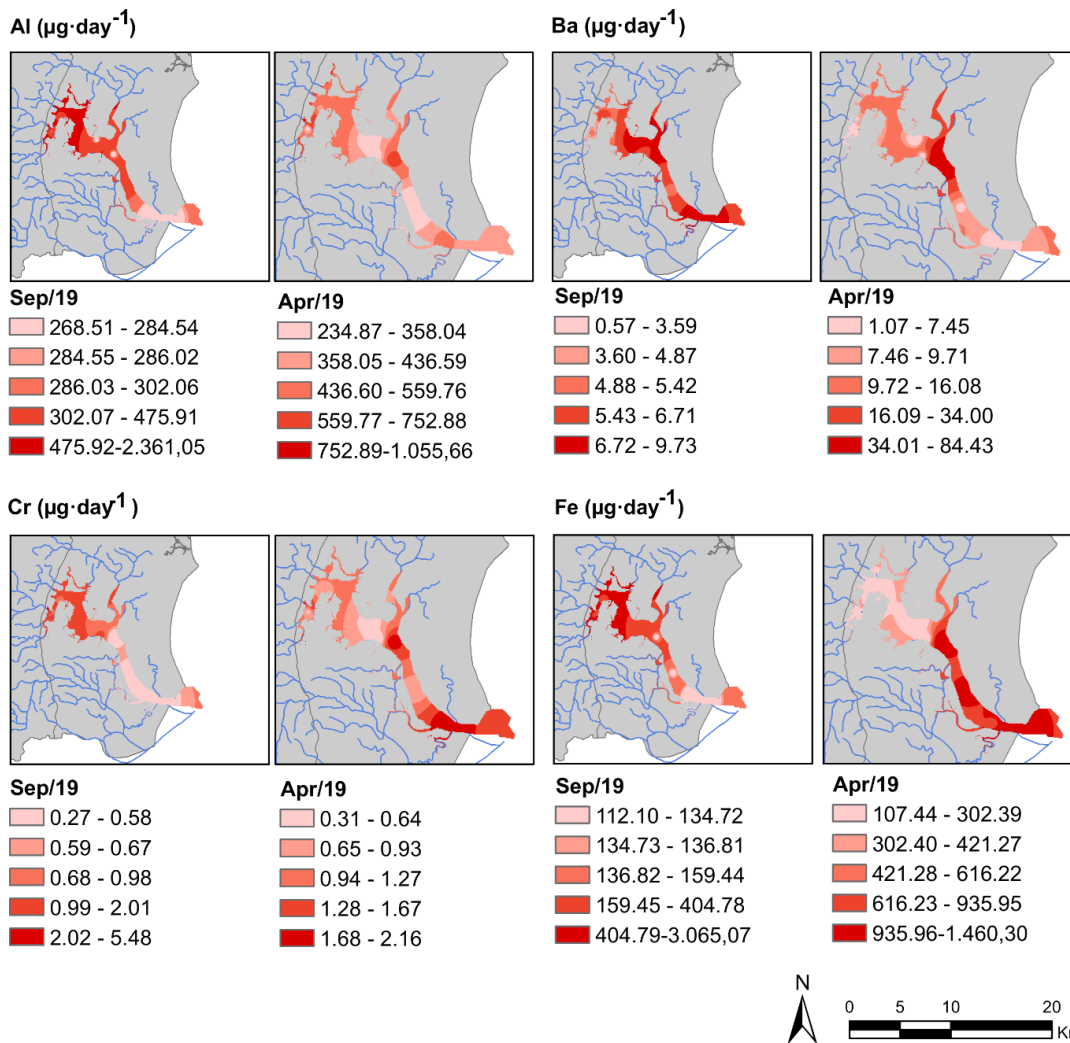


Figure 8 – Flow of trace elements (Al, Ba, Cr and Fe) in the particulate fraction of the water column in both collection campaigns.

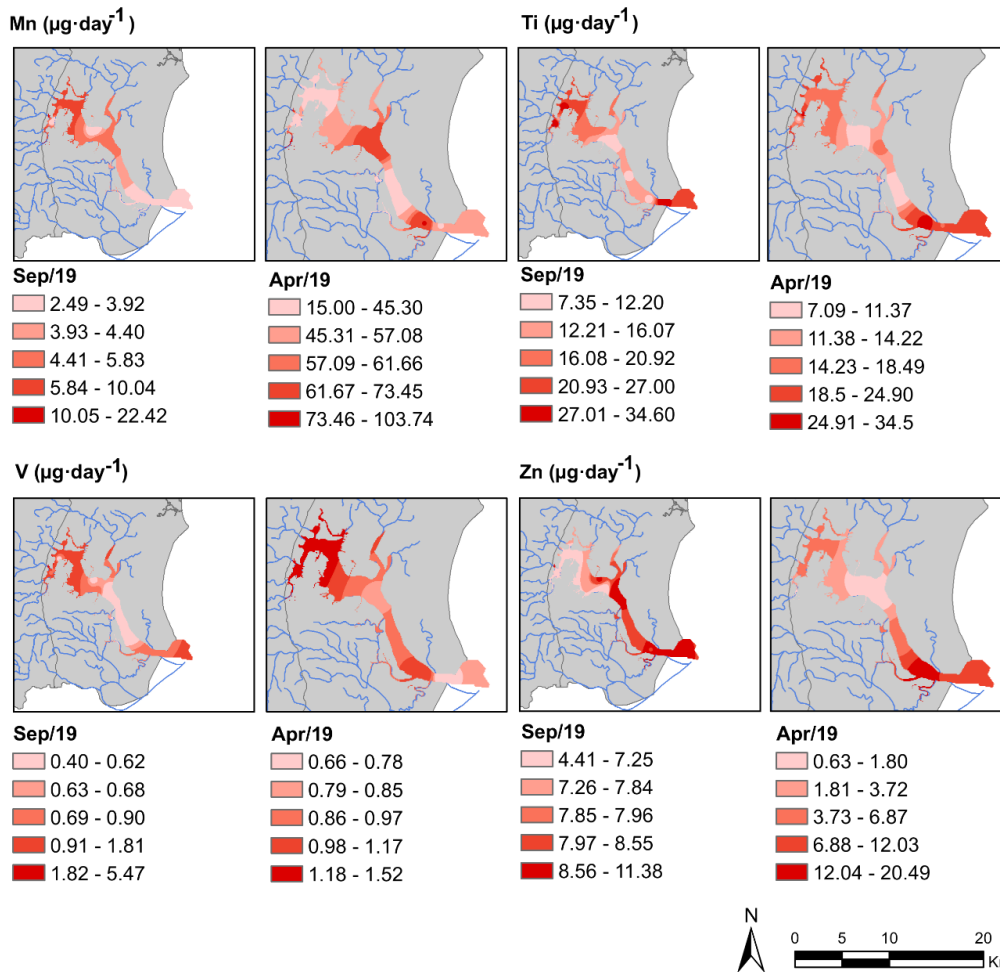


Figure 9 - Flow of trace elements (Mn, Ti, V and Zn) in the particulate fraction in the water column in both collection campaigns.

Supplementary Material

Table S7 - Analytical procedure validation using Nist Standard Reference Material® 1646a from estuarine sediments (mg kg⁻¹ dry weight), N = 3. Data are presented as mean ± SD.

	Al	Fe	Ba	Mn	Cr	Zn	Cd	Cu	Ni	Pb
Obtained concentrations	16979.0 ± 3086.28	19302.9 ± 132.56	145.9 ± 7.58	171.3 ± 1.35	28.0 ± 0.4	35.3 ± 0.69	0.74 ± 0.2	7.4 ± 0.62	15.2 ± 0.03	7.6 ± 0.69
Certified concentrations	22970	20080	210	234.5	40.9	48.9	0.817	10	23	11.7
Recovery (%)	74±13	96±1	69±4	73±1	69±1	72±1	90±1	74±6	66±1	65±5

Table S8 - Dissolved flows – Rainy.

Rainy ($\mu\text{g}\cdot\text{L}^{-1}$)											
Samples	Al	Ba	Cd	Cr	Cu	Fe	Mn	Pb	V	Zn	Discharge ($\text{m}^3\cdot\text{s}^{-1}$)
Nacente	4.00	24.78	1.76	0.60	5.51	106.19	69.87	2.26	1.99	6.86	4.4
Juliana	1.90	26.69	1.68	0.58	8.58	204.22	34.06	<LOD	1.86	37.21	
Serinhaem	10.20	22.41	1.72	0.63	6.63	103.90	8.42	<LOD	1.90	13.27	
E1	14.70	12.84	1.00	0.79	1.53	1.94	7.45	4.82	1.87	7.53	
E2	16.16	14.21	1.00	0.58	1.16	1.95	7.05	4.36	1.86	<LOD	
E3	12.88	13.41	0.99	0.56	1.12	<LOD	4.52	4.24	1.81	<LOD	
E4	15.89	12.79	1.04	0.54	1.23	<LOD	5.95	4.49	1.86	<LOD	
E5	17.30	12.12	1.10	0.54	1.44	<LOD	2.28	3.68	1.88	4.89	
E6	18.64	12.73	1.12	0.54	1.88	<LOD	1.43	<LOD	2.18	6.80	
E7	19.59	12.17	1.12	0.41	2.01	<LOD	0.87	3.67	2.19	<LOD	
E8	21.79	10.23	1.17	0.47	2.56	<LOD	1.19	4.80	2.25	<LOD	
E9	23.30	10.31	1.26	0.48	4.48	<LOD	0.79	3.20	2.13	5.04	
Fluxes ($\mu\text{g}\cdot\text{day}^{-1}$)											
Samples	Al	Ba	Cd	Cr	Cu	Fe	Mn	Pb	V	Zn	
Nacente	17.60	109.05	7.76	2.62	24.25	467.25	307.45	9.96	8.77	30.18	
Juliana	8.36	117.42	7.38	2.55	37.75	898.59	149.85	<LOD	8.18	####	
Serinhaem	44.88	98.62	7.55	2.77	29.18	457.16	37.03	<LOD	8.35	58.38	
E1	64.68	56.49	4.41	3.49	6.71	8.52	32.78	21.21	8.22	33.11	
E2	71.10	62.51	4.38	2.56	5.12	8.57	31.03	19.17	8.16	<LOD	
E3	56.66	59.02	4.34	2.47	4.91	<LOD	19.88	18.64	7.96	<LOD	
E4	69.91	56.28	4.58	2.37	5.40	<LOD	26.19	19.78	8.19	<LOD	
E5	76.11	53.32	4.83	2.36	6.33	<LOD	10.01	16.20	8.28	21.51	
E6	82.00	56.01	4.92	2.36	8.27	<LOD	6.29	<LOD	9.60	29.94	
E7	86.21	53.54	4.92	1.81	8.85	<LOD	3.82	16.16	9.63	<LOD	
E8	95.89	45.00	5.15	2.09	11.25	<LOD	5.22	21.10	9.92	<LOD	
E9	102.53	45.37	5.56	2.12	19.69	<LOD	3.49	14.06	9.37	22.17	

Table S9 – Dissolved Flows – Dry.

Dry ($\mu\text{g}\cdot\text{L}^{-1}$)											
Samples	Al	Ba	Cd	Cr	Cu	Fe	Mn	Pb	V	Zn	Discharge ($\text{m}^3\cdot\text{s}^{-1}$)
Nascente	64.29	21.97	0.77	1.61	3.80	300.86	12.92	<LOD	2.62	6.17	4.84
Juliana	68.18	21.03	0.79	1.90	3.72	488.36	16.62	<LOD	2.69	5.66	
Serinhaém	34.51	10.42	0.75	1.76	3.06	292.80	34.68	<LOD	2.53	<LOD	
E1	31.93	17.33	0.78	1.28	1.31	16.98	11.52	6.54	2.39	3.32	
E2	31.97	17.60	0.74	1.18	1.34	16.40	12.68	5.92	2.41	3.33	
E3	34.34	15.70	0.75	1.19	0.91	13.05	11.82	6.40	2.34	<LOD	
E4	37.38	15.94	0.74	1.21	1.35	2.31	4.59	4.67	2.36	5.00	
E5	34.97	11.75	0.75	1.19	1.93	1.06	4.50	5.46	2.31	2.17	
E6	45.95	13.30	0.74	1.17	1.55	1.51	2.60	6.96	2.53	2.53	
E7	55.44	14.65	0.73	1.21	1.84	2.05	2.26	6.38	2.63	5.08	
E8	53.61	11.70	0.79	1.20	1.76	0.96	1.74	4.44	2.87	<LOD	
E9	57.43	12.47	0.75	1.14	1.73	0.95	1.71	4.47	3.00	3.83	

Fluxes ($\mu\text{g}\cdot\text{day}^{-1}$)											
Samples	Al	Ba	Cd	Cr	Cu	Fe	Mn	Pb	V	Zn	
Nascente	311.14	106.33	3.74	7.77	18.40	1456.14	62.54	<LOD	12.70	29.84	
Juliana	329.97	101.76	3.81	9.18	17.99	2363.67	80.43	<LOD	13.00	27.41	
Serinhaém	167.02	50.43	3.63	8.53	14.80	1417.13	167.84	<LOD	12.22	<LOD	
E1	154.56	83.85	3.80	6.20	6.36	82.19	55.77	31.63	11.59	16.08	
E2	154.75	85.18	3.59	5.70	6.48	79.39	61.35	28.64	11.66	16.10	
E3	166.22	76.00	3.61	5.75	4.40	63.15	57.20	30.98	11.31	<LOD	
E4	180.92	77.16	3.58	5.86	6.54	11.17	22.22	22.60	11.44	24.22	
E5	169.27	56.89	3.64	5.74	9.33	5.14	21.80	26.40	11.18	10.52	
E6	222.40	64.39	3.57	5.67	7.52	7.32	12.59	33.66	12.24	12.24	
E7	268.32	70.92	3.55	5.86	8.92	9.90	10.94	30.90	12.75	24.60	
E8	259.46	56.63	3.81	5.81	8.53	4.65	8.44	21.51	13.91	<LOD	
E9	277.95	60.34	3.62	5.51	8.37	4.60	8.26	21.63	14.52	18.56	

Table S10 – Particulate Flows – Rainy.

Samples	Rainy ($\mu\text{g}\cdot\text{g}^{-1}$)									Discharge ($\text{m}^3\cdot\text{s}^{-1}$)
	Al	Fe	Ti	Mn	Zn	Ba	V	Pb	Cr	
Nascente	15258.05	9385.29	388.56	<LOD	<LOD	22.60	<LOD	<LOD	233.26	4.4
Juliana	28490.53	11947.68	776.80	103.79	27.55	200.90	<LOD	<LOD	52.90	
Serinhaém	24393.56	21676.60	1398.84	107.92	112.07	224.09	56.48	66.46	88.70	
E1	43095.04	1005.62	74.81	19.29	<LOD	8.53	<LOD	<LOD	4.62	
E2	2888.95	2971.72	253.07	48.73	42.45	77.93	<LOD	<LOD	12.79	
E3	8108.62	1425.06	123.90	14.93	46.12	91.65	<LOD	<LOD	5.49	
E4	3707.87	806.44	72.17	<LOD	5.44	23.70	<LOD	<LOD	3.03	
E5	2056.46	1120.74	75.18	<LOD	15.44	41.89	<LOD	<LOD	2.76	
E6	3313.94	10660.52	113.27	70.99	4.61	616.42	6.00	<LOD	14.74	
E7	5565.25	7721.75	55.27	17.73	40.30	53.28	<LOD	4.11	5.76	
E8	2196.02	8144.88	242.38	74.28	180.34	58.99	9.57	5.33	16.74	
E9	4791.06	9182.98	153.37	44.16	78.80	55.22	5.52	<LOD	14.18	
Samples	Fluxes ($\mu\text{g}\cdot\text{day}^{-1}$)									SPM ($\text{mg}\cdot\text{L}^{-1}$)
	Al	Fe	Ti	Mn	Zn	Ba	V	Pb	Cr	
Nascente	449.81	276.68	11.45	<LOD	<LOD	0.67	<LOD	<LOD	6.88	0.0067
Juliana	752.15	315.42	20.51	2.74	0.73	5.30	<LOD	<LOD	1.40	0.0060
Serinhaém	654.72	581.80	37.54	2.90	3.01	6.01	1.52	1.78	2.38	0.0061
E1	5088.09	118.73	8.83	2.28	<LOD	1.01	<LOD	<LOD	0.55	0.0268
E2	309.31	318.17	27.09	5.22	4.54	8.34	<LOD	<LOD	1.37	0.0243
E3	981.14	172.43	14.99	1.81	5.58	11.09	<LOD	<LOD	0.66	0.0275
E4	493.52	107.34	9.61	<LOD	0.72	3.15	<LOD	<LOD	0.40	0.0303
E5	226.21	123.28	8.27	<LOD	1.70	4.61	<LOD	<LOD	0.30	0.0250
E6	454.45	1461.91	15.53	9.73	0.63	84.53	0.82	<LOD	2.02	0.0312
E7	714.21	990.96	7.09	2.27	5.17	6.84	<LOD	0.53	0.74	0.0292
E8	249.61	925.80	27.55	8.44	20.50	6.70	1.09	0.61	1.90	0.0258
E9	572.69	1097.67	18.33	5.28	9.42	6.60	0.66	<LOD	1.69	0.0272

Table S11 - Particulate Flows – Dry.

Dry ($\mu\text{g}\cdot\text{g}^{-1}$)										
Samples	Al	Fe	Ti	Mn	Zn	Ba	V	Pb	Cr	Discharge ($\text{m}^3\cdot\text{s}^{-1}$)
Nascente	55866.17	141249.08	827.27	874.83	908.05	689.83	117.52	<LOD	106.74	4.84
Juliana	5681.35	13260.61	104.20	151.46	62.72	8.02	13.03	<LOD	14.36	
Serinhaém	64631.89	84348.56	572.19	612.16	269.35	39.79	149.49	<LOD	149.51	
E1	4332.26	4342.32	535.72	37.74	106.87	83.07	10.78	<LOD	14.46	
E2	4808.19	4544.36	188.60	43.20	79.53	63.40	12.66	<LOD	11.62	
E3	3334.42	1647.67	316.09	58.38	71.34	66.14	4.89	<LOD	7.12	
E4	3846.78	3249.81	276.93	38.24	123.63	137.82	8.27	<LOD	11.25	
E5	4600.78	2238.49	86.86	47.24	44.85	54.19	6.93	<LOD	10.39	
E6	3079.39	1370.78	125.48	54.52	130.73	82.71	4.55	<LOD	3.12	
E7	2931.98	1287.88	114.47	40.78	80.63	50.75	4.20	<LOD	4.11	
E8	2782.90	1157.78	103.84	28.09	88.18	74.73	0.00	<LOD	3.84	
E9	3150.03	1450.05	362.53	36.56	102.49	76.63	0.00	0.40	0.00	
Fluxes ($\mu\text{g}\cdot\text{day}^{-1}$)										
Samples	Al	Fe	Ti	Mn	Zn	Ba	V	Pb	Cr	SPM ($\text{mg}\cdot\text{L}^{-1}$)
Nascente	3316.81	8386.05	49.12	51.94	53.91	40.96	6.98	<LOD	6.34	0.012
Juliana	399.63	932.77	7.33	10.65	4.41	0.56	0.92	<LOD	1.01	0.015
Serinhaém	2731.95	3565.36	24.19	25.88	11.39	1.68	6.32	<LOD	6.32	0.009
E1	281.32	281.98	34.79	2.45	6.94	5.39	0.70	<LOD	0.94	0.013
E2	308.35	291.43	12.10	2.77	5.10	4.07	0.81	<LOD	0.74	0.013
E3	309.32	152.85	29.32	5.42	6.62	6.14	0.45	<LOD	0.66	0.019
E4	271.52	229.38	19.55	2.70	8.73	9.73	0.58	<LOD	0.79	0.015
E5	478.76	232.94	9.04	4.92	4.67	5.64	0.72	<LOD	1.08	0.022
E6	268.28	119.42	10.93	4.75	11.39	7.21	0.40	<LOD	0.27	0.018
E7	302.74	132.98	11.82	4.21	8.33	5.24	0.43	<LOD	0.42	0.021
E8	269.39	112.07	10.05	2.72	8.54	7.23	<LOD	<LOD	0.37	0.020
E9	279.51	128.67	32.17	3.24	9.09	6.80	<LOD	0.04	<LOD	0.018

Table S12 – Correlation values (r) and p from the April collection.

	April (r)																								
	Ald ($\mu\text{g}\cdot\text{L}^{-1}$)	Alp ($\mu\text{g}\cdot\text{g}^{-1}$)	Bad ($\mu\text{g}\cdot\text{L}^{-1}$)	Bap ($\mu\text{g}\cdot\text{g}^{-1}$)	Cdd ($\mu\text{g}\cdot\text{L}^{-1}$)	Crd ($\mu\text{g}\cdot\text{L}^{-1}$)	Crp ($\mu\text{g}\cdot\text{g}^{-1}$)	Cud ($\mu\text{g}\cdot\text{L}^{-1}$)	Fed ($\mu\text{g}\cdot\text{L}^{-1}$)	Fep ($\mu\text{g}\cdot\text{g}^{-1}$)	Mnd ($\mu\text{g}\cdot\text{L}^{-1}$)	Mnp ($\mu\text{g}\cdot\text{g}^{-1}$)	Pbd ($\mu\text{g}\cdot\text{L}^{-1}$)	Vd ($\mu\text{g}\cdot\text{L}^{-1}$)	Vp ($\mu\text{g}\cdot\text{g}^{-1}$)	Znd ($\mu\text{g}\cdot\text{L}^{-1}$)	Znp ($\mu\text{g}\cdot\text{g}^{-1}$)	Tip ($\mu\text{g}\cdot\text{g}^{-1}$)	pH	Conductivity ($\mu\text{S}\cdot\text{cm}^{-1}$)	DO ($\text{mg}\cdot\text{L}^{-1}$)	Salinity (‰)	DOC ($\text{mg}\cdot\text{L}^{-1}$)	TN ($\text{mg}\cdot\text{L}^{-1}$)	SPM ($\text{mg}\cdot\text{L}^{-1}$)
Ald ($\mu\text{g}\cdot\text{L}^{-1}$)		-0.63	-0.94	-0.01	-0.71	-0.45	-0.67	-0.66	-0.93	-0.29	-0.80	-0.47	0.43	0.56	-0.94	-0.69	0.24	-0.56	0.15	0.90	-0.32	0.88	-0.77	-0.45	0.84
Alp ($\mu\text{g}\cdot\text{g}^{-1}$)	0.0293		0.79	0.23	0.82	0.28	0.51	0.80	0.62	0.83	0.36	0.79	-0.68	-0.26	1.00	0.51	0.26	0.99	-0.36	-0.86	0.82	-0.87	0.33	0.90	-0.86
Bad ($\mu\text{g}\cdot\text{L}^{-1}$)	4.20E-06	0.0021		0.11	0.88	0.32	0.74	0.83	0.95	0.56	0.79	0.70	-0.66	-0.37	0.97	0.69	-0.08	0.74	-0.28	-0.97	0.52	-0.97	0.58	0.56	-0.95
Bap ($\mu\text{g}\cdot\text{g}^{-1}$)	0.9708	0.4800	0.7371		0.10	-0.05	-0.06	0.13	0.65	0.46	-0.13	0.46	0.13	0.27	-0.07	0.11	-0.24	0.20	0.08	-0.02	0.05	-0.06	-0.10	0.14	0.01
Cdd ($\mu\text{g}\cdot\text{L}^{-1}$)	0.0099	0.0010	0.0002	0.7459		0.10	0.81	0.93	0.85	0.78	0.73	0.84	-0.84	-0.03	0.97	0.51	0.27	0.78	-0.41	-0.92	0.63	-0.94	0.18	0.55	-0.94
Crd ($\mu\text{g}\cdot\text{L}^{-1}$)	0.1404	0.3800	0.3065	0.8734	0.7481		0.19	0.09	-0.53	-0.07	0.24	0.01	0.24	-0.61	0.91	0.04	-0.13	0.25	-0.12	-0.33	0.17	-0.35	0.70	0.49	-0.30
Crp ($\mu\text{g}\cdot\text{g}^{-1}$)	0.0174	0.0912	0.0054	0.8566	0.0016	0.5594		0.58	0.38	0.44	0.91	0.84	-0.75	-0.04	1.00	0.03	0.34	0.44	-0.06	-0.77	0.15	-0.78	0.25	0.30	-0.76
Cud ($\mu\text{g}\cdot\text{L}^{-1}$)	0.0202	0.0018	0.0008	0.6882	1.01E-05	0.7786	0.0493		0.98	0.77	0.57	0.78	-0.81	-0.05	0.84	0.76	0.23	0.78	-0.62	-0.85	0.74	-0.87	0.16	0.51	-0.88
Fed ($\mu\text{g}\cdot\text{L}^{-1}$)	0.0225	0.2637	0.0144	0.2324	0.0711	0.3584	0.5267	0.0045		0.63	0.50	0.85	-0.99	0.17	NA	0.84	-0.16	0.58	-0.75	-0.88	0.58	-0.88	0.26	0.18	-0.88
Fep ($\mu\text{g}\cdot\text{g}^{-1}$)	0.3688	0.0008	0.0593	0.1331	0.0029	0.8231	0.1499	0.0036	0.2501		0.21	0.82	-0.59	0.29	0.97	0.35	0.42	0.84	-0.35	-0.61	0.70	-0.65	-0.18	0.66	-0.65
Mnd ($\mu\text{g}\cdot\text{L}^{-1}$)	0.0017	0.2525	0.0020	0.6787	0.0075	0.4511	3.31E-05	0.0518	0.3886	0.5072		0.52	-0.70	-0.19	1.00	0.27	-0.18	0.28	-0.10	-0.76	0.06	-0.76	0.44	0.11	-0.73
Mnp ($\mu\text{g}\cdot\text{g}^{-1}$)	0.2069	0.0114	0.0356	0.2149	0.0043	0.9714	0.0043	0.0131	0.1466	0.0068	0.1482		0.20	0.01	0.88	0.64	0.25	0.80	-0.36	-0.73	0.81	-0.77	0.13	0.59	-0.78
Pbd ($\mu\text{g}\cdot\text{L}^{-1}$)	0.2481	0.0440	0.0522	0.7342	0.0043	0.5318	0.0190	0.0088	0.1089	0.0926	0.0352	0.7009		-0.18	1.00	0.25	0.33	-0.47	0.21	0.68	0.19	0.67	0.18	0.36	0.72
Vd ($\mu\text{g}\cdot\text{L}^{-1}$)	0.0558	0.4141	0.2298	0.3901	0.9368	0.0341	0.9103	0.8890	0.7847	0.3594	0.5646	0.9898	0.6506		-0.92	-0.44	0.42	-0.23	0.14	0.38	-0.15	0.32	-0.88	-0.38	0.30
Vp ($\mu\text{g}\cdot\text{g}^{-1}$)	0.0620	0.0030	0.0293	0.9342	0.0312	0.0941	0.0009	0.1588	NA	0.0253	0.0040	0.1206	NA	0.0809		0.98	0.23	1.00	-0.07	-0.99	0.92	-1.00	0.87	1.00	-0.99
Znd ($\mu\text{g}\cdot\text{L}^{-1}$)	0.0881	0.2427	0.0837	0.8083	0.2383	0.9393	0.9494	0.0461	0.1609	0.4437	0.5527	0.2421	0.7511	0.3175	0.1255		-0.08	0.51	-0.39	-0.60	0.61	-0.60	0.59	0.28	-0.60
Znp ($\mu\text{g}\cdot\text{g}^{-1}$)	0.4970	0.4635	0.8359	0.5115	0.4441	0.7257	0.3344	0.5280	0.8974	0.2296	0.6139	0.5453	0.4685	0.2258	0.7734	0.9042		0.35	-0.11	-0.07	0.36	-0.14	-0.38	0.31	-0.23
Tip ($\mu\text{g}\cdot\text{g}^{-1}$)	0.0582	2.27E-10	0.0064	0.5231	0.0026	0.4361	0.1562	0.0027	0.3032	0.0007	0.3817	0.0092	0.2038	0.4667	0.0006	0.2374	0.3273		-0.38	-0.81	0.85	-0.82	0.29	0.91	-0.83
pH	0.6527	0.2466	0.3820	0.8012	0.1899	0.6995	0.8512	0.0306	0.1464	0.2682	0.7570	0.3426	0.5798	0.6693	0.9313	0.3882	0.7614	0.2178		0.34	-0.63	0.35	0.00	-0.22	0.35
Conductivity ($\mu\text{S}\cdot\text{cm}^{-1}$)	7.85E-05	0.0004	9.45E-08	0.9386	2.20E-05	0.2872	0.0033	0.0004	0.0496	0.0344	0.0042	0.0250	0.0426	0.2237	0.0054	0.1542	0.8484	0.0014	0.2765		-0.61	0.99	-0.53	-0.66	0.97
DO ($\text{mg}\cdot\text{L}^{-1}$)	0.3038	0.0012	0.0850	0.8678	0.0295	0.6007	0.6397	0.0059	0.3059	0.0106	0.8501	0.0088	0.6227	0.6355	0.0787	0.1477	0.3087	0.0004	0.0272	0.0335		-0.62	0.13	0.76	-0.63
Salinity (‰)	0.0002	0.0003	1.26E-07	0.8626	7.56E-06	0.2588	0.0027	0.0002	0.0498	0.0218	0.0040	0.0149	0.0495	0.3101	0.0014	0.1519	0.6973	0.0010	0.2692	7.94E-11	0.0302		-0.50	-0.67	0.98
DOC ($\text{mg}\cdot\text{L}^{-1}$)	0.0031	0.2998	0.0472	0.7639	0.5830	0.0109	0.4366	0.6123	0.6756	0.5673	0.1512	0.7387	0.6344	0.0002	0.1329	0.1630	0.2789	0.3681	0.9906	0.0752	0.6940	0.0983		0.39	-0.45
TN ($\text{mg}\cdot\text{L}^{-1}$)	0.1378	5.81E-05	0.0558	0.6689	0.0642	0.1038	0.3430	0.0874	0.7772	0.0192	0.7395	0.0929	0.3397	0.2257	0.0016	0.5403	0.3775	3.45E-05	0.4875	0.0195	0.0044	0.0170	0.2124		-0.66
SPM ($\text{mg}\cdot\text{L}^{-1}$)	0.0007	0.0003	3.19E-06	0.9708	7.49E-06	0.3457	0.0039	0.0002	0.0474	0.0224	0.0065	0.0139	0.0296	0.3450	0.0142	0.1561	0.5313	0.0008	0.2612	1.96E-07	0.0286	1.41E-08	0.1462	0.0196	

April (p)

Table S13 - Correlation values (r) and p from the September collection.

	September (r)																							pH	Conductivity ($\mu\text{S}\cdot\text{cm}^{-1}$)	DO ($\text{mg}\cdot\text{L}^{-1}$)	Salinity (%)	DOC ($\text{mg}\cdot\text{L}^{-1}$)	TN ($\text{mg}\cdot\text{L}^{-1}$)	SPM ($\text{mg}\cdot\text{L}^{-1}$)
	Ald ($\mu\text{g}\cdot\text{L}^{-1}$)	Alp ($\mu\text{g}\cdot\text{g}^{-1}$)	Bad ($\mu\text{g}\cdot\text{L}^{-1}$)	Bap ($\mu\text{g}\cdot\text{g}^{-1}$)	Cdd ($\mu\text{g}\cdot\text{L}^{-1}$)	Crd ($\mu\text{g}\cdot\text{L}^{-1}$)	Crp ($\mu\text{g}\cdot\text{g}^{-1}$)	Cud ($\mu\text{g}\cdot\text{L}^{-1}$)	Fed ($\mu\text{g}\cdot\text{L}^{-1}$)	Fep ($\mu\text{g}\cdot\text{g}^{-1}$)	Mnd ($\mu\text{g}\cdot\text{L}^{-1}$)	Mnp ($\mu\text{g}\cdot\text{g}^{-1}$)	Pbd ($\mu\text{g}\cdot\text{L}^{-1}$)	Vd ($\mu\text{g}\cdot\text{L}^{-1}$)	Vp ($\mu\text{g}\cdot\text{g}^{-1}$)	Znd ($\mu\text{g}\cdot\text{L}^{-1}$)	Znp ($\mu\text{g}\cdot\text{g}^{-1}$)	Tip ($\mu\text{g}\cdot\text{g}^{-1}$)												
Ald ($\mu\text{g}\cdot\text{L}^{-1}$)		-0.63	-0.94	-0.01	-0.71	-0.45	-0.67	-0.66	-0.93	-0.29	-0.80	-0.47	0.43	0.56	-0.94	-0.69	0.24	-0.56	0.15	0.90	-0.32	0.88	-0.77	-0.45	0.84					
Alp ($\mu\text{g}\cdot\text{g}^{-1}$)	0.0293		0.79	0.23	0.82	0.28	0.51	0.80	0.62	0.83	0.36	0.79	-0.68	-0.26	1.00	0.51	0.26	0.99	-0.36	-0.86	0.82	-0.87	0.33	0.90	-0.86					
Bad ($\mu\text{g}\cdot\text{L}^{-1}$)	4.20E-06	0.0021		0.11	0.88	0.32	0.74	0.83	0.95	0.56	0.79	0.70	-0.66	-0.37	0.97	0.69	-0.08	0.74	-0.28	-0.97	0.52	-0.97	0.58	0.56	-0.95					
Bap ($\mu\text{g}\cdot\text{g}^{-1}$)	0.971	0.4800	0.7371		0.10	-0.05	-0.06	0.13	0.65	0.46	-0.13	0.46	0.13	0.27	-0.07	0.11	-0.24	0.20	0.08	-0.02	0.05	-0.06	-0.10	0.14	0.01					
Cdd ($\mu\text{g}\cdot\text{L}^{-1}$)	0.010	0.0010	0.0002	0.7459		0.10	-0.10	0.81	0.93	0.85	0.78	0.84	-0.84	-0.03	0.97	0.51	0.27	0.78	-0.41	-0.92	0.63	-0.94	0.18	0.55	-0.94					
Crd ($\mu\text{g}\cdot\text{L}^{-1}$)	0.140	0.3800	0.3065	0.8734	0.7481		0.19	0.09	-0.53	-0.07	0.24	0.01	0.24	-0.61	0.91	0.04	-0.13	0.25	-0.12	-0.33	0.17	-0.35	0.70	0.49	-0.30					
Crp ($\mu\text{g}\cdot\text{g}^{-1}$)	0.017	0.0912	0.0054	0.8566	0.0016	0.5594		0.58	0.38	0.44	0.91	0.84	-0.75	-0.04	1.00	0.03	0.34	0.44	-0.06	-0.77	0.15	-0.78	0.25	0.30	-0.76					
Cud ($\mu\text{g}\cdot\text{L}^{-1}$)	0.020	0.0018	0.0008	0.6882	1.01E-05	0.7786	0.0493		0.98	0.77	0.57	0.78	-0.81	-0.05	0.84	0.76	0.23	0.78	-0.62	-0.85	0.74	-0.87	0.16	0.51	-0.88					
Fed ($\mu\text{g}\cdot\text{L}^{-1}$)	0.022	0.2637	0.0144	0.2324	0.071	0.3584	0.5267	0.0045		0.63	0.50	0.85	-0.99	0.17	NA	0.84	-0.16	0.58	-0.75	-0.88	0.58	-0.88	0.26	0.18	-0.88					
Fep ($\mu\text{g}\cdot\text{g}^{-1}$)	0.369	0.0008	0.0593	0.1331	0.003	0.8231	0.1499	0.0036	0.2501		0.21	0.82	-0.59	0.29	0.97	0.35	0.42	0.84	-0.35	-0.61	0.70	-0.65	-0.18	0.66	-0.65					
Mnd ($\mu\text{g}\cdot\text{L}^{-1}$)	0.002	0.2525	0.0020	0.6787	0.008	0.4511	3.31E-05	0.0518	0.3886	0.5072		0.52	-0.70	-0.19	1.00	0.27	-0.18	0.28	-0.10	-0.76	0.06	-0.76	0.44	0.11	-0.73					
Mnp ($\mu\text{g}\cdot\text{g}^{-1}$)	0.207	0.0114	0.0356	0.2149	0.004	0.9714	0.0043	0.0131	0.1466	0.0068	0.1482		0.20	0.01	0.88	0.64	0.25	0.80	-0.36	-0.73	0.81	-0.77	0.13	0.59	-0.78					
Pbd ($\mu\text{g}\cdot\text{L}^{-1}$)	0.248	0.0440	0.0522	0.7342	0.004	0.5318	0.0190	0.0088	0.1089	0.0926	0.0352	0.7009		-0.18	1.00	0.25	0.33	-0.47	0.21	0.68	0.19	0.67	0.18	0.36	0.72					
Vd ($\mu\text{g}\cdot\text{L}^{-1}$)	0.056	0.4141	0.2298	0.3901	0.937	0.0341	0.9103	0.8890	0.7847	0.3594	0.5646	0.9898	0.6506		-0.92	-0.44	0.42	-0.23	0.14	0.38	-0.15	0.32	-0.88	-0.38	0.30					
Vp ($\mu\text{g}\cdot\text{g}^{-1}$)	0.062	0.0030	0.0293	0.9342	0.031	0.0941	0.0009	0.1588	NA	0.0253	0.0040	0.1206	NA	0.0809		0.98	0.23	1.00	-0.07	-0.99	0.92	-1.00	0.87	1.00	-0.99					
Znd ($\mu\text{g}\cdot\text{L}^{-1}$)	0.088	0.2427	0.0837	0.8083	0.238	0.9393	0.9494	0.0461	0.1609	0.4437	0.5527	0.2421	0.7511	0.3175	0.1255		-0.08	0.51	-0.39	-0.60	0.61	-0.60	0.59	0.28	-0.60					
Znp ($\mu\text{g}\cdot\text{g}^{-1}$)	0.497	0.4635	0.8359	0.5115	0.444	0.7257	0.3344	0.5280	0.8974	0.2296	0.6139	0.5453	0.4685	0.2258	0.7734	0.9042		0.35	-0.11	-0.07	0.36	-0.14	-0.38	0.31	-0.23					
Tip ($\mu\text{g}\cdot\text{g}^{-1}$)	0.058	2.27E-10	0.0064	0.5231	0.003	0.4361	0.1562	0.0027	0.3032	0.0007	0.3817	0.0092	0.2038	0.4667	0.0006	0.2374	0.3273		-0.38	-0.81	0.85	-0.82	0.29	0.91	-0.83					
pH	0.653	0.2466	0.3820	0.8012	0.190	0.6995	0.8512	0.0306	0.1464	0.2682	0.7570	0.3426	0.5798	0.6693	0.9313	0.3882	0.7614	0.2178		0.34	-0.63	0.35	0.00	-0.22	0.35					
Conductivity ($\mu\text{S}\cdot\text{cm}^{-1}$)	7.85E-05	0.0004	9.45E-08	0.9386	2.20E-05	0.2872	0.0033	0.0004	0.0496	0.0344	0.0042	0.0250	0.0426	0.2237	0.0054	0.1542	0.8484	0.0014	0.2765		-0.61	0.99	-0.53	-0.66	0.97					
DO ($\text{mg}\cdot\text{L}^{-1}$)	0.3038	0.0012	0.0850	0.8678	0.0295	0.6007	0.6397	0.0059	0.3059	0.0106	0.8501	0.0088	0.6227	0.6355	0.0787	0.1477	0.3087	0.0004	0.0272	0.0335		-0.62	0.13	0.76	-0.63					
Salinity (%)	0.0002	0.0003	1.26E-07	0.8626	7.56E-06	0.2588	0.0027	0.0002	0.0498	0.0218	0.0040	0.0149	0.0495	0.3101	0.0014	0.1519	0.6973	0.0010	0.2692	7.94E-11	0.0302		-0.50	-0.67	0.98					
DOC ($\text{mg}\cdot\text{L}^{-1}$)	0.0031	0.2998	0.0472	0.7639	0.5830	0.0109	0.4366	0.6123	0.6756	0.5673	0.1512	0.7387	0.6344	0.0002	0.1329	0.1630	0.2789	0.3681	0.9906	0.0752	0.6940	0.0983		0.39	-0.45					
TN ($\text{mg}\cdot\text{L}^{-1}$)	0.1378	5.81E-05	0.0558	0.6689	0.0642	0.1038	0.3430	0.0874	0.7772	0.0192	0.7395	0.0929	0.3397	0.2257	0.0016	0.5403	0.3775	3.45E-05	0.4875	0.0195	0.0044	0.0170	0.2124		-0.66					
SPM ($\text{mg}\cdot\text{L}^{-1}$)	0.0007	0.0003	3.19E-06	0.9708	7.49E-06	0.3457	0.0039	0.0002	0.0474	0.0224	0.0065	0.0139	0.0296	0.3450	0.0142	0.1561	0.5313	0.0008	0.2612	1.96E-07	0.0286	1.41E-08	0.1462	0.0196						

September (p)

Table S8 - Table of the distribution of river and estuarine loads.

Element	Dissolved Loads (%)		Particulate Loads (%)		Ecosystem
	Rainy	Dry	Rainy	Dry	
Al	9.13	30.36	16.96	69.96	River
	90.87	69.64	83.04	30.04	Estuary
Ba	40.00	29.05	8.27	42.92	River
	60.00	70.95	91.73	57.08	Estuary
Cd	34.49	25.45	-	-	River
	65.51	74.55	-	-	Estuary
Cr	26.86	32.85	52.48	72.11	River
	73.14	67.15	47.52	27.89	Estuary
Cu	54.37	43.52	-	-	River
	45.63	56.48	-	-	Estuary
Fe	99.07	95.14	18.09	88.45	River
	0.93	4.86	81.91	11.55	Estuary
Mn	78.09	54.59	13.86	72.73	River
	21.91	45.41	86.14	27.27	Estuary
Pb	6.37	0.00	-	-	River
	93.63	100.00	-	-	Estuary
V	24.17	25.53	37.09	77.61	River
	75.83	74.47	62.91	22.39	Estuary
Zn	70.27	31.88	7.18	50.11	River
	29.73	68.12	92.82	49.89	Estuary

Table S9 -Distribution coefficient (Kd).

Logkd	Rainy	Dry	Ecosystem
Al	6.58	5.94	River
	5.44	4.94	Estuary
Fe	5.01	5.19	River
	5.95	5.83	Estuary
Mn	3.80	4.35	River
	4.19	3.98	Estuary
Zn	3.40	4.61	River
	3.51	4.42	Estuary
Ba	3.61	3.55	River
	3.67	3.71	Estuary
V	4.47	4.37	River
	3.49	3.45	Estuary
Cr	5.23	4.54	River
	4.13	3.77	Estuary

Discussão geral

A contribuição fluvial de elementos traço é a principal fonte de contaminantes para os Oceanos. Todas as alterações realizadas ao longo das bacias de drenagem afetam a concentração e tipo dos contaminantes exportados. Os eventos naturais como a precipitação também influenciam nos contaminantes transportados através dos sistemas fluviais para os Oceanos. Os fluxos de As e Pb dentro da bacia do rio Doce são diretamente influenciados pelas atividades antrópicas, principalmente pela mineração e industrialização (**Capítulo 1**). Sofrem também influencia dos parâmetros naturais, como a precipitação e vazão, que atuam no transporte desses elementos ao longo da bacia. Sendo assim, a variação sazonal dessa região é bem marcante e por ser uma região muito impactada pela presença da mineração existe uma grande preocupação com os acidentes provenientes dessa atividade.

Um exemplo foi o acidente de 2015, com o rompimento da barragem de Fundão em Mariana, MG, que causou grandes impactos nos ecossistemas aquáticos e continentais da região. O grande movimento gerado pela lama de rejeitos, liberada pelo rompimento da barragem, levou a um alto transporte de materiais, a um aumento das concentrações de As e Pb em áreas anteriormente não impactadas por essa atividade e em uma maior exportação desses elementos para o Oceano Atlântico. O monitoramento existente nessa região facilitou a constatação dos impactos provenientes desse acidente. Assim, monitoramentos físico-químicos, hidrológicos e de contaminantes se provam necessários para o controle das alterações antrópicas ocorridas nos ecossistemas aquáticos e para que sejam realizadas ações mitigatórias nesses locais quando for preciso.

Os monitoramentos de bacias de drenagem devem incluir os dados hidrológicos (vazão e precipitação), uso da terra, concentrações de contaminantes, entre outros. Quando não há a disponibilidade desses dados os modelos de predição (**Capítulo 2**) se tornam de suma importância. Além de predizer dados hidrológicos essas ferramentas estatísticas vêm sendo muito utilizadas para usos variados como, prever concentrações de carbono, disseminação de doenças, concentração de nutrientes e etc. As regiões tropicais geralmente apresentam variações sazonais marcantes, entretanto, as mudanças climáticas que vêm ocorrendo nas últimas décadas têm ocasionando mudanças drásticas nas épocas sazonais de precipitação e seca (Konapala et al., 2020; Trenberth et al., 2014). Esse fato, acarreta em impactos

para a biota local e para o transporte de contaminantes ao longo dos ecossistemas aquáticos, fazendo com que ocorra uma maior concentração desses nos sedimentos superficiais. Essa maior concentração de elementos pode vir a causar contaminações mais expressivas para a biota e para as populações que utilizam essa água contaminada tanto para consumo, como para irrigação.

Apesar disso, em algumas regiões, como é o caso do estuário de Serinhaém, BA, épocas mais longas de seca não afetaram diretamente nos dados hidrológicos da região, conforme foi observado no **Capítulo 2**. Esse fato, só ocorreu por essa ser uma região na qual a precipitação acontece durante o ano inteiro, sem uma época marcante de seca. Assim, o transporte de contaminantes ao longo da bacia de drenagem se torna constante ao longo dos anos, sendo influenciado diretamente pelo aumento das atividades antrópicas. No estuário de Serinhaém, BA, a presença das atividades humanas não gerou tantos impactos, provavelmente pelo fato do estuário ser inserido em uma área de proteção ambiental, onde as atividades devem ocorrer de forma sustentável (**Capítulo 3**). Contudo, essa região apresenta um transporte constante de elementos pra o Oceano Atlântico, mesmo que em concentrações dentro das estabelecidas pela legislação brasileira.

No estuário de Serinhaém, BA, a concentração dos elementos traço são correlacionadas aos parâmetros físico-químicos, com processos de adsorção e floculação acontecendo ao mesmo tempo na fração dissolvida e na particulada. Além disso, ambas as frações (dissolvida e particulada) são influenciadas pelo metabolismo do manguezal existente nas margens do estuário. Outro fator relevante para o estudo de elementos traço nessa região é a composição da geologia local. Esse estuário pertence a Baía de Camamu, que é uma região rica em minério de barita, explicando as concentrações de Ba na região.

Comparando os achados dos 3 capítulos, fica evidente a importância de estudos constantes de monitoramento das bacias de drenagem com a coleta de dados hidrológicos, químicos, físicos e biológicos da região estudada. Falta de informações básicas afeta a tomada de decisões importantes que deveriam ser realizadas pelo poder público em prol da conservação dos recursos hídricos naturais e aumenta a probabilidade que ocorram grandes impactos negativos ocasionados pelas atividades antrópicas. Além disso, a falta de planejamento da conservação dos recursos naturais, leva a consequências negativas na economia local quando há a existência de uma

contaminação impactando a biota, que pertence ao ciclo alimentar humano e ao turismo que sustenta muitas populações regionais.

Considerações Finais

A bacia de drenagem do rio Doce, MG apresenta décadas de impactos por mineração e esse fato é evidenciado em todos os estudos realizados ao longo dos anos de 2009 a 2019, a partir dos contaminantes encontrados na coluna d'água e nos sedimentos de todos os ecossistemas aquáticos existentes na bacia. Outro fator relevante que deve ser levado em consideração dentro dessa bacia são os acidentes oriundos da mineração, cujo impacto de contaminação é substancial.

O monitoramento constante da região do rio Doce, realizado pelo IGAM, é de extrema importância para averiguar todos os impactos antrópicos na área. Apesar disso, ficou evidente que o número de postos de monitoramento é ínfimo comparado ao tamanho da bacia de drenagem do rio Doce, tornando necessário que haja uma ampliação desses pontos de amostragem, para que sejam obtidos resultados mais detalhados em relação as concentrações de contaminantes existentes na área e para que medidas mitigatórias sejam tomadas pelo poder público alcançando um uso sustentável da região. Foi observado que a variação sazonal acarreta em um aumento da exportação de elementos traço dos ecossistemas continentais para os Oceanos na época chuvosa, conseqüentemente impactando outras regiões e também deve ser levada em consideração.

A conjunção entre as ferramentas estatísticas, métodos de interpolação, métodos de mapeamento e as metodologias mais básicas de quantificação de contaminantes facilita a visualização de ambientes impactados por consequência de atividades antrópicas e reduz a possibilidade de impedimento no uso de água para irrigação e consumo, além da ingestão da biota pelas comunidades. Essa harmonização de ferramentas facilita a realização de estudos em bacias de drenagem, que são áreas normalmente com grande território.

Os parâmetros físico-químicos se relacionam com disponibilidade de contaminantes nos ecossistemas aquáticos ao controlarem processos de remoção e liberação, como floculação, adsorção e deposição dos elementos traço. No estuário de Serinhaém, BA o fluxo de elementos em direção ao Oceano Atlântico é constante,

diferente dos fluxos do rio Doce os quais apresentavam variação sazonal, e eram maiores na época de chuva, devido ao maior transporte das partículas.

Por fim, fica clara a importância da coleta correta de informações ambientais nas regiões brasileiras e que devem ser realizados estudos constantes de monitoramento que englobem a maior porção possível da bacia de drenagem em questão, o maior número de informações ambientais e de postos de coleta de dados, hidrológicos e ambientais, que permita um uso responsável dos recursos naturais.

Referências

- Almeida, C. A., Oliveira, A. F. de, Pacheco, A. A., Lopes, R. P., Neves, A. A., & Lopes Ribeiro de Queiroz, M. E. (2018). Characterization and evaluation of sorption potential of the iron mine waste after Samarco dam disaster in Doce River basin – Brazil. *Chemosphere*, 209, 411–420. <https://doi.org/10.1016/j.chemosphere.2018.06.071>
- Bianchi, T. S. (2007). *Biogeochemistry of Estuaries* (1st ed.). Oxford University Press, Inc.
- Bibi, R., Kang, H. Y., Kim, D., Jang, J., Kim, C., Kundu, G. K., & Kang, C. K. (2021). Biochemical composition of seston reflecting the physiological status and community composition of phytoplankton in a temperate coastal embayment of Korea. *Water (Switzerland)*, 13(22). <https://doi.org/10.3390/w13223221>
- Boyle, E. A., Edmond, J. M., & Sholkovitz, E. R. (1977). The mechanism of iron removal in estuaries. *Geochimica et Cosmochimica Acta*, 41(9), 1313–1324. [https://doi.org/10.1016/0016-7037\(77\)90075-8](https://doi.org/10.1016/0016-7037(77)90075-8)
- Chen, M., Li, F., Tao, M., Hu, L., Shi, Y., & Liu, Y. (2019). Distribution and ecological risks of heavy metals in river sediments and overlying water in typical mining areas of China. *Marine Pollution Bulletin*, 146(March), 893–899. <https://doi.org/10.1016/j.marpolbul.2019.07.029>
- Chowdhary, P., Bharagava, R. N., Mishra, S., & Khan, N. (2020). Role of Industries in Water Scarcity and Its Adverse Effects on Environment and Human Health. In *Environmental Concerns and Sustainable Development* (pp. 235–256). Springer, Singapore. https://doi.org/10.1007/978-981-13-5889-0_12
- Cohen, A., & Davidson, S. (2011a). The watershed approach: Challenges, antecedents, and the transition from technical tool to governance unit. *Water Alternatives*, 4(1), 1–14.
- Cohen, A., & Davidson, S. (2011b). The watershed approach: Challenges, antecedents, and the transition from technical tool to governance unit. *Water Alternatives*, 4(1), 1–14.
- Das, B., Nordin, R., & Mazumder, A. (2009). Watershed land use as a determinant of metal concentrations in freshwater systems. *Environmental Geochemistry and Health*, 31(6), 595–607. <https://doi.org/10.1007/s10653-008-9244-z>

- Elimelech, M. (2006). The global challenge for adequate and safe water. *Journal of Water Supply: Research and Technology - AQUA*, 55(1), 3–10. <https://doi.org/10.2166/aqua.2005.064>
- Fan, J., Jian, X., Shang, F., Zhang, W., Zhang, S., & Fu, H. (2021). Underestimated heavy metal pollution of the Minjiang River, SE China: Evidence from spatial and seasonal monitoring of suspended-load sediments. *Science of the Total Environment*, 760, 142586. <https://doi.org/10.1016/j.scitotenv.2020.142586>
- Fettweis, M., & Lee, B. J. (2017). Spatial and Seasonal Variation of Biomineral Suspended Particulate Matter Properties in High-Turbid Nearshore and Low-Turbid Offshore Zones. *Water (Switzerland)*, 9(9). <https://doi.org/10.3390/w9090694>
- Gäbler, H. E. (1997). Mobility of heavy metals as a function of pH of samples from an overbank sediment profile contaminated by mining activities. *Journal of Geochemical Exploration*, 58(2–3), 185–194. [https://doi.org/10.1016/S0375-6742\(96\)00061-1](https://doi.org/10.1016/S0375-6742(96)00061-1)
- Gaillardet, J., Viers, J., & Dupré, B. (2014). Trace Elements in River Waters. In *Treatise on Geochemistry: Second Edition* (Vol. 7). <https://doi.org/10.1016/B978-0-08-095975-7.00507-6>
- Gleick, P. H., & Cooley, H. (2021). Freshwater Scarcity. *Annual Review of Environment and Resources*, 46, 319–348. <https://doi.org/10.1146/annurev-environ-012220-101319>
- Gönenc, E. I., Vadineanu, A., Wolflin, J. P., & Russo, R. C. (2007). *Sustainable Use and Development of Watersheds NATO Science for Peace and Security Series* (1st ed.). Springer, Dordrecht. <https://doi.org/https://doi.org/10.1007/978-1-4020-8558-1>
- González-Ortegón, E., Laiz, I., Sánchez-Quiles, D., Cobelo-Garcia, A., & Tovar-Sánchez, A. (2019). Trace metal characterization and fluxes from the Guadiana, Tinto-Odiel and Guadalquivir estuaries to the Gulf of Cadiz. *Science of the Total Environment*, 650, 2454–2466. <https://doi.org/10.1016/j.scitotenv.2018.09.290>
- Goudie, A. S., & Viles, H. A. (2012). Weathering and the global carbon cycle: Geomorphological perspectives. *Earth-Science Reviews*, 113(1–2), 59–71. <https://doi.org/10.1016/j.earscirev.2012.03.005>
- Guillou, N., & Chapalain, G. (2021). Machine learning methods applied to sea level predictions in the upper part of a tidal estuary. *Oceanologia*, 63(4), 531–544. <https://doi.org/10.1016/j.oceano.2021.07.003>
- Hecky, R. E., & Kilham, P. (1988). Nutrient limitation of phytoplankton in freshwater and marine environments: A review of recent evidence on the effects of enrichment. *Limnology and Oceanography*, 33(4part2), 796–822. <https://doi.org/10.4319/lo.1988.33.4part2.0796>
- Ho, Q. N., Fettweis, M., Spencer, K. L., & Lee, B. J. (2022). Flocculation with heterogeneous composition in water environments: A review. *Water Research*, 213(July 2021), 118147. <https://doi.org/10.1016/j.watres.2022.118147>
- Ip, C. C. M., Li, X.-D., Zhang, G., Wai, O. W. H., & Li, Y.-S. (2007). Trace metal distribution in sediments of the Pearl River Estuary and the surrounding coastal area, South China.

- Jia, Z., Li, S., Liu, Q., Jiang, F., & Hu, J. (2021). Distribution and partitioning of heavy metals in water and sediments of a typical estuary (Modaomen, South China): The effect of water density stratification associated with salinity. *Environmental Pollution*, 287(April), 117277. <https://doi.org/10.1016/j.envpol.2021.117277>
- Kang, Y., Kang, Y. H., Kim, J. K., Kang, H. Y., & Kang, C. K. (2020). Year-to-year variation in phytoplankton biomass in an anthropogenically polluted and complex estuary: A novel paradigm for river discharge influence. *Marine Pollution Bulletin*, 161(September), 111756. <https://doi.org/10.1016/j.marpolbul.2020.111756>
- Karbassi, A. R., & Ayaz, G. O. (2007). Flocculation of Cu, Zn, Pb, Ni and Mn during mixing of Talar River Water with Caspian Seawater. *International Journal of Environmental Research*, 1(1), 66–73.
- Kim, J. S., Oh, S. Y., & Oh, K. Y. (2006). Nutrient runoff from a Korean rice paddy watershed during multiple storm events in the growing season. *Journal of Hydrology*, 327(1–2), 128–139. <https://doi.org/10.1016/j.jhydrol.2005.11.062>
- Konapala, G., Mishra, A. K., Wada, Y., & Mann, M. E. (2020). Climate change will affect global water availability through compounding changes in seasonal precipitation and evaporation. *Nature Communications*, 11(1). <https://doi.org/10.1038/s41467-020-16757-w>
- Kretzschmar, R., & Schafer, T. (2005). Metal Retention and Transport on Colloidal Particles in the Environment. *Elements*, 1(4), 205–210. <https://doi.org/10.2113/gselements.1.4.205>
- Lee, G., Bigham, J. M., & Faure, G. (2002). Removal of trace metals by coprecipitation with Fe, Al and Mn from natural waters contaminated with acid mine drainage in the Ducktown Mining District, Tennessee. *Applied Geochemistry*, 17(5), 569–581. [https://doi.org/10.1016/S0883-2927\(01\)00125-1](https://doi.org/10.1016/S0883-2927(01)00125-1)
- Lee, M. K., & Saunders, J. A. (2003). Effects of pH on metals precipitation and sorption: Field bioremediation and geochemical modeling approaches. *Vadose Zone Journal*, 2(2), 177–185. <https://doi.org/10.2113/2.2.177>
- Lee, S., Roh, Y., & Koh, D. C. (2019). Oxidation and reduction of redox-sensitive elements in the presence of humic substances in subsurface environments: A review. *Chemosphere*, 220, 86–97. <https://doi.org/10.1016/j.chemosphere.2018.11.143>
- Li, L. Y., Hall, K., Yuan, Y., Mattu, G., McCallum, D., & Chen, M. (2009). Mobility and bioavailability of trace metals in the water-sediment system of the highly urbanized brunette watershed. *Water, Air, and Soil Pollution*, 197(1–4), 249–266. <https://doi.org/10.1007/s11270-008-9808-7>
- Macdonald, F. A., Swanson-Hysell, N. L., Park, Y., Lisiecki, L., & Jagoutz, O. (2019). Arc-continent collisions in the tropics set Earth's climate state. *Science*, 364(6436), 181–184. <https://doi.org/10.1126/science.aav5300>

- Machado, A. de S. A., Spencer, K., Kloas, W., Toffolon, M., & Zarfl, C. (2016). Metal fate and effects in estuaries : A review and conceptual model for better understanding of toxicity. *Science of the Total Environment*, *541*, 268–281. <https://doi.org/10.1016/j.scitotenv.2015.09.045>
- Manning, A. J., Langston, W. J., & Jonas, P. J. C. (2010). A review of sediment dynamics in the Severn Estuary: Influence of flocculation. *Marine Pollution Bulletin*, *61*(1–3), 37–51. <https://doi.org/10.1016/j.marpolbul.2009.12.012>
- Millward, G. E. (1995). Processes affecting trace-element speciation in estuaries - A review. *Analyst*, *120*(3), 609–614. [https://doi.org/Doi 10.1039/An9952000609](https://doi.org/Doi%2010.1039/An9952000609)
- Mosley, L. M., & Liss, P. S. (2020). Particle aggregation, pH changes and metal behaviour during estuarine mixing: Review and integration. *Marine and Freshwater Research*, *71*(3), 300–310. <https://doi.org/10.1071/MF19195>
- Oliver, B. G., Thurman, E. M., & Malcolm, R. L. (1983). The contribution of humic substances to the acidity of colored natural waters. *Geochimica et Cosmochimica Acta*, *47*(11), 2031–2035. [https://doi.org/10.1016/0016-7037\(83\)90218-1](https://doi.org/10.1016/0016-7037(83)90218-1)
- Perret, D., Gaillard, J. F., Dominik, J., & Atteia, O. (2000). The diversity of natural hydrous iron oxides. *Environmental Science and Technology*, *34*(17), 3540–3546. <https://doi.org/10.1021/es0000089>
- Plathe, K. L., von der Kammer, F., Hassellöv, M., Moore, J. N., Murayama, M., Hofmann, T., & Hochella, M. F. (2013). The role of nanominerals and mineral nanoparticles in the transport of toxic trace metals: Field-flow fractionation and analytical TEM analyses after nanoparticle isolation and density separation. *Geochimica et Cosmochimica Acta*, *102*, 213–225. <https://doi.org/10.1016/j.gca.2012.10.029>
- Pouget, F., Gil-Díaz, T., Blanc, G., Coynel, A., Bossy, C., & Schäfer, J. (2022). Historical mass balance of cadmium decontamination trends in a major European continent-ocean transition system: Case study of the Gironde Estuary. *Marine Environmental Research*, *176*, 105594. <https://doi.org/10.1016/j.marenvres.2022.105594>
- Prabakaran, K., Eswaramoorthi, S., Nagarajan, R., Anandkumar, A., & Franco, F. M. (2020). Geochemical behaviour and risk assessment of trace elements in a tropical river, Northwest Borneo. *Chemosphere*, *252*, 126430. <https://doi.org/10.1016/j.chemosphere.2020.126430>
- Rani, S., Ahmed, M. K., Xiongzi, X., Keliang, C., Islam, M. S., & Habibullah-Al-Mamun, M. (2021). Occurrence, spatial distribution and ecological risk assessment of trace elements in surface sediments of rivers and coastal areas of the East Coast of Bangladesh, North-East Bay of Bengal. *Science of the Total Environment*, *801*, 149782. <https://doi.org/10.1016/j.scitotenv.2021.149782>
- Riba, I., Del Valls, T. Á., Forja, J. M., & Gómez-Parra, A. (2004). The influence of pH and salinity on the toxicity of heavy metals in sediment to the estuarine clam *Ruditapes philippinarum*. *Environmental Toxicology and Chemistry*, *23*(5), 1100–1107. <https://doi.org/10.1897/023-601>

- Salomons, W., & Förstner, U. (1980). Trace metal analysis on polluted sediments . Part II . Evaluation of environmental impact. *Environmental Technology Letters*, 1(December 2012), 506. <https://doi.org/10.1080/09593338009384007>
- Salomons, W., & Förstner, U. (1984). Metals in the Hydrocycle. In *Eos, Transactions American Geophysical Union* (Vol. 66, Issue 33). <https://doi.org/10.1007/978-3-642-69325-0>
- Samanta, S., Dalai, T. K., Tiwari, S. K., & Rai, S. K. (2018). Quantification of source contributions to the water budgets of the Ganga (Hooghly) River estuary, India. *Marine Chemistry*, 207(June), 42–54. <https://doi.org/10.1016/j.marchem.2018.10.005>
- Santos, S. M., Marini, M., de Souza, P., Augusto, G., Bircol, C., & Ueno, M. (2020). *Planos de Bacia e seus desafios: o caso da Bacia Hidrográfica do alto tietê-sP 1* (Vol. 23). <https://orcid.org/0000-0001-8254-5167>
- Shimizu, Y., Yamazaki, S., & Terashima, Y. (1992). Sorption of anionic pentachlorophenol (PCP) in aquatic environments: The effect of pH. In *Wal. Sci. Tech* (Vol. 25). <https://iwaponline.com/wst/article-pdf/25/11/41/102807/41.pdf>
- Sholkovitz, E. R. (1976). Flocculation of dissolved organic and inorganic matter during the mixing of river water and seawater. *Geochimica et Cosmochimica Acta*, 40(1966), 831–845.
- Sinclair, P., Beckett, R., & Hart, B. T. (1989). Trace elements in suspended particulate matter from the Yarra River, Australia. *Sediment/Water Interactions. Proc. 4th Symposium, Melbourne, 1987*, 239–251. https://doi.org/10.1007/978-94-009-2376-8_22
- Sultan, K., Shazili, N. A., & Peiffer, S. (2011). Distribution of Pb, As, Cd, Sn and Hg in soil, sediment and surface water of the tropical river watershed, Terengganu (Malaysia). *Journal of Hydro-Environment Research*, 5(3), 169–176. <https://doi.org/10.1016/j.jher.2011.03.001>
- Tepe, N., & Bau, M. (2014). Importance of nanoparticles and colloids from volcanic ash for riverine transport of trace elements to the ocean: Evidence from glacial-fed rivers after the 2010 eruption of Eyjafjallajökull Volcano, Iceland. *Science of the Total Environment*, 488–489(1), 243–251. <https://doi.org/10.1016/j.scitotenv.2014.04.083>
- Thill, A., Moustier, S., Garnier, J. M., Estournel, C., Naudin, J. J., & Bottero, J. Y. (2001). Evolution of particle size and concentration in the Rhône river mixing zone: Influence of salt flocculation. *Continental Shelf Research*, 21(18–19), 2127–2140. [https://doi.org/10.1016/S0278-4343\(01\)00047-4](https://doi.org/10.1016/S0278-4343(01)00047-4)
- Trenberth, K. E., Dai, A., van der Schrier, G., Jones, P. D., Barichivich, J., Briffa, K. R., & Sheffield, J. (2014). Global warming and changes in drought. In *Nature Climate Change* (Vol. 4, Issue 1, pp. 17–22). <https://doi.org/10.1038/nclimate2067>
- Turner, A., & Millward, G. E. (2002). Suspended particles: Their role in Estuarine biogeochemical cycles. *Estuarine, Coastal and Shelf Science*, 55(6), 857–883. <https://doi.org/10.1006/ecss.2002.1033>

- Upping, E., Thompson, D. W., Ohnstad, M., & Hetherington, N. B. (1986). Effects of pH on the release of metals from naturally-occurring oxides of Mn and Fe. *Environmental Technology Letters*, 7(1–12), 109–114. <https://doi.org/10.1080/09593338609384396>
- Violante, A., Cozzolino, V., Perelomov, L., Caporale, A. G., & Pigna, M. (2010). Mobility and bioavailability of heavy metals and metalloids in soil environments. *Journal of Soil Science and Plant Nutrition*, 10(3), 268–292. <https://doi.org/10.4067/S0718-95162010000100005>
- Wagena, M. B., Goering, D., Collick, A. S., Bock, E., Fuka, D. R., Buda, A., & Easton, Z. M. (2020). Comparison of short-term streamflow forecasting using stochastic time series, neural networks, process-based, and Bayesian models. *Environmental Modelling and Software*, 126. <https://doi.org/10.1016/j.envsoft.2020.104669>
- Walther, J. V. (1996). Relation between rates of aluminosilicate mineral dissolution, pH, temperature, and surface charge. In *American Journal of Science* (Vol. 296, Issue 7, pp. 693–728). <https://doi.org/10.2475/ajs.296.7.693>
- Yan, X., Wei, Z., Hong, Q., Lu, Z., & Wu, J. (2017). Phosphorus fractions and sorption characteristics in a subtropical paddy soil as influenced by fertilizer sources. *Geoderma*, 295, 80–85. <https://doi.org/10.1016/j.geoderma.2017.02.012>
- Yang, L., Wang, L., Wang, Y., & Zhang, W. (2015). Geochemical speciation and pollution assessment of heavy metals in surface sediments from Nansi Lake, China. *Environmental Monitoring and Assessment*, 187(5), 1–9. <https://doi.org/10.1007/s10661-015-4480-z>
- Yaseen, Z. M. (2021). An insight into machine learning models era in simulating soil, water bodies and adsorption heavy metals: Review, challenges and solutions. *Chemosphere*, 277, 130126. <https://doi.org/10.1016/j.chemosphere.2021.130126>